Middle Rio Grande
Elephant Butte Reach Report:

Morpho-dynamic Processes and
Silvery Minnow Habitat from
the Southern Boundary of the
Bosque Del Apache National Wildlife Refuge to
the Elephant Butte Reservoir

Joshua Sperry
Andrew Schied
Dr. Pierre Julien

May 2022
Final report prepared for the
United States Bureau of Reclamation

Colorado State University
Engineering Research Center
Department of Civil and Environmental Engineering
Fort Collins, Colorado 80523

Abstract

The Elephant Butte Reach spans approximately 39 miles of the Middle Rio Grande (MRG), from the southern boundary of Bosque Del Apache National Wildlife Refuge to Elephant Butte Reservoir in New Mexico. This reach report, prepared for the United States Bureau of Reclamation (USBR), presents a summary of results for a better understanding of the morpho-dynamic processes within the Elephant Butte Reach. The reach is divided into six subreaches (EB1, EB2, EB3, EB4, EB5 and EB6) to illustrate the spatial and temporal trends of the channel geometry and morphology of the dynamic river, which are still changing in response to anthropogenic impacts over the last century (Posner, 2017).

Discharge and sediment data from the United States Geological Survey were used to identify the seasons of peak discharge and sediment load in the reach. While spring snowmelt brings water discharge volumes, monsoonal thunderstorms often transport the greatest amount of suspended sediment. Since 2006, the two main stream gages (HWY 380 near San Antonio and Floodway at San Marcial) recorded an average discharge of 0.47 million acre-ft/yr and 0.42 million acre-ft/yr respectively. Since 2011, the average measured suspended sediment loads at these two gages reached about 7,000 tons per day and 5,000 tons per day respectively.

Aerial photographs dating back to 1918 were analyzed through GIS (geographic information system) to evaluate the changes in channel width and sinuosity. Anthropogenic changes and droughts led to significant river narrowing to values between 100 and 200 feet since 1918. The sinuosity of the Elephant Butte Reach has remained low (slightly above 1) for most sub-reaches, but increased slightly in recent years. The river essentially changed from a braided planform to a single-thread nearly-straight planform, mainly due to the channelization and constriction from levee formation.

Changes to bed elevation were observed using cross-section geometry files provided by the USBR Technical Service Center. The Elephant Butte reach has shown cycles of degradation and aggradation, where the magnitude of this cycle greatly decreases moving upward from the Elephant Butte Reservoir. After the initial degradation between 1962 and 1972, EB1 aggraded a maximum of around 5 feet and EB5 aggraded up to 15 feet from 1972 to 2002. From 2002 to 2012, subreach EB1 degraded a maximum of 3 feet where EB5 degraded as much as 13 feet. These significant changes are linked to the water levels in Elephant Butte Reservoir. Water levels increased from 1972 to 2002 and caused aggradation of the main channel due to backwater flow. The subsequent water level drop from 2002 to 2012 caused head cutting and degradation of the entire reach. The reservoir level changes greatly affect the erosion and sedimentation processes and the river morphology of the Elephant Butte Reach. A reservoir water level conceptual model is proposed to better understand the effects of the Elephant Butte water levels on the delta and channel formation of the reach.

The application of the Massong et al. (2010) geomorphic conceptual model to the Middle Rio Grande resulted in a classification of the Elephant Butte sub-reaches into migrating or aggrading stages. The reach as a whole follows similar trends whereby the channel enters a stage M4 or stage 3 (1962-1972), then transitions to rapid aggradation with perching (1972-2002) under the characteristics of A3/A4 stages, then stays in an A4 stage where the banks are aggrading faster than the main channel, and finally with instances where the banks aggrade while the bed degrades is representative of an A4 overbank, M4 main channel (2002-2012).

Additional work was performed with HEC-RAS to understand habitat availability for the endangered Rio Grande Silvery Minnow (RGSM) throughout the Elephant Butte Reach. A width-slice method in HEC-RAS was developed to calculate the hydraulically suitable RGSM habitat based on flow velocity and depth criteria for the larval, juvenile, and adult stages at various discharges. Calculations for a wide range of discharges up to 10,000 cfs were conducted for four geometric river conditions over a span of 50 years. At flow rates below 3,000 cfs, sub-reaches EB2, EB3, and EB4 provided the least amount of hydraulically suitable habitat, while sub-reaches EB1 and EB5 showed better adult habitat suitability. At flows above 4000 cfs, EB1 provided the greatest possible habitat for all life stages and EB4 provides the least RGSM habitat. Detailed mapping for year 2012 was performed based on detailed LiDAR data at a 10-foot resolution to illustrate the RGSM habitat areas within the Elephant Butte Reach. A large portion of the floodplain met the RGSM velocity and depth criteria but remained disconnected from the main channel due to perching. The wide cycles of aggradation and degradation associated with changes in water levels in the Elephant Butte Reservoir resulted in significant head cutting in sub-reach EB5, resulting in the need for excessively large flow discharges to inundate the floodplain.

Acknowledgement

This final report has been prepared for the United States Bureau of Reclamation under Award Number R17AC00064. The authors gratefully acknowledge the numerous constructive comments and thoughtful suggestions to improve a draft version of this report. We are particularly thankful to Ari Posner, Drew Baird, Nathan Holste and Nate Bradley at Reclamation. The detailed discussions contributed to key improvements including the addition of a synthesis section, a review of HEC-RAS files, and fine-tuning of multiple graphics and calculation procedures.

These reports have been prepared in collaboration with the University of New Mexico (UNM) and the American Southwest Ichthyological Researchers (ASIR). We specifically treasure our collaboration with Tom Turner, Steven Platania, Robert Dudley and Jake Mortensen whose aquatic habitat expertise on the Rio Grande Silvery Minnow (RGSM) provided an underlying framework for this reach report.

Table of Contents

Abstract I

Acknowledgement II

List of Tables V

List of Figures VI

Appendix A List of Figures VIII

Appendix B List of Figures IX

Appendix C List of Figures IX

Appendix D List of Figures IX

Appendix E List of Figures X

Appendix F List of Figures XII

Introduction 1

1.1 Site Description 2

1.2 Aggradation/Degradation Lines and Rangelines 3

1.3 Subreach Delineation 3

2. Precipitation, Flow and Sediment Discharge Analysis 9

2.1 Precipitation 9

2.2 River Flow 11

2.2.1 Cumulative Discharge Curves 14

2.2.2 Flow Duration 16

2.3 Suspended Sediment Load 23

2.3.1 Single Mass Curve 23

2.3.2 Double Mass Curve 25

2.3.3 Monthly Sediment Variation 26

3. River Geomorphology 29

3.1 Wetted Top Width 29

3.2 Width (Defined by Vegetation) 32

3.3 Bed Elevation 34

3.4 Bed Material 37

3.5 Sinuosity 37

3.6 Hydraulic Geometry 38

3.7 Mid-Channel Bars and Islands 41

3.8 Reservoir Effects 44
3.9 Channel Response Models 47
3.10 Geomorphic Conceptual Model 49
4. HEC-RAS Modeling for Silvery Minnow Habitat 62
4.1 Modeling Data and Background 62
4.2 Width Slices Methodology 63
4.3 Width Slices Habitat Results 64
4.4 RAS-Mapper Methodology 70
4.5 RAS-Mapper Habitat Results in 2012 70
4.6 Disconnected Areas 71
5. Elephant Butte Reservoir Synthesis 73
5. Conclusions 78
6. Bibliography 81
Appendix A A-1
Appendix B B-1
Appendix C C-1
Wetted Top Width Plots C-2
Appendix D D-1
Width Slices: Habitat Bar Charts D-2
Stacked Habitat Charts D-10
Appendix E E-1
Appendix F F-1

List of Tables

Table 1 Elephant Butte Subreach Delineation 4
Table 2 List of gages used in this study 11
Table 3 Probabilities of Exceedance 16
Table 4 Julien Wargadalam channel width prediction 48
Table 5 Rio Grande Silvery Minnow habitat velocity and depth range requirements (from Mortensen et al., 2019) 62
Table 6 Observed Trends Of The Elephant Butte Reach 76
Table 7 Years used in JW Calculations for D50 ..... B-4

List of Figures

Figure 1 Map with the Middle Rio Grande outlined in blue. It begins at the Cochiti Dam (top) and continues downstream to the Narrows in Elephant Butte Reservoir (bottom). The lime green highlights the Elephant Butte Reach. 1
Figure 2 Timeline of Significant events for the Middle Rio Grande River (Makar2006) 3
Figure 3 Width (top) and cumulative width (bottom) throughout the Elephant Butte Reach for the years 2002 (orange) and 2012 (blue). 5
Figure 4 Overall Elephant Butte Subreach Delineation 6
Figure 5 Subreaches EB1 through EB3 Delineation Magnified 7
Figure 6 Subreach EB4 through EB6 Delineation Magnified 8
Figure 7 BEMP data collection sites (figure source: http://bemp.org) 9
Figure 8 Precipitation near the Elephant Butte Reach over time 10
Figure 9 Cumulative precipitation near the Elephant Butte Reach 10
Figure 10 Raster hydrograph of daily discharge at USGS 08358500 Rio Grande at San Marcial, NM 12
Figure 11 Raster hydrograph of daily discharge at USGS 08358400 Rio Grande Floodway at San Marcial, NM 12
Figure 12 Raster hydrograph of daily discharge at USGS Station 08355490 near San Antonio, NM 13
Figure 13 Raster hydrograph of daily discharge at USGS Station 08359500 at Narrows In Elephant Butte, NM 13
Figure 14 Discharge single mass curve of the San Marcial gages and HWY 380 NR San Antonio gage (top) and San Marcial gages (bottom) 15
Figure 15 Cumulative discharge plotted against cumulative precipitation at the USG Floodway at San Marcial, NM 16
Figure 16 Flow Duration Curve for USGS Gage 08358400 Rio Grande Floodway at San Marcial, NM (left) and USGS Gage 08359500 Rio Grande at Narrows in Elephant Butte Reservoir, NM (right) using the mean daily flow discharge values. 17
Figure 17 Comparison of flow duration curves. The Elephant Butte, Floodway at San Marcial, HWY 380 Gages include data starting from the years 1951, 1949, and 2005 respectively. 17
Figure 18 Flow Duration Curve for USGS Gage 08358400 Rio Grande Floodway at San Marcial, NM using the maximum yearly discharge values. 18
Figure 19 Yearly Peak Flow Events 19
Figure 20 Number of days over an identified discharge at the Floodway at San Marcial gage ..... **Error! Bookmark not defined.**
Figure 21 Number of days over an identified discharge at the Narrows in Elephant Butte Reservoir gage 21
Figure 22 Number of days over an identified discharge at the Narrows in EB Reservoir gage including historical gage data 21
Figure 23 Number of days over an identified discharge above US HWY 380 gage 22
Figure 24 Number of days over an identified discharge above US HWY 380 gage including historical gage data 22

Figure 25 Suspended sediment discharge single mass curve for US HWY 380 Bridge USGS gage Near San Antonio, NM (top) and San Marcial Floodway, NM (bottom) 24
Figure 26 Double Mass Curve for the US HWY 380 Bridge Gage near San Antonio, NM 25
Figure 27 Cumulative suspended sediment (data from the Floodway at San Marcial gage, NM) versus cumulative precipitation at the Lemitar gage..... 26
Figure 28 Monthly average suspended sediment and water discharge at gage 08355490 Near San Antonio, NM..... 27
Figure 29 Monthly average suspended sediment concentration and water discharge at gage 08355490 Near San Antonio, NM 27
Figure 30 Monthly average suspended sediment and water discharge at gage 08358400 at San Marcial, NM 28
Figure 31 Monthly average suspended sediment concentration and water discharge at gage 08358400 at San Marcial, NM..... 28
Figure 32 Moving cross-sectional average of the wetted top width at a discharge of 1,000 cfs (With Levees) 29
Figure 33 Moving cross-sectional average of the wetted top width at a discharge of 3,000 cfs (With Levees) 30
Figure 34 Cumulative top width at a discharge of 1,000 cfs (With Levees)..... 31
Figure 35 Average top width for EB1 (top left), EB2 (top right), EB3 (middle left), EB4 (middle right), and EB5 (bottom) at discharges 500 to 5,000 cfs (Without Levees) 32
Figure 36 Averaged active channel width by subreach 33
Figure 37 Longitudinal profiles of bed elevation 35
Figure 38 Degradation and Aggradation by subreach 36
Figure 39 Median grain diameter size of samples taken throughout the Elephant Butte Reach 37
Figure 40 Sinuosity by subreach 38
Figure 41 HEC-RAS Wetted top width of channel at 1,000 cfs (left) and 3,000 cfs (right) 39
Figure 42 HEC-RAS Hydraulic depth at 1,000 cfs (left) and 3,000 cfs (right) 39
Figure 43 Example cross section indicating that the banks are going through a cycle of degradation / aggradation. Throughout the reach, the top wetted width has decreased then increased. 40
Figure 44 Wetted Perimeter at 1000 cfs (left) and 3000 cfs (right)..... 40
Figure 45 Water Surface Slope (500 cfs) and Channel Bed Slope..... 41
Figure 46 Average Number of Mid-Channel bars and Islands in Each Subreach..... 42
Figure 47 Aerial Photograph of subreach EB3 when multiple alternating bars, point bars, and islands were present in 2002 (left) and in 2012 (right) after vegetation encroachment. 43
Figure 48 Elephant Butte Reservoir Water Level (USBR, 2021) 44
Figure 49 Elephant Butte Reservoir water surface elevation (WSE) over time compared to Elephant Butte narrows range line elevations over time (Owen, 2012) 45
Figure 50 Elephant Butte Reservoir water surface elevation (WSE) over time compared to Elephant Butte narrows range line elevations over time 46
Figure 51 Julien and Wargadalam predicted widths and observed widths of the channel..... 48

Figure 52 Planform evolution model from Massong et al. (2010). The river undergoes stages 1-3 first and then continues to stages A4-A6 or stages M4-M8 depending on the sediment transport capacity. 49
Figure 53 Planform evolution model from Massong et al. (2010) applied to channel cross sectional view (Schied et al., 2022). 50
Figure 54 Downstream view of the 2005 Tiffany Plug (Owen et al., 2011) 51
Figure 55 Channel evolution of a representative cross section from subreach EB1 52
Figure 56 Subreach EB1: historical cross section profiles and corresponding aerial images 53
Figure 57 Channel evolution of a representative cross section from subreach EB2 54
Figure 58 Subreach EB2: historical cross section profiles and corresponding aerial images 55
Figure 59 Channel evolution of a representative cross section from subreach EB3 56
Figure 60 Subreach EB3: historical cross section profiles and corresponding aerial images 57
Figure 65 Subreach EB3: historical cross section profiles and corresponding aerial images 57
Figure 61 Channel Evolution of a representative cross section of subreach EB4 58
Figure 62 Subreach EB4: historical cross section profiles and corresponding aerial images 59
Figure 63 Channel evolution of a representative cross section of subreach EB5 60
Figure 64 Subreach EB5: historical cross section profiles and corresponding aerial images 61
Figure 65 Comparing the overbanking discharge values at various years. The dashed line (indicating 25% of cross sections in a reach experiencing overbanking) determines the discharge at which computational levees are removed for habitat analysis. 63
Figure 66 Cross-section with flow distribution from HEC-RAS with 20 vertical slices in the floodplains and 5 vertical slices in the main channel. The yellow and green slices are small enough that the discrete color changes look more like a gradient. 64
Figure 67 Larval RGSM habitat availability throughout the Elephant Butte Reach- the scale of the y-axis is lower for the larval habitat to better see the trends in the hydraulically suitable habitat. 65
Figure 68 Juvenile RGSM habitat availability throughout the Elephant Butte Reach 66
Figure 69 Adult RGSM habitat availability throughout the Elephant Butte Reach 66
Figure 70 Stacked habitat charts to display spatial variations of habitat throughout the Elephant Butte Reach in 2012 67
Figure 71 Stacked habitat charts at different scales to display spatial variations of habitat throughout the Elephant Butte Reach in 2012 68
Figure 72 Subreach EB6 habitat charts displays available RGSM life stage habitat at various flow rates in 2012 69
Figure 73 Hydraulically suitable habitat in 2012 for each life stage in subreach EB1 at 1,500 cfs (left) and 5,000 cfs (right) 71
Figure 74 Example of a disconnected area that contains water, but no access to or from the main channel 72
Figure 75 Disconnected area showing hydraulically suitable habitat for RGSM adult (green), juvenile (orange cross hatch), and larvae (green) 72
Figure 76 Reservoir Evolution Model 77

Appendix A List of Figures

Figure A- 1 Width (top) and cumulative width (bottom) throughout the Escondida reach for the years 2002 (orange) and 2012 (blue).EB1 ..... A-2
Figure A- 2 *2012 Aerial imagery with agg/deg line labels* A-3
Figure A- 3 2012 Aerial imagery with agg/deg line labels A-4
Figure A- 4 2012 Aerial imagery with agg/deg line labels A-5
Figure A- 5 2012 Aerial imagery with agg/deg line labels A-6
Figure A- 6 2012 Aerial imagery with agg/deg line labels A-7
Figure A- 7 2012 Aerial imagery with agg/deg line labels A-8
Figure A- 8 2012 Aerial imagery with agg/deg line labels A-9
Figure A- 9 2012 Aerial imagery with agg/deg line labels A-10
Figure A- 10 2012 Aerial imagery with agg/deg line labels A-11
Figure A- 11 2012 Aerial imagery with agg/deg line labels A-12
Figure A- 12 2012 Aerial imagery with agg/deg line labels A-13
Figure A- 13 Thalweg Elevation Profile from Agg/Deg Surveys (Owens, 2012) A-14

Appendix B List of Figures

Figure B- 1 Comparison between predicted and measured total sediment load (left) and percent difference vs u*/w (right) B-2
Figure B- 2 Total sediment rating curve at the San Acacia gage B-3
Figure B- 3 the ratio of measured to total sediment discharge vs depth; and (b) the ratio of suspended to total sediment discharge vs h/ds at the San Acacia gage B-3

Appendix C List of Figures

Figure C- 1 Wetted top width at each agg/deg line throughout the Elephant Butte Reach at a discharge of 1,000 cfs C-2
Figure C- 2 Wetted top width at each agg/deg line throughout the Elephant Butte Reach at a discharge of 3,000 cfs C-2
Figure C- 3 Example of annual habitat interpolating using the sediment rating curve and alpha technique C-3

Appendix D List of Figures

Figure D- 1 Subreach EB1 larva habitat ---------- D-2
Figure D- 2 Subreach EB1 Juvenile habitat---------- *D*-2
Figure D- 3 Subreach EB1 Adult habitat---------- *D*-3
Figure D- 4 Subreach EB2 larva habitat----------*D*-3
Figure D- 5 Subreach EB2 juvenile habitat----------*D*-4

Figure D- 6 Subreach EB2 adult habitat----------*D*-4
Figure D- 7 Subreach EB3 Larva Habitat----------D-5
Figure D- 8 Subreach EB3 Juvenile Habitat----------D-5
Figure D- 9 Subreach EB3 Adult Habitat----------*D*- 6
Figure D- 10 Subreach EB4 Larva Habitat----------*D*-6
Figure D- 11 Subreach EB4 Juvenile Habitat----------*D*-7
Figure D- 12 Subreach EB4 Adult Habitat----------*D*-7
Figure D- 13 Subreach EB5 Larva Habitat----------*D*-8
Figure D- 14 Subreach EB5 Juvenile Habitat----------*D*-8
Figure D- 15 Subreach EB5 Adult Habitat----------*D*-9
Figure D- 16 Stacked habitat charts to display spatial variations of habitat throughout the Elephant Butte Reach in 1962 ----------D-10
Figure D- 17Stacked habitat charts to display spatial variations of habitat throughout the Elephant Butte Reach in 1972 ----------D-11
Figure D- 18 Stacked habitat charts to display spatial variations of habitat throughout the Elephant Butte Reach in 1992 ----------D-12
Figure D- 19 Stacked habitat charts to display spatial variations of habitat throughout the Elephant Butte Reach in 2002 ----------D-13
Figure D- 20 Life stage habitat curves for subreach EB1 at the years 1962 (top), 1972 (middle), and 1992 (bottom). ----------D-14
Figure D- 21 Life stage habitat curves for subreach EB1 for the years 2002 (top) and 2012 (bottom).--D-15
Figure D- 22 Life stage habitat curves for subreach EB2 at the years 1962 (top), 1972 (middle), and 1992 (bottom). ----------D-16
Figure D- 23 Life stage habitat curves for subreach EB2 for the years 2002 (top) and 2012 (bottom).--D-17
Figure D- 24 Life stage habitat curves for subreach EB3 at the years 1962 (top), 1972 (middle), and 1992 (bottom) ----------D-18
Figure D- 25 Life stage habitat curves for subreach EB3 for the years 2002 (top) and 2012 (bottom) --D-19
Figure D- 26 Life stage habitat curves for subreach EB4 at the years 1962 (top), 1972 (middle), and 1992 (bottom).----------D-20
Figure D- 27 Life stage habitat curves for subreach EB4 for the years 2002 (top) and 2012 (bottom).--D-21
Figure D- 28 Life stage habitat curves for subreach EB5 at the years 1962 (top), 1972 (middle), and 1992 (bottom).----------D-22
Figure D- 29 Life stage habitat curves for subreach EB5 for the years 2002 (top) and 2012 (bottom). -D-23
Figure D- 30 Life stage habitat curves for subreach EB6 2012.----------D-24

Appendix E List of Figures

Figure E- 1 RGSM Habitat in subreach EB1 at 1500 cfs with hydraulically suitable areas labeled for larvae (green), juvenile (orange), and adult (light blue) and unsuitable inundated areas in dark blue. E-2
Figure E- 2 RGSM Habitat in subreach EB2 1500 cfs with hydraulically suitable areas labeled for larvae (green), juvenile (orange), and adult (light blue) and unsuitable inundated areas in dark blue.....E-3

Figure E- 3 RGSM Habitat in subreach EB3 at 1500 cfs with hydraulically suitable areas labeled for larvae (green), juvenile (orange), and adult (light blue) and unsuitable inundated areas in dark blue..... E-4
Figure E- 4 RGSM Habitat in subreach EB4 at 1500 cfs with hydraulically suitable areas labeled for larvae (green), juvenile (orange), and adult (light blue) and unsuitable inundated areas in dark blue..... E-5
Figure E- 5 RGSM Habitat in subreach EB5 at 1500 cfs with hydraulically suitable areas labeled for larvae (green), juvenile (orange), and adult (light blue) and unsuitable inundated areas in dark blue..... E-6
Figure E- 6 RGSM Habitat in subreach EB6.1 at 1500 cfs with hydraulically suitable areas labeled for larvae (green), juvenile (orange), and adult (light blue) and unsuitable inundated areas in dark blue.... E-7
Figure E- 7 RGSM Habitat in subreach EB6.2 at 1500 cfs with hydraulically suitable areas labeled for larvae (green), juvenile (orange), and adult (light blue) and unsuitable inundated areas in dark blue.... E-8
Figure E- 8 RGSM Habitat in subreach EB6.3) at 1500 cfs with hydraulically suitable areas labeled for larvae (green), juvenile (orange), and adult (light blue) and unsuitable inundated areas in dark blue.... E-9
Figure E- 9 RGSM Habitat in subreach EB6.4 at 1500 cfs with hydraulically suitable areas labeled for larvae (green), juvenile (orange), and adult (light blue) and unsuitable inundated areas in dark blue.. E-10
Figure E- 10 RGSM Habitat in subreach EB6.5 at 1500 cfs with hydraulically suitable areas labeled for larvae (green), juvenile (orange), and adult (light blue) and unsuitable inundated areas in dark blue. . E-11
Figure E- 11 RGSM Habitat in subreach EB6.6 at 1500 cfs with hydraulically suitable areas labeled for larvae (green), juvenile (orange), and adult (light blue) and unsuitable inundated areas in dark blue. . E-12
Figure E- 12 RGSM Habitat in subreach EB1 at 3000 cfs with hydraulically suitable areas labeled for larvae (green), juvenile (orange), and adult (light blue) and unsuitable inundated areas in dark blue. . E-13
Figure E- 13 RGSM Habitat in subreach EB2 at 3000 cfs with hydraulically suitable areas labeled for larvae (green), juvenile (orange), and adult (light blue) and unsuitable inundated areas in dark blue. . E-14
Figure E- 14 RGSM Habitat in subreach EB3 at 3000 cfs with hydraulically suitable areas labeled for larvae (green), juvenile (orange), and adult (light blue) and unsuitable inundated areas in dark blue. . E-15
. Figure E- 15 RGSM Habitat in subreach EB4 at 3000 cfs with hydraulically suitable areas labeled for larvae (green), juvenile (orange), and adult (light blue) and unsuitable inundated areas in dark blue. . E-16
Figure E- 16 RGSM Habitat in subreach EB5 at 3000 cfs with hydraulically suitable areas labeled for larvae (green), juvenile (orange), and adult (light blue) and unsuitable inundated areas in dark blue. . E-17
Figure E- 17 RGSM Habitat in subreach EB6.1 at 3000 cfs with hydraulically suitable areas labeled for larvae (green), juvenile (orange), and adult (light blue) and unsuitable inundated areas in dark blue. . E-18
Figure E- 18 RGSM Habitat in subreach EB6.2 at 3000 cfs with hydraulically suitable areas labeled for larvae (green), juvenile (orange), and adult (light blue) and unsuitable inundated areas in dark blue. . E-19
Figure E- 19 RGSM Habitat in subreach EB6.3 at 3000 cfs with hydraulically suitable areas labeled for larvae (green), juvenile (orange), and adult (light blue) and unsuitable inundated areas in dark blue. . E-20
Figure E- 20 RGSM Habitat in subreach EB6.4 at 3000 cfs with hydraulically suitable areas labeled for larvae (green), juvenile (orange), and adult (light blue) and unsuitable inundated areas in dark blue. . E-21
Figure E- 21 RGSM Habitat in subreach EB6.5 at 3000 cfs with hydraulically suitable areas labeled for larvae (green), juvenile (orange), and adult (light blue) and unsuitable inundated areas in dark blue. . E-22
Figure E- 22 RGSM Habitat in subreach EB6.6 at 3000 cfs with hydraulically suitable areas labeled for larvae (green), juvenile (orange), and adult (light blue) and unsuitable inundated areas in dark blue. . E-23

Figure E-23 RGSM Habitat in subreach EB1 at 5000 cfs with hydraulically suitable areas labeled for larvae (green), juvenile (orange), and adult (light blue) and unsuitable inundated areas in dark blue. E-24
Figure E- 24 RGSM Habitat in subreach EB2 at 5000 cfs with hydraulically suitable areas labeled for larvae (green), juvenile (orange), and adult (light blue) and unsuitable inundated areas in dark blue. .E-25
Figure E- 25 RGSM Habitat in subreach EB3 at 5000 cfs with hydraulically suitable areas labeled for larvae (green), juvenile (orange), and adult (light blue) and unsuitable inundated areas in dark blue ..E-26
Figure E- 26 RGSM Habitat in subreach EB4 at 5000 cfs with hydraulically suitable areas labeled for larvae (green), juvenile (orange), and adult (light blue) and unsuitable inundated areas in dark blue..E-27
Figure E- 27 RGSM Habitat in subreach EB5 at 5000 cfs with hydraulically suitable areas labeled for larvae (green), juvenile (orange), and adult (light blue) and unsuitable inundated areas in dark blue ..E-28
Figure E-28 RGSM Habitat in subreach EB6.1 at 5000 cfs with hydraulically suitable areas labeled for larvae (green), juvenile (orange), and adult (light blue) and unsuitable inundated areas in dark blue. .E-29
Figure E-29 RGSM Habitat in subreach EB6.2 at 5000 cfs with hydraulically suitable areas labeled for larvae (green), juvenile (orange), and adult (light blue) and unsuitable inundated areas in dark blue. .E-30
Figure E-30 RGSM Habitat in subreach EB6.3 at 5000 cfs with hydraulically suitable areas labeled for larvae (green), juvenile (orange), and adult (light blue) and unsuitable inundated areas in dark blue. .E-31
Figure E-31 RGSM Habitat in subreach EB6.4 at 5000 cfs with hydraulically suitable areas labeled for larvae (green), juvenile (orange), and adult (light blue) and unsuitable inundated areas in dark blue. .E-32
Figure E-32 RGSM Habitat in subreach EB6.5 at 5000 cfs with hydraulically suitable areas labeled for larvae (green), juvenile (orange), and adult (light blue) and unsuitable inundated areas in dark blue. .E-33
Figure E-33 RGSM Habitat in subreach EB6.6 at 5000 cfs with hydraulically suitable areas labeled for larvae (green), juvenile (orange), and adult (light blue) and unsuitable inundated areas in dark blue. .E-34

Appendix F List of Figures

Figure F- 1 Geomorphology and habitat connections collage for subreach EB1.....F-2
Figure F- 2 Geomorphology and habitat connections collage for subreach EB2.....F-3
Figure F- 3 Geomorphology and habitat connections collage for subreach EB3.....F-4
Figure F- 4 Geomorphology and habitat connections collage for subreach EB4.....F-5
Figure F- 5 Geomorphology and habitat connections collage for subreach EB5.....F-6

Introduction

The purpose of this research/study is to evaluate the morpho-dynamic conditions of the Middle Rio Grande (MRG) which extends from the Cochiti Dam to the Narrows in Elephant Butte Reservoir. The report focuses on the Elephant Butte Reach, which begins at the southern boundary of the Bosque Del Apache Wildlife Refuge near San Antonio, New Mexico, and continues downstream to the Elephant Butte Reservoir near Truth or Consequences, New Mexico (Figure 1).

The presented report is part of a series of reports commissioned by the USBR, which includes morpho-dynamic reach reports, reports on the biological-habitat conditions for the Rio Grande Silvery Minnow, and process linkage reports. The process linkage reports will ultimately connect morpho-dynamic conditions with the required biological-habitat conditions. This report focuses on understanding trends of the physical conditions of the Elephant Butte Reach based on literature and provided data. Specific objectives include:

- Delineate the reach into subreaches based on shared geomorphic characteristics;
- Summarize the flow and sediment discharge conditions and trends for the period of record available from United States Geological Survey (USGS) gages;
- Analyze geomorphic characteristics at a subreach level (sinuosity, width, bed elevation, bed material, and other hydraulic parameters);
- Link changes in the river geomorphology with changes in sediment and flow trends;
- Classify subreaches using a geomorphic conceptual model; and

Finally, in preparation for a future process linkage report, attempts were made to characterize the Rio Grande Silvery Minnow habitat of the Elephant Butte Reach. These methods were based on HEC-RAS one-dimensional hydraulic models, which were used to understand and predict the conditions on the Middle Rio Grande. This series of reports will support USBR's mission for the Middle Rio Grande to improve habitat for species listed by the Endangered Species Act and to support channel sustainability while continuing to provide effective water delivery (U.S. Bureau of Reclamation, 2012).

Figure 1 Map with the Middle Rio Grande outlined in blue. It begins at the Cochiti Dam (top) and continues downstream to the Narrows in Elephant Butte Reservoir (bottom). The lime green highlights the Elephant Butte reach.

1.1 Site Description

The Rio Grande begins in the San Juan Mountain range of Colorado and continues into New Mexico. It follows along the Texas-Mexico border before reaching the Gulf of Mexico. The Middle Rio Grande is the stretch from the Cochiti Dam to Elephant Butte Reservoir. The MRG has historically been affected by periods of drought and large spring flooding events due to snowmelt. Monsoons have causes some of the largest peak flows the river has seen. These floods often caused large scale shifts in the course of the river and rapid aggradation (Massong et al., 2010). Floods helped maintain aquatic ecosystems by enabling connection of water between the main channel and the floodplains (Scurlock, 1998), but consequently threatened human establishments that were built near the Rio Grande. Beginning in the 1930s, levees were installed to prevent flooding. Beginning in the 1950s, the USBR undertook a significant channelization effort involving jetty jacks, river straightening and other techniques. The low flow conveyance channel was in operation from the 1950's to the 1980's which diverted a portion of the water from the main channel, lessoning the water available to the river. Upstream dams built in the 1950s were used to store and regulate flow in the river. While these efforts enabled agriculture and large-scale human developments to thrive along the MRG, they also fundamentally changed the river, which led to reduced peak flows and sediment supply while altering the channel geometry and vegetation (Makar, 2006). In parts of the MRG, narrowing of the river continues, with channel degradation due to limited sediment supply and the formation of vegetated bars that encroach into the channel (Varyu, 2013; Massong et al., 2010). Farther downstream, closer to Elephant Butte Reservoir, aggradation and sediment plugs have been observed. The San Marcial plug, is an example of one of these sediment plugs that formed near the San Marcial railroad crossing located close to agg/deg line 1702. These factors have created an ecologically stressed environment, as seen in the decline of species such as the Rio Grande Silvery Minnow (Mortensen et al., 2019).

The Elephant Butte Reach is a part of the Middle Rio Grande located in central New Mexico. This reach begins at the downstream end of the Bosque Del Apache National Wildlife Refuge on the Rio Grande and continues approximately 39 miles downstream to the Elephant Butte Reservoir near Truth or Consequences, New Mexico. Figure 2 shows an excellent timeline of events by (Makar 2006) that have occurred from 1870 to 2010. While there is sediment transported due to erosion from the upstream reaches, ephemeral tributaries are the largest source of sediment to Elephant Butte Reach (Fitzner 2018). Below the San Acacia dam there are no major tributaries that enter the MRG but there are several small arroyos that enter the river and two flood controlled channels (Towne 2007). The Elephant Butte Reservoir located at the end of the Elephant Butte Reach, has a very large impact on the morpho dynamics of the Elephant Butte Reach. It has been observed that the water level in the reservoir has a direct impact on the head cutting and backwater effects which can subsequently lead to degradation or aggradation.

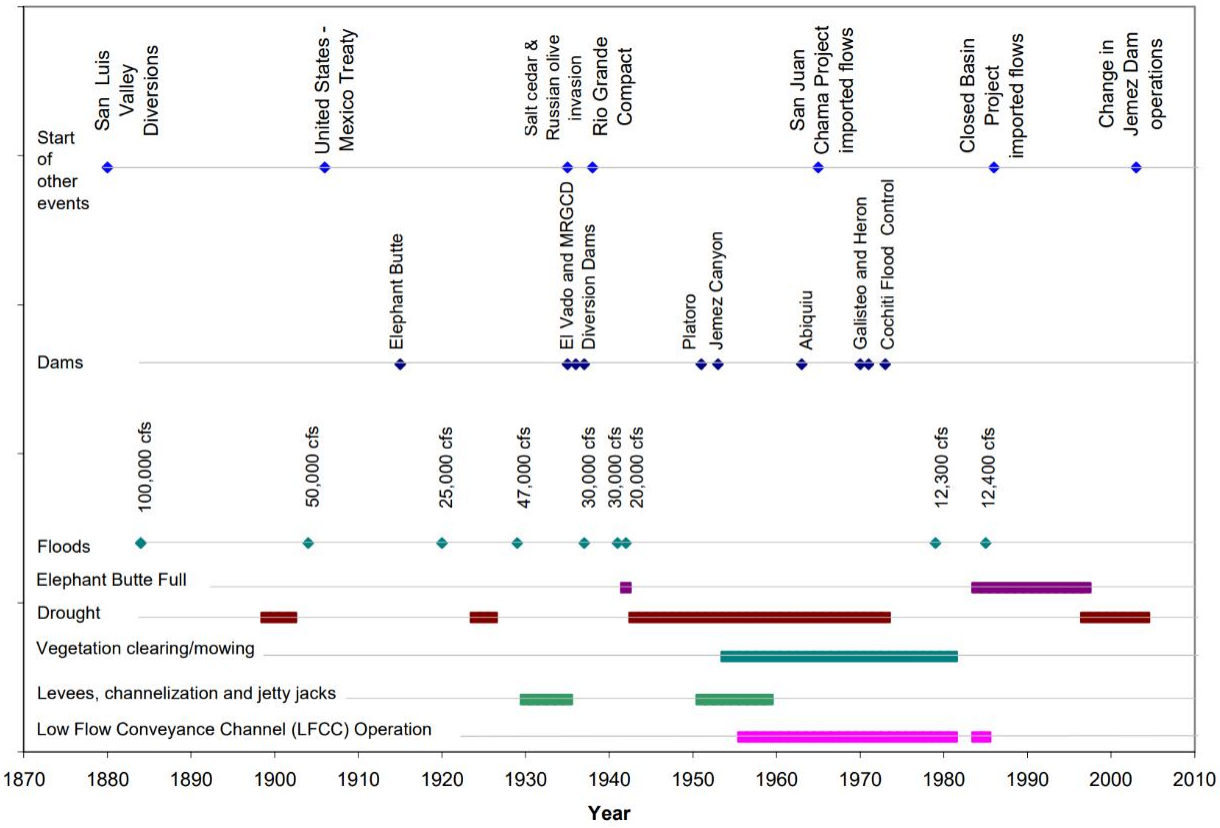

Figure 2 Timeline of Significant events for the Middle Rio Grande River (Makar2006)

1.2 Aggradation/Degradation Lines and Rangelines

Aggradation/degradation lines (agg/deg lines) are "spaced approximately 500-feet apart and are used to estimate sedimentation and morphological changes in the river channel and floodplain for the entire MRG" (Posner, 2017). Each agg/deg line is surveyed approximately every 10 years and is established as a cross-section in the Rio Grande HEC-RAS models. The most recent entire MRG survey used was performed in 2012. Cross-sectional geometry at each agg/deg line is available from models developed by the Technical Service Center (Varyu, 2013). Models are available for 1962, 1972, 1992, 2002 and 2012. The 2012 model was developed from LiDAR data, but models prior to 2012 used photogrammetry techniques. All models use the NAVD88 vertical datum. In addition to agg/deg lines, rangelines are used as location identifiers in this analysis. 'The rangelines, created at the same time as agg/deg lines, were determined in association with geomorphic factors, such as migrating bends, incision, or river maintenance issues. Where agg/deg line cross sections were determined from aerial photographs with an estimated underwater prism. The underwater prism was estimated using the measured water surface elevation and the flow on the date the aerial photograph was taken using HEC-RAS' (Baird, pers.comm.). Repeat surveys are implemented along these cross-section lines, as well as bed material samples.

1.3 Subreach Delineation

To analyze the hydraulic trends, the Elephant Butte Reach was divided into six subreaches. Within these subreaches there were no major distinguishing confluence and or structures that were used to delineate the subreaches. While the San Marcial railroad bridge crossing is located at agg/deg line 1702 this was not used to delineate the river into it's subreaches. The subreach definitions of Owens (2012) were adopted

for consistency to delineate the Elephant Butte Reach into it's respective subreaches. The cumulative plots of hydraulic variables such as channel top width and flow depth were used to cross check Tracey Owens (2012) report. Subreaches were designated when there was a noticeable change in the slope of the cumulative plots. All cumulative plots used in the delineations can be found in Appendix A. These plots were developed using a HEC-RAS model with the 2002 and 2012 geometry provided by the USBR. A flow of 3,000 cfs was selected for cumulative plots of hydraulic variables to be consistent with previous reach reports (LaForge et al., 2019; Yang et al., 2019; Beckwith et al., 2020; Schied et al. 2022). While in 2012, 3,000 cfs isn't the nominal discharge that achieve bankfull discharge for the Elephant Butte Reach (Figure 72), it was chosen to be consistent with previous reports and a good median approximate for overbanking through time. The daily percent exceedance for 3,000 cfs is approximately 4.8% at USGS 08358400 Rio Grande Floodway at San Marcial, NM gage located in subreach EB3. A downstream boundary condition slope of 0.0007 was selected based on the average slope of the reach as a whole.

Figure 3 shows the cumulative width analysis to delineate the Elephant Butte Reach into its respective subreaches. Subreach Elephant Butte 1 (EB1) extends from the Bosque Del Apache National Wildlife Refuge (agg/deg line 1637) downstream to where there is a change in slope of cumulative width plot and the river gets narrower (agg/deg line 1672). Subreach EB2 continues from this decrease in slope of cumulative width and ends just before the San Marcial Bridge where the slope of the cumulative width increases (agg/deg line 1696). Subreach EB3 continues until about the end of the large radial bend where the river gets narrower (agg/deg line 1728). Subreach EB4 continues from this location until there is there is an expansion in the river (agg/deg line 1751). Subreach EB5 begins at the expansion of the river and ends where the formal low flow conveyance channel stops (agg/deg line 1794) and the agg/ deg delineation data available from 1962 to 2002 ends. Lastly, subreach EB6, continues from this point (agg/deg line 1794) to the Elephant Butte reservoir (EB-63). The EB reservoir range line naming convention begins in the narrows of Elephant Butte are used to determine the deposition volume of sediment in the reservoir. Subreach six, EB6, is not split up into subsequent subreaches because of an absence of historical cross-sectional data. Therefore, this subreach will be kept together as whole and will only be included where possible in the report when enough data is available for comparison. The subreaches are shown in Figure 4 through 6. The subreach delineation is summarized in Table 1. Aerial images with every agg/deg line labeled are included in Appendix A. Tracey Owen's (2012) delineation can be seen in Figure A-14.

Table 1 Elephant Butte Subreach Delineation

Elephant Butte Reach			
Subreach	Agg/Deg Lines	Length (Miles)	Justification
EB1	1637-1672	3.3	Start: Southern Boundary of Bosque Del Apache New Mexico End: Marks a decrease in slope of cumulative width plot
EB2	1672-1696	2.3	Start: Marks a decrease in slope of the cumulative width plot End: Marks an increase in slope of the cumulative width plot
EB3	1696-1728	3.1	Start: Marks an increase in slope of the cumulative width plot End: Marks a decrease in slope of the cumulative width plot
EB4	1728-1751	2.2	Start: Marks a decrease in slope of the cumulative width plot End: Marks an increase in slope of the cumulative width plot
EB5	1751-1794	4.5	Start: Marks an increase in slope of the cumulative width plot End: Previous temporary outfall of the low-flow conveyance channel
EB6	1794-EB-63	23.4	Start: Previous temporary outfall of the low-flow conveyance channel End: Beginning of Elephant Butte Reservoir

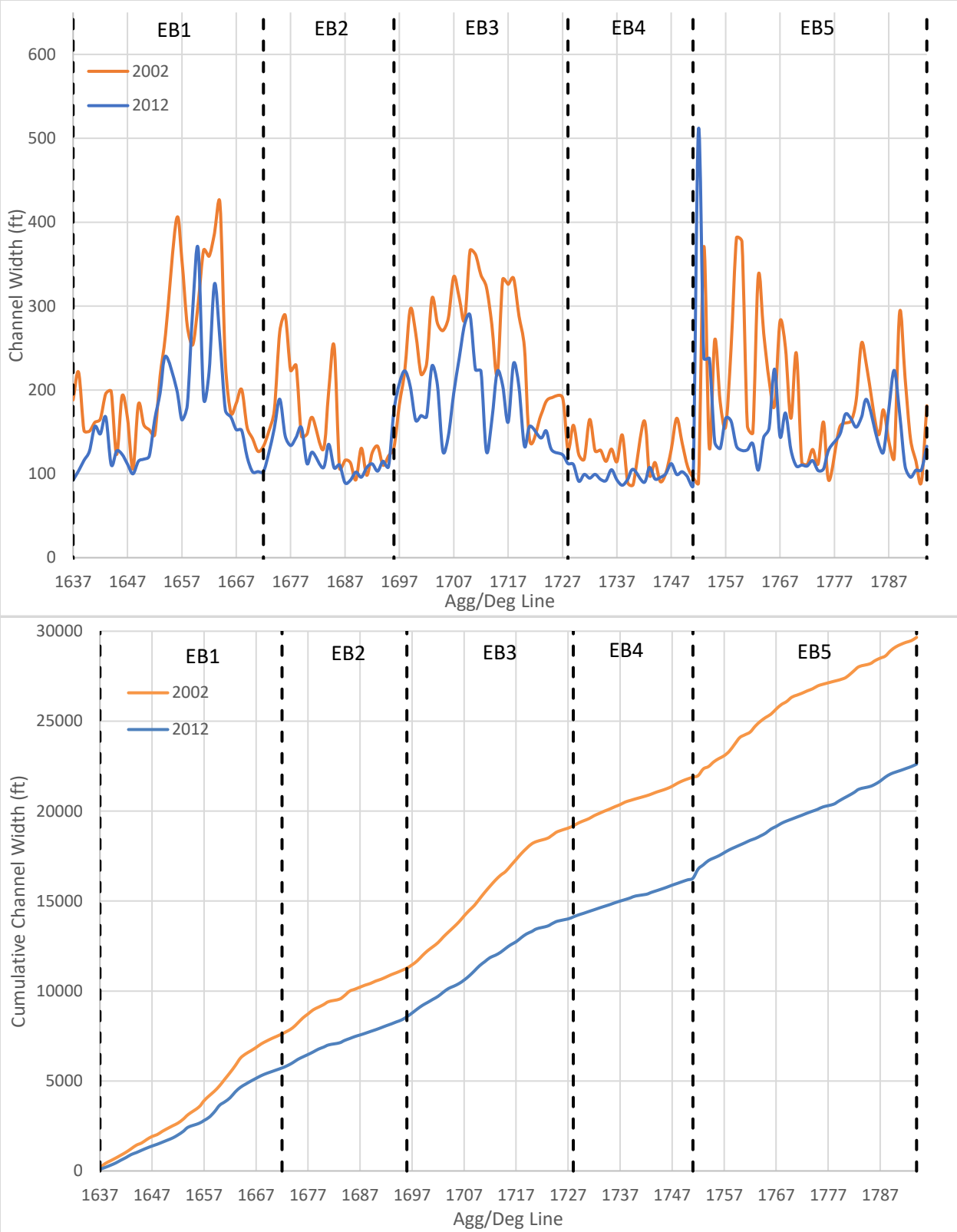

Figure 3 Width (top) and cumulative width (bottom) throughout the Elephant Butte Reach for the years 2002 (orange) and 2012 (blue).

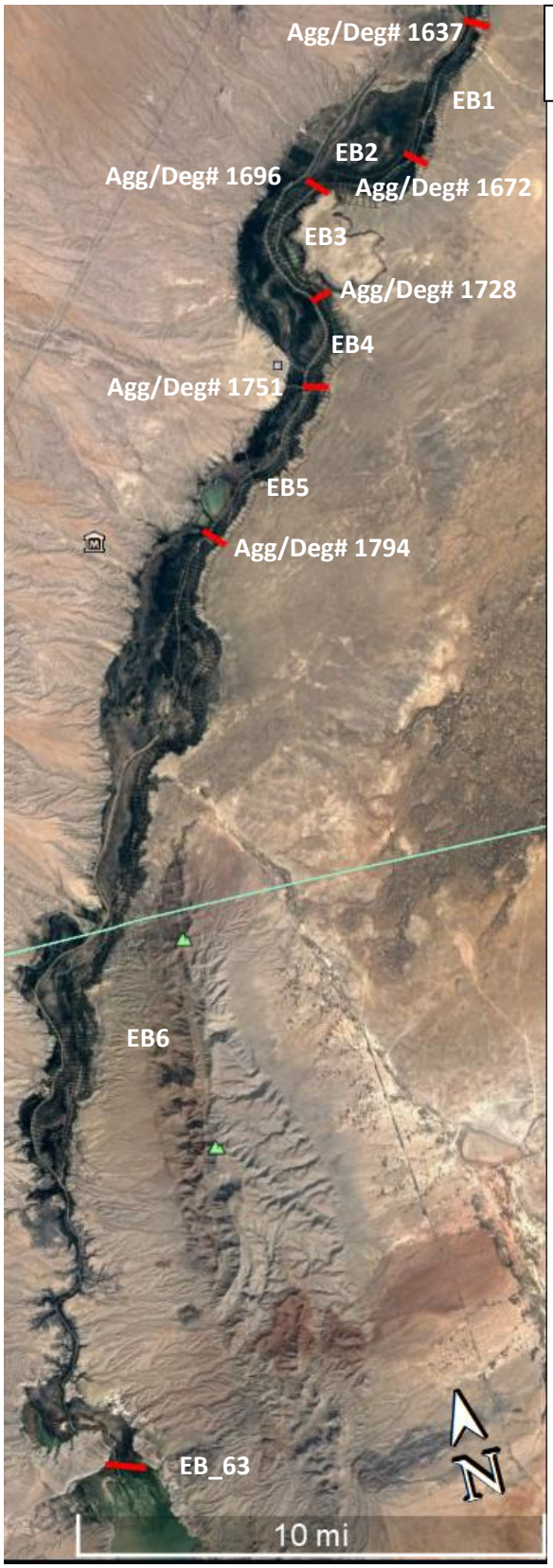

Figure 4 Overall Elephant Butte Subreach Delineation

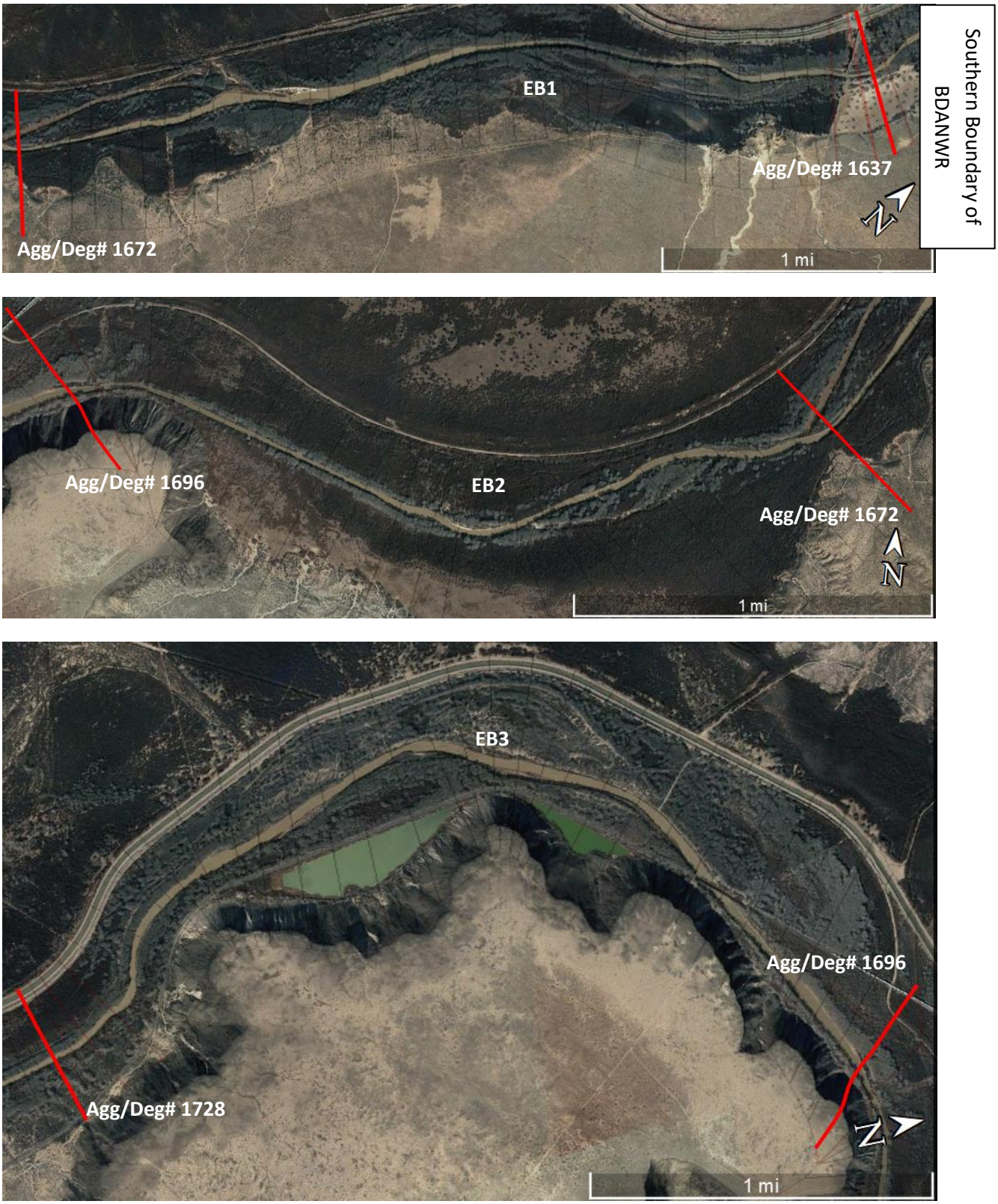

Figure 5 Subreaches EB1 through EB3 Delineation Magnified

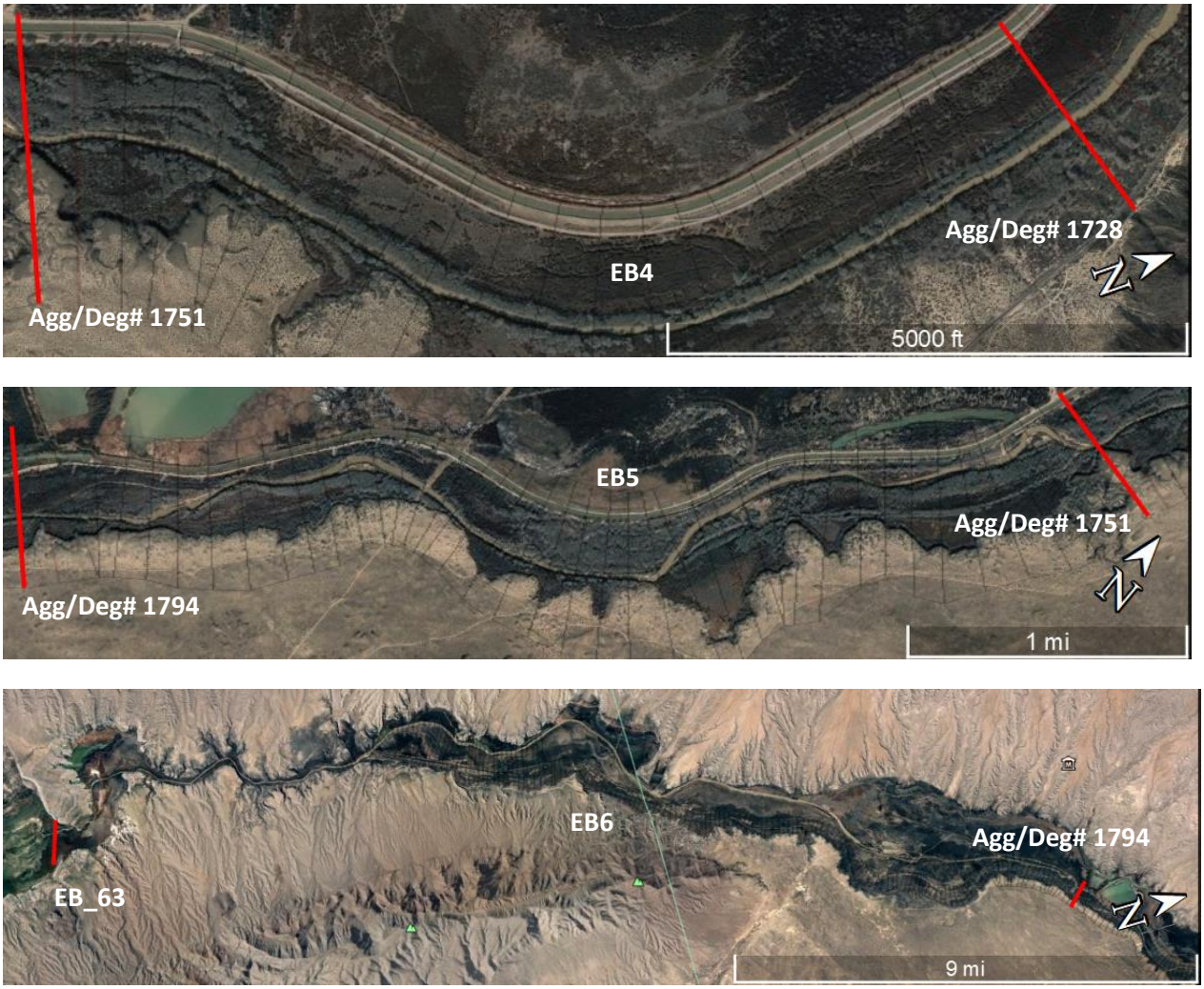

Figure 6 Subreach EB4 through EB6 Delineation Magnified

2. Precipitation, Flow and Sediment Discharge Analysis

2.1 Precipitation

Precipitation data is collected along the MRG by the Bosque Ecosystem Monitoring Program from University of New Mexico (BEMP Data, 2017). The locations of the data collection are shown in Figure 7. The Sevilleta site is near the San Acacia Diversion Dam, the Lemitar site is North of Escondida just outside of Lemitar, and the Mesilla site is just outside of Las Cruces, New Mexico. These three sites were used in the precipitation analysis.

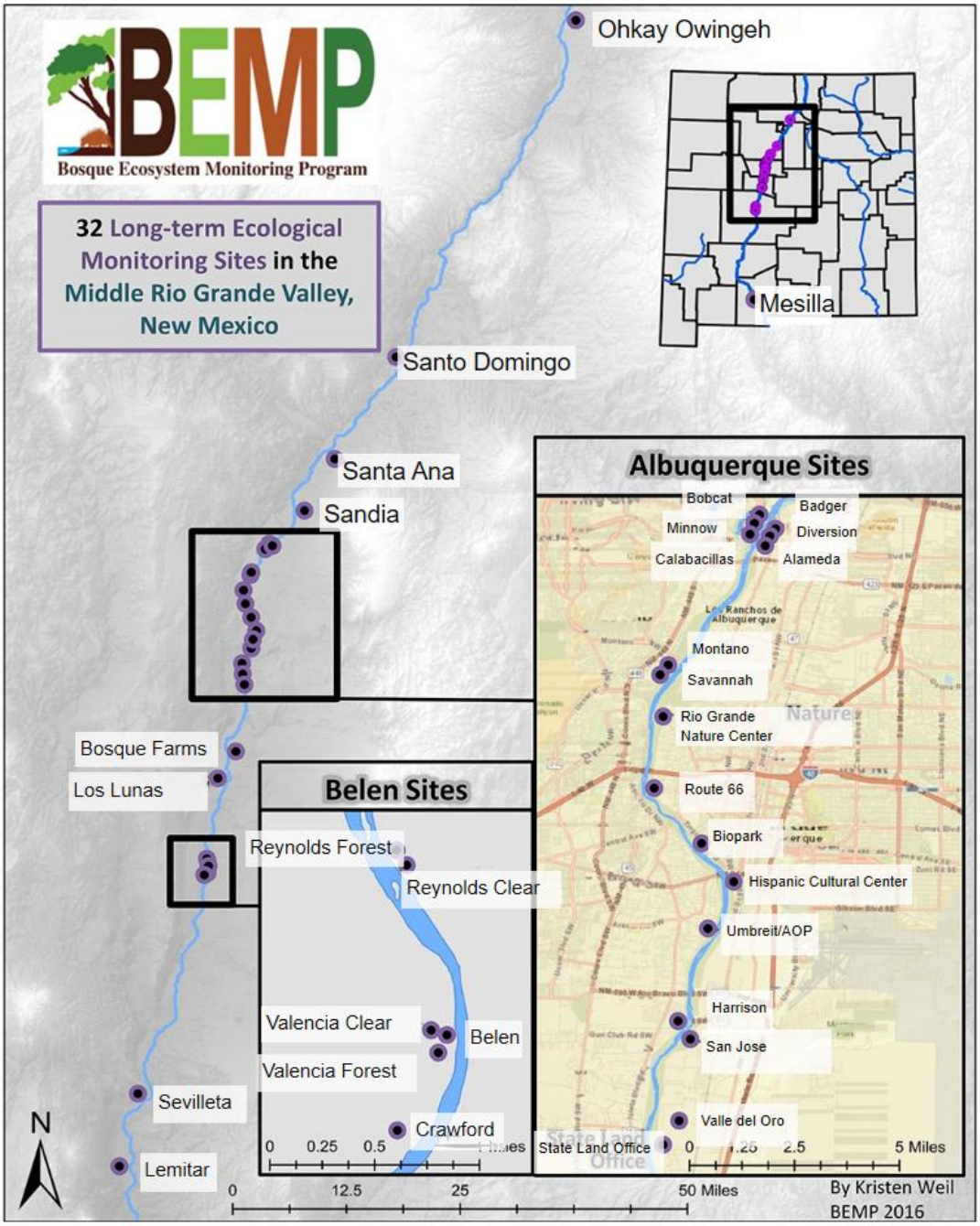

Figure 7 BEMP data collection sites (figure source: http://bemp.org)

The precipitation data are shown in Figure 8. The highest precipitation peak occurred in August of 2006 at the Lemitar gage, with 5.5 inches of rainfall. A general trend was observed with highest precipitation values occurring during monsoon season (late July through early September). A cumulative plot of rainfall (Figure 9) shows that individual rain events can greatly affect the overall trend of the data. It further highlights the monsoonal rains, which create a "stepping" pattern with higher rainfall in August and September, and lower levels throughout the rest of the year. The comparison of the cumulative precipitation at the three sites also shows that the Lemitar gage recieves more precipitation than the Sevilleta and the Mesilla gages throughout the time observed.

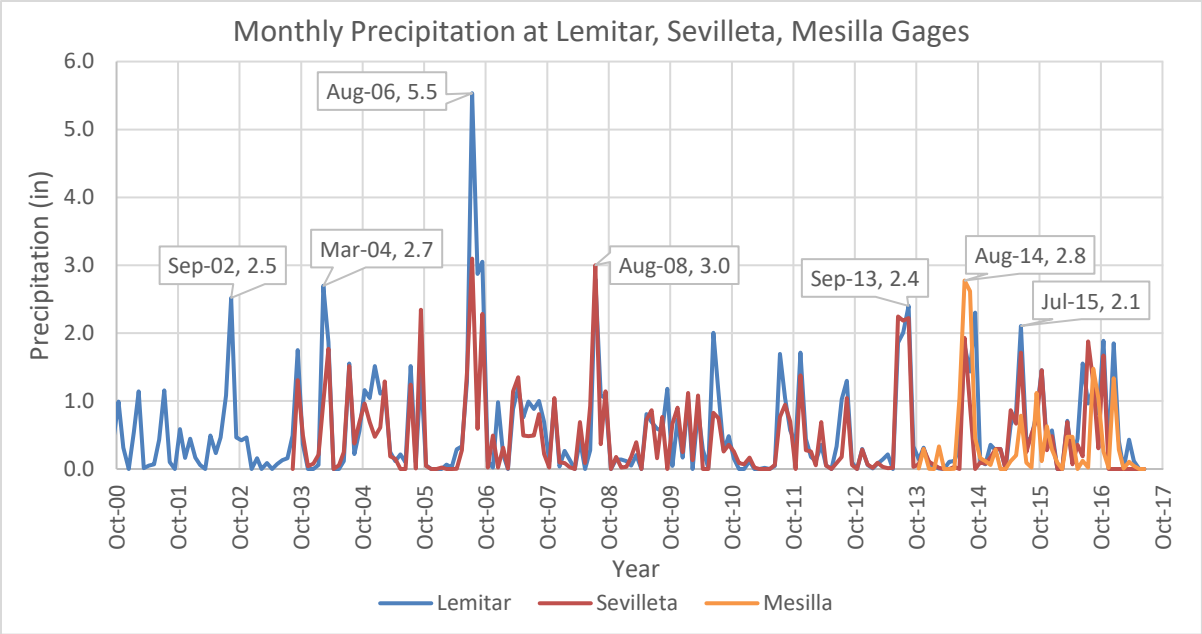

Figure 8 Precipitation near the Elephant Butte Reach over time

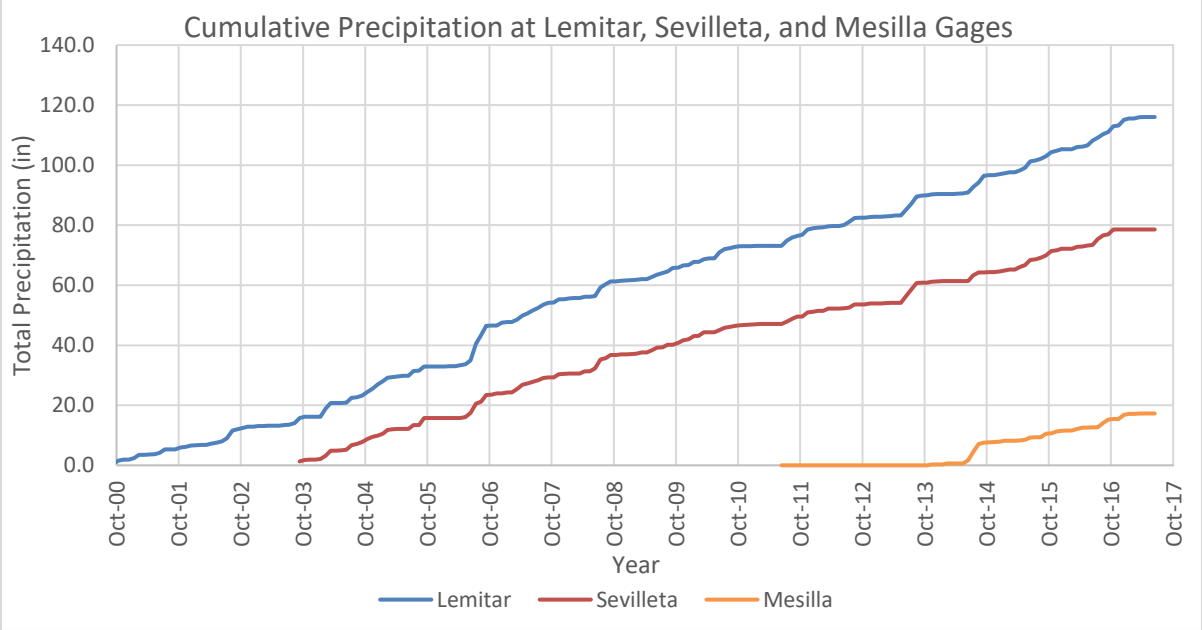

Figure 9 Cumulative precipitation near the Elephant Butte Reach

2.2 River Flow

Information regarding river flow was gathered from the United States Geological Survey (USGS) National Water Information System. The gages in the area relevant to the study are included in Table 2.

Table 2 List of gages used in this study

Station	Station Number	Mean Daily Discharge	Suspended Sediment
Rio Grande Floodway at San Marcial	08358400	October 1, 1949 to present	October 1, 1956 to September 30, 2019
Rio Grande at Narrows in Elephant Butte Reservoir, NM	08359500	April 1, 1951 to September 29, 1957 May 21, 2012 to May 25, 2021	No data
Rio Grande above US HWY 380 near San Antonio, NM	08355490	September 30, 2005 to present	October 1, 2011 to September 30, 2018
Rio Grande at San Marcial, NM (Inactive Site)	08358500	January 1, 1899 to September 29, 1964 Intermittently	July 1, 1946 to July 31, 1947
Rio Grande Conveyance Channel at San Marcial, NM	0835300	December 1, 1951 to present	October 1, 1955 to August 29, 1994

The gage at San Marcial (08358400) is located below Bosque Del Apache National Wildlife Refuge (beginning of subreach EB3) and has the longest record for both the mean daily discharge and suspended sediment. The raster hydrographs of the daily discharge at the Rio Grande at San Marcial (08358500), Rio Grande Floodway at San Marcial (08358400), US HWY 380 near San Antonio (08355490), and Rio Grande at Narrows in Elephant Butte Reservoir (08359500) gages are shown in Figures 10, 11, 12, and 13 respectively. The raster hydrograph from the inactive site at San Marcial (08358500), which only recorded data between 1899 and 1964, is shown in Figure 10.

The figures show seasonal flow patterns, with peak flow often occurring from snowmelt runoff April through June, low flow throughout the rest of the summer (except for strong summer thunderstorms), and medium flow from November onwards representing the end of the irrigation season. It can be seen in Figure 11, at the Rio Grande Floodway at San Marcial there was a 15-year drought between 1960 and 1975. This lack of water can also be attributed to a Low Flow Conveyance Channel diverting the water away from the main channel.

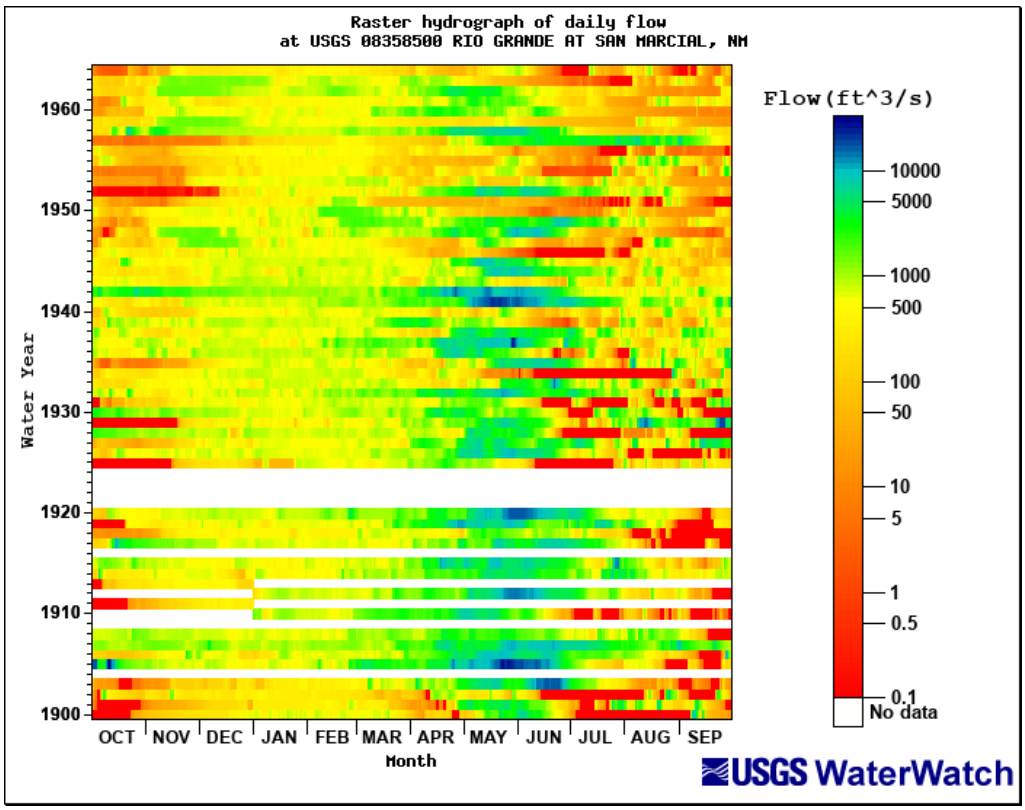

Figure 10 Raster hydrograph of daily discharge at USGS 08358500 Rio Grande at San Marcial, NM

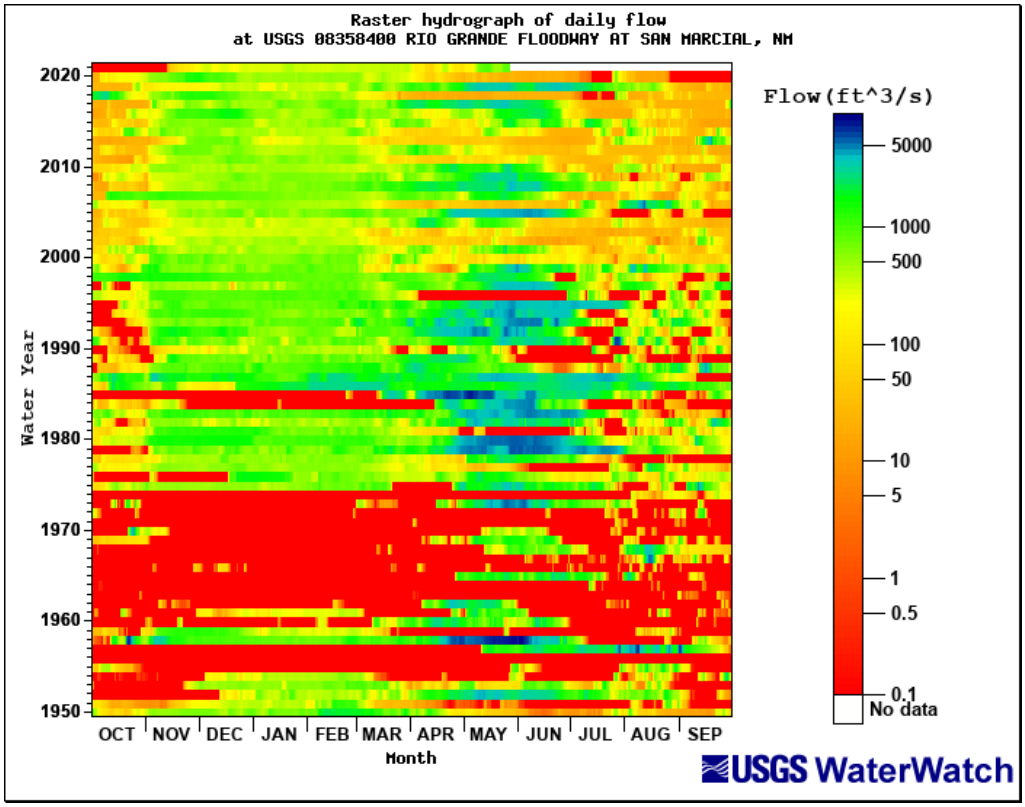

Figure 11 Raster hydrograph of daily discharge at USGS 08358400 Rio Grande Floodway at San Marcial, NM

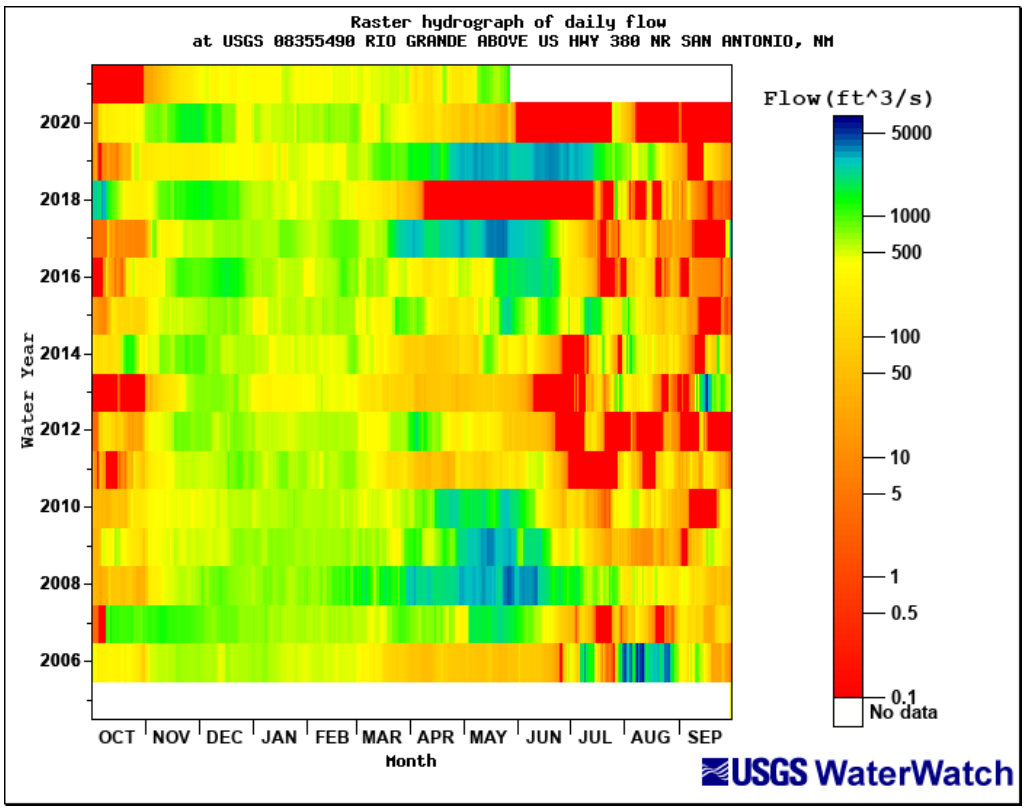

Figure 12 Raster hydrograph of daily discharge at USGS Station 08355490 near San Antonio, NM

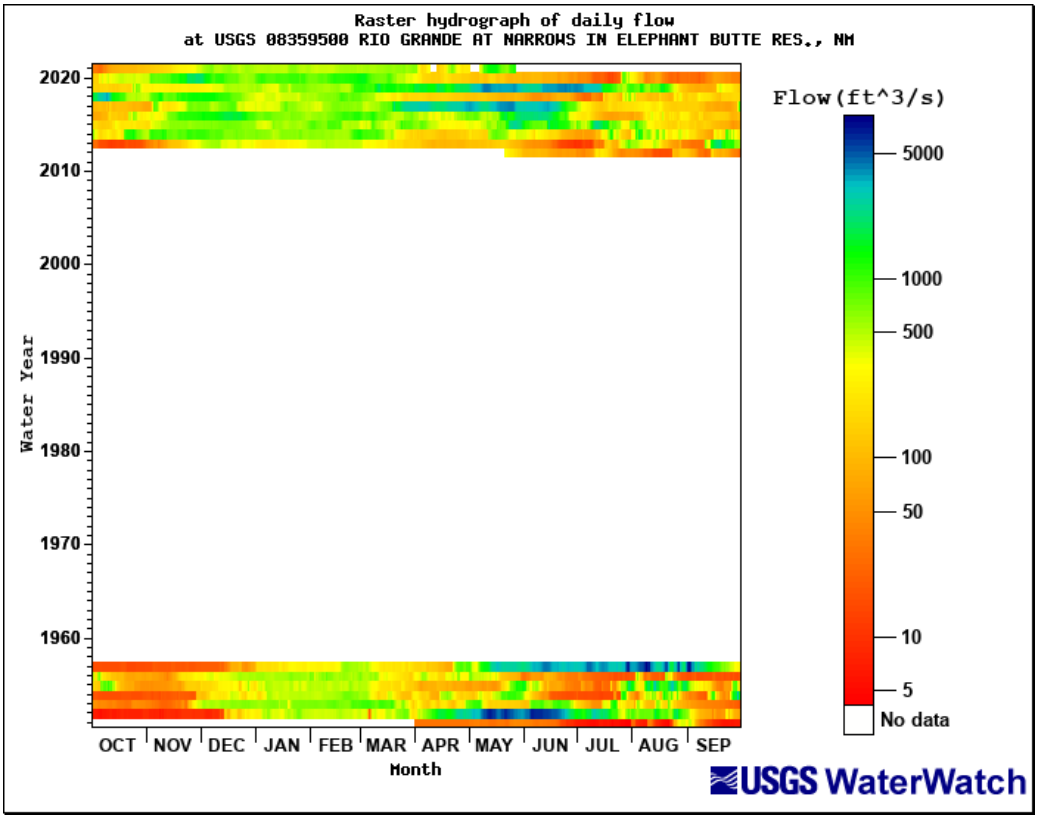

Figure 13 Raster hydrograph of daily discharge at USGS Station 08359500 at Narrows In Elephant Butte, NM

2.2.1 Cumulative Discharge Curves

Cumulative discharge curves show changes in annual flow volume over a given time period. The slope of the line of the mass curve gives the mean annual discharge, while breaks in the slope show changes in flow volume. Figure 14 shows the mass curves of the gages near San Marcial and HWY 380 near San Antonio. While the San Marcial gage has a longer period of data, the single mass curve comparison between San Marcial and San Antonio gages start in 2005 for a fair comparison between the two gages. A one-week moving average was used to determine significant breaks in slope. The data callout points are dates labeled on the figures below which represent changes in slope that were greater than the 97.5th percentile of moving-average slope values. This helps to depict the times in which the greatest increase in cumulative discharge occurred. These large increases typically occur between April and June (likely from snowmelt), although noticeable increases can also occur in late August or September from seasonal thunderstorms.

Figure 14 also includes a single mass curve from the gage locate at San Marcial, NM to show the full historic trends of the discharge in the Elephant Butte Reach. This gage has data for a much longer period of record which can help in identifying long term trends. The single mass curve was developed from 1949 which is before the installation of the Cochiti Dam in 1975. Based on the San Marcial's single mass curve, there were a few periods where the discharge volume in the river was higher, such as in the mid to late 1950s, late 70's, mid to late 80's, early to mid-90s, and smaller local increases in 2005 and 2019. Given the longer time period analyzed, the detail for many specific events becomes harder to analyze due to their decrease in magnitude over the whole time period. However, a sharper increase in the cumulative discharge in 2017 and 2019 is present, which was also seen in the Elephant Butte and San Antonio gages. The top graph of Figure 14 shows this in more clarity due to the interval of time presented only starting in 2005. Similarly, the cumulative discharge plots at the gages in the Elephant Butte Reach, the steeper slopes at the San Antonio and San Marcial gages often occur in the spring months, indicating that snowmelt may have the greatest impact on the Middle Rio Grande's discharge.

Figure 15, relates the cumulative precipitation and cumulative monthly discharges, can further demonstrate the time periods that experience higher discharges. A steeper slope indicates that the discharges are increasing with relatively little precipitation. This increase in slope is from spring runoff and could possibly be from regulation structures releasing water. As seen in Figure 14, there are several noticeable increases in cumulative discharge in October and November. This occurrence is likely due to the end of the irrigation season and the drying out of all the irrigation infrastructure that would otherwise be utilizing their allocated water.

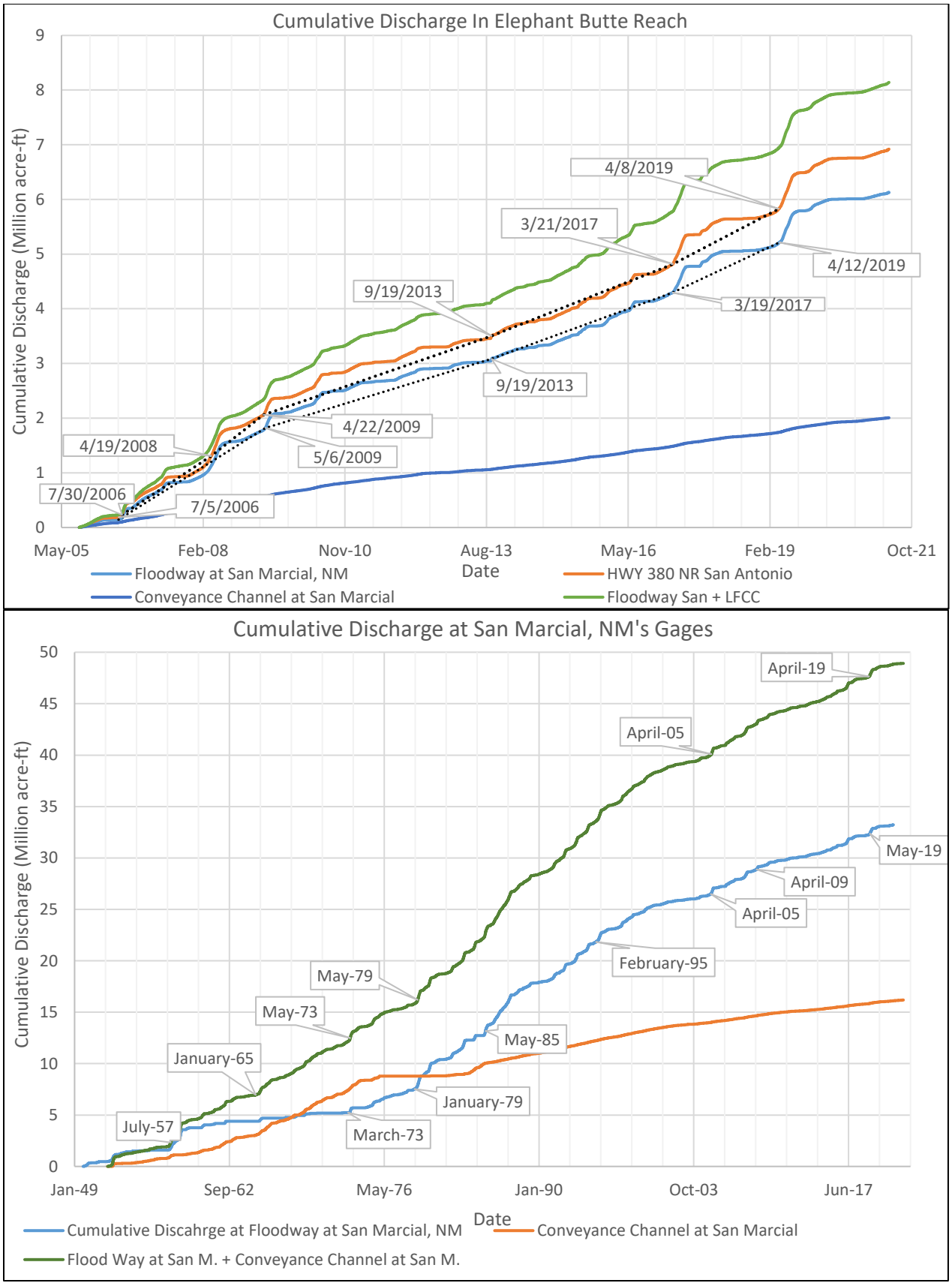

Figure 14 Discharge single mass curve of the San Marcial gages and HWY 380 NR San Antonio gage (top) and San Marcial gages (bottom)

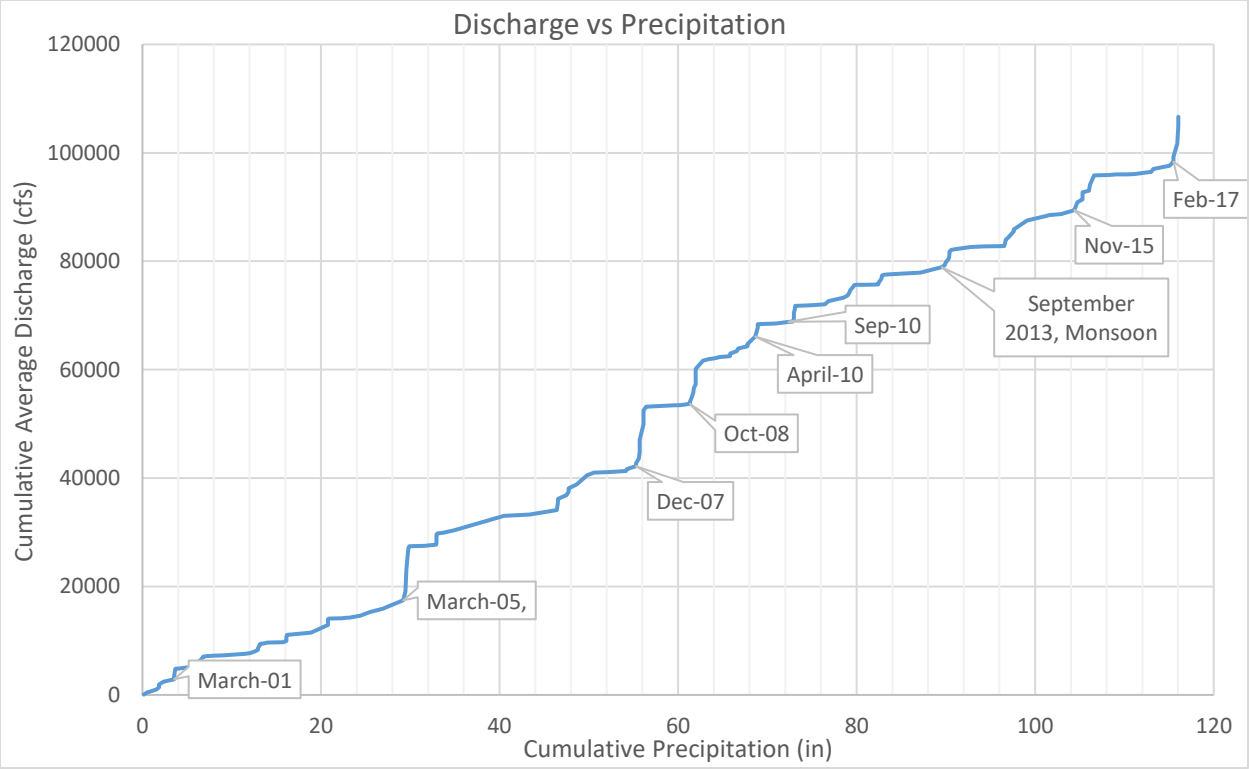

Figure 15 Cumulative discharge plotted against cumulative precipitation at the USG Floodway at San Marcial, NM

2.2.2 Flow Duration

Flow duration curves were developed using the mean daily flow discharge values for the Floodway at San Marcial (years 1949 to 2021) and Narrows at Elephant Butte Reservoir (years 1951 to 2021) and for the San Antonio (years 2005 to 2021) gages. The exceedance probability curves are shown in Figures 16 and 17. Table 3 shows exceedance values calculated from the flow duration curves. The values for the San Marcial gage are very low for the greater exceedance probabilities, showing that there were a larger number of low flows and no flows that were measured.

Table 3 Probabilities of Exceedance

	Daily Discharge (cfs)			**Annual Peak Discharge (cfs)**
Probability of Exceedance	08358400 Rio Grande Floodway at San Marcial, NM (October 1, 1949 – May 25, 2021)	08359500 Rio Grande at Narrows in Elephant Butte Reservoir, NM (April 1, 1951 – May 25, 2021)	08355490 Rio Grande Above US HWY 380 NR San Antonio, NM (September 30, 2005 – May 25, 2021)	08358400 Rio Grande Floodway at San Marcial, NM (October 1, 1949 – May 25, 2021)
1%	4926	4483	3739	12144
10%	1870	1449	1602	6216
25%	775	681	723	4880
50%	232	330	461	3230
75%	0.009	100	82	1860
90%	0.004	29	4	732

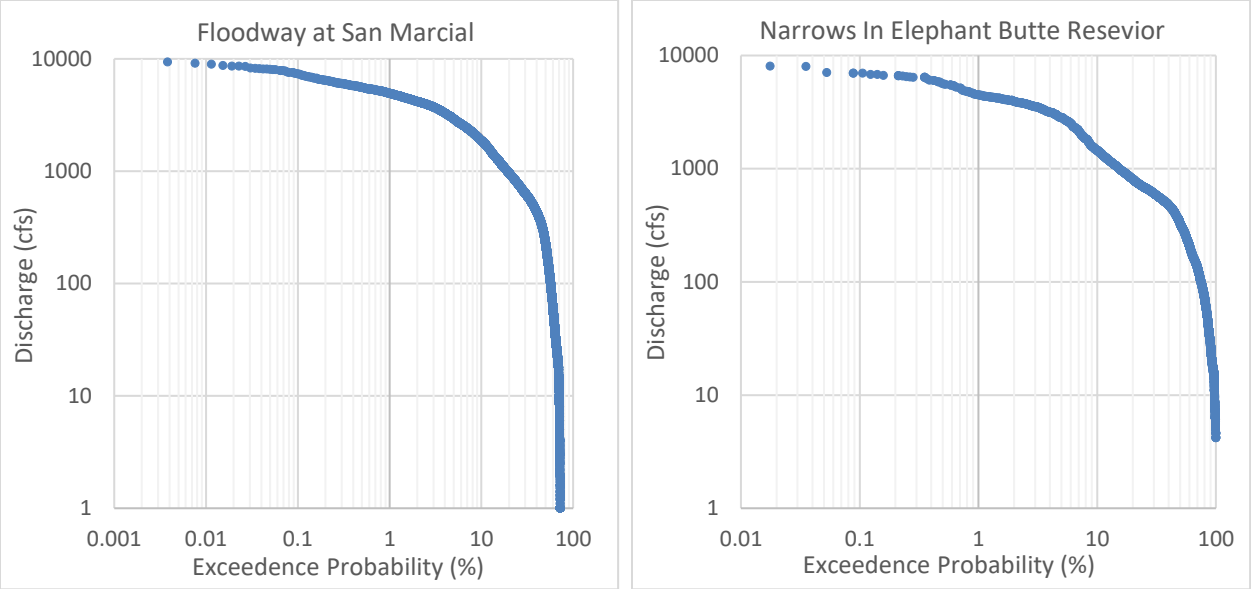

Figure 16 Flow Duration Curve for USGS Gage 08358400 Rio Grande Floodway at San Marcial, NM (left) and USGS Gage 08359500 Rio Grande at Narrows in Elephant Butte Reservoir, NM (right) using the mean daily flow discharge values.

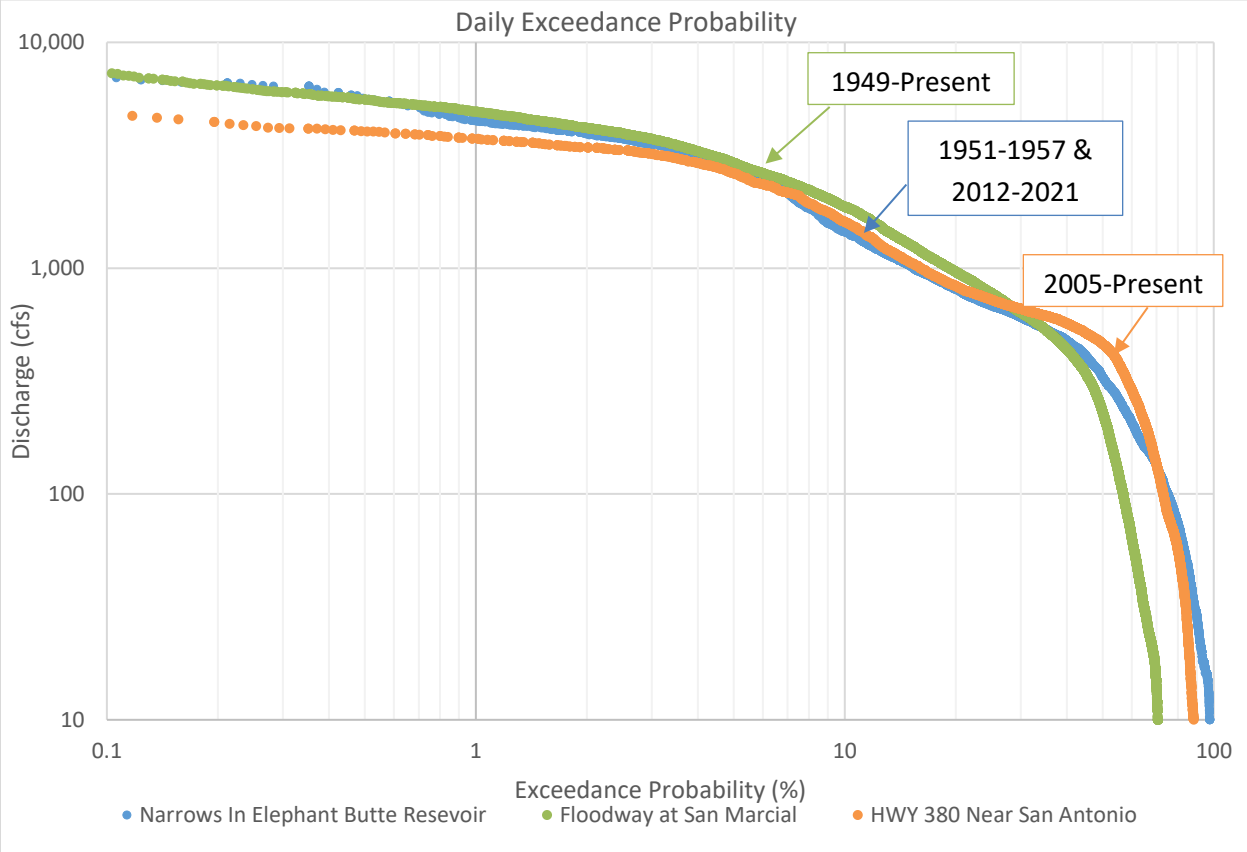

Figure 17 Comparison of flow duration curves. The Elephant Butte, Floodway at San Marcial, HWY 380 Gages include data starting from the years 1951, 1949, and 2005 respectively.

Figure 18 displays exceedance probability of the annual peak discharge at the San Marcial Floodway. The annual peak discharge exceedance probability is helpful to show what the return period for different maximum discharges are. These peak flows in the Elephant Butte Reach are important for inundation of the floodplain and ultimately allow for the Rio Grande Silvery Minnow fish habitat to be available.

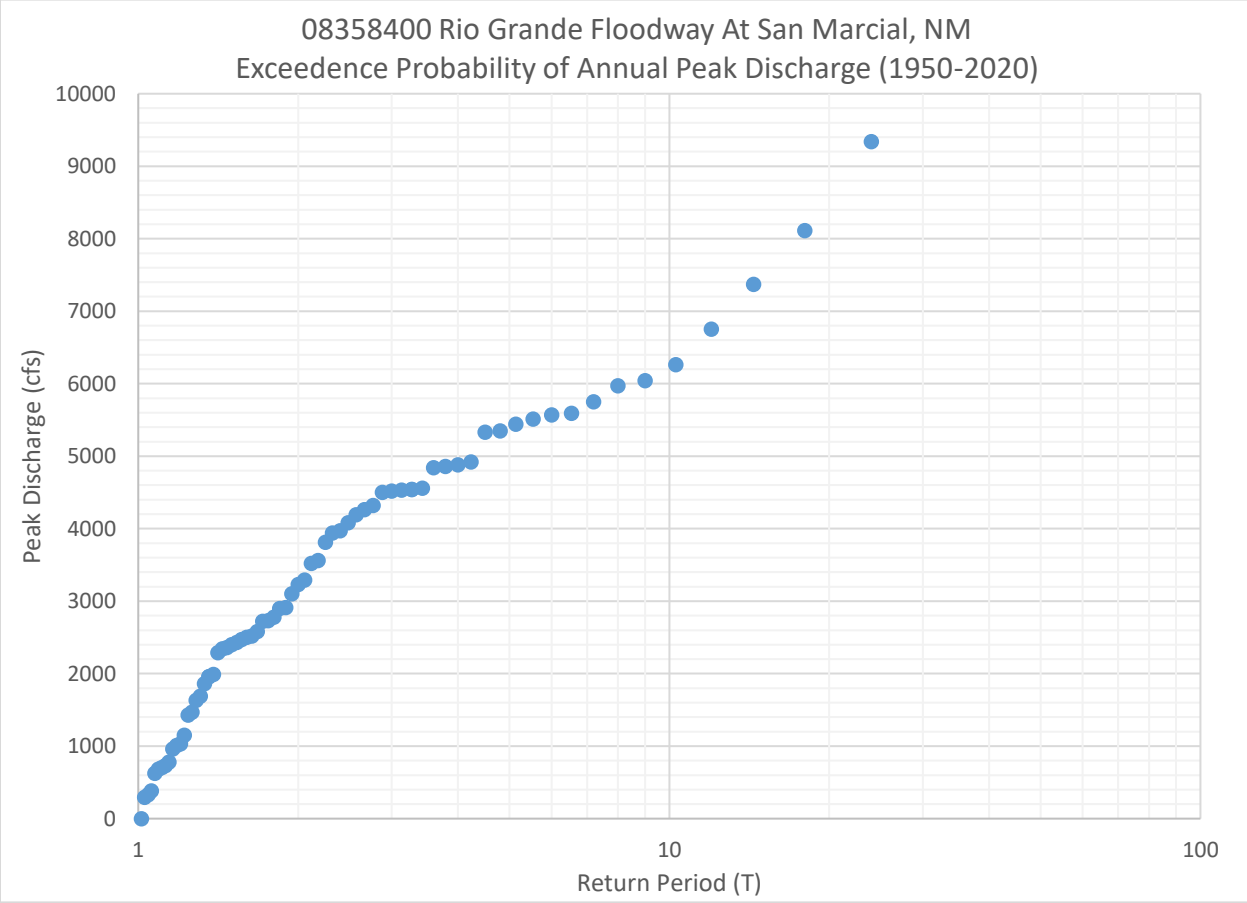

Figure 18 Flow Duration Curve for USGS Gage 08358400 Rio Grande Floodway at San Marcial, NM using the maximum yearly discharge values.

Figure 19 is a simple bar graph of the yearly peak discharges available across the different flow gages. For the available data, the HWY 380 Near San Antonio and the Narrows in Elephant Butte gages have had higher discharges then both San Marcial gages. This is due to the water being split between the river and the conveyance channel, decreasing the in-channel flows. After 1980's the conveyance channel was taken offline but still is able to convey water. From 2005 to present the Floodway at San Marcial gage's peaks matches more closely to the rest of the gages. The amount of water that is carried in the conveyance channel decreases after 1975 and stays at lower discharges There is an overall increasing trend of peak flows from 1972 and 2002. This also corroborates the water level rise in the Elephant Butte Reservoir during this period in Section 3.8.

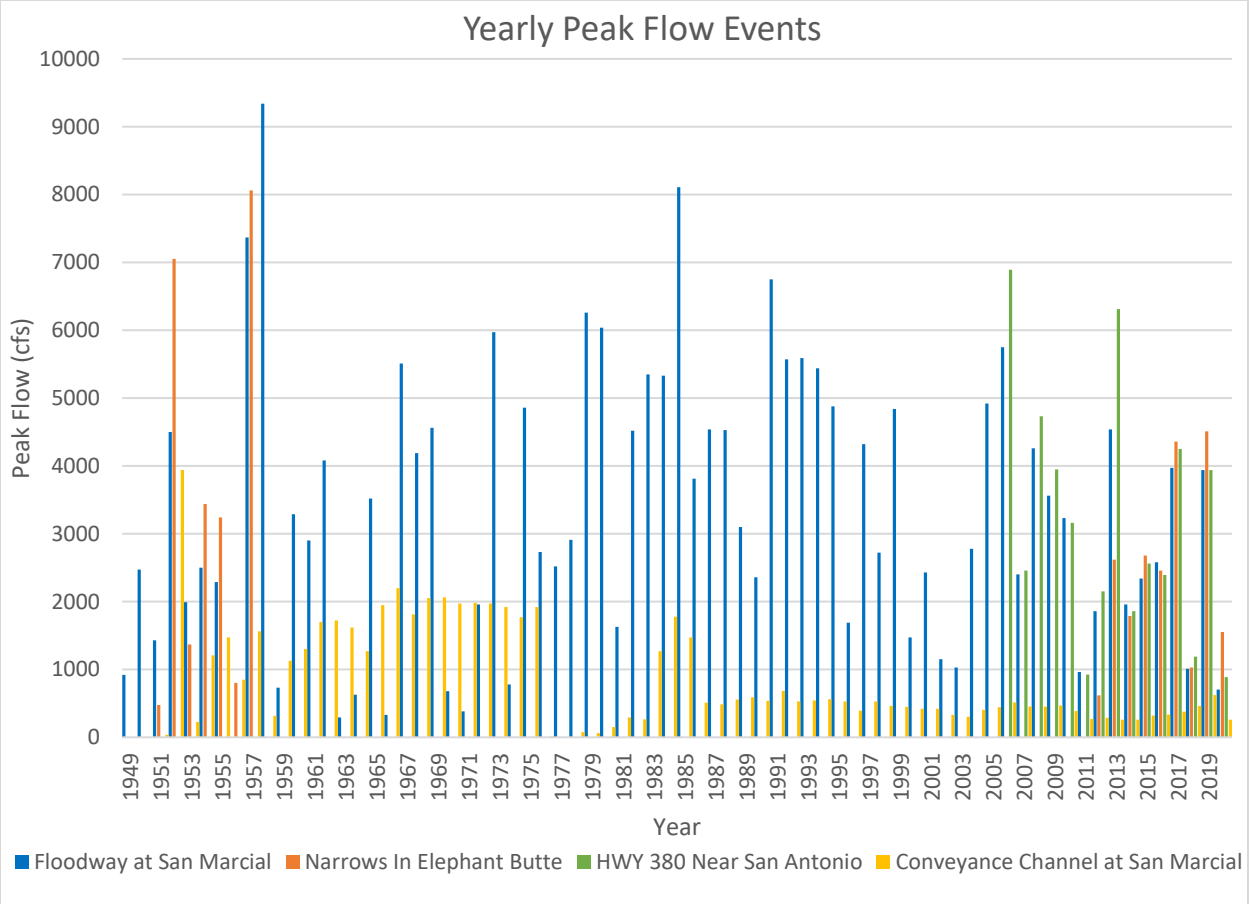

Figure 19 Yearly Peak Flow Events

In addition to flow duration curves, the number of days in the water year exceeding specified flow values at each gage was analyzed. Where the white space on the figure indicates the number of days that did not exceed any of the values tested. This analysis is a count of days in which the flow exceeds a threshold flow level within each water year. The analysis was performed for the entire record for both the San Marcial and Elephant Butte gages and was corrected to be fitted to a water year. Figure 20, 21, and 22 show a period of lower flow from 2011 to 2014. Figure 21 shows a small increase in the number of high flow days 2017 and 2019. The river had the greatest number of low flow days in 2002, 2003, 2011 to 2014 (not exceeding 500 cfs). In 2017 and 2019 the river had a few days that achieved a flow rate of 3,000 cfs. These high outlier values are associated with a monsoonal storm event that occurred in September of 2013 (Pinson, et. al, 2014). The remnants of the two hurricanes pushed warm humid air north, which clashed with a cold front, resulting in heavy rainstorms throughout Colorado and New Mexico (Pinson et al., 2014). Figures 20, 21, 22 show the Rio Grande ‘s flow has been decreasing and becoming drier since 1995. It can be seen in Figure 20 that in more recent years that the river has decreased in number of high flow days year-round. It is rare to have multiple days where the flow reading is above 4,000 cfs in present day. There are months that can be seen that have no flow present in the channel. The cumulative discharge plot’s slope, Figure 14, decreases around 1995.

Figure 22 and 24 shows the whole data record of both Elephant Reservoir and US 380 gage data near San Antonio respectively. Through all available data records Figure 20-24 it appears that prior to the Cochiti

dam and operation of the Low Flow Conveyance Channel, there were more days that exceeded 6,000 cfs (or higher discharge values in general).

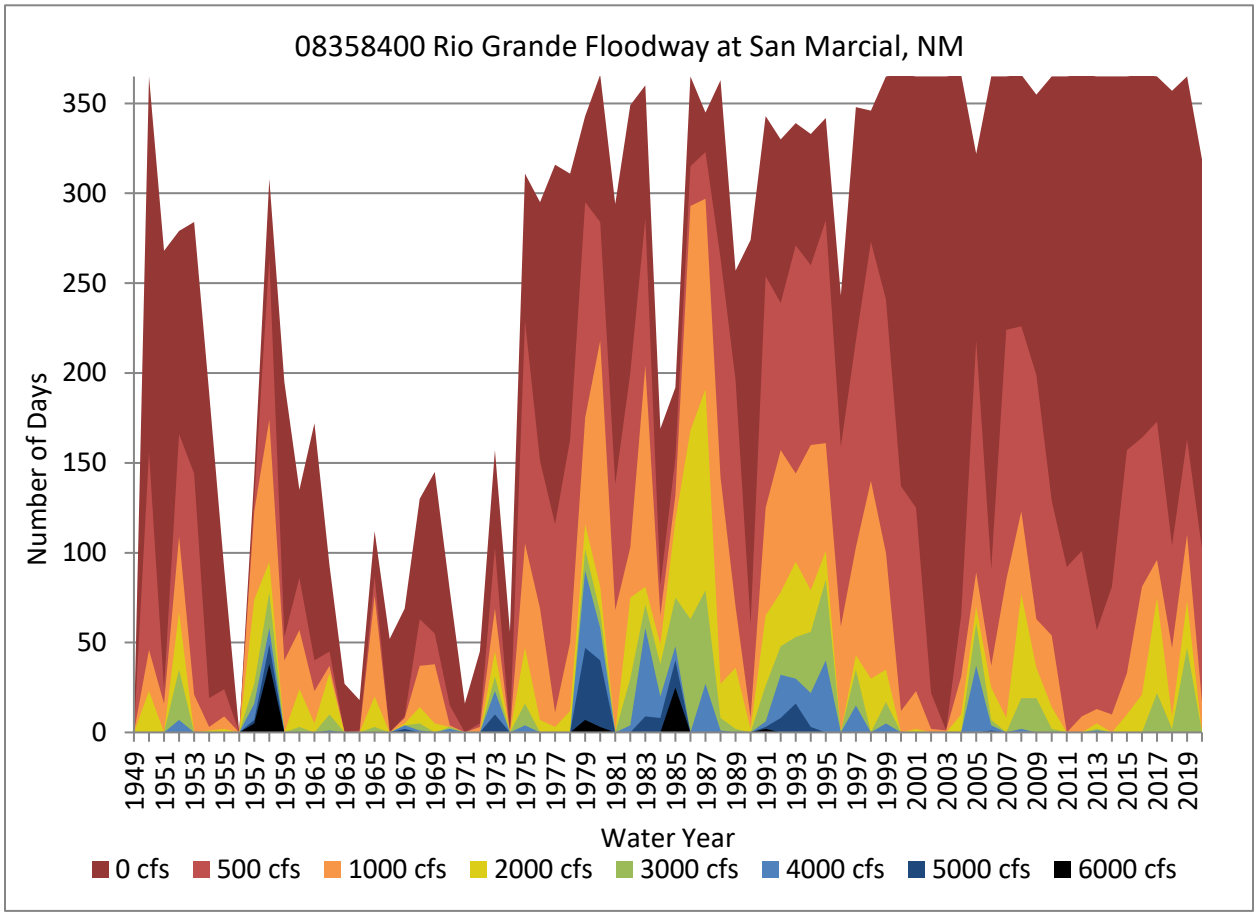

Figure 20 Number of days over an identified discharge at the Floodway at San Marcial gage

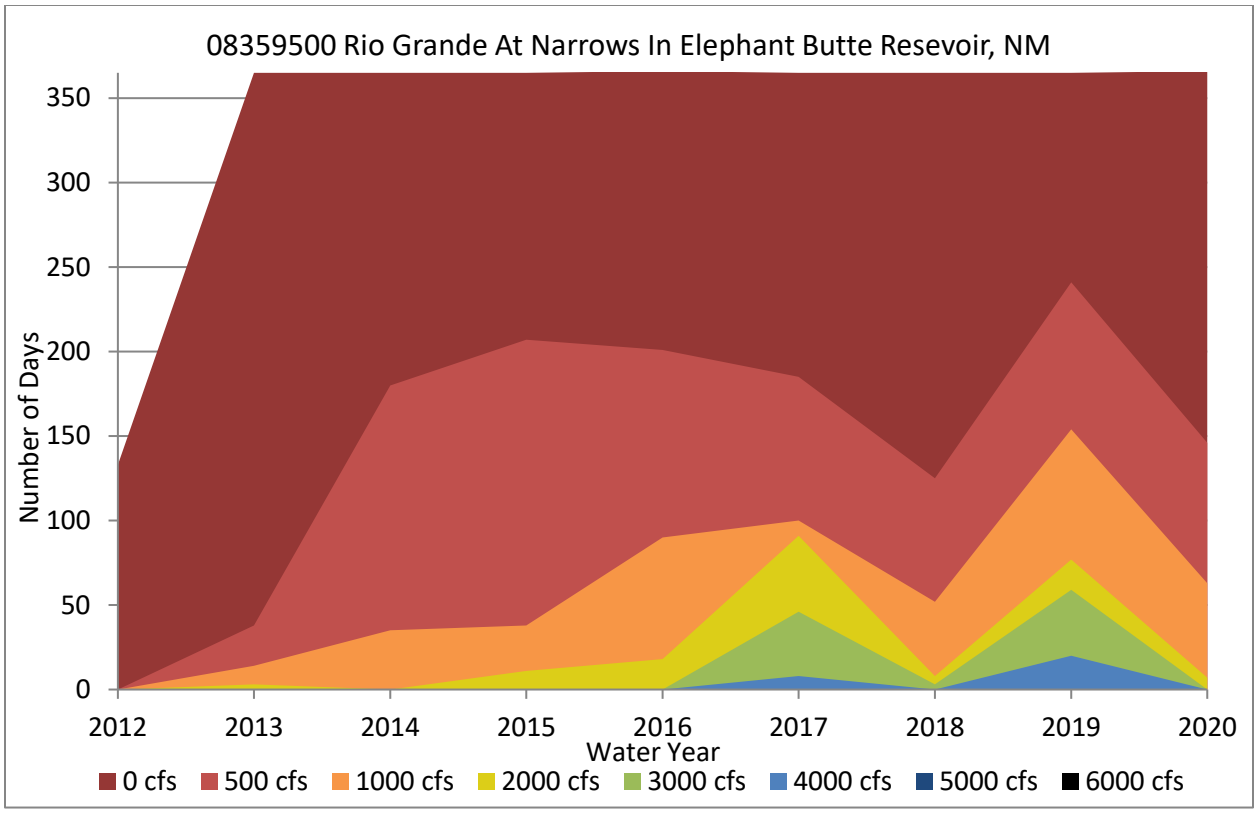

Figure 21 Number of days over an identified discharge at the Narrows in Elephant Butte Reservoir gage

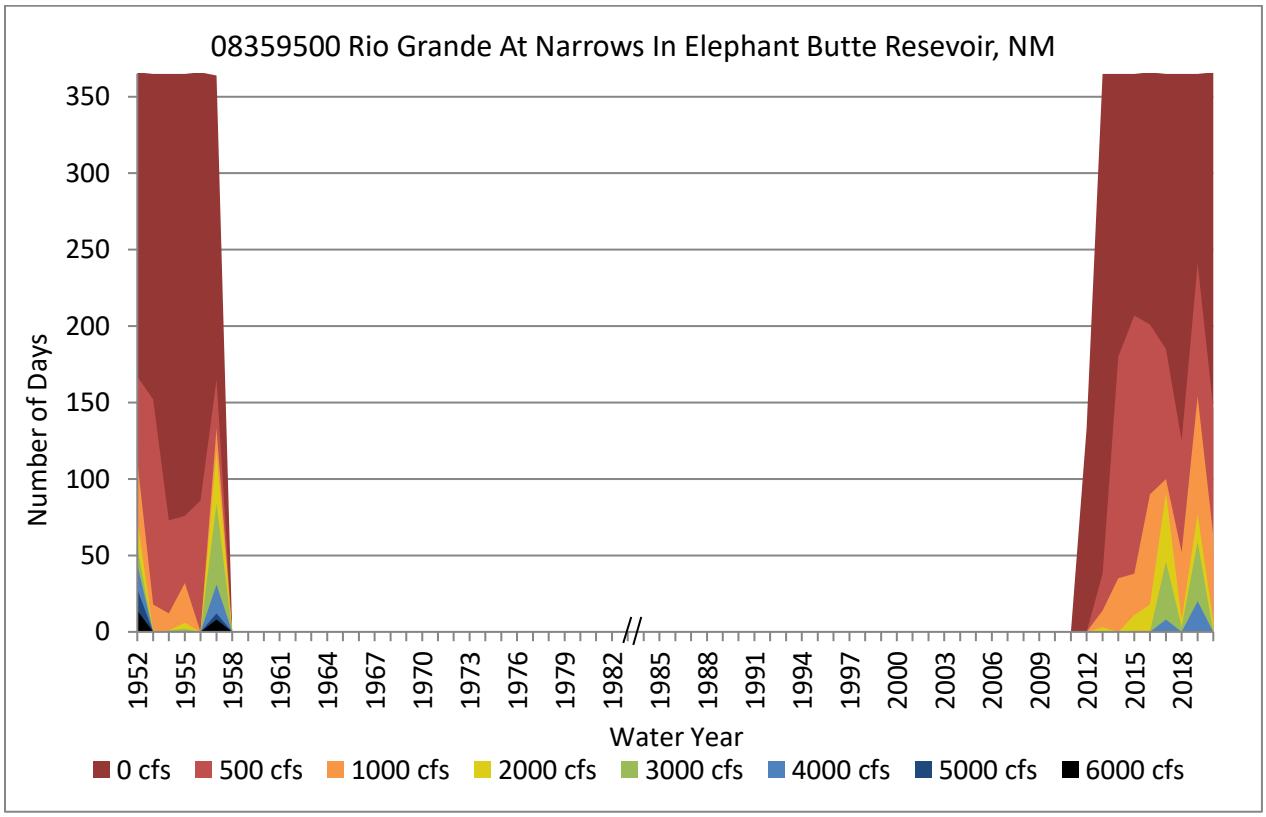

Figure 22 Number of days over an identified discharge at the Narrows in EB Reservoir gage including historical gage data

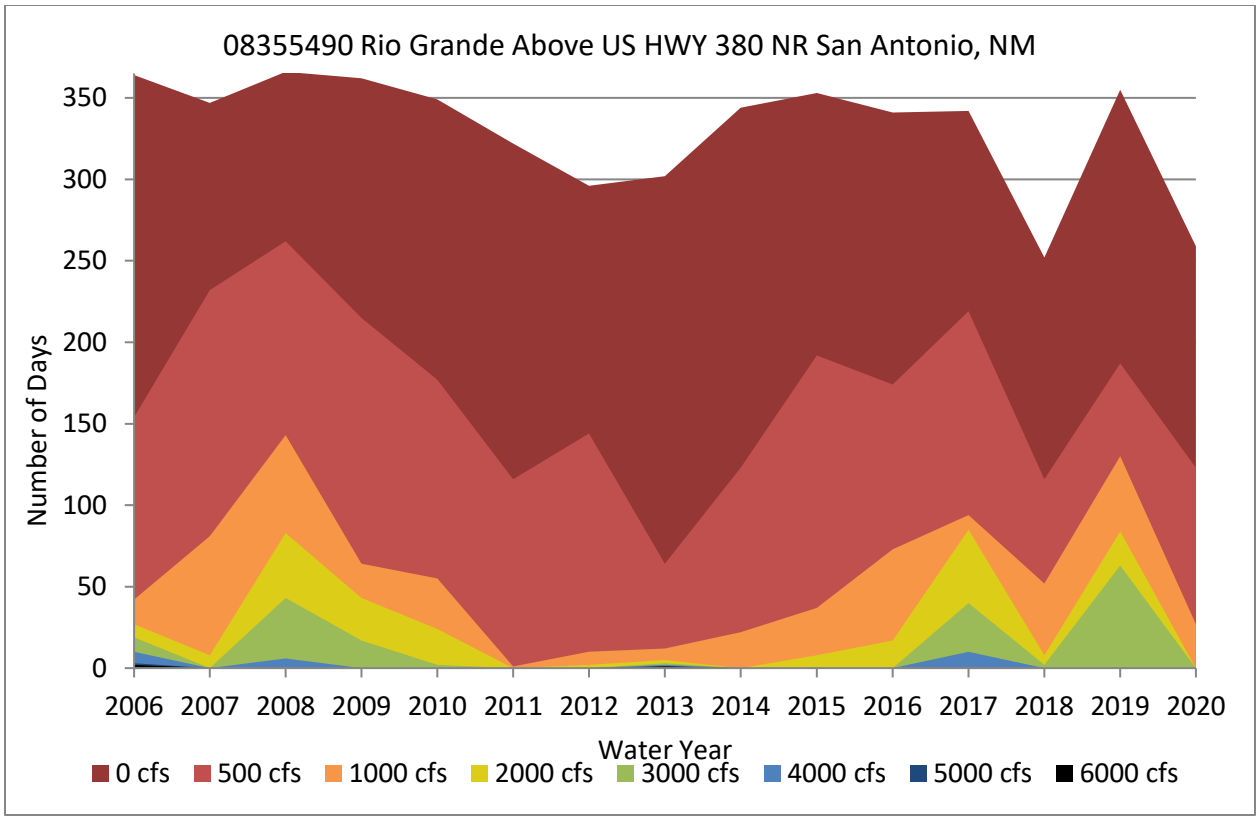

Figure 23 Number of days over an identified discharge above US HWY 380 gage

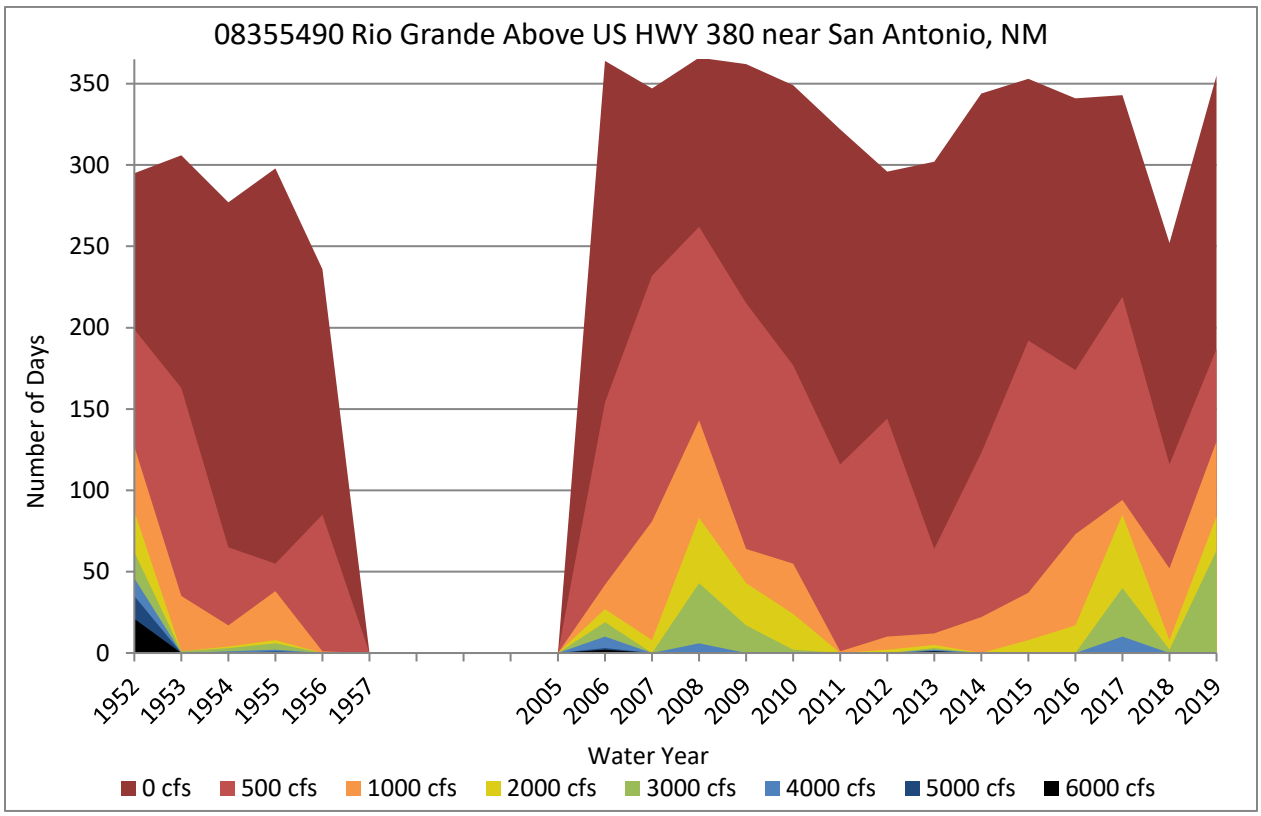

Figure 24 Number of days over an identified discharge above US HWY 380 gage including historical gage data

2.3 Suspended Sediment Load

2.3.1 Single Mass Curve

Single mass curves of cumulative suspended sediment (in millions of tons) at the San Antonio gage and the San Marcial gage are shown in Figure 25. Data comes from the USGS gage near US HWY 380 in San Antonio, NM (08355490) and the USGS gage at the Rio Grande San Marcial Floodway, NM (08355490). There is no sediment data record present for the USGS gage at Elephant Butte Narrows. For the San Antonio single mass curve, the analysis was performed in water years beginning in 2011, when the collection of suspended sediment data began. The dashed line was created using the same technique as the previous cumulative discharge plot by plotting only the inflection points that are greater than the 97.5th percentile of slope changes. A one-week moving average was used to determine the 97.5th percentile of slope changes. If a slope change is greater than this value, a point is created along the line indicating a time with one of the greatest increases in sediment transport.

The breaks in slope along the single mass curve show the changes in sediment flux. As previously determined from the cumulative discharge plot in Section 2.2.1, the large increases in flow in the Elephant Butte Reach occurred in the spring from snowmelt, with some increases in the summer from seasonal thunderstorms. However, the cumulative sediment discharge curve shows that the greatest increases in sediment occur during the monsoonal storms that occur in the summer. The monsoonal event mentioned earlier is seen by the large increase in suspended sediment in September of 2013. The second largest increase in sediment flux occurred as a result of a series of heavy thunderstorms in the summer of 2014. These monsoonal events make the river a very flashy system which allows for large amounts of sediment to be transported. As mentioned in section 1.1, the ephemeral tributaries are the sole source of sediment input into to MRG (Fitzner 2018). Where below the San Acacia dam there are no major tributaries that enter the MRG but there are several small arroyos that enter the river and two flood controlled channels (Towne 2007). Thus, the sediment flux into the river seems to be primarily driven not by snowmelt but rainfall that allows for these arroyos wash sediment into the MRG.

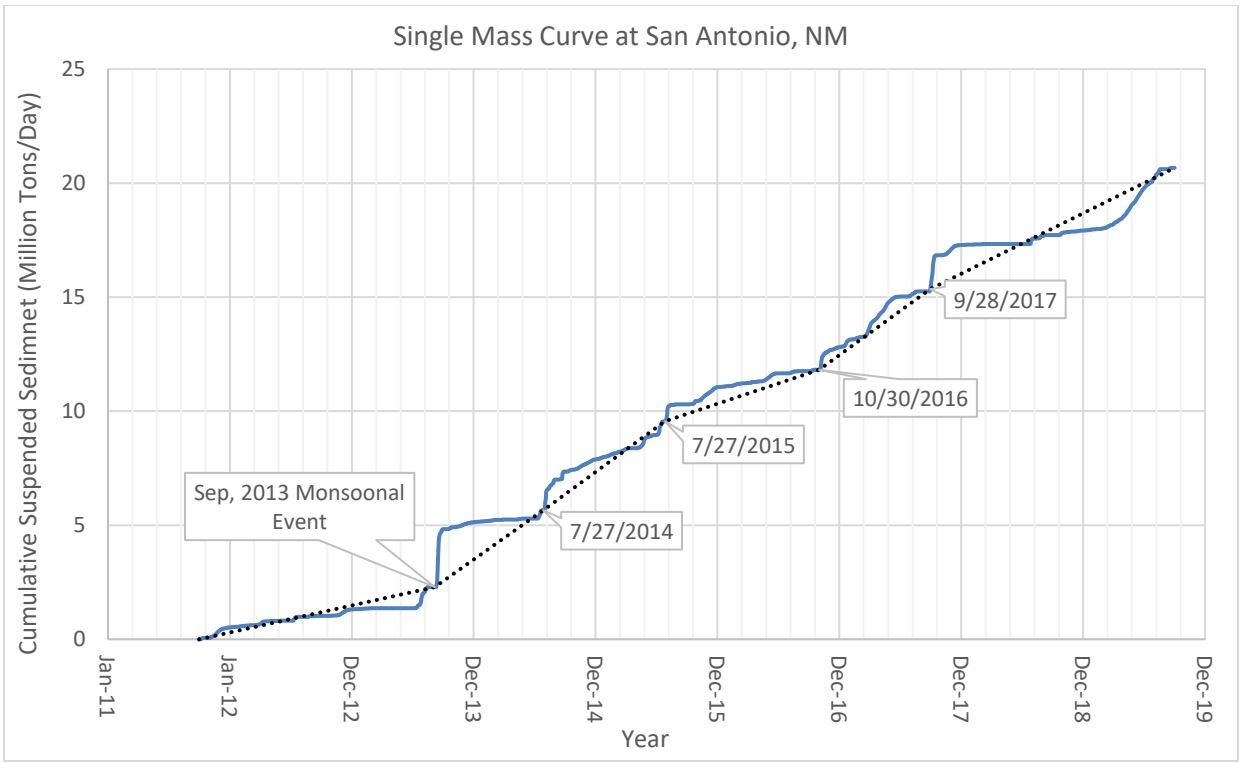

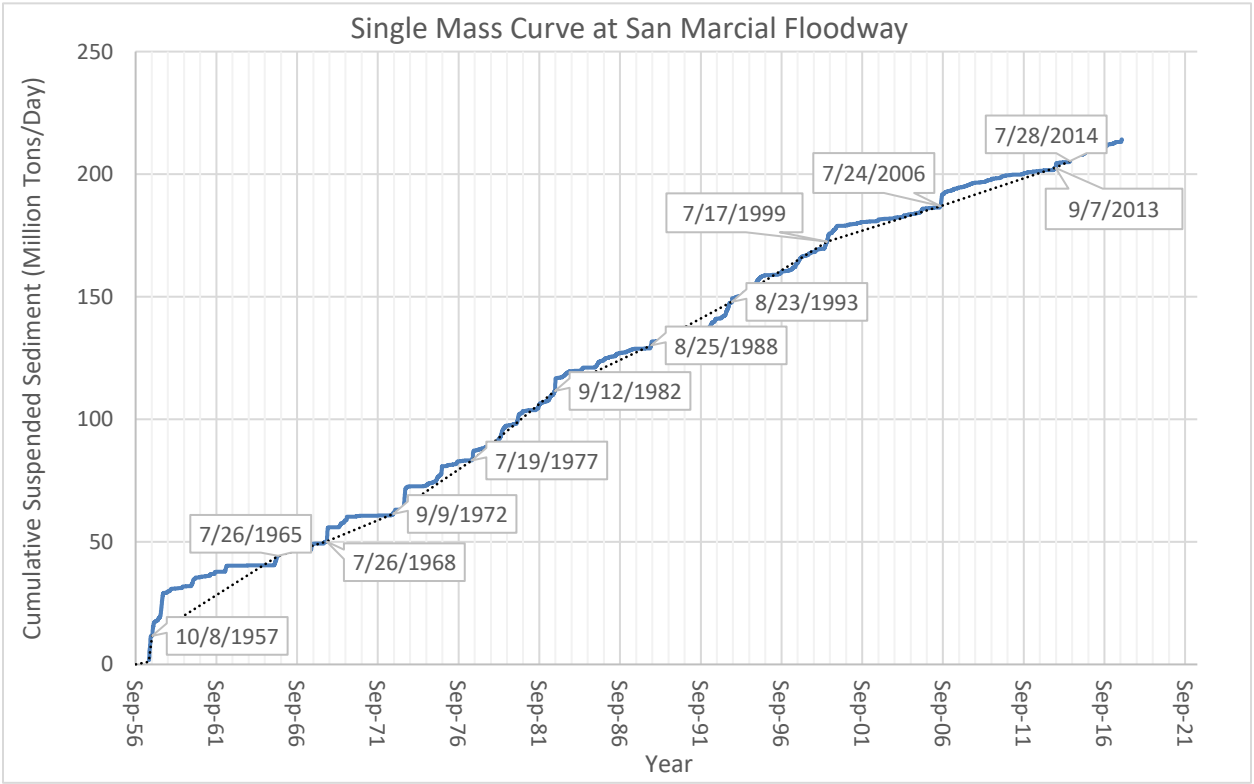

Figure 25 Suspended sediment discharge single mass curve for US HWY 380 Bridge USGS gage Near San Antonio, NM (top) and San Marcial Floodway, NM (bottom)

2.3.2 Double Mass Curve

Double mass curves show how suspended sediment volume relates to the daily discharge volume. The slope of the double mass curve represents the mean sediment concentration. The double mass curve in Figure 26 is for USGS gage at Floodway at San Marcial (08358400). The greatest changes in cumulative sediment load with respect to cumulative discharge typically occur during the summer months between June and September when thunderstorms are more prevalent, thus further indicating that the thunderstorms have a greater impact on sediment load than the spring snowmelt.

Figure 27 relates the cumulative average monthly suspended sediment at the Floodway at San Marcial gage to the cumulative precipitation at the Lemitar gage to further demonstrate the effects of monsoon-related sediment transport. A steeper slope indicates that there was an increase in suspended sediment with very little change in the cumulative precipitation. Specific monsoon events can clearly be seen in the figure, such as the monsoonal event from August 2013 to September 2013 and a series of thunderstorms from July 2014 to August 2014. These events impact the suspended sediment in the Elephant Butte Reach. Where the main sediment input into the MRG is due to ephemeral tributaries (Fitzner 2018). Where within the Elephant Butte Reach there are no major tributaries but small arroyos that enter the river (Towne 2007).

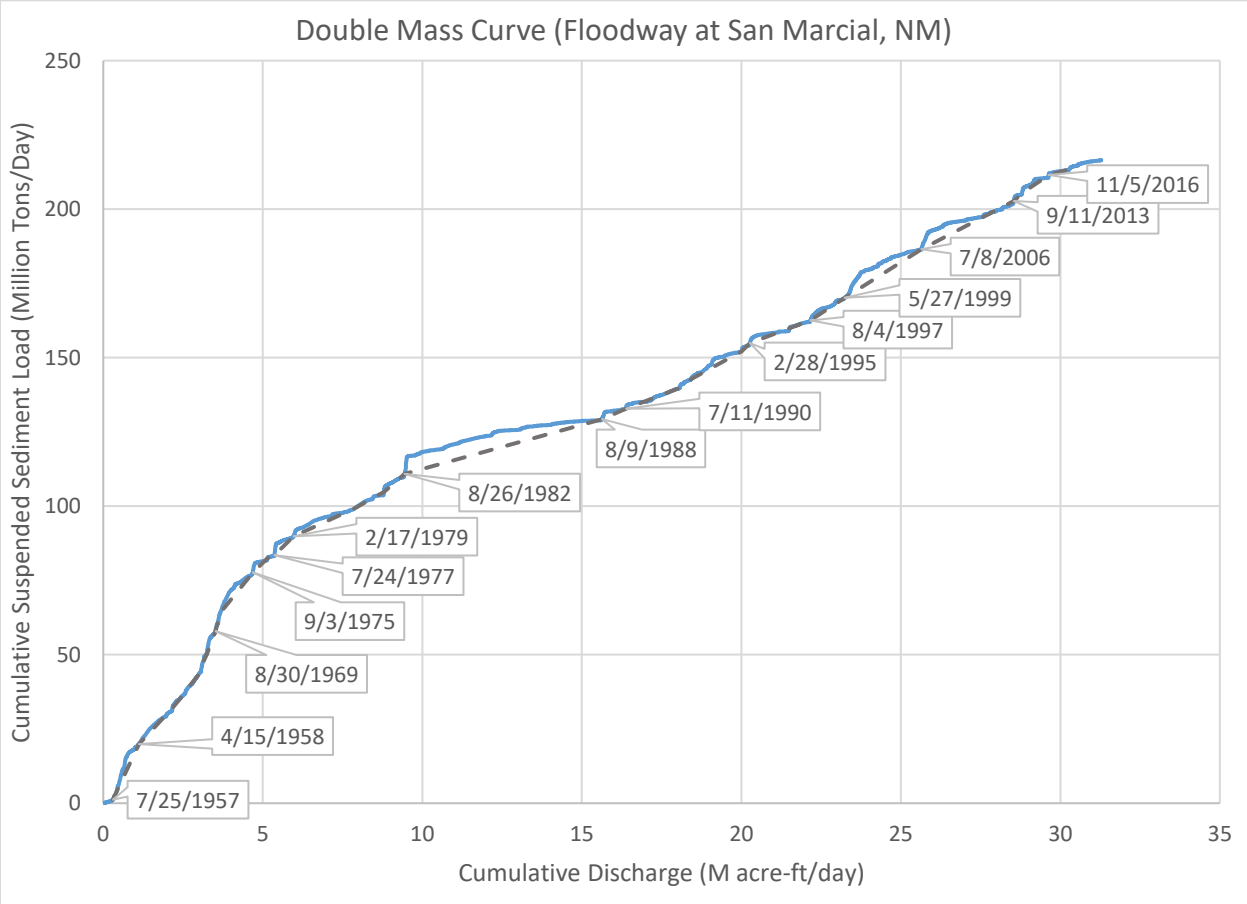

Figure 26 Double Mass Curve for the US HWY 380 Bridge Gage near San Antonio, NM

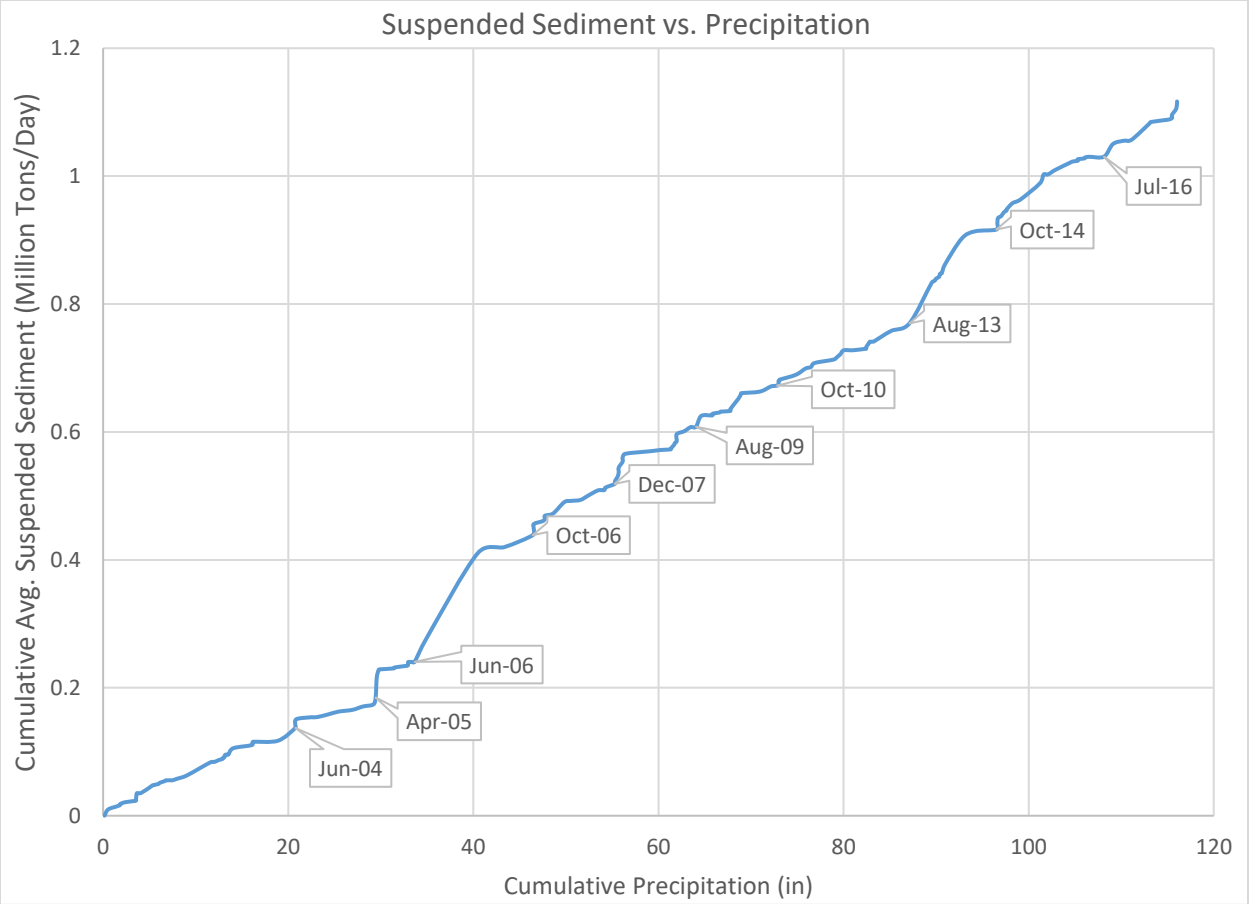

Figure 27 Cumulative suspended sediment (data from the Floodway at San Marcial gage, NM) versus cumulative precipitation at the Lemitar gage.

2.3.3 Monthly Sediment Variation

A plot of monthly average discharge and suspended sediment was created for the gage near San Antonio and for the floodway at San Marcial to help reveal any important seasonal trends. Figures 28 through 31 show the seasonal trends of suspended sediment load and concentration, respectively, along with the discharges that correspond with the years. Although the spring snowmelt brings some of the larger flow rates, the increased flows from the monsoonal storm events transports the most sediment. Peaks in suspended sediment occur in the summer months around June. A SEMEP analysis of total sediment load in the MRG can be found in Appendix B.

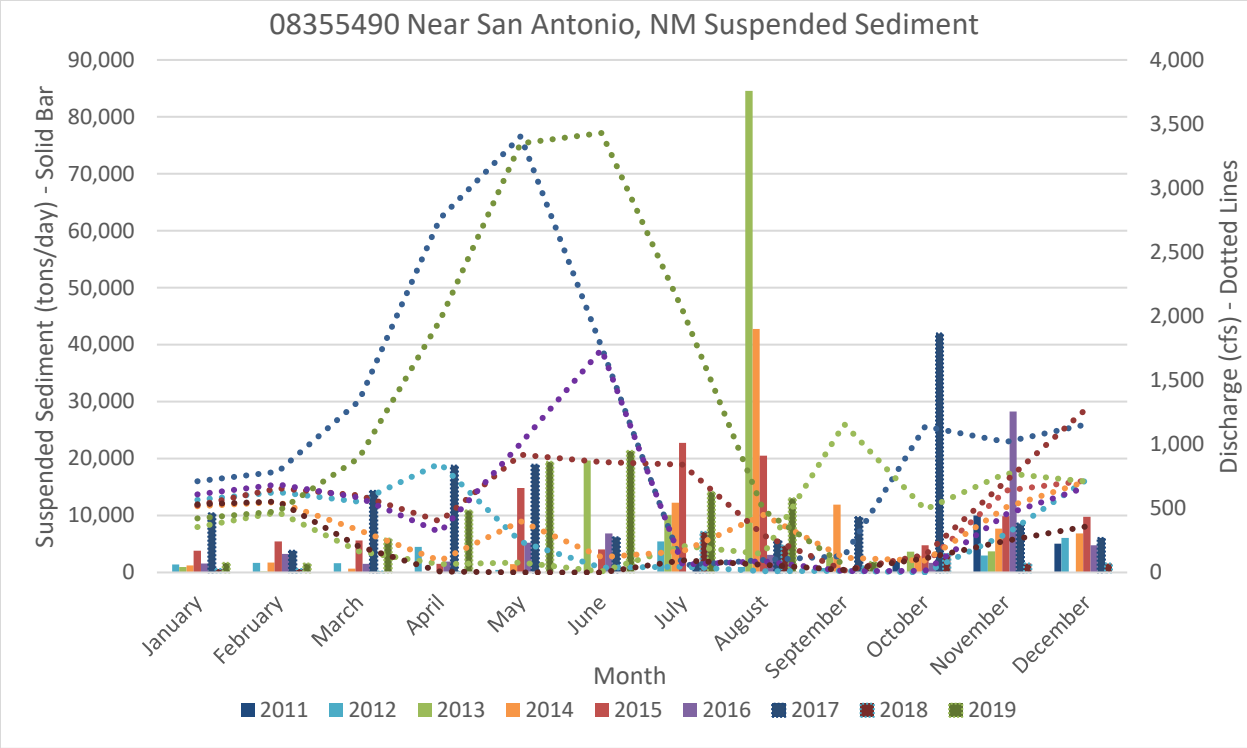

Figure 28 Monthly average suspended sediment and water discharge at gage 08355490 Near San Antonio, NM

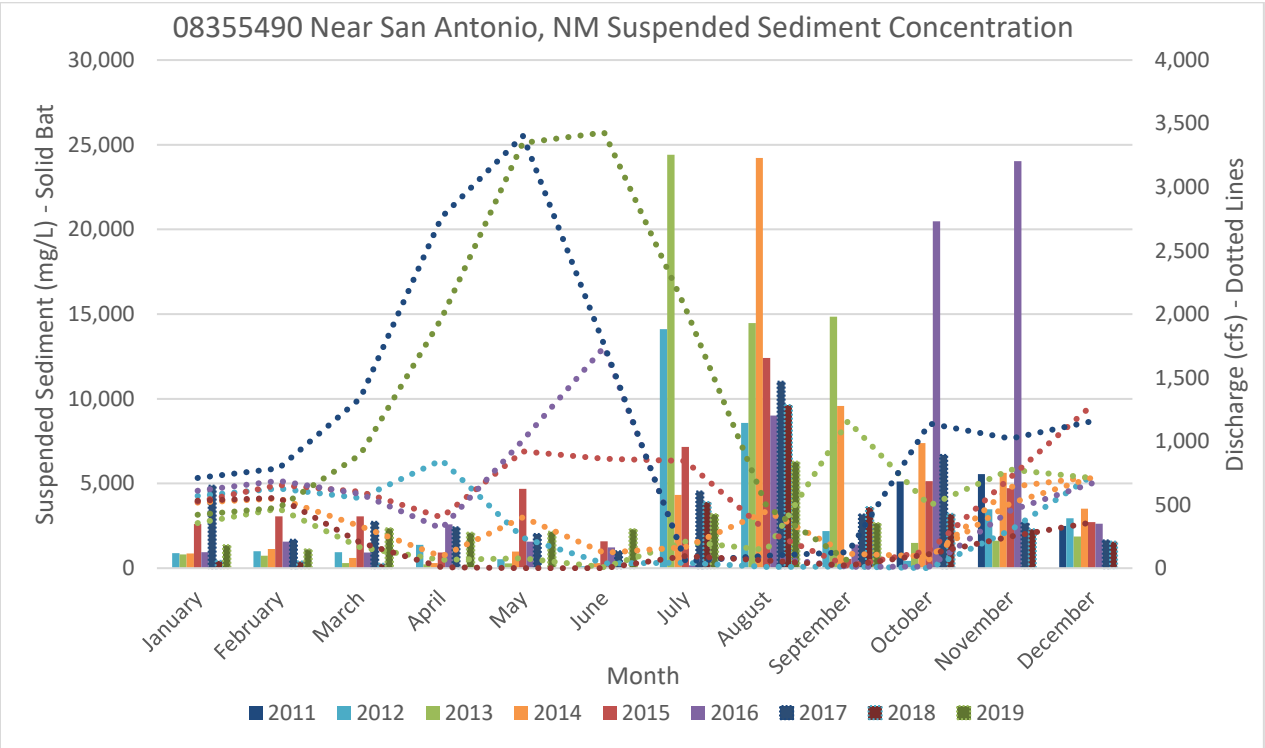

Figure 29 Monthly average suspended sediment concentration and water discharge at gage 08355490 Near San Antonio, NM

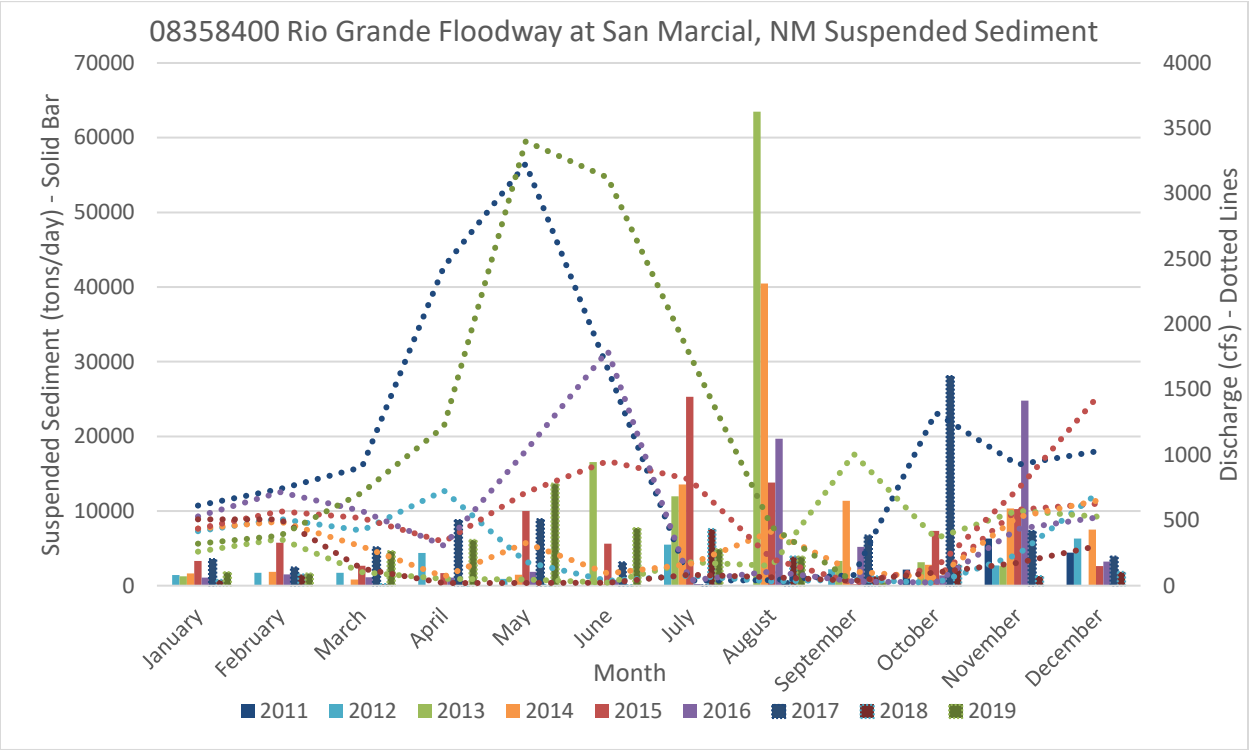

Figure 30 Monthly average suspended sediment and water discharge at gage 08358400 at San Marcial, NM

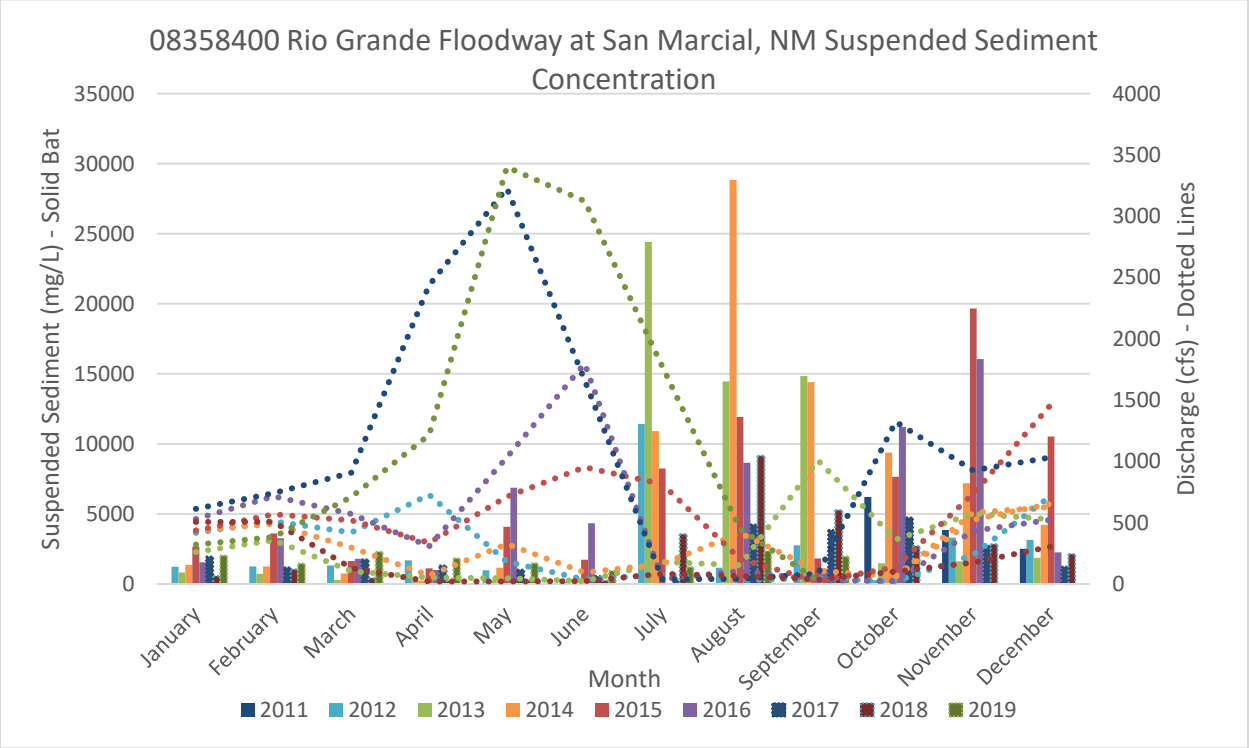

Figure 31 Monthly average suspended sediment concentration and water discharge at gage 08358400 at San Marcial, NM

3. River Geomorphology

3.1 Wetted Top Width

Wetted top width can provide significant insight into at-a-station hydraulic geometry. Typically, wetted top width in a compound trapezoidal channel would slowly increase as discharge values increase until there is a connection with the floodplain. At this point, the top wetted width would quickly increase as the water spills onto the floodplains. Then, a gradual increase in width would continue after this point. Analysis of the wetted top width can be used to help understand bankfull conditions and how they vary spatially and temporally in the Elephant Butte Reach. A HEC-RAS model was created to analyze a variety of top width metrics. Levee points in HEC-RAS were set on the tops of the natural levee of the channel, confining the flows bellow this bank elevation to the main channel. An increment of 500 cfs up to 10,000 cfs was used in the top width analysis for the years with available data: 1962, 1972, 1992, 2002 and 2012.

Figure 32 show the moving cross sectional averaged top wetted width at 1,000 from the HEC-RAS model results. The top width shown at each agg/deg line comes from the moving average from five consecutive cross sections: the identified agg/deg line, two upstream agg/deg lines, and two downstream agg/deg lines. Based on the analysis, subreaches EB1, EB2 and EB5 have experienced the most dramatic change in top width. Majority of the EB1 and EB2 subreaches have shown a trend of narrowing since 1962. Subreach EB3 has consistently gone through a narrowing and widening phase. Subreach EB4's wetted top width has stayed relatively constant. Subreach EB5 has widened since 1962 but has started narrowing from the maximum width that it experienced in 2002. Additional figures from this analysis can be found in Appendix C, including plots with the corresponding top width for each agg/deg line rather than the moving average.

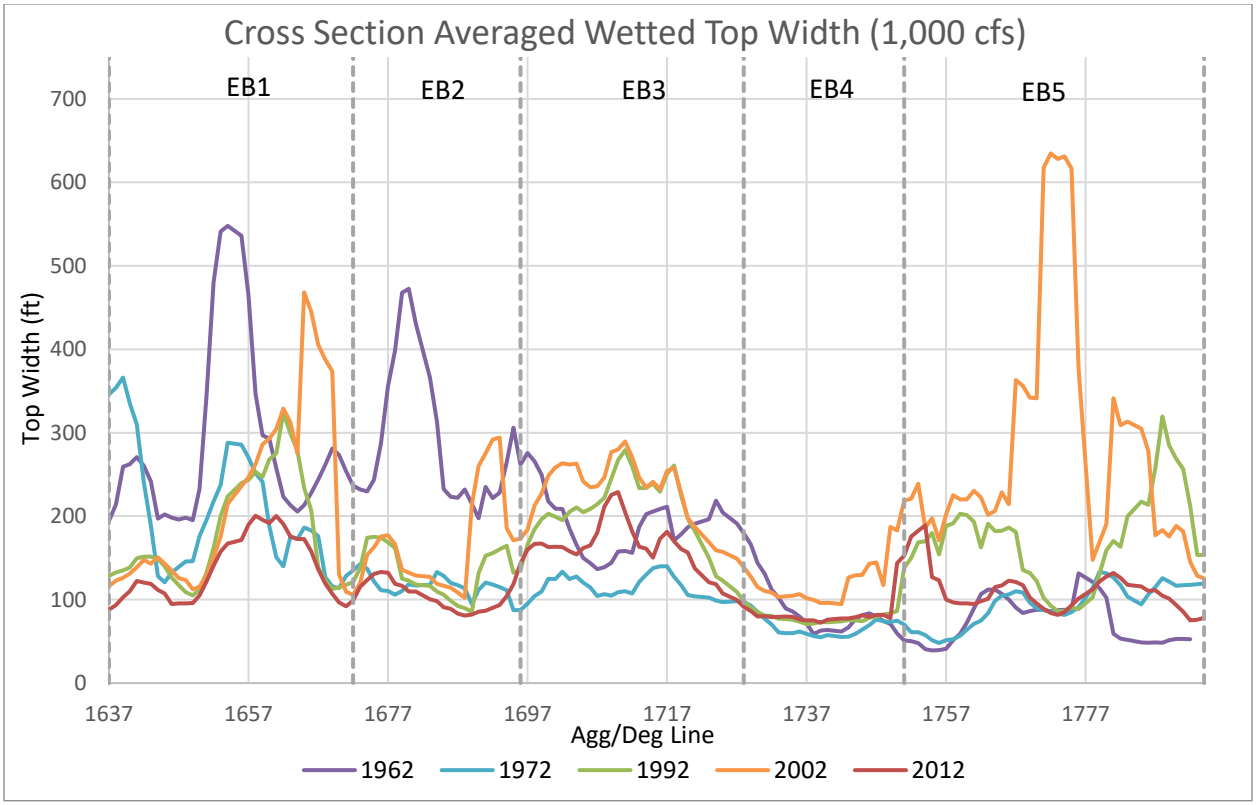

Figure 32 Moving cross-sectional average of the wetted top width at a discharge of 1,000 cfs (With Levees)

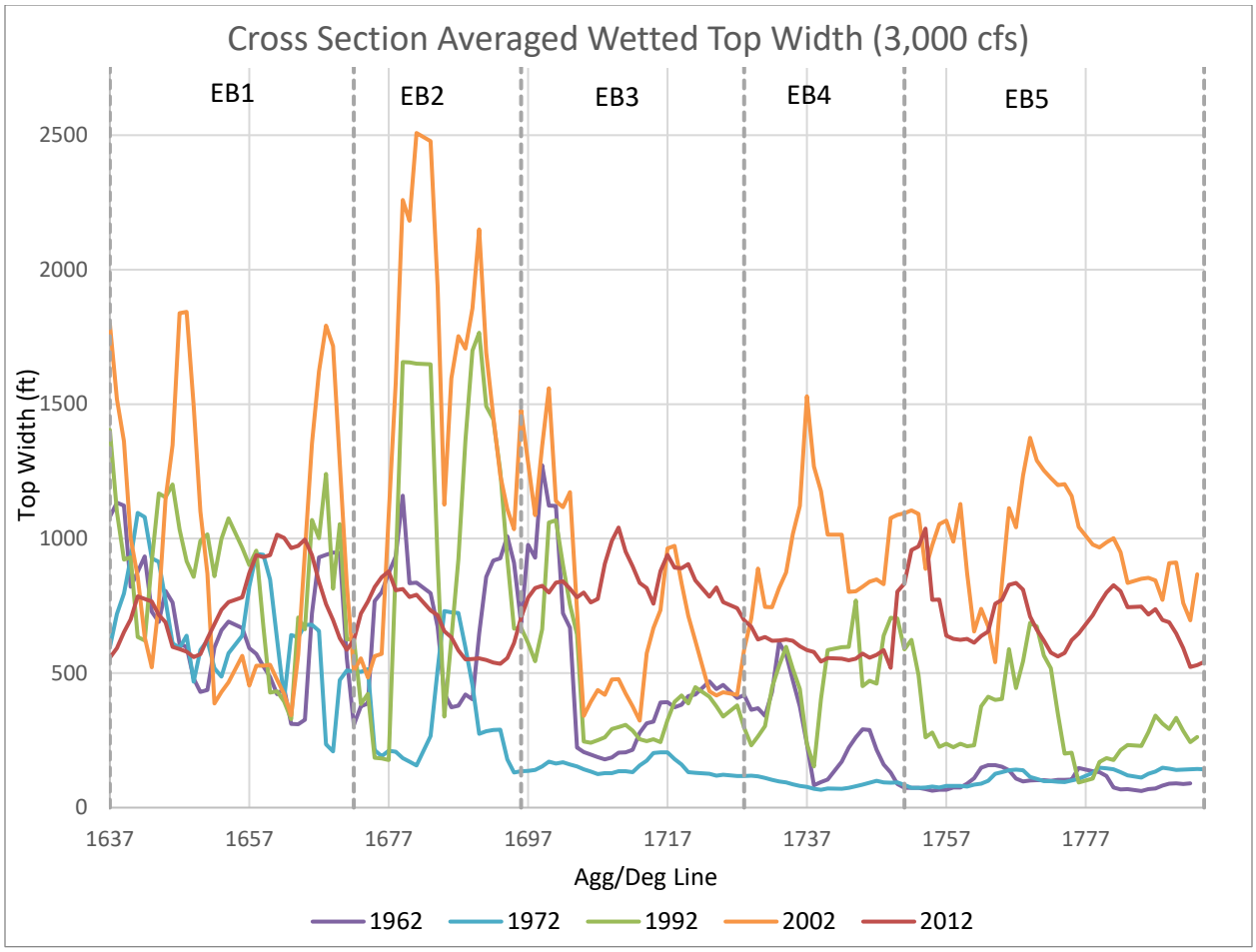

Figure 33 Moving cross-sectional average of the wetted top width at a discharge of 3,000 cfs (With Levees)

Figure 33 show the moving cross sectional averaged top wetted width at 3,000 cfs from the HEC-RAS model results. The channel width decreased dramatically in 1972 compared to 1962. In the subsequent years at flow of 3,000 cfs there is a rapid increase in top width compared to the 1,000 cfs flow. This indicates that the floodplain is being utilized and filled. The top width at 3,000 cfs flow has increased from 1972 to 2002. This may indicate that the hydraulic depth of the channel has decreased allowing for the floodplain to be inundated at this flow, increasing the top width. Between 2002 and 2012 the top width of the river decreases. This may be an indicator that the hydraulic depth is increasing, and the channel is narrowing.

The discussed channel characteristics are further corroborated in Section 3.2, 3.3, and 4.1. Where reservoir effects play a major role in the river geometry and is discussed in section 3.8 and the synthesis section, section 5, of the report. Another potential contributor to the top width increase is the mowing operations that occurred from the 1950s to the 1980s. Where when the main channel aggrades the

floodplain is inundated at a lower flow rate and there is potentially less bank stability due to the clearing of vegetation, Figure 2.

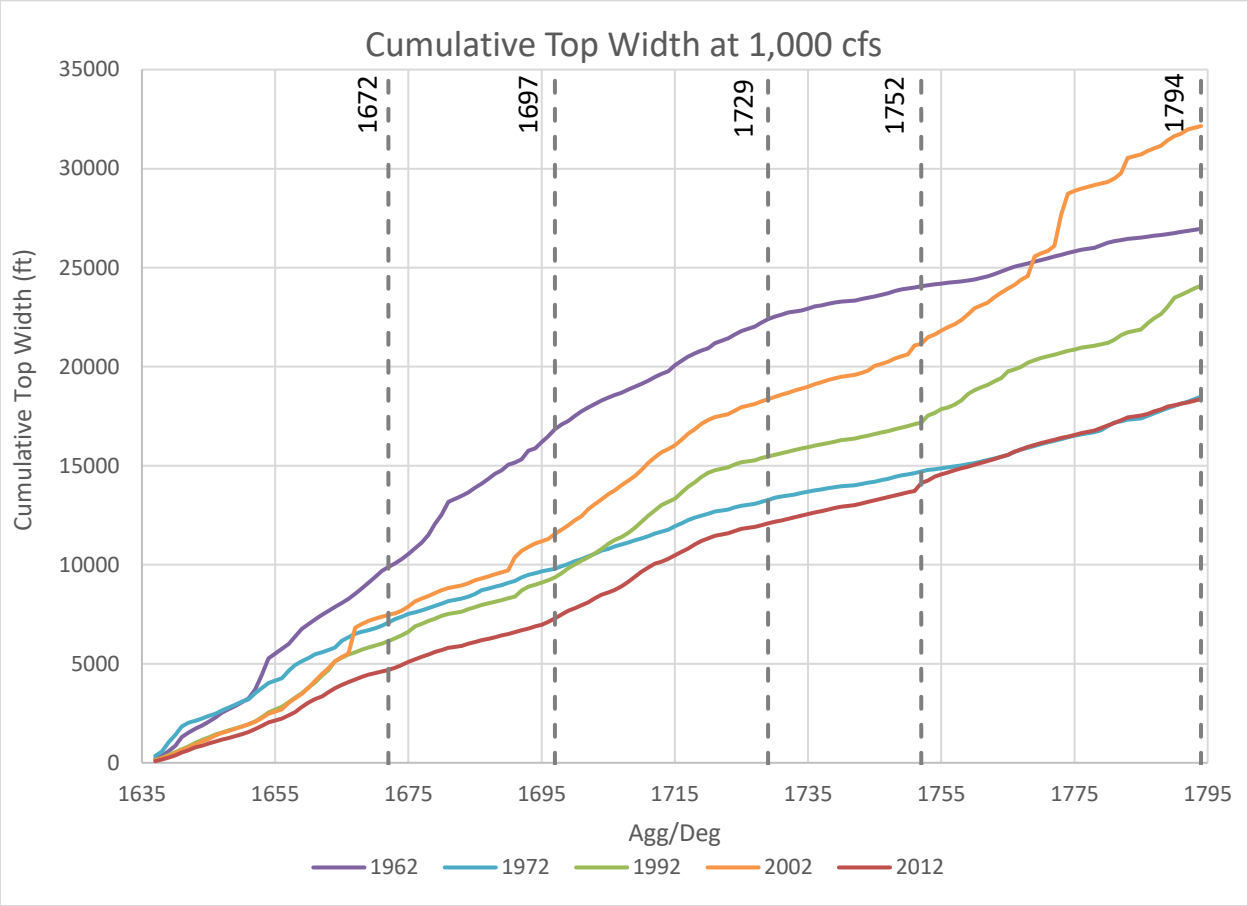

Figure 34 Cumulative top width at a discharge of 1,000 cfs (With Levees)

Figure 34 shows the cumulative top width of the wetted cross sections. The cumulative width shows how the width through time varies within each subreach. Where in general 1962 had the greatest widths until around subreach 4 where the slope of the line decreases. Then in 1972 the channel is narrower and has a less steep cumulative width slope. When the channel aggrades from 1972 to 2002 the top widths all increase allow for a greater slope of the top width line from 1992 to 2002. Then when the channel degrades when the water level in the reservoir drops from 2002 to 2012 the top width of the channel narrows again.

The average top width for each subreach was also plotted for the years analyzed in Figure 35 for discharges up to 5,000 cfs. The average top width for all reaches generally increased between 1962 and 2002. Then for the 2012 data shows a dramatic decrease in width generally for all subreaches showing narrowing of the channel. EB1, EB2, EB3 and EB5 show a large range of top width changes throughout the years of widening then narrowing of the channel.

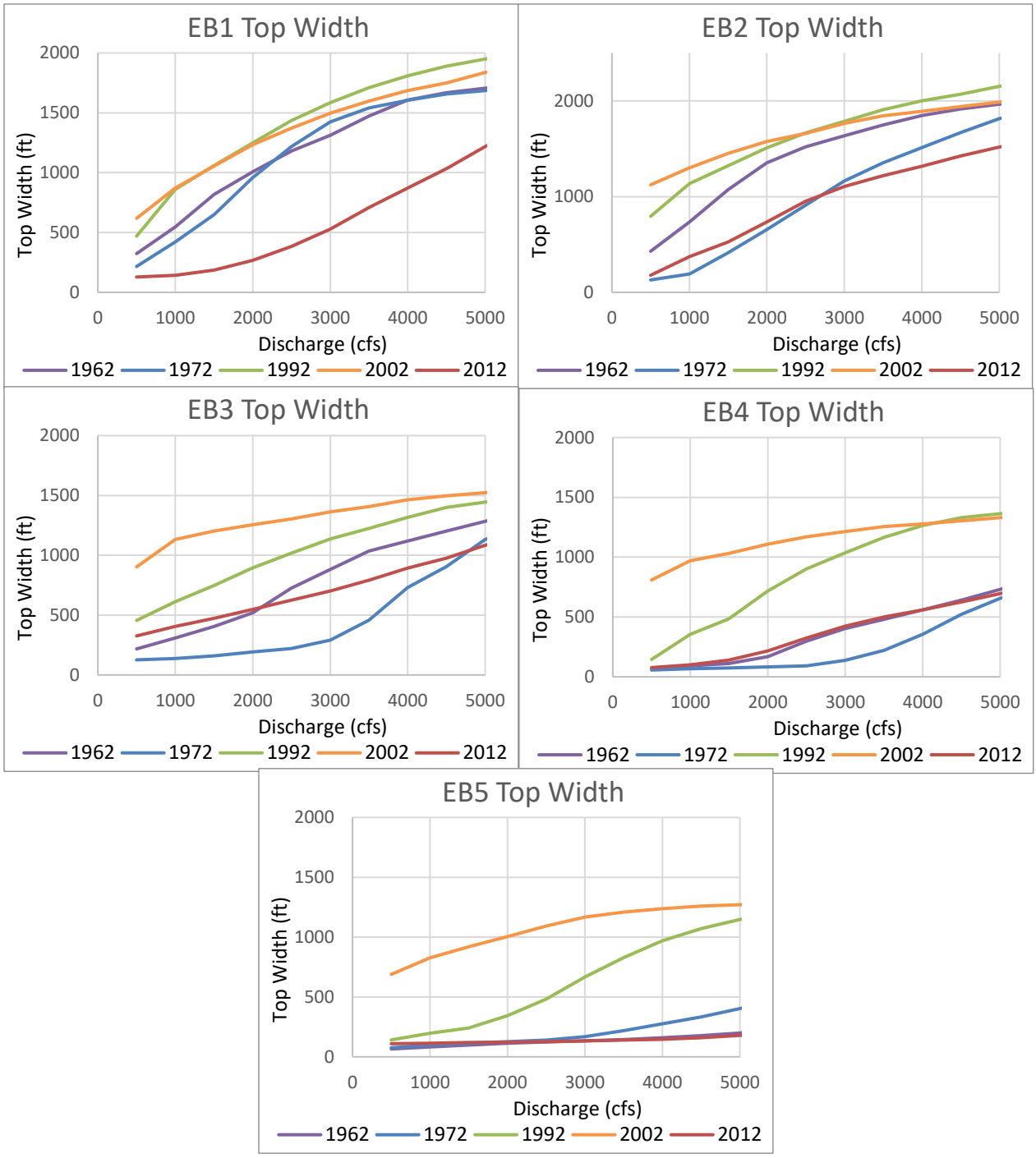

Figure 35 Average top width for EB1 (top left), EB2 (top right), EB3 (middle left), EB4 (middle right), and EB5 (bottom) at discharges 500 to 5,000 cfs (Without Levees)

3.2 Width (Defined by Vegetation)

The width of the active channel, defined as the non-vegetated channel, was found by clipping the agg/deg line to the width of the active channel polygon provided by the USBR's GIS and Remote Sensing Group. The widths of the clipped agg/deg lines were exported from ArcMap for each agg/deg line. Then the average width of each subreach was calculated by averaging the width of all agg/deg lines within the

subreach. Aerial photographs and accompanying digital shapefiles were provided for years 1935, 1962, 1972, 1987, 1992, 2001, 2002, 2003, 2004, 2005, 2006, 2007, 2012 and 2019. The results are shown in Figure 36.

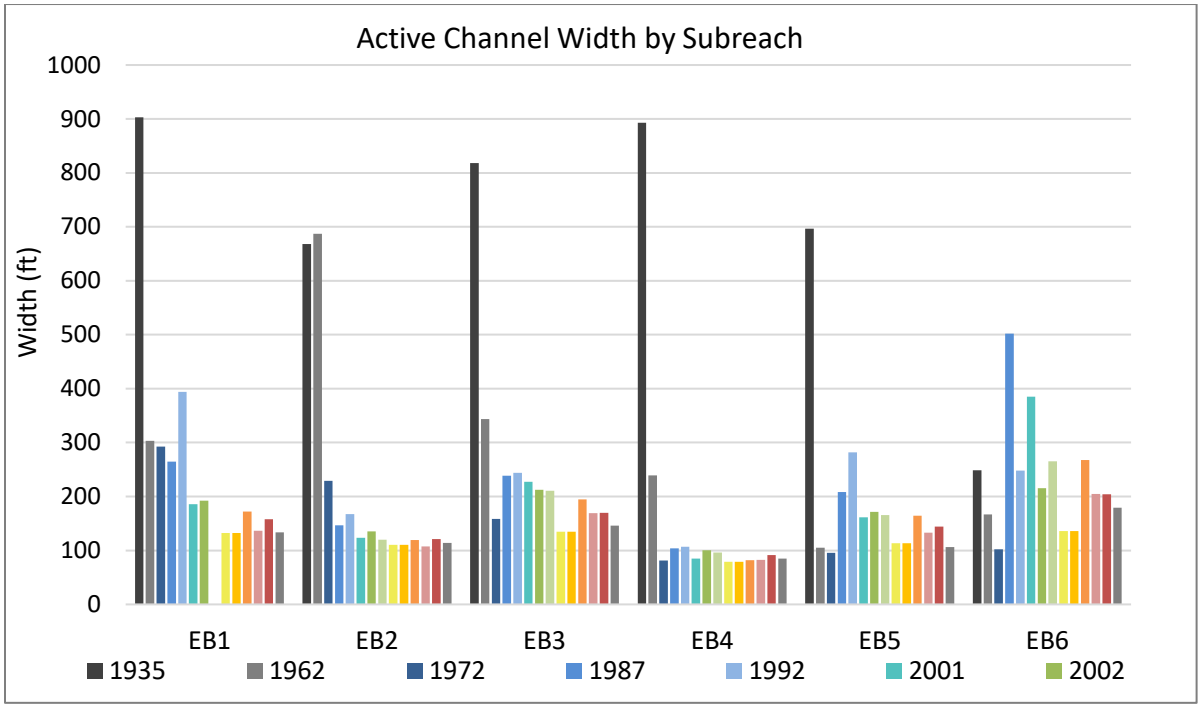

Figure 36 Averaged active channel width by subreach

Figure 36 shows that the active channel width in 1935 was the largest in subreaches EB1, EB3, EB4, and EB5. After 1962 the width decreased in subreach EB2. Subreach EB6 has had a lot of fluctuations through time which may be directly linked to reservoir effects. Generally, there is a sharp decrease in width after 1935. A reduction in peak flows lead to a decline in the active channel width of the river. An extended period of drought beginning in the 1940s and installation of jetty jacks in the 1950s resulted in additional narrowing of the active channel (Scurlock, 1998). "The construction of the Tiffany levee in the early 1950s is the primary driver of changes through this reach, but in particular beginning at EB3. The levee constricted the river to a much smaller portion of the valley and cut off many old channels." (Posner, pers.comm.). Upstream dams and reservoir storage also lead to a decrease in peak flows during this time period. Furthermore, installation of the Low Flow Conveyance Channel reduced the discharges in the Rio Grande by diverting the flow from the 1960s to the 1980s, further decreasing the width as seen in Figure 36. Mowing operations cleared vegetation along the riverbanks from the 1950s to the 1980s (and into the early 1990s in various locations along the MRG), which may have played a part in a slight widening of the river seen in 1987 and 1992, in addition to the increased flows as the period of drought came to an end and operation of the Low Flow Conveyance Channel was stopped (Makar, 2006). Another period of drought began in the 1990s and is still on going. There have been periods of larger spring runoffs in 2005, 2008, 2017, and 2019 but not enough to end this drought trend. Since the 1990s the active channel width of the river has decreased once again and has remained relatively stable for the upper subreaches EB1 through EB4, where the closer to Elephant Butte Reservoir the more fluctuation in width seem to be present due to more pronounced reservoir effects.

3.3 Bed Elevation

The minimum channel bed elevation is used to evaluate the change in the longitudinal profile of the Elephant Butte Reach. The bed elevation of the channel comes from an estimate generated by HEC-RAS, which is based on the discharge and the water surface elevation on the day of the aerial photography. Based on national mapping standards, 95% of the points need to be within 6 inches of the true ground elevation (Varyu, 2013). While the minimum channel elevation points may not be exact, the overall trends can still be identified throughout the Elephant Butte Reach. The minimum channel elevation was obtained at each cross-section from the HEC-RAS geometry files to generate a plot of the bed elevation throughout the reach, as seen in Figure 37.

Across all reaches there has been net aggradation occurring. This aggradation and degradation cycle of sediment at the beginning of the Elephant Butte subreach is consistent with a previous report by Andrew Schied, which focused on the Bosque reach (Schied et al., 2022). The cycle of aggradation degradation can be observed in Figure 37. This trend becomes more pronounced and extreme moving downstream. The cycle for most of the observed reach is as follows: degradation (1962-1992), aggradation (1992-2002), to degradation (2002-2012). What distinguishes Elephant Butte from previous reaches is the pronounced aggradation degradation cycle due caused by the reservoir effects. The upstream cycle of the Elephant Butte Reach is consistent with the downstream most portion of the Bosque Reach, where the river shows a small amount of degradation from 1962 to 1972 then switch to aggradation from 1972 to 2002 (Scheid, 2021). These trends can be observed and are analyzed in Figure 38. The bed elevation has had a net increase from 1962 to 2012 but is degrading back towards the 1962 elevation. Where the 1962 and 2012 water surface elevation (WSE) in the Elephant Butte Reservoir is at a similar stage (Figure 48). It can be seen in Figure 20 that there is a decrease in precipitation starting in 1990's starting another period of drought that is still continuing which will have an effect on the reservoir water level.

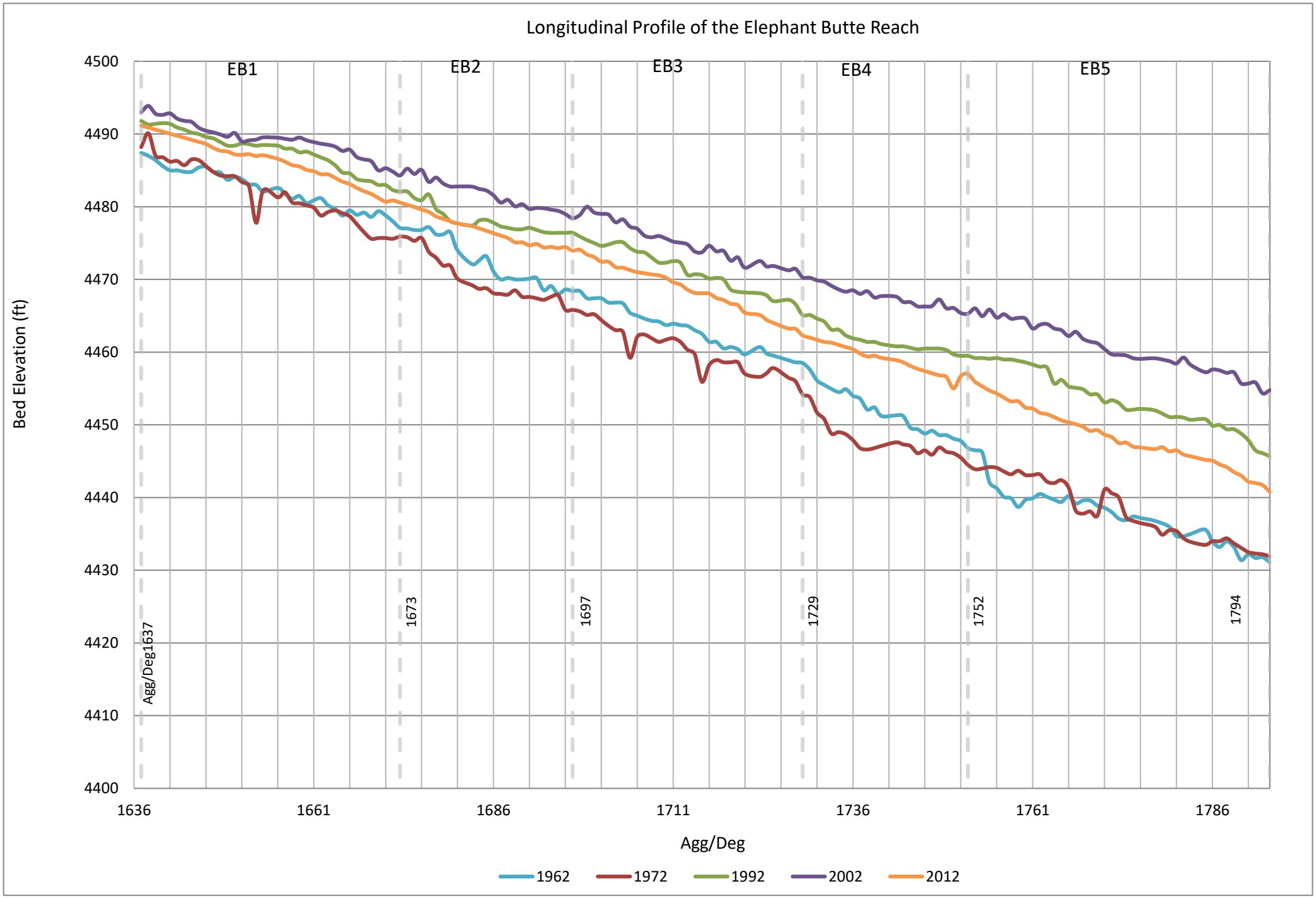

Figure 37 Longitudinal profiles of bed elevation

The reservoir effect is the main driving of the cycles of aggradation and degradation seen in the Elephant Butte Reach which is discussed in Section 3.8 and represented by Figure 48 showing the reservoir's stage record. The water level was highest from 1988 to 2000. This is where we see the greatest aggradation in the channel. Then the water level drops due to. During this time this is where degradation of the channel is seen in 2012. Figure 38 shows the main channel aggradation and degradation of each subreach, which was found by first finding the average minimum channel elevation for each subreach and then subtracting the average bed elevation of the earlier year from the later year. A positive number indicates aggradation, and a negative number indicates degradation. This figure shows an interesting trend happening across all subreaches and gets more pronounced moving downstream toward Elephant Butte Reservoir. The physical trend shown is that in all subreaches between the time interval spanning between 1962 to 1972 there is degradation of the river occurring. Where then the river switches to an aggradation state for the time interval 1972 to 1992. Then decreases the ability for aggradation to occur from the time interval 1992 to 2002. Where then the river totally switches to a degradation state from 2002 to 2012. Moving down stream towards the Elephant Butte reservoir increases the aggradation and degradation potential of the river. This may be due to the reservoir effects and the types of sediment that is present in the river allowing the downstream subreaches to display a higher sensitivity to geomorphic change.

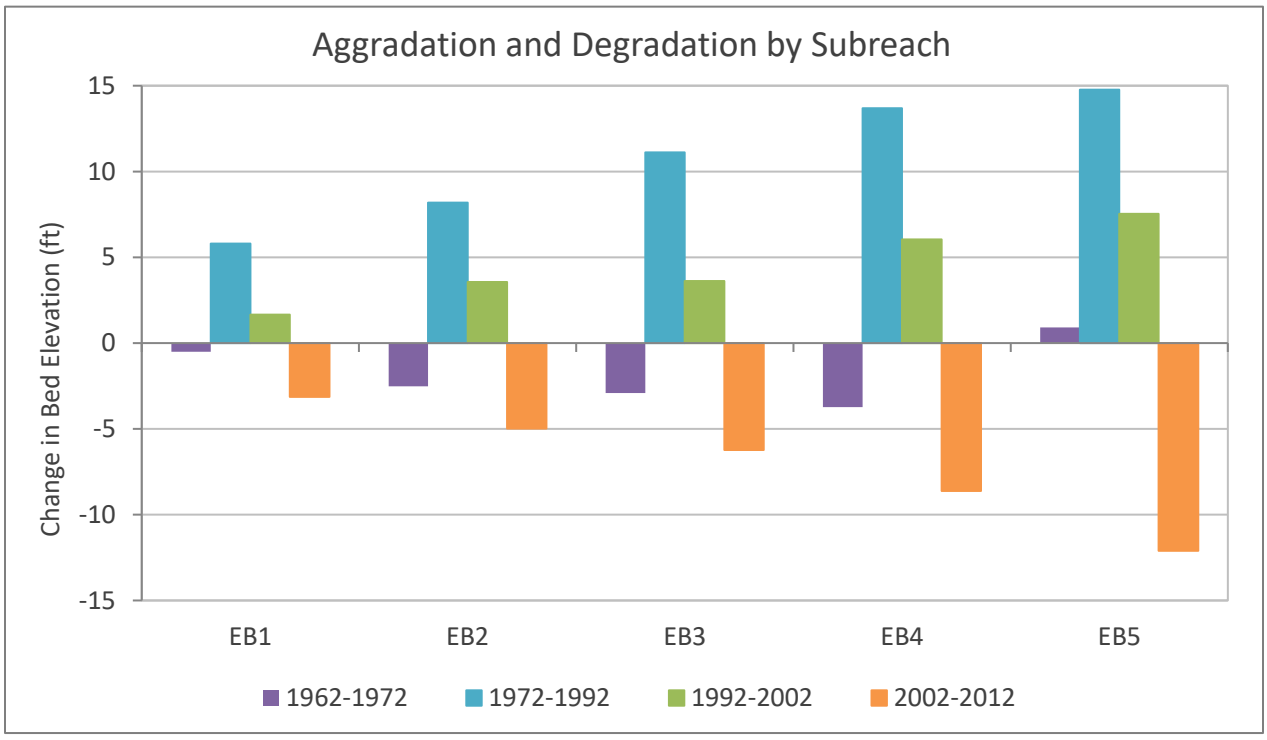

Figure 38 Degradation and Aggradation by subreach

3.4 Bed Material

Bed material samples were collected at various location in the rive reach denoted by Agg/Deg locations. There are bed material samples available for analysis of the Elephant Butte Reach from the years 1990 to 1998. Figure 39 shows the median grain diameter of each sample versus Agg/Deg location downstream of the Bosque Del Apache National Wildlife Refuge (i.e. the start of the Elephant Butte Reach).

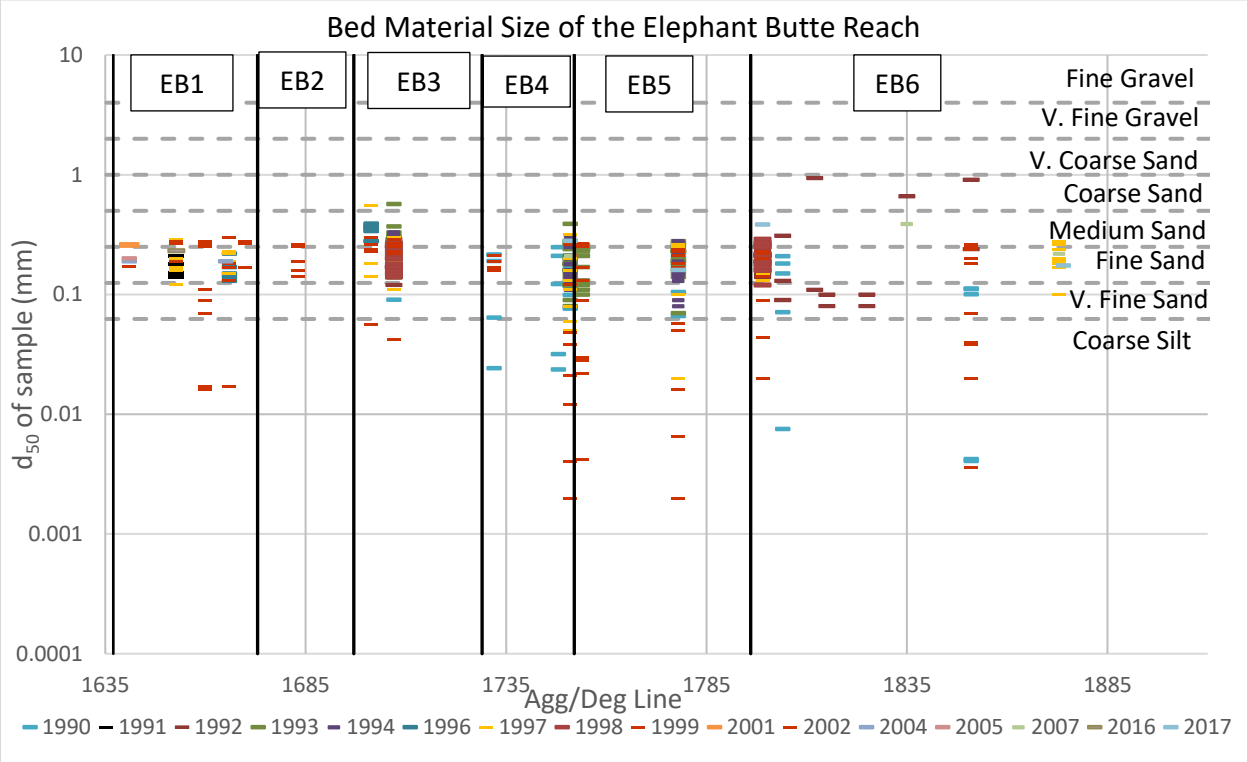

Figure 39 Median grain diameter size of samples taken throughout the Elephant Butte Reach

Throughout the reach the median diameter size of the samples is typically between 0.0625 millimeter and 1 millimeter for the years in which data were collected. These grain size diameters correspond with classifications of fine sand to coarse sand, emphasizing the majority of Elephant Butte Reach is a sand-bed river with some coarse silt.

3.5 Sinuosity

The sinuosity was calculated at each subreach using digitized channel centerlines provided by the USBR's GIS and Remote Sensing Group. Aerial photographs and accompanying digital shapefiles were provided for the years 1918, 1935, 1949, 1962, 1972, 1985, 1992, 2001, 2002, 2006, 2008, 2012 and 2019. To analyze the sinuosity of each subreach, the centerlines were split at each subreach boundary. Then, for each subreach, the length of the centerline (channel length) was divided by the valley length (shortest distance between the top and bottom of the subreach) to get the sinuosity value.

Overall, the sinuosity values in the Elephant Butte Reach are low, measuring just above 1 throughout the reach, as seen in Figure 40. Both subreaches EB1 and EB2 have remained relatively constant and low in their sinuosity values. The sinuosity in EB3 dropped in 1935 and increased slightly over the time interval of 1935 to 1972 and has remained relatively constant around 1.3 since. Subreach EB3 remains the most

sinuous subreach in the Elephant Butte Reach which is due to the large radial bend, around the Mesa del Contadero, located in this reach. Both EB4 and EB5 had a significant decrease in sinuosity between 1949 and 1962. Where EB4 increased slightly but has stayed relatively constant whereas EB5 has been generally increasing in sinuosity.

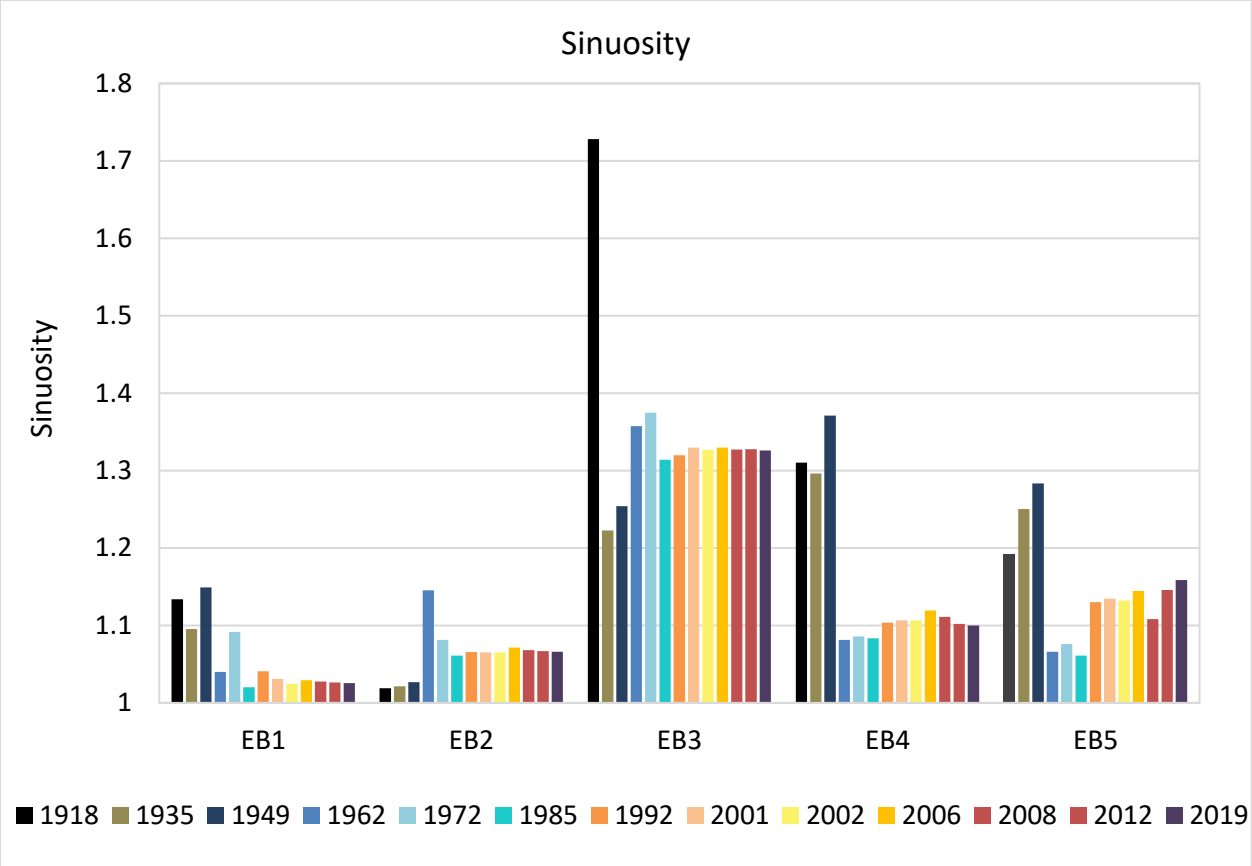

Figure 40 Sinuosity by subreach

3.6 Hydraulic Geometry

Flow depth, velocity, width, wetted perimeter of the main channel, and bed slope are obtained using HEC-RAS 5.0.3 with a discharge of 3,000 cfs, which was selected based on the fact that this discharge represents bankfull conditions with limited likelihood of overbanking (LaForge et al., 2019 and Yang et al., 2019). Where for certain years analyzed 3,000 cfs does indeed activate the flood plain and is not bankfull discharge. This can be seen in Figure 62 and in appendix E. A discharge of 3,000 cfs has a daily exceedance of 4.9% at the Elephant Butte Narrows gage 08359500. A 1,000 cfs, has a daily exceedance probability around 15.4%. For the plots of the hydraulic geometry variables, the values were averaged by subreach for each year analyzed.

The HEC-RAS results (Figure 39) show a cycle of the river's wetted top width. This analysis can indicate at what years the channel may be activating the floodplain and how the main channel morphology may be changing. For 1000 cfs, represented in Figure 41, EB1 appears to be narrowing which is likely caused by channel degradation. EB2, EB3, EB4, and EB5 at a 1000 cfs show a cycle of degradation and aggradation, showing a decrease and then increase in top width. Additionally, 3000 cfs is activating the

floodplain in 1992 to 2002. As stated above this is corroborated with Figure 62 and in Appendix E. Where 3,000 cfs in 1962, 1972, and 2012 seems to be still confined to the main channel. These trends are due to reservoir effects, which induces the aggradation / degradation cycles within the reach. From 1962 the river's main channel has narrowed or stayed relatively consistent, with EB5 being the exception. For EB5, the effects of aggradation have widened the top width of the channel slightly.

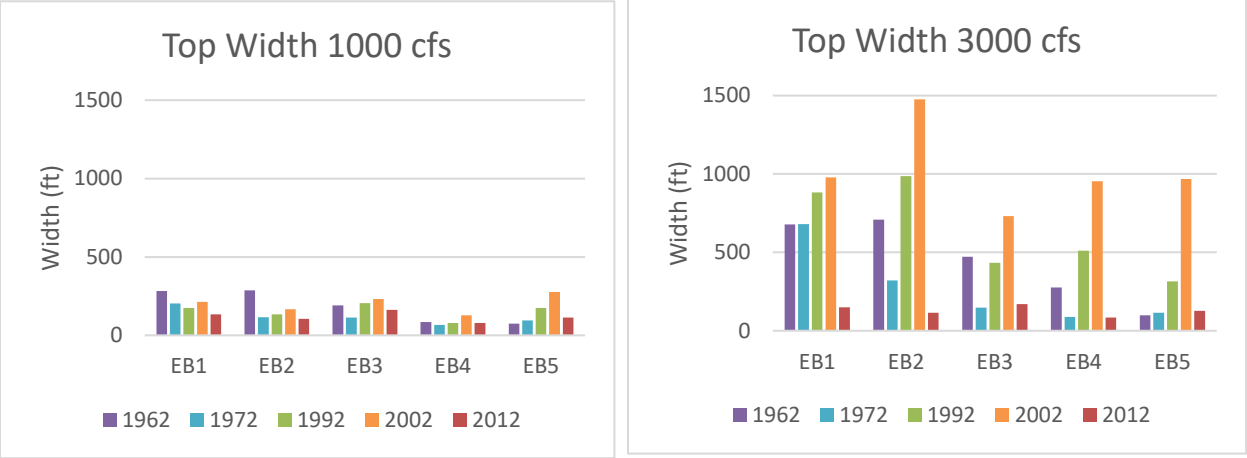

Figure 41 HEC-RAS Wetted top width of channel at 1,000 cfs (left) and 3,000 cfs (right)

Figure 42 accompanies the observed trends of Figure 41 of the Elephant Butte Reach. When narrowing occurs it is expected that there will be an increase in flow depth. The inverse is true for widening of the channel. This trend can be confidently applied to the 1,000 cfs flow rate because the flow is still confined to the main channel. Figure 42 shows the HEC-RAS calculated hydraulic depths (area over top width) at discharges of 1,000 cfs and 3,000 cfs. Generally, there is a slight increase in hydraulic depth from 1962 to 1972 showing slight incision occurring which will increase the area. Then between 1972 and 2002 the hydraulic depth decreases showing a deposition of sediment decreasing the cross sectional area. From 2002 to 2012 there is a slight increase in hydraulic depth show more degradation and incision occur. These events can be tied to the reservoir effects discussed in section 3.8.

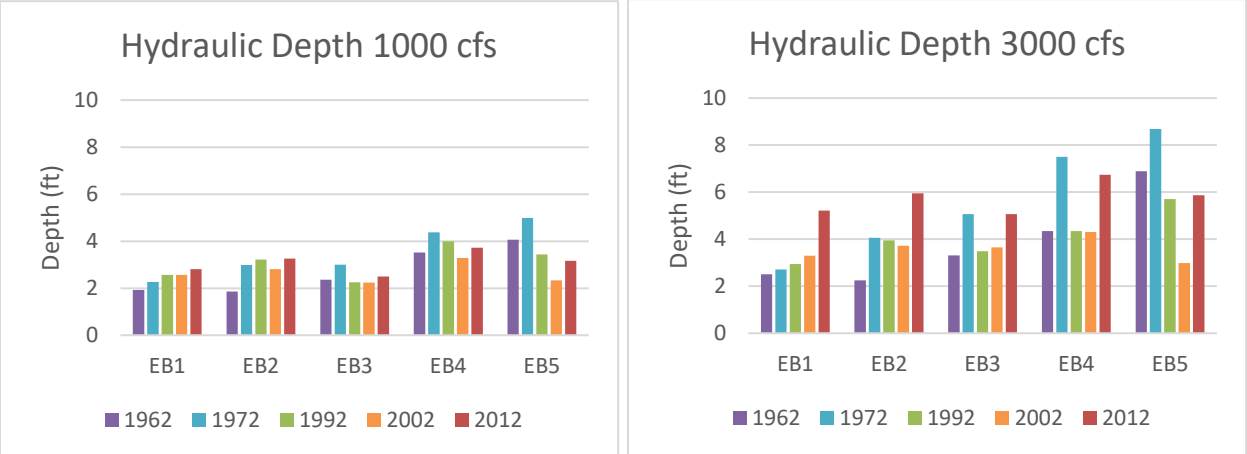

Figure 42 HEC-RAS Hydraulic depth at 1,000 cfs (left) and 3,000 cfs (right)

Figure 43 shows one cross section in Subreach EB2. This example shows that although the main channel has gone through a degradation / aggradation cycle and the banks become perched. A notable pattern that

occurs within the Elephant Butte Reach is that the banks are aggrading faster than the main channel, which is another factor leading to an average increase in the hydraulic depth. This deposition of sediment on the banks creates a perched channel and the formation of natural levees. When the river starts to degrade the main channel degrades but the natural levees that were built up stay at their aggraded elevation. This increases the flow required to inundate the floodplain.

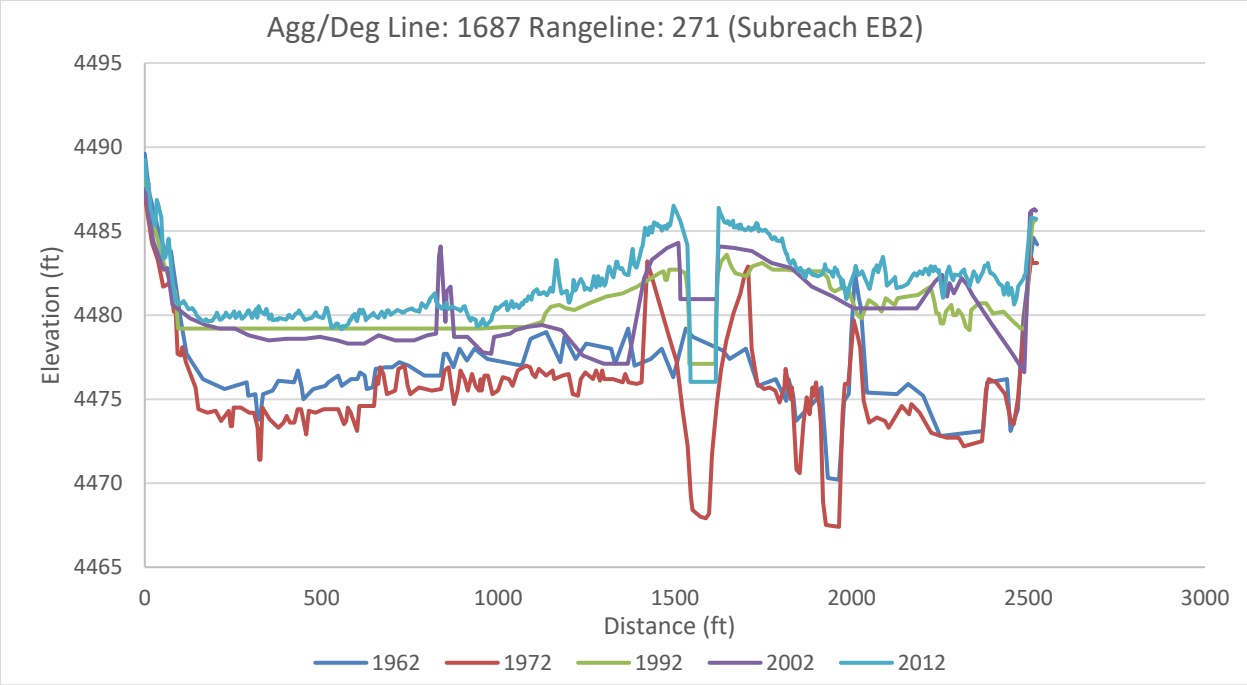

Figure 43 Example cross section indicating that the banks are going through a cycle of degradation / aggradation. Throughout the reach, the top wetted width has decreased then increased.

The results for the wetted perimeter of the main channel were obtained by using HEC-RAS and is represented by Figure 44. Generally, the main channel wetted perimeter follows a similar trend to the top width. Subreach EB1 has a steady decline in the main channel wetted perimeter throughout the time interval analyzed. Where EB2, EB3, EB4, and EB5 loosely follows the similar trends of the wetted perimeter decreasing from 1962 to 1972 then increase between 1972 and 2002. Then the main channel wetted perimeter decreases from 2002 to 2012. Which is a very similar trend as seen in Figure 41 for the wetted top width. This is due to the degradation and aggradation cycle that is present in the channel. It is

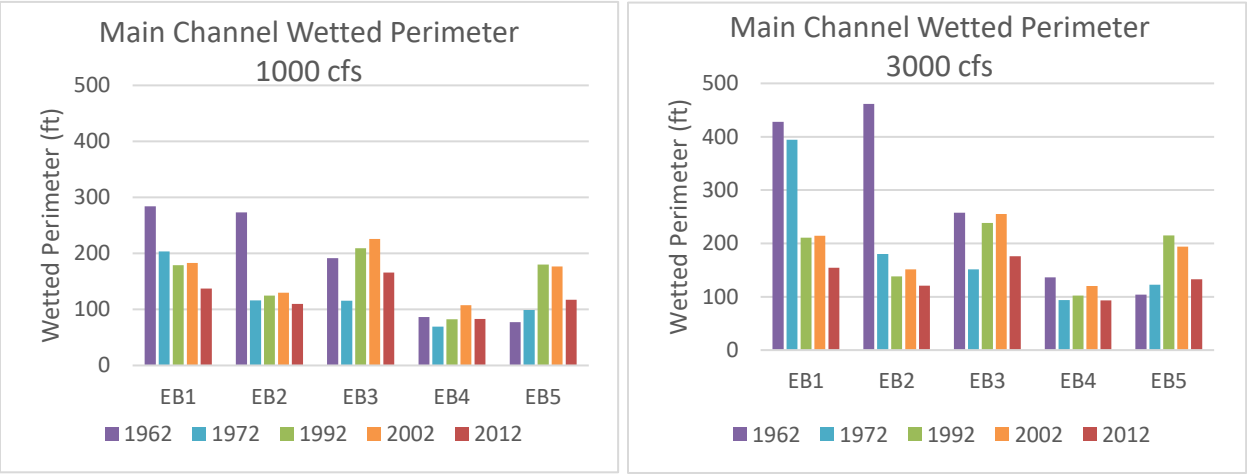

Figure 44 Wetted Perimeter at 1000 cfs (left) and 3000 cfs (right)

important to note that the wetted perimeter is confined to the main channel and shows how the main channel has changed over time.

The bed slope was calculated by taking the slope of a linear fitted line for each subreach. A bar chart of the bed slope of the linear fitted line is shown in Figure 45. The bed slope calculated off of the water surface profile at 500 cfs for EB1, EB3, and EB5 has fluctuated but has stayed relatively stable, with a bed slope around 0.0005, 0.0006, and 0.0006 respectively, over the time interval of 1962 to 2012. Subreach EB2 and EB4 ultimately both dropped in bed slope from around 0.0075 to 0.00055 and 0.0008 to 0.0065 respectively over the time interval. Changes in flow depth and slope often have an inverse relationship. In general, as slope decreases the flow depth increases. This trend can be seen in the Elephant Butte Reach, while not very pronounced, it is indicated in subreach EB1. Each subreach has undergone different trends through the time interval. The bed slope has overall remained the same or decreased from 1962 to 2012, and the hydraulic depth has increased since the river started incising from 2002 to 2012. It is importat to note that these subreaches each have there own characteristics and trends where between 1962 and 2012.

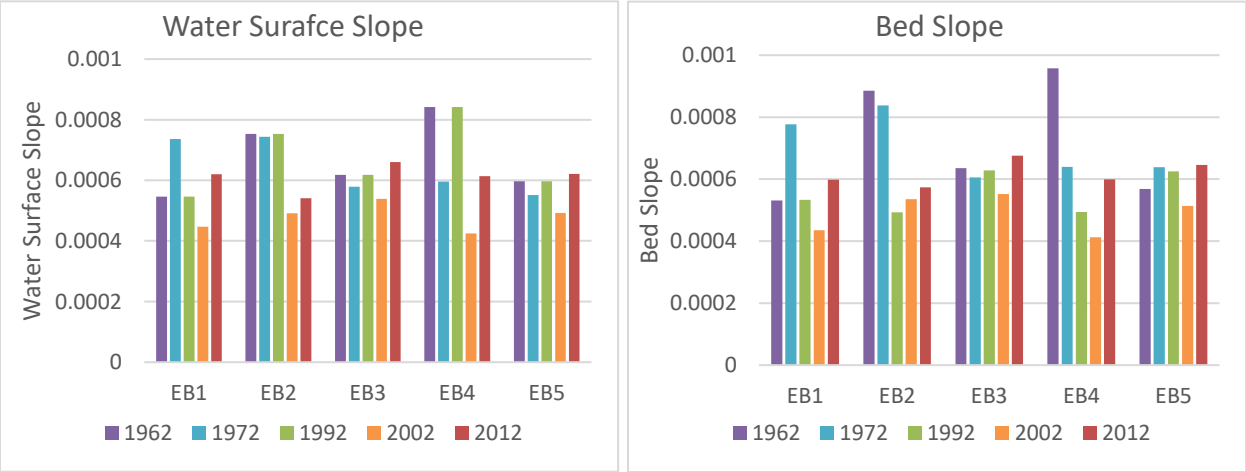

Figure 45 *Water Surface Slope (500 cfs) and Channel Bed Slope*

3.7 Mid-Channel Bars and Islands

The number of mid-channel bars and islands at each agg/deg line is counted from digitized planforms from the aerial photographs provided by the USBR. This led to several limitations to this analysis, the main one being the inconsistency between time and flow rate. There is no indication that the photos used are taken at the same time of the year. Due to there only being a year for the photo and no exact date does not allow for an understanding of the current flow rate in the river at that point in time. Thus, these limitations make it hard to say with certainty what the river's evolution model state is. Regardless this information is useful track the formation of more permanent islands and mid channel bars that may be forming in the river. In some locations, multiple channels were present at one agg/deg line due to a vegetated bar or island bifurcating the flow. The number of channels at each agg/deg line were averaged throughout each subreach and the results are presented in Figure 46. EB1 and EB3 typically has a slightly higher average number of mid-channel bars and islands which may indicate migration. In contrast, EB4 has remained nearly a single-thread channel throughout the time period analyzed. Although there are

slight changes by subreach, the average number of mid-channel bars and islands throughout the reach is still only just above 1 for majority of the years analyzed.

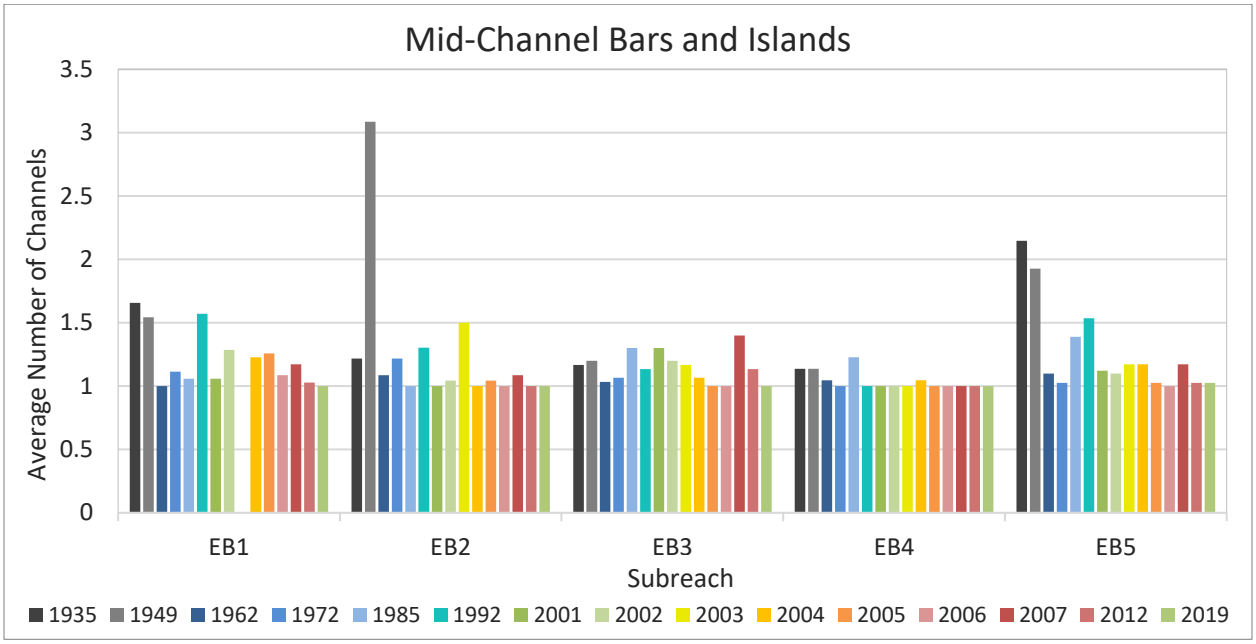

Figure 46 Average Number of Mid-Bars and Islands in Each Subreach

Based on the analysis of the digitized planforms, the years 1935 and 1949 appeared to have a slight increase in number of mid-channel bars and islands. Majority of the Elephant Butte Reach has had around 1 channel with some instances of a mid-channel bar or island. This shows that pre 1949 there typically was a few more geomorphic features in the river. Figure 47 shows an aerial photograph comparison of subreach EB3 between 2002 and 2012. The arial imagery from 2002 shows that there is a lot less vegetation along the banks of the river exposing point bars and alternate bars along the banks. These have the potential to become mid-channel bars depending on how the river evolves under environmental conditions. In 2012 there is vegetation encroachment. This will decrease the number of point bars and alternate bars along the banks. Overall the Elephant Butte Reach is currently almost all a single threaded channel.

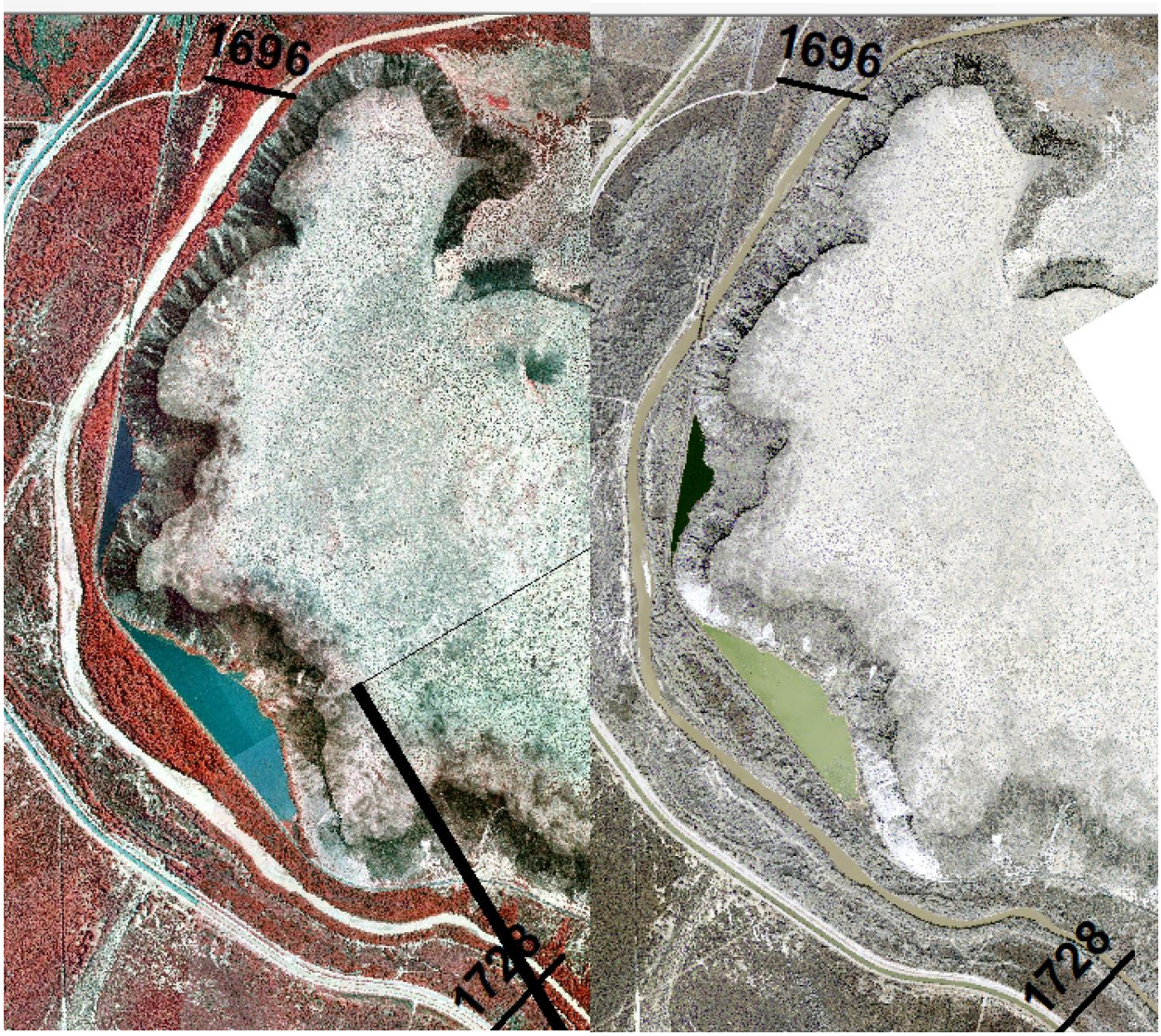

Figure 47 Aerial Photograph of subreach EB3 when multiple alternating bars, point bars, and islands were present in 2002 (left) and in 2012 (right) after vegetation encroachment.

3.8 Reservoir Effects

The reservoir water level was plotted by using data from USBR, 2021 in order to understand the longitudinal profiles (Figure 37) and aggradation / degradation effects (Figure 38) that have occurred in the Elephant Butte Reach. When the reservoir is filled there is a backwater effect that occurs. This causes water levels to rise upstream, decreasing sediment transport capacity of a river, leading to aggradation. When the reservoirs water level decreases the backwater effects diminish, depth decrease, velocity increases, sediment transport capacity increases, allowing for head cutting of deposited material to occur. These effects can change locations of delta formations and cause incision of the main channel.

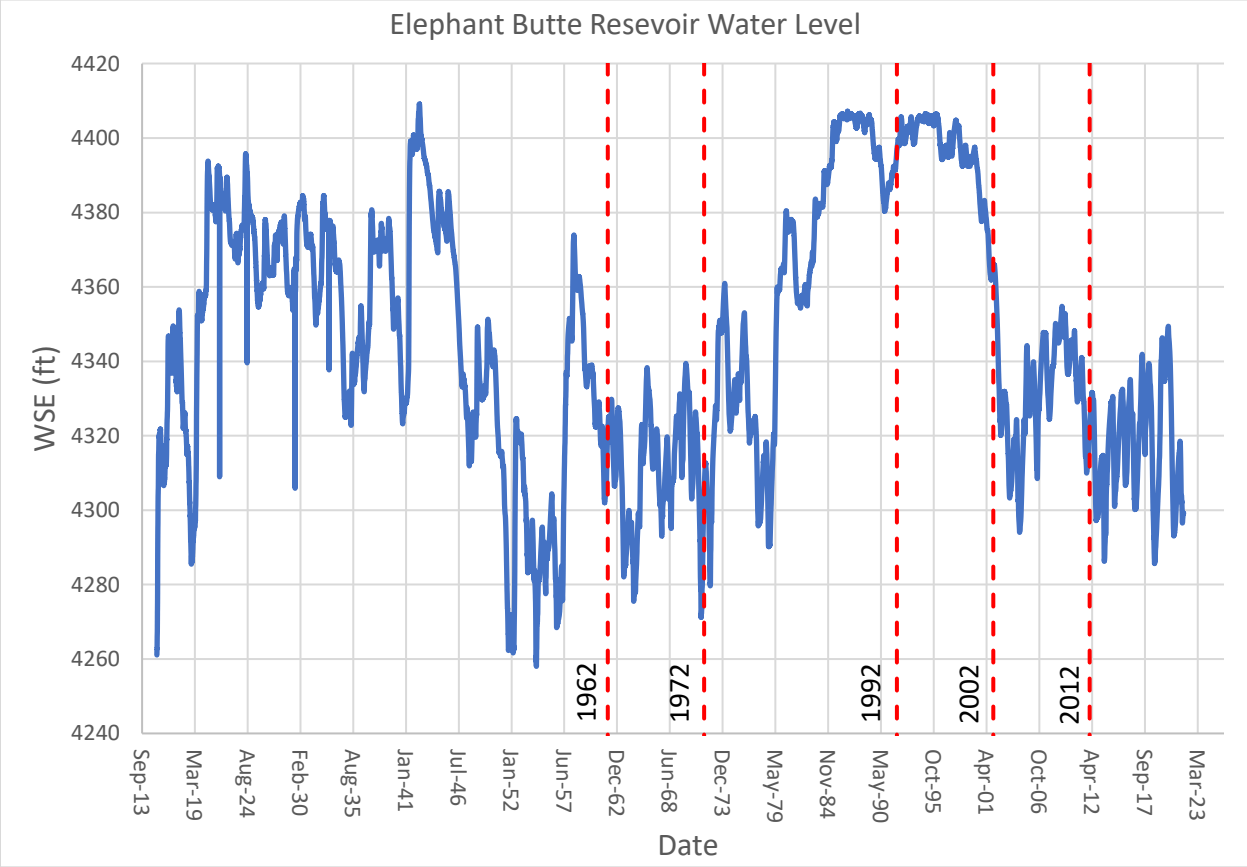

Figure 48 Elephant Butte Reservoir Water Level (USBR, 2021)

As seen in Figure 48 between 1962 and 1972 that the reservoir water level stayed relatively constant. From 1962 to 1964 there is a drop in the reservoir water level then a rise. Relating this to the effect on the river, Figure 38 shows that there is degradation of the main channel in subreaches EB1 to EB4. This is due to the backwater effect shifting downstream. From 1972 to 2002 there is around a 120-foot rise in the reservoir water level. Figure 38 shows that there is a large amount of aggradation occurring where close to the reservoir there is a larger amount of sediment deposition. This allows a delta to form and backwater effects to propagate upstream. Then post 2002 the reservoir water level decreases around 90 feet. This leads to a large amount of head cutting to propagate upstream (Figure 38) leading to an increase in hydraulic depth and required discharge (Figure 62) to achieve 25% of the cross section to overtop.

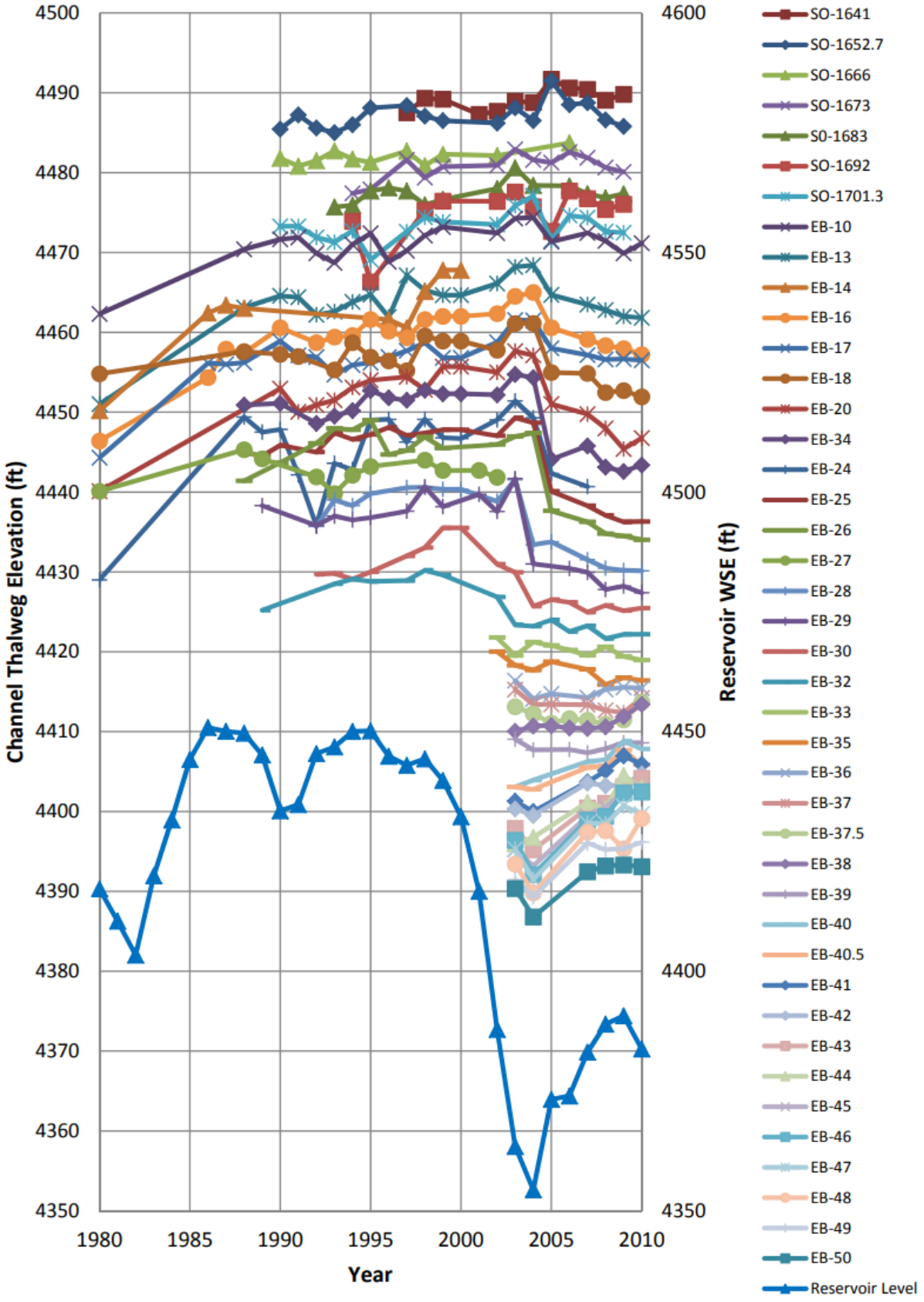

Figure 49 Elephant Butte Reservoir water surface elevation (WSE) over time compared to Elephant Butte narrows range line elevations over time (Owen, 2012)

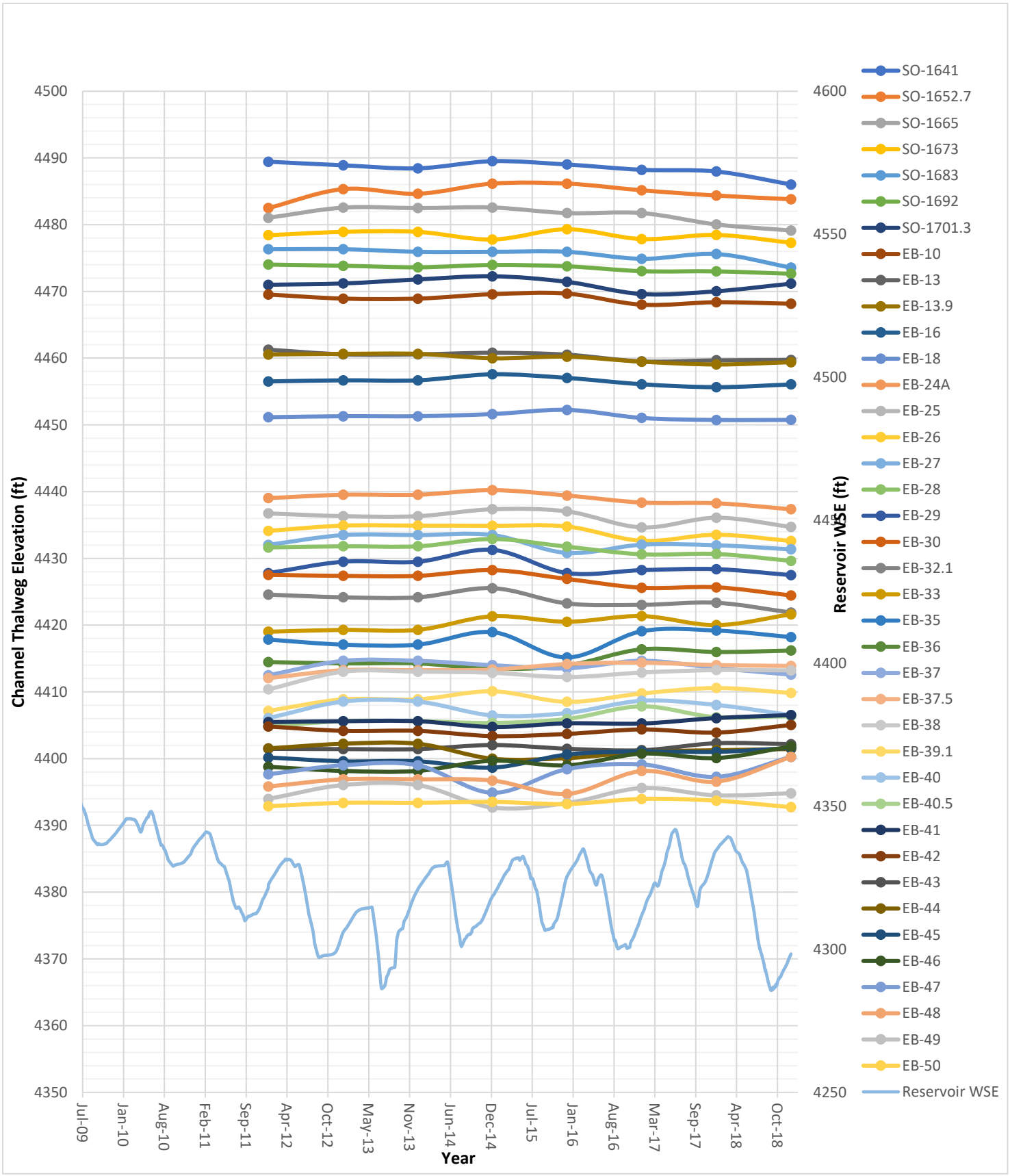

Figure 50 Elephant Butte Reservoir water surface elevation (WSE) over time compared to Elephant Butte narrows range line elevations over time

Figure 49 and Figure 50 shows what is occurring in the 6th subreach and how each EB reservoir range line changes compared to the fluctuation of the Elephant Butte Reservoir water level through time. When the reservoir water level rises there is an increase in the EB reservoir range line elevations. From 1982 to 1995 there is a large increase in the reservoirs water surface elevation (WSE). The reaction is also true for the EB range lines which also increased. From 2002 to 2004 there is a decrease in the Elephant Butte WSE where the range line's elevations closer to the reservoir EB-27 to EB-32 decrease sooner. This shows that the effect of incision propagates upstream and is not felt equally through the whole reach. This is also shown in Figure 38, where the lower subreaches have a greater amount of aggradation and degradation then subreaches farther upriver. After 2012 the reservoir water level fluctuates and stays close to the same WSE. The main channel elevation of the EB range lines also fluctuate a small amount. It can be concluded that the morphology of the river and the habitat has not changed all that much between 2012 and 2018 closer to the reservoir but there may still be head cutting occurring that is propagating upstream (Figure 50). This could mean that farther upstream the hydraulic depth is increasing, leading to a larger required discharge for floodplain inundation.

3.9 Channel Response Models

The Julien and Wargadalam (JW) equations were used to predict the downstream hydraulic geometry of rivers (Julien and Wargadalam, 1995). These equations were based on empirical analysis of over 700 single-threaded rivers and channels, and predicted the width and depth likely to result from a given discharge, grain size and slope:

$$h = 0.2Q^{\frac{2}{6m+5}}D_s^{\frac{6m}{6m+5}}S^{\frac{-1}{6m+5}}$$

$$W = 1.33Q^{\frac{4m+2}{6m+5}}D_s^{\frac{-4m}{6m+5}}S^{\frac{-1-2m}{6m+5}}$$

Where $m = 1/\left[2.3\log\left(\frac{2h}{D_s}\right)\right]$, h is the flow depth, W is the channel width, Q is the flow discharge, D_s is the median grain size, and S is the slope. A discharge of 3,000 cfs, the same discharge as in the previous HEC-RAS analysis, was used. The values for slope and grain size were obtained from 3.3 Bed Elevation and 3.4 Bed Material, respectively. Due to missing grain size data for every year, the median D_{50} with a (*) symbol indicates data that was that does not match the specified year in Table 1. If data was unavailable for the specific year presented in Table 1 it was attempted to keep the data used for the median D_{50} of 1992 within the 1990s, median D_{50} of 2002 within the 2000s, and median D_{50} of 2012 within the 2010s. The results are compared to the observed active channel widths (from the GIS analysis of the digitized planforms) in Table 4 and plotted in Figure 51. The percent difference was calculated as:

$$\text{Percent Difference} = 100 * \left(\frac{\text{predicted width} - \text{observed width}}{\text{observed width}}\right)$$

Table 4 Julien Wargadalam channel width prediction

Year	Subreach	D_s (mm)	Slope	Predicted Width (ft)	Observed Width (ft)	Percent difference
1992	EB1	0.167*	0.0006	266	394	266
	EB2	0.200*	0.0005	273	167	273
	EB3	0.194	0.0006	262	244	262
	EB4	0.186*	0.0005	270	107	270
	EB5	0.202*	0.0013	226	282	226
2002	EB1	0.172	0.0005	275	192	275
	EB2	0.200*	0.0005	277	136	277
	EB3	0.230	0.0004	280	212	280
	EB4	0.230	0.0005	277	100	277
	EB5	0.240	0.0005	274	171	274
2012	EB1	0.233*	0.0006	262	158	262
	EB2	0.200*	0.0005	269	121	269
	EB3	0.282*	0.0007	257	170	257
	EB4	0.161*	0.0005	271	91	271
	EB5	0.385*	0.0007	251	144	251

**See Table B-1 in Appendix B, for specific years used for D_{50} values.*

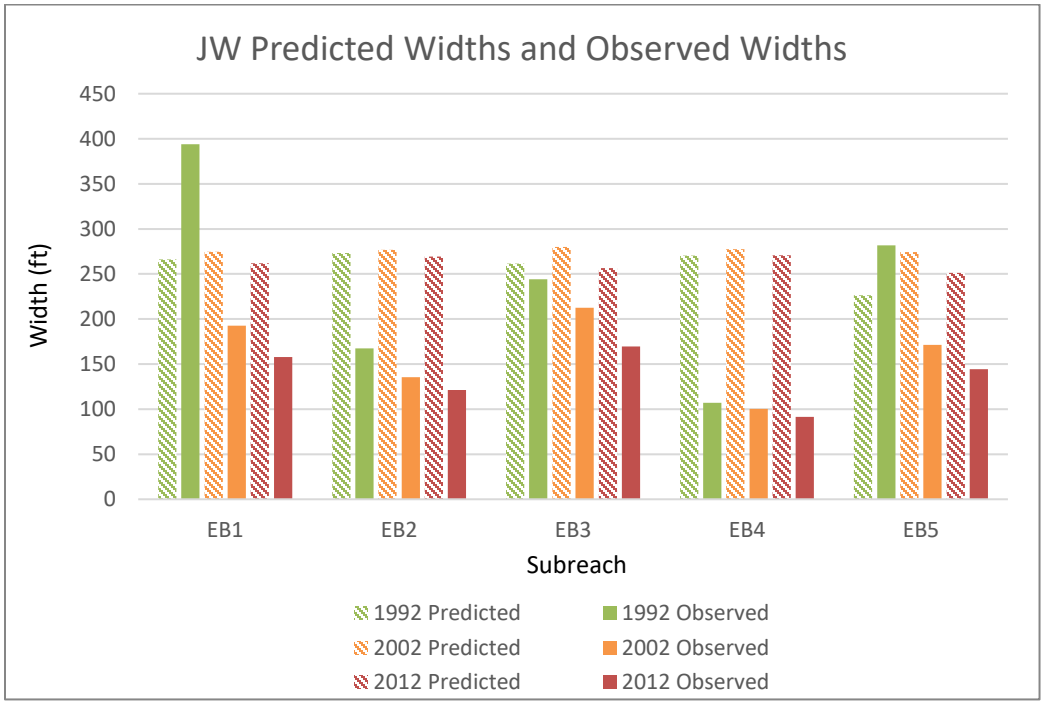

Figure 51 Julien and Wargadalam predicted widths and observed widths of the channel

The predicted JW widths are wider than the observed widths for all subreaches if the Elephant Butte Reach. In 1992 subreaches EB1 and EB5 observed widths were greater than the predicted widths. The JW equations predict that the channel width for all subreaches should be wider, 240 to 270 feet, than observed. When calculating the predicted width, the bankfull discharge was used, when in reality varying discharges would be occurring in the river. This could lead to the greater variability in the observed width values. It is important to note that the JW equations represent a river whose morpho dynamics are in equilibrium. The morpho dynamic equilibrium is assuming there would be no aggradation nor degradation occurring. The Elephant Butte Reach has been going through cycles of aggradation and degradation showing that the river is not in equilibrium and is continuously changing.

3.10 Geomorphic Conceptual Model

Massong et al. (2010) developed a channel planform evolution model for the Rio Grande based on historic observations. The sequence of planform evolution is outlined in Figure 45. Stage 1 describes a large channel with a high sediment load and large floods, which results in an active channel with constantly changing bars and dunes and little vegetation encroachment. The evolution from dunes to islands and bars transitions the river into Stage 2. As the islands and bars are stabilized by vegetation, they begin to act like floodplains indicating that the river is transitioning to Stage 3. The sediment transport capacity then becomes the determining factor of the future course of the river to either an aggrading river (stages A4-A6) or a migrating river (stages M-4 to M-8). A deficiency in sediment transport capacity, meaning the sediment supply is exceeding the transport capacity, leads to aggradation in the main channel and the flow eventually shifts onto the lower surrounding floodplain. When the sediment transport capacity exceeds the sediment supply, bank material erodes both laterally and vertically, leading to a meandering river. Transition between the M stages and the A stages can occur, but a reset to a Stage 1 requires a large, prolonged flood (Massong et al., 2010).

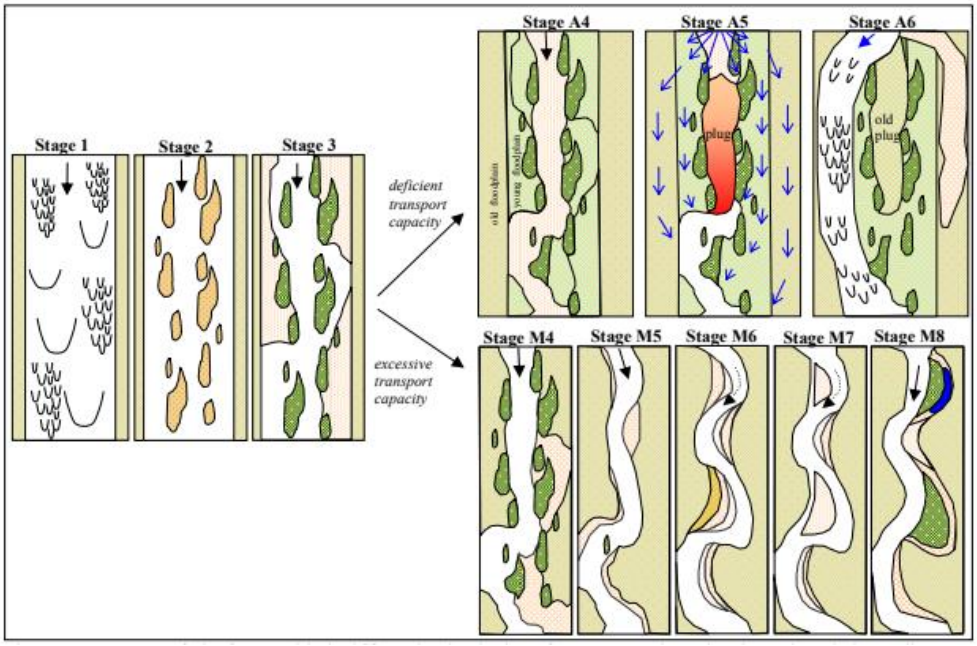

Figure 52 Planform evolution model from Massong et al. (2010). The river undergoes stages 1-3 first and then continues to stages A4-A6 or stages M4-M8 depending on the sediment transport capacity.

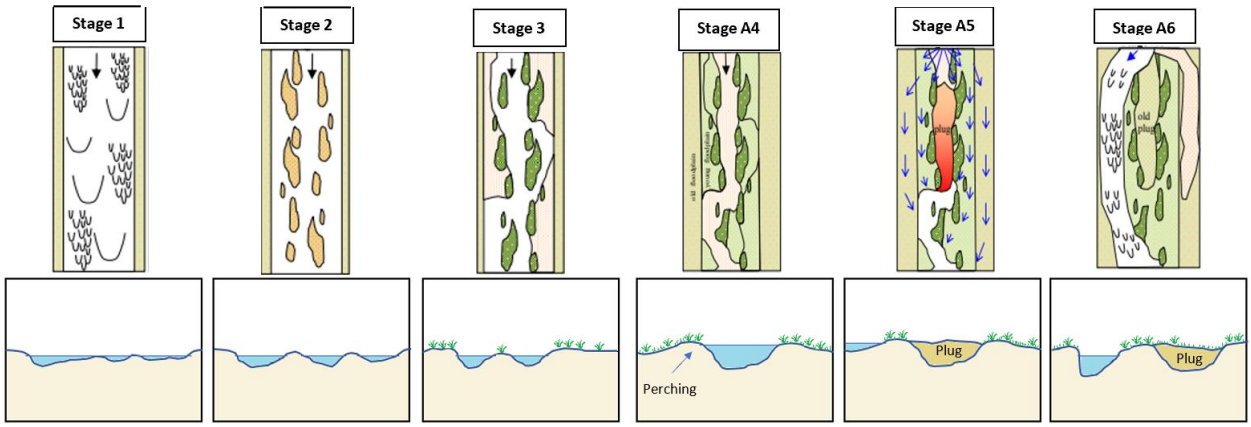

Figure 53 Planform evolution model from Massong et al. (2010) applied to channel cross sectional view (Schied et al., 2022).

Figure 53 give a glimpse of how a channel transitions from stage 1 to stage A6 where the channel avulses and changes locations laterally. The Elephant Butte Reach's aggrading stage happened between 1972 and 2002 when the reservoir water level increased as discussed. There have been plugs, like the Tiffany Plug, that have formed in the river indicating an A5 stage, but usually there is a pilot channel is cut in order for the river to not reach an A6 stage.

Comparisons between channel shifts and the channel slope of the MRG have indicated that transitions into the aggrading reach cycle have a slope of less than 0.0007 ft/ft, while transitions through the migrating reach stages have a slope greater than 0.0009 ft/ft (Massong et al., 2010). The Elephant Butte Reach has slopes ranging between 0.0004 and 0.001 within the analyzed time interval of 1962 to 2012, which has resulted in a river that can transition into either the aggrading or degrading reach stages. This is based on the transport capacity of the reach and if there is deposition or erosion of sediment.

The Elephant Butte Reach has previously had sediment plug studies performed on it by Shrimpton 2012. The Tiffany Plug is located about 1.5 miles upstream of the San Marcial Bridge (Shrimpton, 2012). Coupled with a very abrupt radial bend in the river just south of the San Marcial bridge, inducing backwater effects, led to the Tiffany Plug's formation (Shrimpton, 2012). When a plug forms in the river the Massong et al. planform evolutionary model stage is an A4 through A6. If left alone the channel will avulse and form a secondary channel. Pilot channels have been dug to prevent the river from avulsing and to encourage degradation of the built-up sediment. Shrimpton 2012, also indicates perching of the river to be occurring within Elephant Butte Reach by having natural levees form above the floodplain which causes disconnection of the floodplain to the main channel. These natural levees can be seen in the cross-sectional graphs Figures 55 through 64. Figure 54 is a picture of the Tiffany Plug and is a visual aid to stages A5 and A6 that are represented in the Massong et al. 2010 planform evolution model.

Figure 54 Downstream view of the 2005 Tiffany Plug (Owen et al., 2011)

A trend of aggradation indicates that the sediment supply exceeds the sediment transport capacity of the river. When degradation occurs, the sediment transport capacity exceeds the sediment availability. The cycle of aggradation / degradation is linked to the base level change in the reservoir stage (Section 3.8). "Width changes are more likely a result of vegetation growth due to keeping the river wet during summer months" (Baird, pers.comm.). Geomorphologically aggrading channels tend to widen where degrading channels the main channel narrows. The 2012 data set that was used is offset and may have used a different lateral scale. Shifts in cross sectional data does not mean the channel migrated. Arial imagery was used to determine how the channel has responded over time.

Figure 55 and Figure 56 show the evolution of the approximate midpoint of subreach EB1 along with aerial photos throughout time to accompany the data. Figure 55 shows the main channel has aggraded and narrowed overall from 1962 to 2012. Between 1972 and 2002 the main channel and floodplains aggraded. This deposition of sediment shows that the sediment supply exceeds the sediment transport capacity of the subreach leading to the banks perching, decrease in hydraulic depth, and a small increase in hydraulic width. The planform evolution model stages that best represent the channel for this period is an A4. The main channel has stayed relatively in the same location between the time interval of 1962 to 2002, with the 2012 data seeming to be shifted. Between 2002 and 2012 there is channel incision due to the drop in reservoir level (section 3.8, Figure 48) giving the river the evolutionary model stage of an M4. The sediment transport capacity exceeds the sediment supply from 2002 to 2012 causing the observed incision. Between this period the natural levees remain, increasing the hydraulic depth, which reduces the overbanking potential. The cross section shows the cycle of degradation (1962 to 1972, stage 3), to aggradation (1972 to 2002, A4), back to degradation of the main channel but aggradation / deposition of sediment on the banks (2002 to 2012, A4 overbank, M4 main channel).

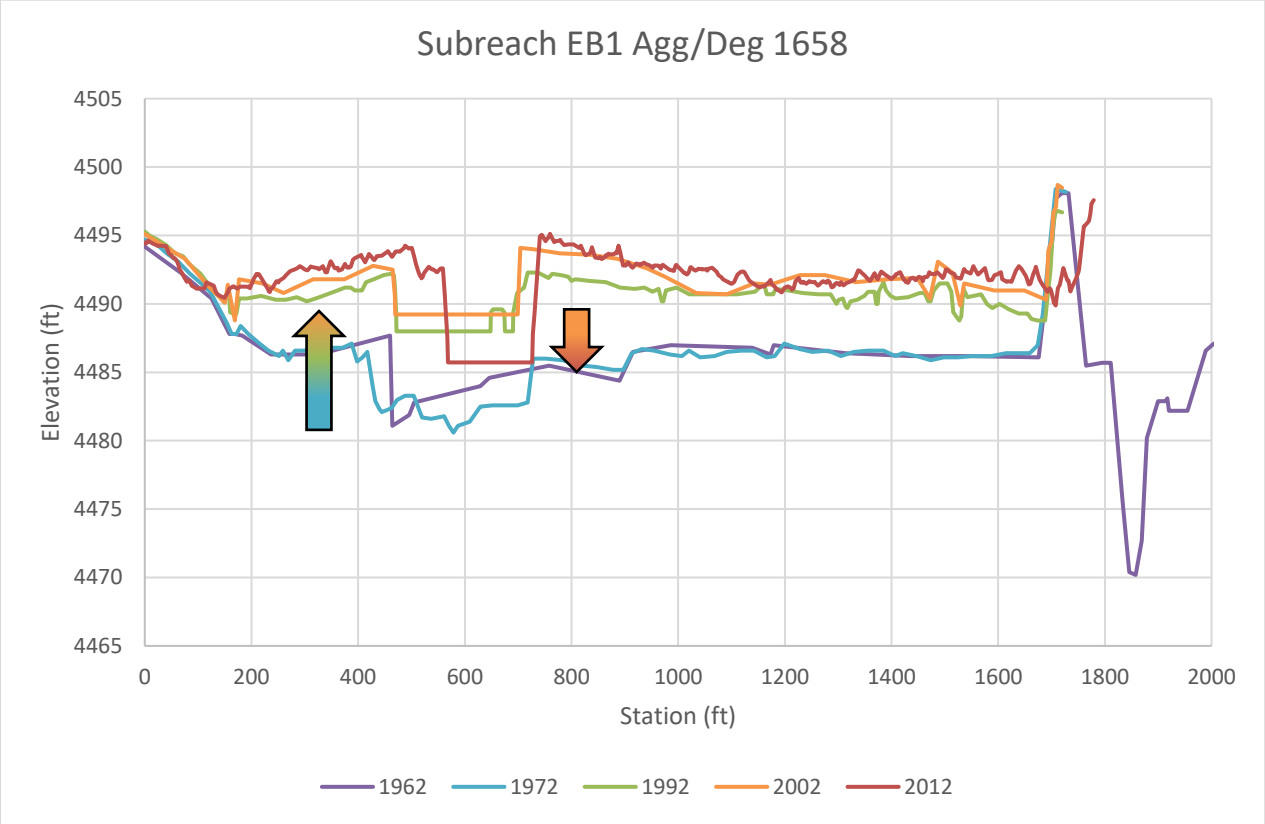

Figure 55 Channel evolution of a representative cross section from subreach EB1

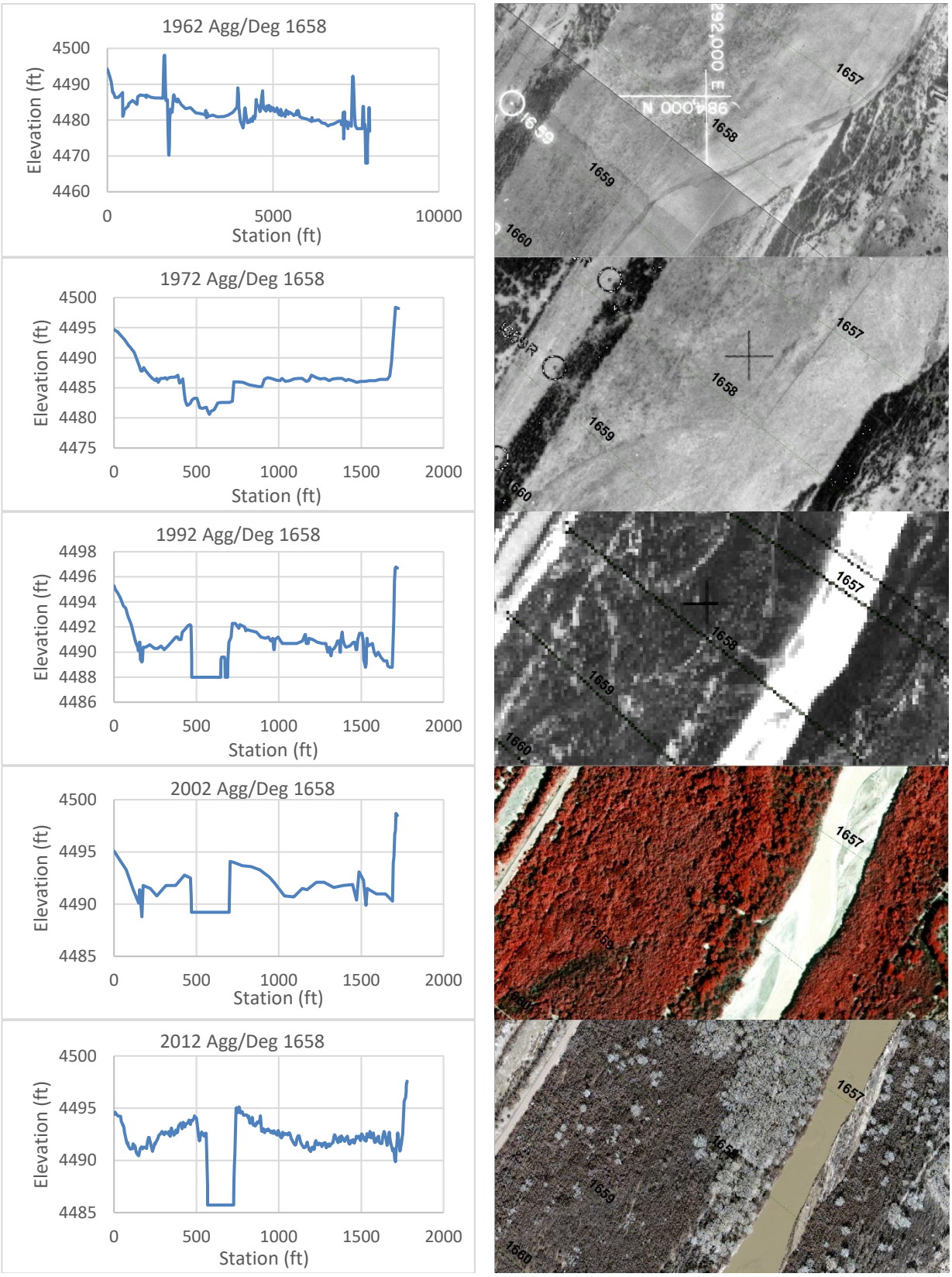

Figure 56 Subreach EB1: historical cross section profiles and corresponding aerial images

Subreach EB2 has had a lot of activity and has change over the time interval of 1962 to 2012. The river has seen major aggradation and degradation, hydraulic depth change, and perching. Subreach EB2 shows that the river sediment capacity was exceeded causing the river to deposit sediment from 1972 to 2002. This caused a large amount of sediment deposition onto the banks creating perching of the channel, creating natural levees. The main channel filled with sediment as well, decreasing the hydraulic depth. This would indicate that sediment supply exceeded the rivers transport capacity. The river shows slight migration between 1972 and 1992. The stages displayed here indicates stage 3 and A4, thus showing slight signs of lateral migration and aggradation of the main channel. From 2002 to 2012 the river starts to incise and changes to a degrading state. When the main channel incises, the natural levees stay, and the required flow rate to achieve bankfull increases. From 2002 to 2012 the evolutionary model stage present is an M4 stage where the transport capacity of the river exceeds the sediment supply. It is important to note that the Tiffany Plug did occur in EB2 in 1991, 1995, and 2005 (Shrimpton, 2012). There may be no indications of evulsion due to pilot channels that were dug to prevent the river from changing locations. The cross section shows the cycle of degradation (1962 to 1972, stage 3), to aggradation (1972 to 2002, stage 3 migrating, A4 main channel), back to degradation of the main channel but aggradation / deposition of sediment on the banks (2002 to 2012, A4 overbank, M4 main channel). The cross-section profile is shown in Figure 57 and a side-by-side view of the cross section and aerial imagery is shown in Figure 58.

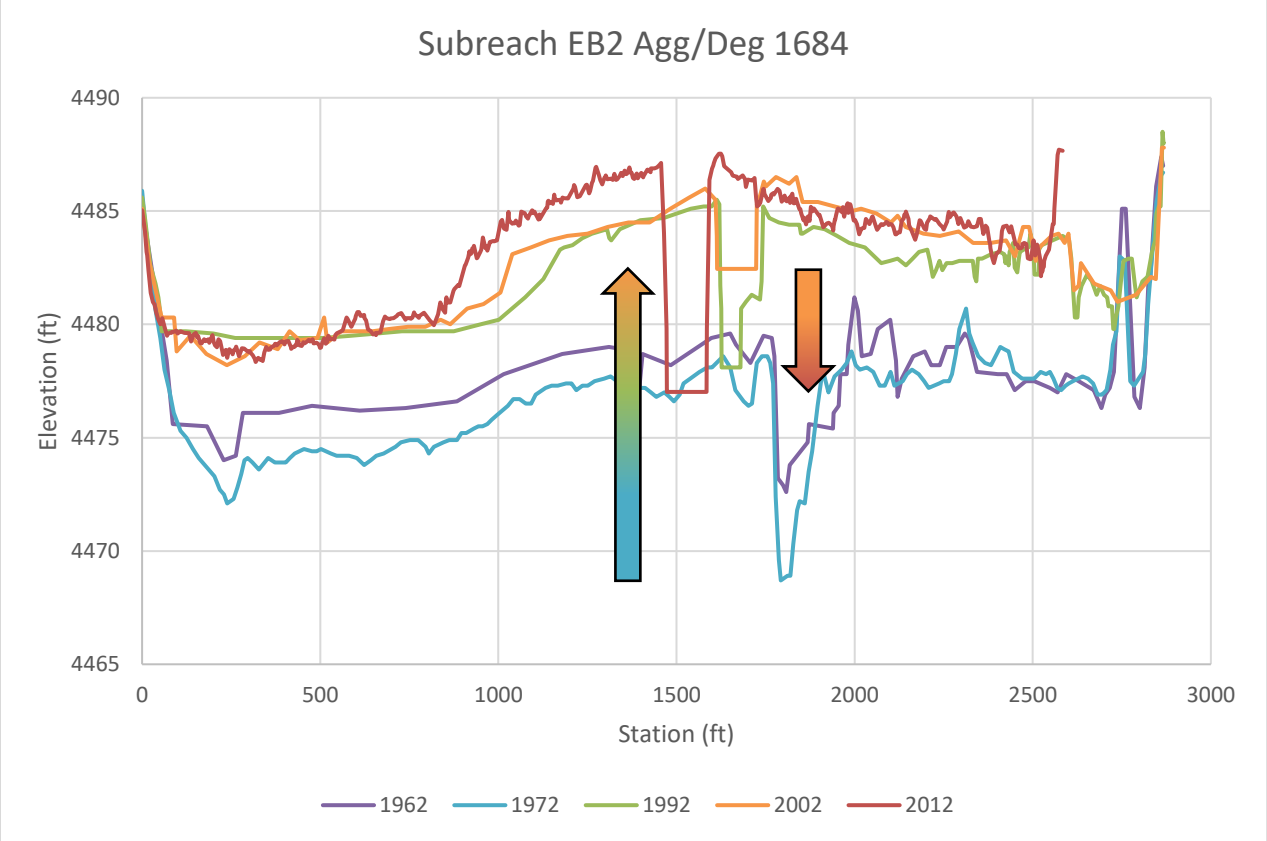

Figure 57 Channel evolution of a representative cross section from subreach EB2

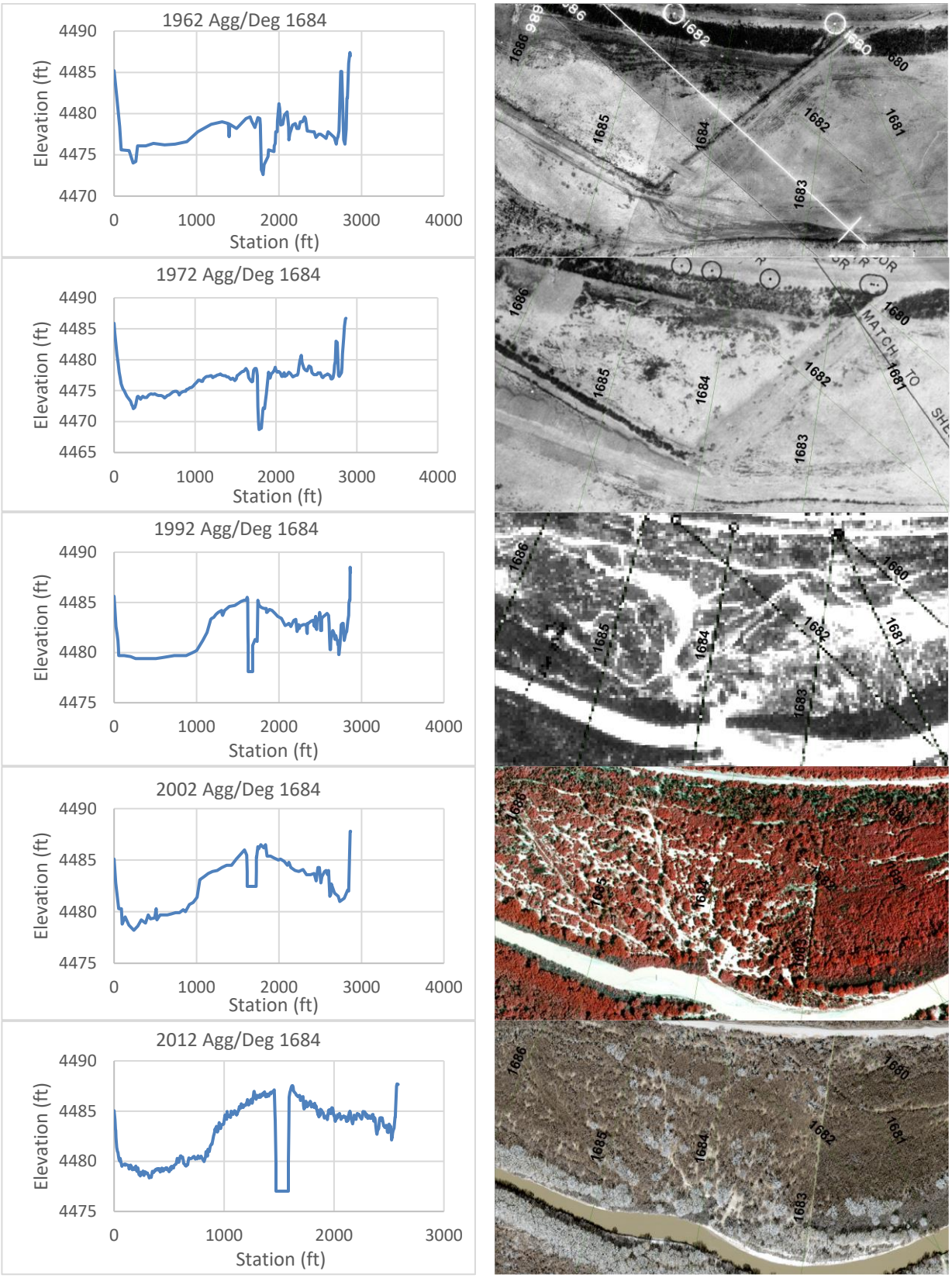

Figure 58 Subreach EB2: historical cross section profiles and corresponding aerial images

Figure 59 shows that subreach EB3 has laterally migrated a large amount between 1972 and 1992. This indicates that this portion of the channel went from M4 to A6 (Figure 59). The channel incised between 1962 and 1972 showing a stage M4. Then from 1972 to 1992 there may have been a plug that formed where the main channel migrated showing A5 to A6 behavior or this could have been cause by a channel realignment. Similarly, to subreach EB2, the sediment supply exceeded the river's transport capacity between 1992 and 2012 causing aggradation and perching to occur. Natural levees are formed from sediment being deposited on the banks of the channel, which is indicative of stage A4 behavior. Subreach EB3 has held the highest sinuosity value of every subreach which is attributed to the bend in the river that occurs (Figure 40 & 47). From 2002 to 2012 the river switches to a degrading state due to the decrease in reservoir level (Section 3.8). As the main channel incises, the natural levees that were built up stay, which increases the hydraulic depth and the required flow rate to reach bankfull discharge. The cross section shows the cycle of degradation (1962 to 1972, stage 3), to aggradation (1972 to 2002, stage 3 migrating, A4 main channel), back to degradation of the main channel but aggradation / deposition of sediment on the banks (2002 to 2012, A4 overbank, M4 main channel). Figure 60 shows the cross-section profile for the various years along with a corresponding aerial image of the river.

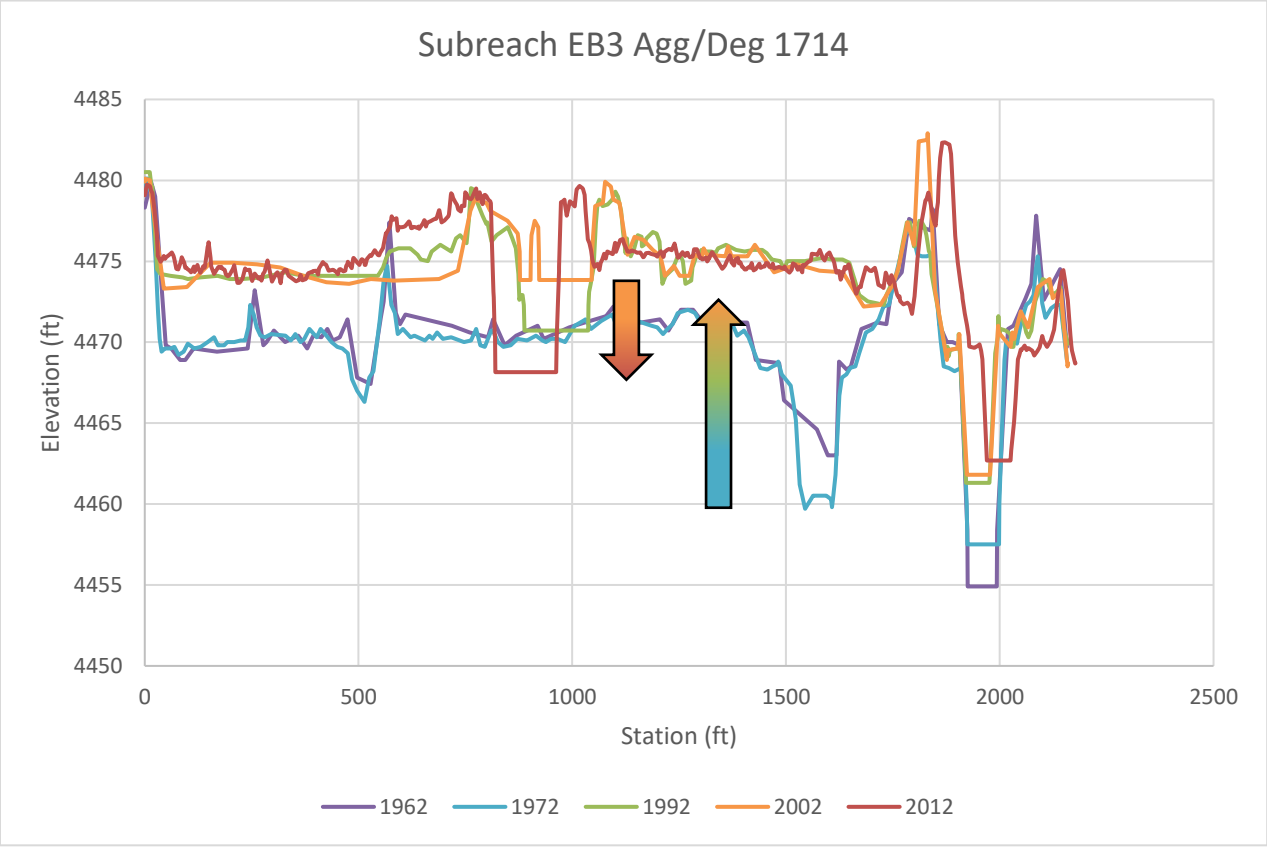

Figure 59 Channel evolution of a representative cross section from subreach EB3

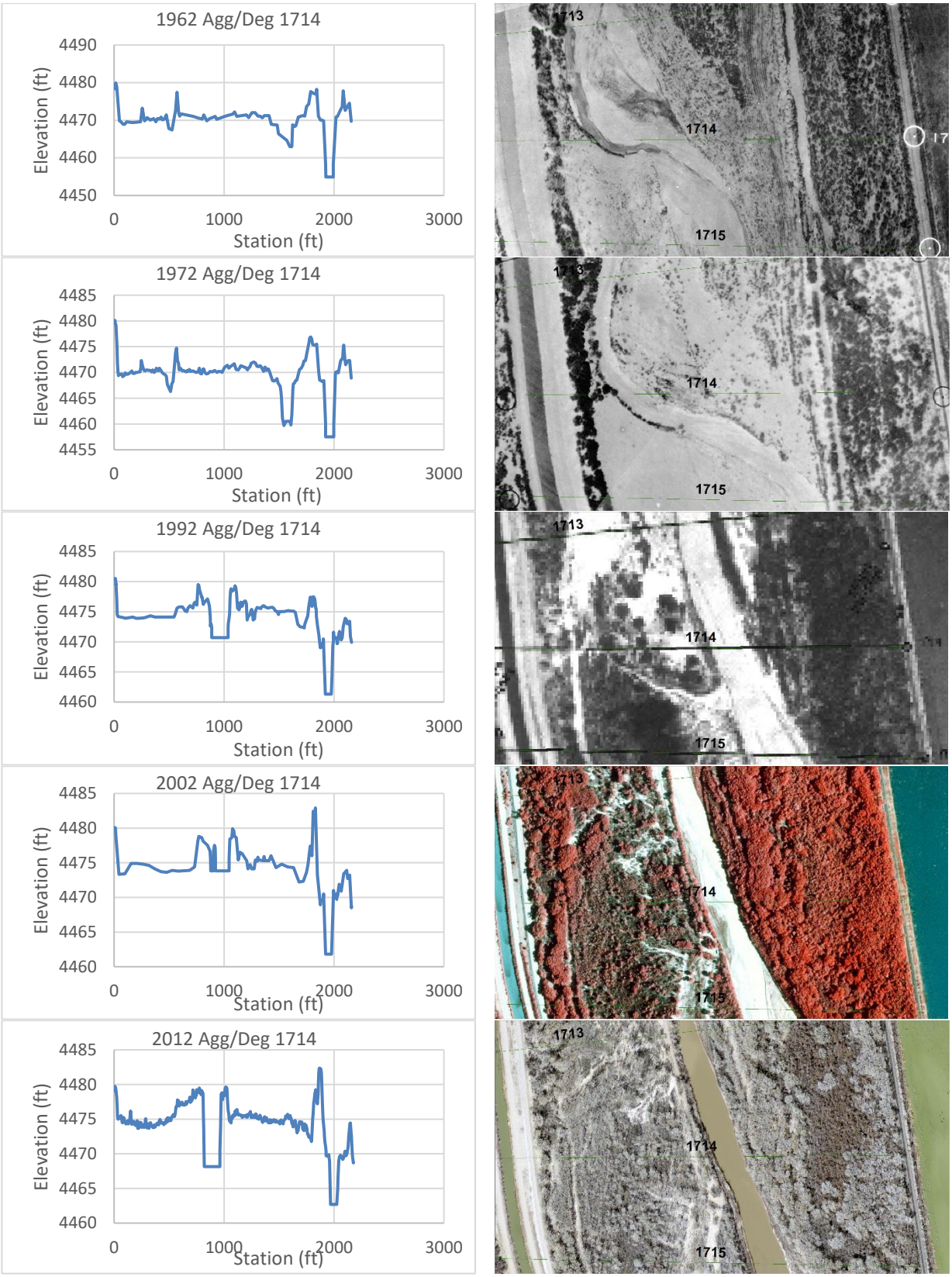

Figure 60 Subreach EB3: historical cross section profiles and corresponding aerial images

Subreach EB4 seems to indicate a perfect example of extreme perching (stages A4). There is a large deposition of sediment which is increasing the bed elevation of the main channel and decreasing the hydraulic depth. This indicates that there is a deficiency of transport capacity of sediment, and sediment is being deposited onto the banks. Between 1962 and 1972 the channel incises showing an M4 stage. After this the channel transitions to an aggradation state, stage A4, from 1972 to 2002. After 2002 the river switches back to degrading state where the main channel is incising. When the river incises the natural levees that were built up previously stay but the hydraulic depth increases. The effect is that the required flow rate to achieve bankfull increases. The cross section shows the cycle of degradation (1962 to 1972, stage 3), to aggradation (1972 to 2002, A4), back to degradation of the main channel but aggradation / deposition of sediment on the banks (2002 to 2012, A4 overbank, M4 main channel). As seen in Figure 61 and Figure 62, the channel in 1992 the channel had aggraded but did not become fully plugged with sediment until 2002-2012. The cycle of degradation and aggradation is tied to reservoir water level as discussed in Section 3.8.

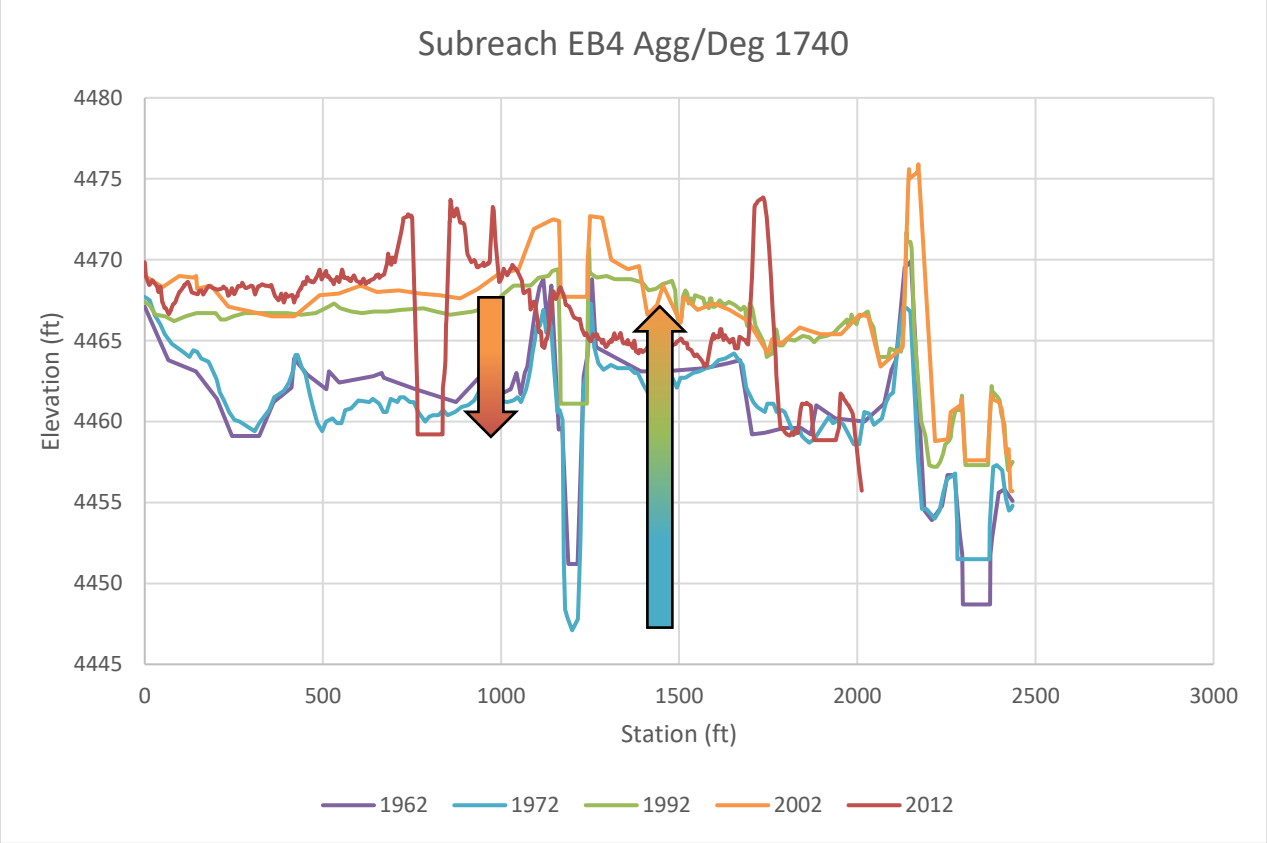

Figure 61 Channel Evolution of a representative cross section of subreach EB4

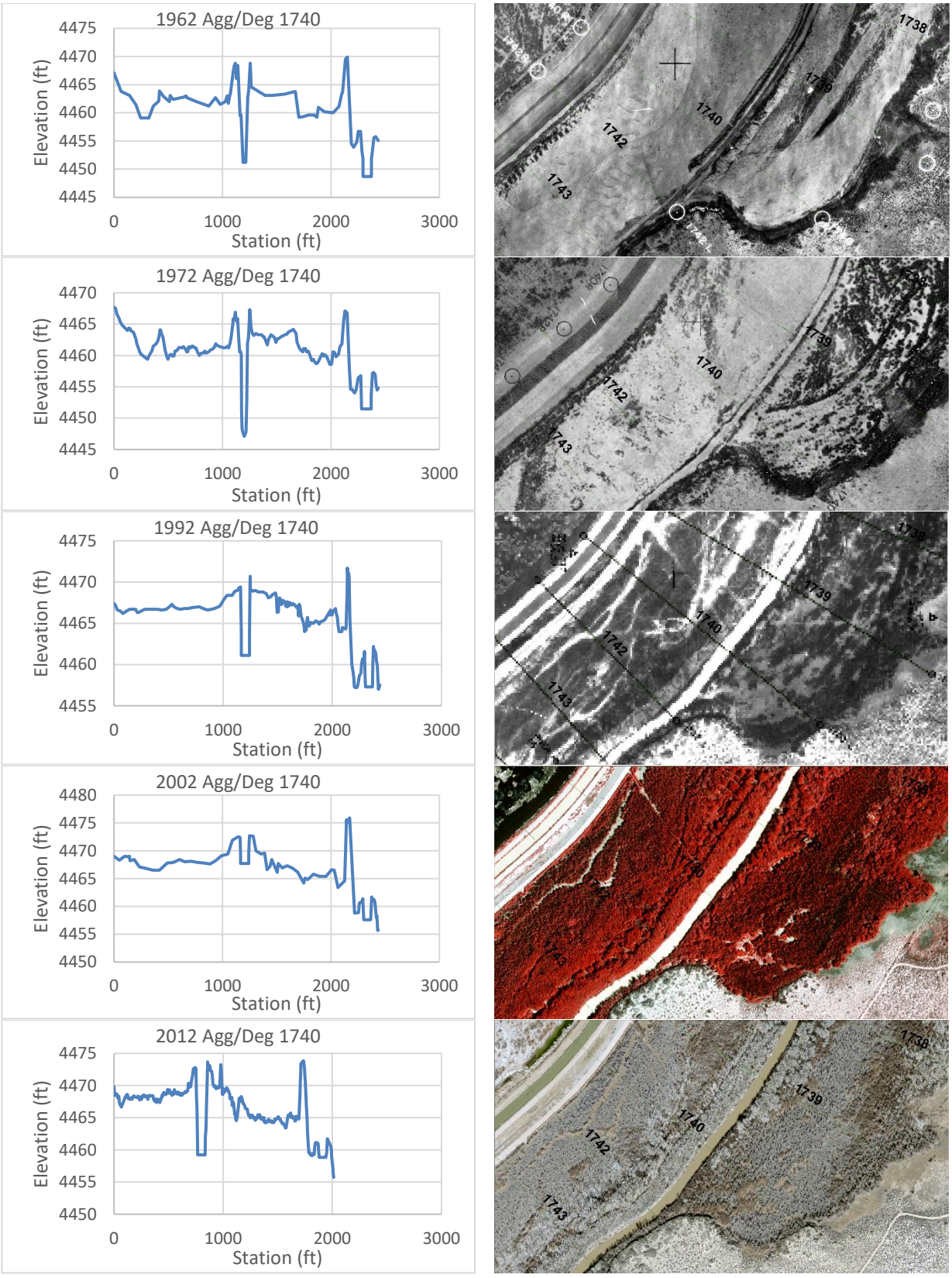

Figure 62 Subreach EB4: historical cross section profiles and corresponding aerial images

Subreach EB5 displays very similar characteristics as EB4 where the channel displays the evolutionary model stages of 3, A4, and M4. From 2962 to 1972 there is very little change in the river's geometry. From 1972 to 2002 the cross-sectional view shows aggradation of the main channel. The banks then become perched between 1992 and 2002 and the main channel is aggraded even more. This ultimately shows the channel is in an A4 state. The sediment supply exceeds the river's transport capacity causing a trend of aggradation and the river to show an A4 stage. From 2002 to 2012 the river switches to a degrading state due to the reservoir water level decreasing (Section 3.8). The main channel incises but the natural levees that were built up remain. This causes the required flow rate to reach bankfull to increase. The cross section for 2012 shows extreme perching. The cross section shows the cycle of aggradation (1972 to 2002, A4), to degradation of the main channel but aggradation / deposition of sediment on the banks (2002 to 2012, A4 overbank, M4 main channel). The imagery and cross-sectional views for each year can be seen in Figure 63 and 64.

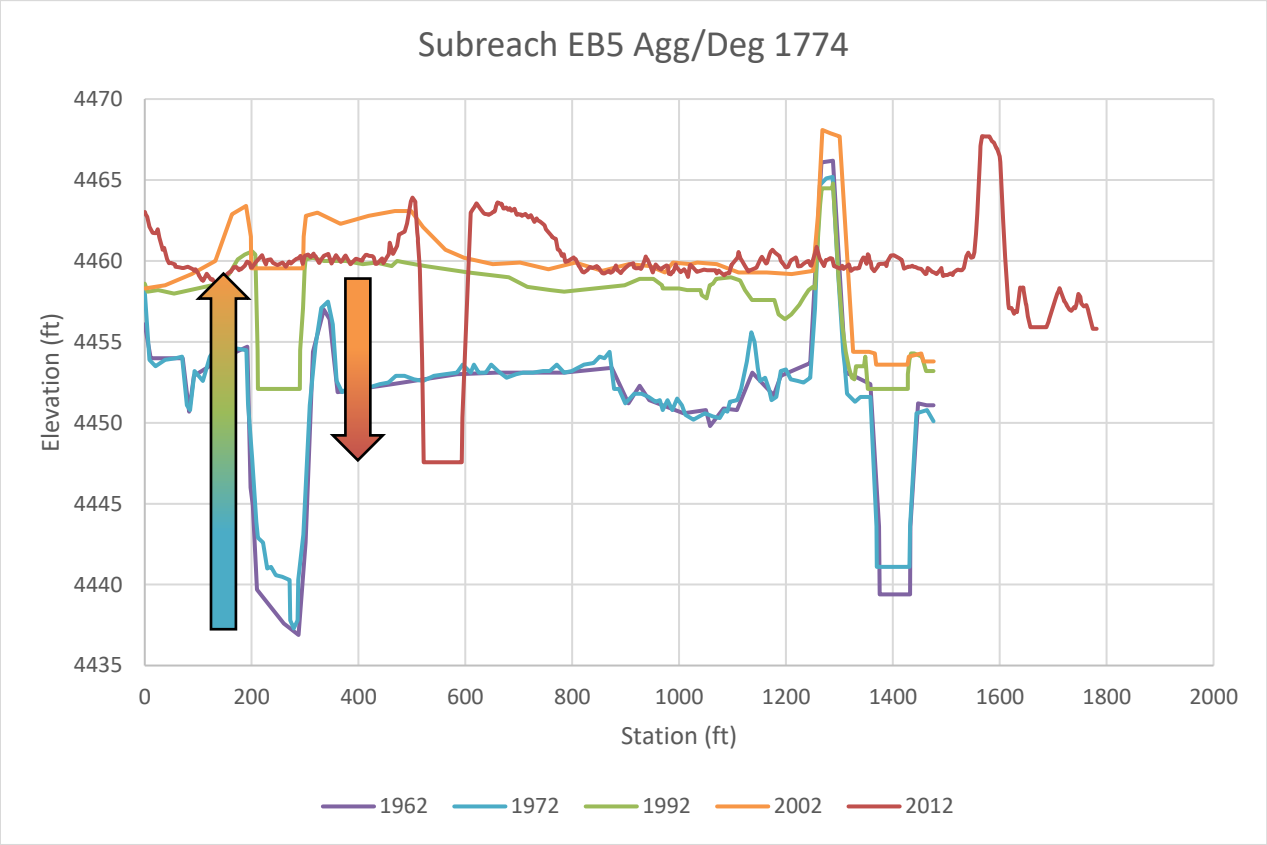

Figure 63 Channel evolution of a representative cross section of subreach EB5

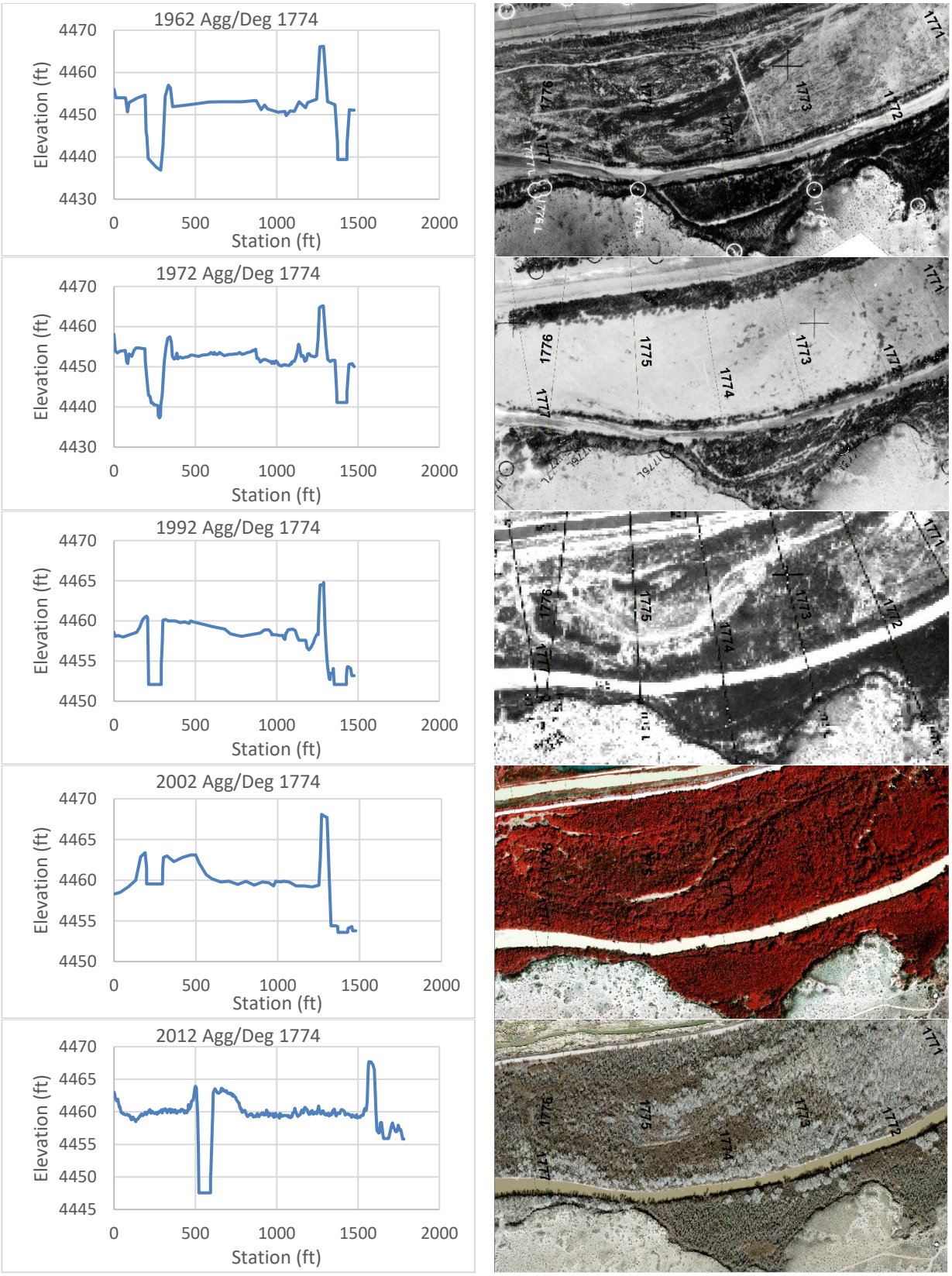

Figure 64 Subreach EB5: historical cross section profiles and corresponding aerial images

4. HEC-RAS Modeling for Silvery Minnow Habitat

The Rio Grande Silvery Minnow (RGSM or silvery minnow) is an endangered fish species that is native to the Middle Rio Grande. Currently, it occupies only about seven percent of its historic range (U.S. Fish and Wildlife Service, 2010). It was listed on the Endangered Species List by the US Fish and Wildlife Service in 1994.

One of the most important aspects of silvery minnow habitat is the connection of the main channel to the floodplain. Spawning is stimulated by peak flows in late April to early June. These flows should create shallow water conditions on the floodplains, which is ideal nursery habitat for the silvery minnow (Mortensen et al., 2019). Silvery minnows require specific velocity and depth ranges depending on the life stage that the fish is in. Table 5 outlines these velocity and depth guidelines. Fish population counts are available prior to 1993 to the present. Therefore, analysis of silvery minnow habitat will not begin prior to 1992. In preparation for the process linkage report, figures relating the geomorphology of the river and RGSM habitat availability are included in Appendix F.

Table 5 Rio Grande Silvery Minnow habitat velocity and depth range requirements (from Mortensen et al., 2019)

	Velocity (cm/s)	Velocity (ft/s)	Depth (cm)	Depth (ft)
Adult Habitat	<40	<1.31	>5 and <60	>0.16 and <1.97
Juvenile Habitat	<30	<0.98	>1 and <50	>0.03 and <1.64
Larvae Habitat	<5	<0.16	<15	<0.49

4.1 Modeling Data and Background

The data available to develop these models varies year by year. Cross section geometry was available for the years 1962, 1972, 1992, 2002, and 2012. In 2012, additional LiDAR data of the floodplain was available, which allowed the development of a terrain for RAS-Mapper. Therefore, RAS-Mapper was used in 2012 only, while comparisons across years are done using 1-D techniques.

HEC-RAS distributes water within the channel by filling each available cross section from the lowest elevation upwards. Much of the MRG is perched, so this can lead to inaccurate predictions of the flow distribution within the cross sections (overpredicting water in the floodplains), therefore, overpredicting hydraulically suitable habitat. Computational levees were used in HEC-RAS to keep the water contained in the channel until bankfull is reached. At the discharge that this occurs, the computational levees were removed to allow water to fill the floodplains from the lowest elevations up. The computational levees are removed at the same discharge throughout the entire reach. This method is described by Holste (2020) which is applied in HEC-RAS by using the cross-sectional data points to determine the “left top of bank” and “right top of bank”. Then the difference between water surface elevation and computational levee elevation can be found. A negative value indicates an overtopping discharge. A sensitivity analysis was completed to determine the percentage of cross sections that should be overtopped before removing the top of bank (TOB) points in HEC-RAS. For this analysis, when 25% of the cross sections in the reach were experiencing overtopping, also signifying 25% of the cross sections had reached bankfull discharge, the computational levees were removed. It is estimate that when about 25% Agg/Deg line banks are overtopped there is sufficient flow to inundate the floodplain from the perched channel. When the computational levees are removed, the flow is not constrained to main channel when filling from the

bottom up allowing for floodplain to be inundated before the channel reaches bankfull. The results from the levee freeboard analysis are shown in Figure 65.

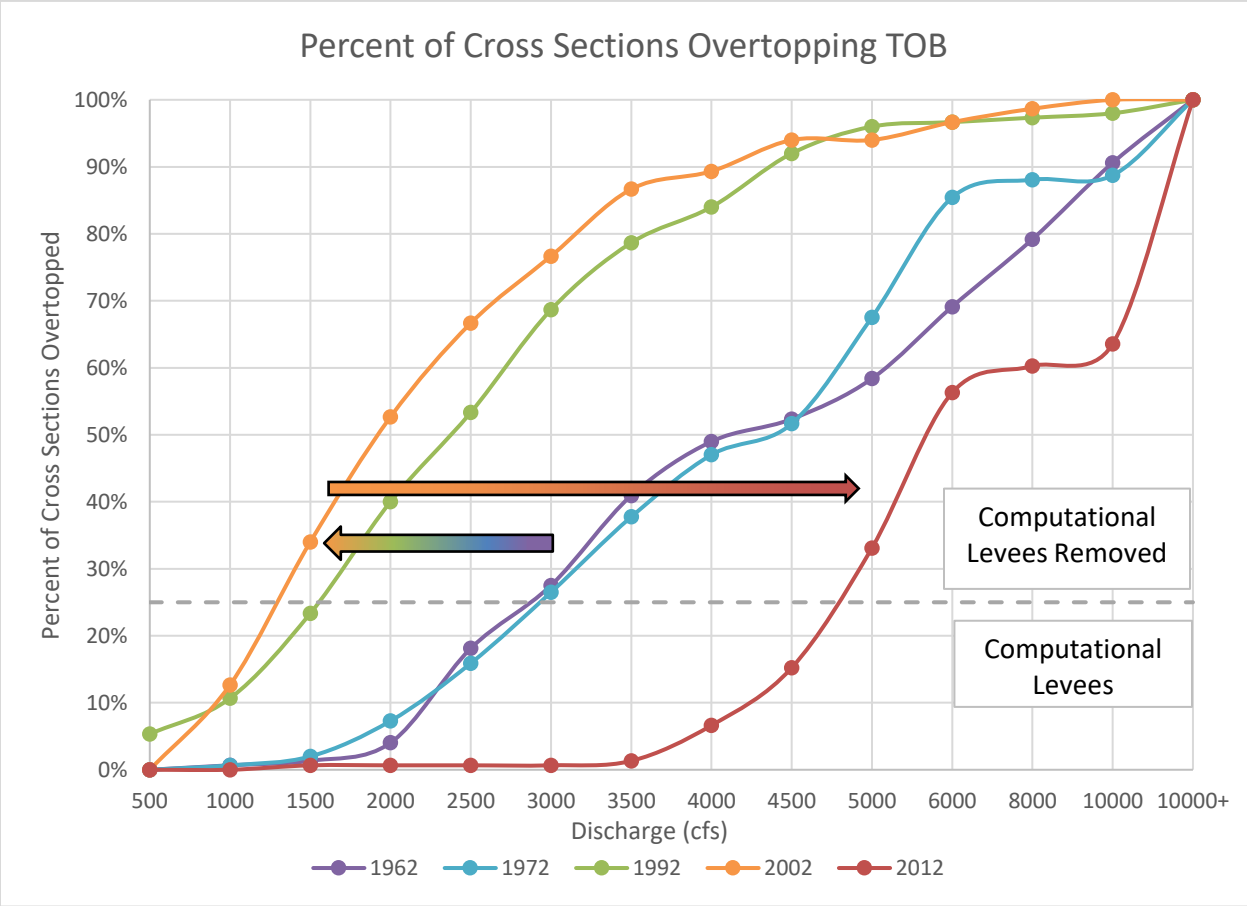

Figure 65 Comparing the overbanking discharge values at various years. The dashed line (indicating 25% of cross sections in a reach experiencing overbanking) determines the discharge at which computational levees are removed for habitat analysis.

Figure 65 shows the effect of the aggradation / degredation cycle that is present in the Elephant Butte Reach. As seen in the cross sectional graphs in Section 3.10, the aggradation / degradation will have a large effect on the required flow for overtopping. From 1962 to 1972 there is only a small amount of overal degradation within the reach, which doesn't change the required flow a lot. From 1972 to 2002 there is a large amount of depositon of sediment, decreasing the hydraulic depth and increasing the amount of perching that occurs. The required flow for 25% overtopping in 1992 and 2002 is around 1,500 cfs. From 2002 to 2012 the reservoir water level drops (Section 3.8) causing the channel to incise. Since the natural levees that were built up remain and the hydrualic depth increases the required flow rate for overtopping increases. The required flow rate in 2012 for 25% overtopping is close to 5,000 cfs.

4.2 Width Slices Methodology

Without a terrain for 2002 and 1992, additional methods had to be considered to determine a metric of fish habitat in area per distance and in length of river. HEC-RAS has the capability to perform a flow distribution analysis to calculate the laterally varying velocities, discharges, and depths throughout a cross section as described in chapter 4 of the HEC-RAS Hydraulic Reference Manual (US Army Corps of

Engineers, 2016). HEC-RAS allows each cross-section to be divided into 45 slices. Because the RGSM relies heavily on floodplains for habitat (due to higher velocities and depths in the main channel) and the floodplains contain more variability than the main channel, 20 width slices were assigned in each floodplain and 5 width slices in the channel. An example of the flow distribution in a cross-section is shown in Figure 66. The velocity and depth of each slice were analyzed to determine the total width at each agg/deg line that meets the RGSM larval, juvenile, and adult criteria. Because the agg/deg lines are spaced approximately 500 feet apart, the hydraulically suitable widths were multiplied by 500 feet to obtain an area of hydraulically suitable habitat per length of river.

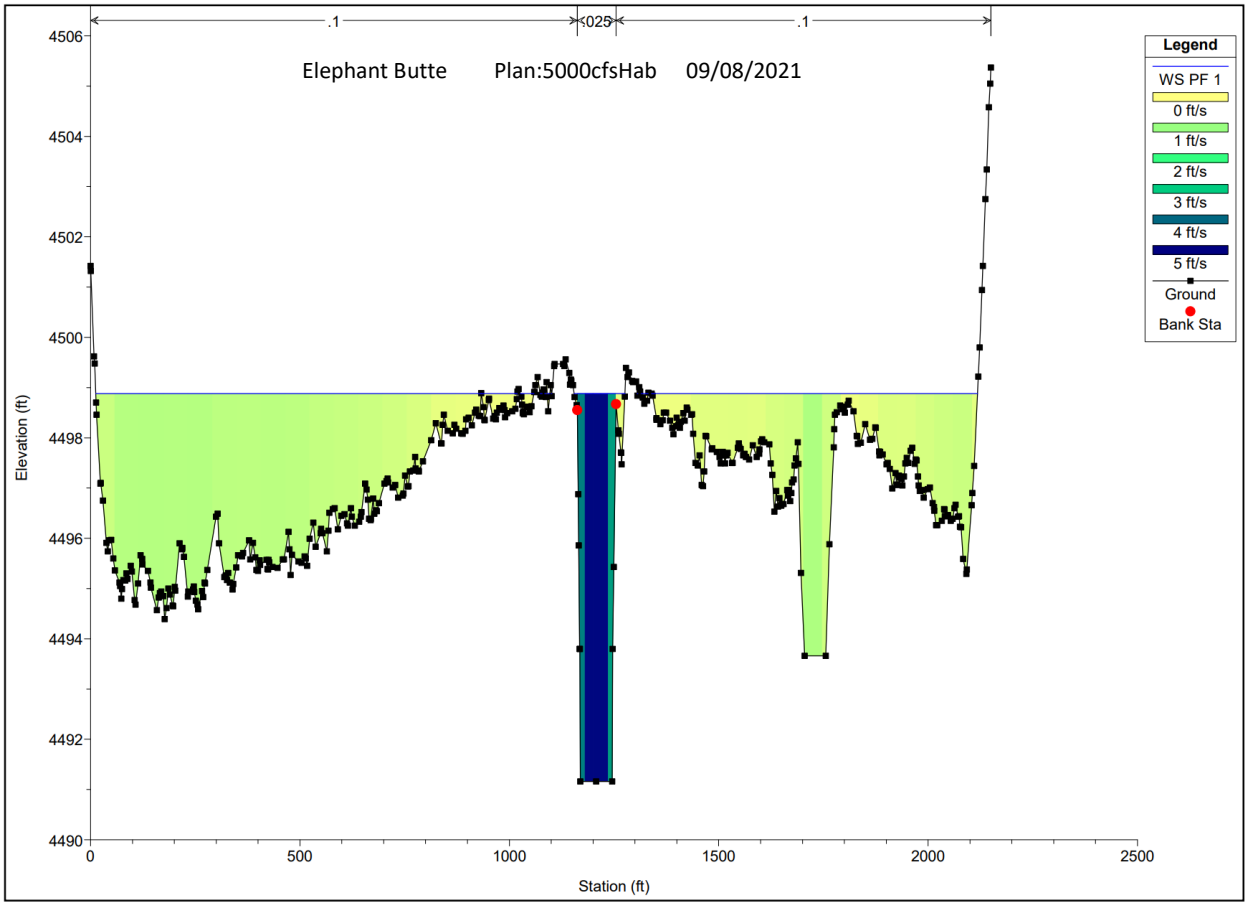

Figure 66 Cross-section with flow distribution from HEC-RAS with 20 vertical slices in the floodplains and 5 vertical slices in the main channel. The yellow and green slices are small enough that the discrete color changes look more like a gradient.

4.3 Width Slices Habitat Results

The width slices method was first used to analyze the habitat availability throughout the Elephant Butte Reach at a reach scale for the years of 1962, 1972, 1992, and 2002. For the discharges at which the water is contained in the main channel, there is less habitat availability. At low discharges, such as 500 cfs, the depth and velocity in the channel remain low enough to provide suitable areas for the Rio Grande Silvery Minnow (RGSM). However, as the discharge increase (but flow is still maintained in the channel) the amount of habitable area that meets the depth and velocity criteria for the Silvery Minnow decreases. When the discharge increases and the water can spill out onto the floodplains, there is suddenly an increase in area where the depth and velocity criteria are met. This is displayed by Figures 67 to 69.

Throughout the Elephant Butte Reach, the results follow the same general pattern for larvae, juvenile, and adult stage habitat. The drastic shift in habitat availability from 1972 to 1992 is due to the channel showing signs of rapid aggradation. The overall trend that the Elephant Butte subreach showed is perching of the banks creating a disconnection of the main channel to the floodplain. This means that as the hydraulic depth of the channel decreases, over topping occurs at lower discharges, which leads to an earlier spike in habitat availability. Once the depth or velocity becomes too high due at higher discharges, the hydraulically suitable habitat availability decreases. In 2012 the habitat availability doesn't increase until 5,000 cfs where the channel has reached 25% bankfull (Figure 65). From 2002 to 2012 there is a large amount of incision causing the required flow rate for floodplain inundation to increase (Figure 37). It is important to note that Figures 67 through 69 accounts for all subreaches in 2012, EB1 through EB6. From 1962 to 2002 subreach EB6 is not included due to unavailable cross-sectional data. Therefore, 2012 will have a much higher available habitat than the rest of the years.

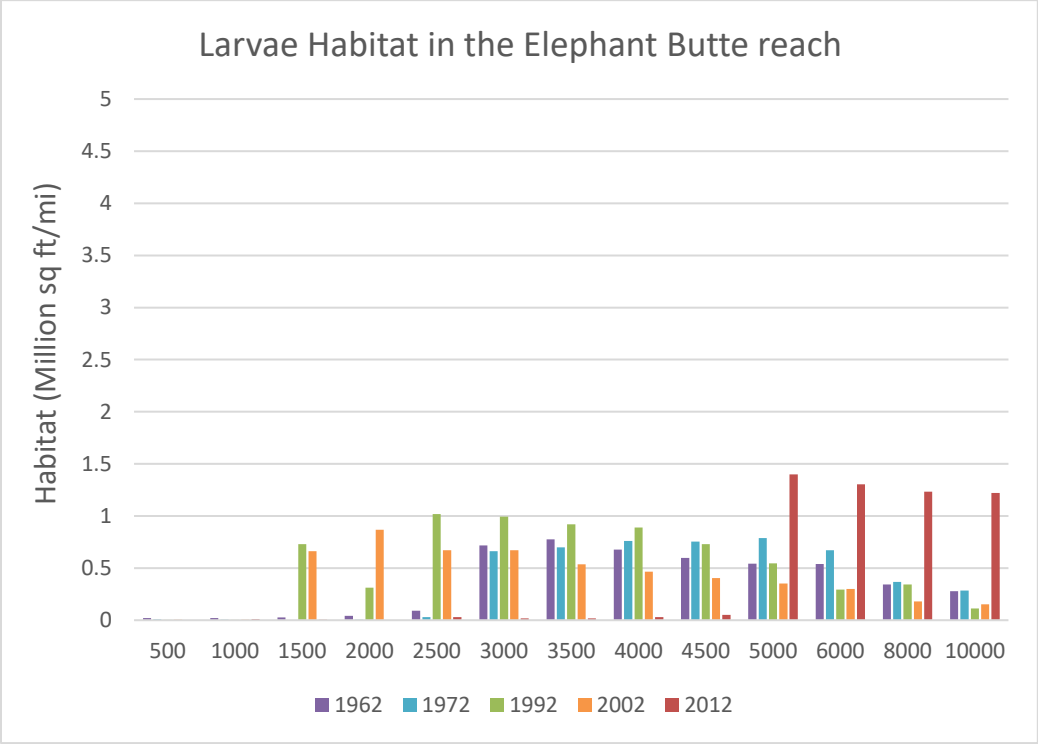

Figure 67 Larval RGSM habitat availability throughout the Elephant Butte Reach- the scale of the y-axis is lower for the larval habitat to better see the trends in the hydraulically suitable habitat.

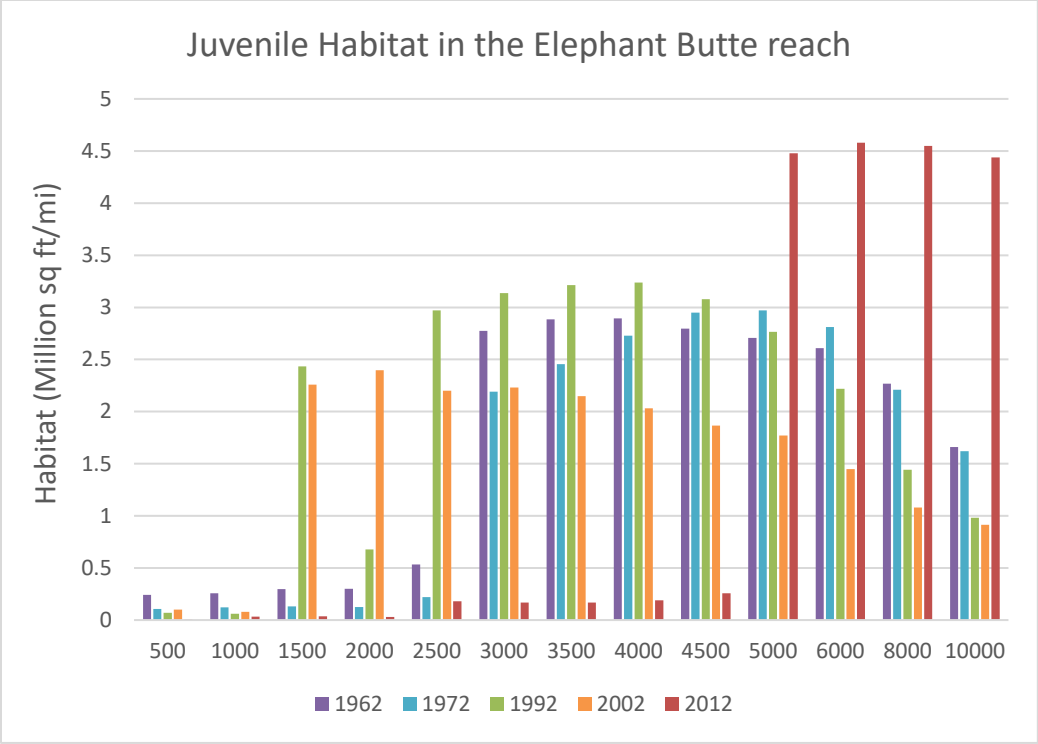

Figure 68 Juvenile RGSM habitat availability throughout the Elephant Butte Reach

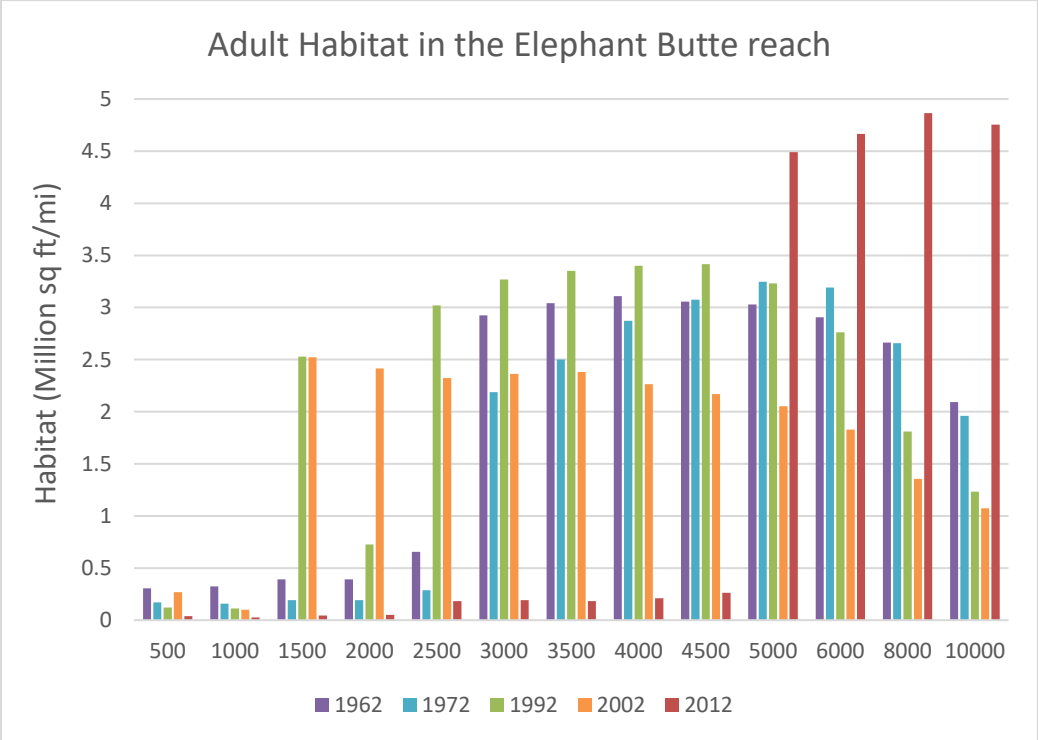

Figure 69 Adult RGSM habitat availability throughout the Elephant Butte Reach

Habitat availability is very much dependent on the river being connected to the floodplain. This allows the specific velocities required by the different life stages of the Silvery Minnow to be met. Looking at Figure 67 through 69 shows that generally across all years, 1992 had the greatest amount of hydraulically suitable habitat for the Silvery Minnow up until 5,000 cfs. This may have been because the channel was aggrading and depositing sediment, thus allowing for connection to the floodplain to occur at lower flows. In 2012 there is the least hydraulically suitable habitat across all life stages for the Silvery minnow until 5,000 cfs when the floodplain is inundated. This may be due to the degradation of the channel that occurred between 2002 and 2012 and the natural levees that formed between 1972 and 2002 that remained when the channel bed lowered after 2002. As a result, higher discharges are required in 2012 for the river to be connected to the floodplain preventing appropriate conditions for the life stages of the Silvery Minnow from being met at discharges that provided habitat in the prior data sets.

The width slices method was also used to analyze the habitat availability throughout the Elephant Butte Reach at a subreach level. Figure 70 was created to show stacked habitat trends at lower flow rates for the adult life stage of the Silvery Minnow. Based on this method, subreach EB5 consistently had the most hydraulic suitable habitat at lower discharges while, subreach EB1 had the next greatest habitat availability above 500 cfs. EB5 has more habitat which lend itself to the incision and narrowing of the channel. The channel form of EB5 may be more efficient at reaching the RGSM's habitat criteria of velocity and flow depth. Additional bar charts for all subreaches are located in Appendix D.

Stacked habitat bar charts were created to portray the spatial variation of hydraulically suitable habitat of the RGSM throughout the Elephant Butte Reach. The bar charts display the width of habitat at different discharges for 2012. To convert the hydraulically suitable habitat to an area, these values would be multiplied by 500 ft, which is approximate the distance between each agg/deg line. Figure 71 shows the 2012 habitat availability from 500 cfs to 10,000 cfs for subreach EB1 through EB5. EB6 is not included in Figure 71 due to its disproportionate total length compared to the other subreaches and so it is included in Figure 72. Habitat for other years can be found in Appendix D.

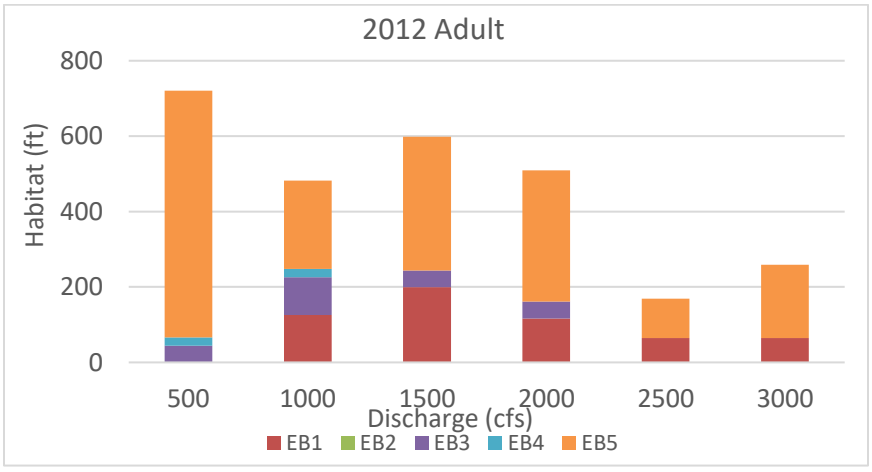

Figure 70 Stacked habitat charts to display spatial variations of habitat throughout the Elephant Butte Reach in 2012

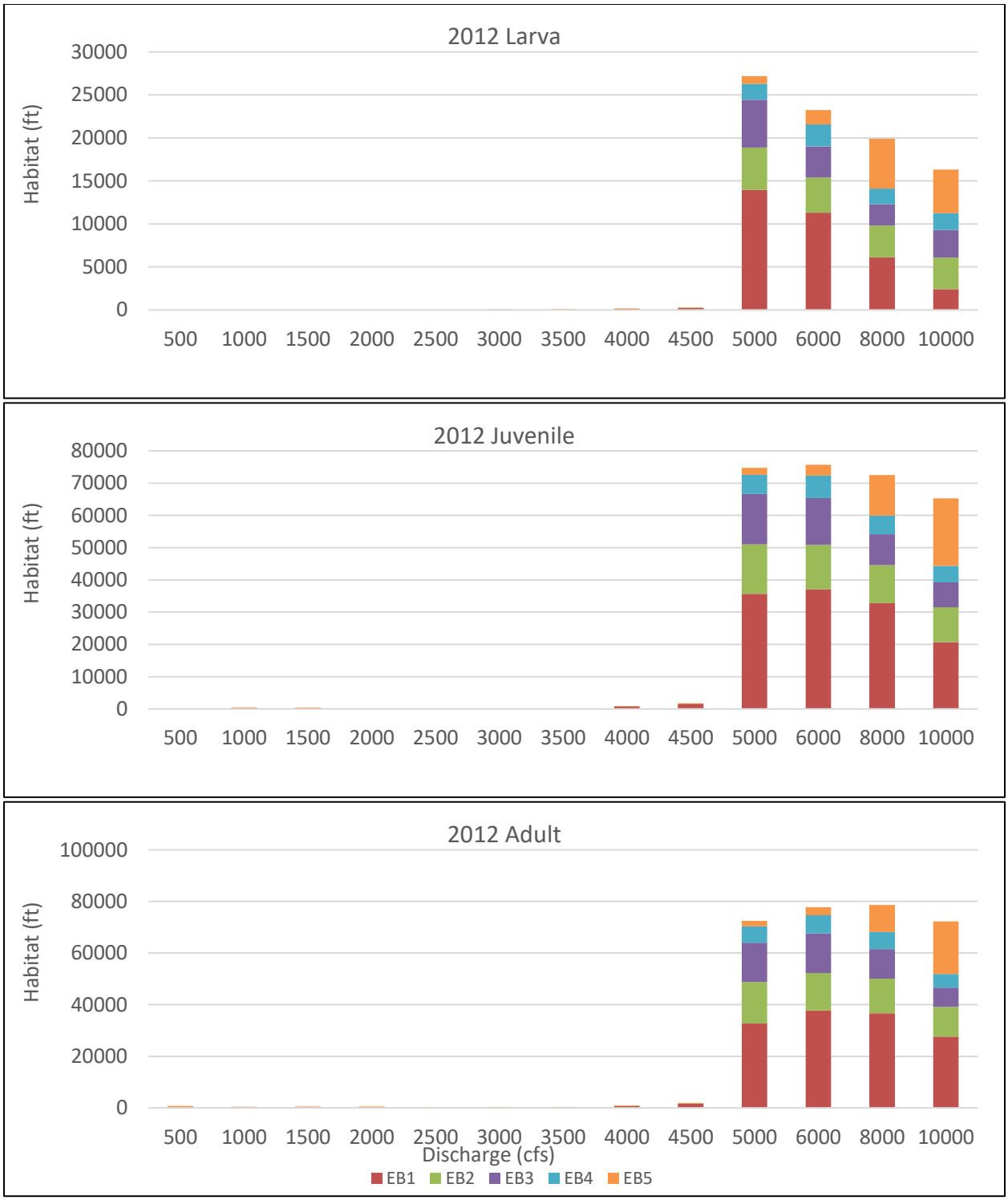

Figure 71 Stacked habitat charts at different scales to display spatial variations of habitat throughout the Elephant Butte reach in 2012

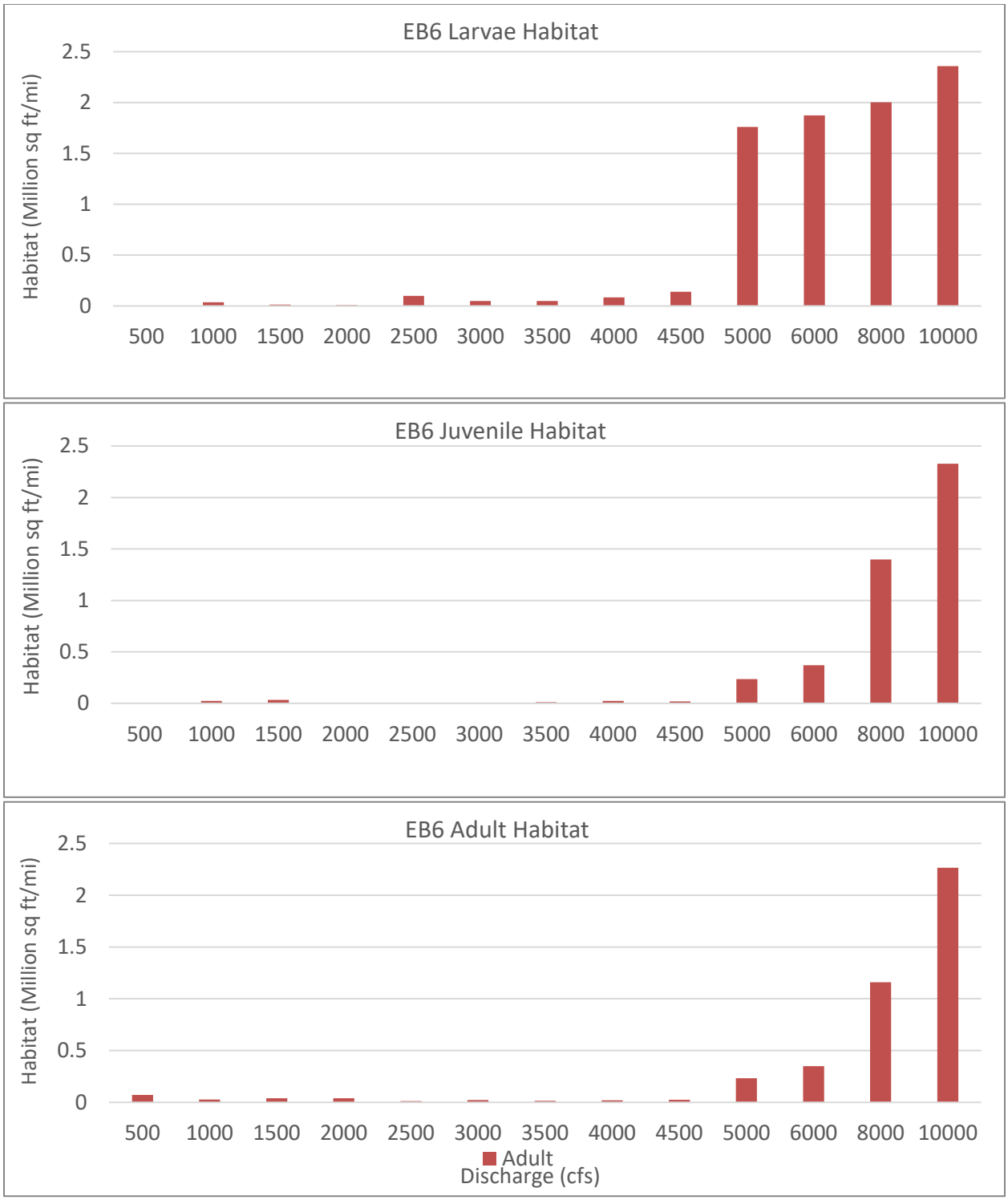

Figure 72 Subreach EB6 habitat charts displays available RGSM life stage habitat at various flow rates in 2012

4.4 RAS-Mapper Methodology

By using RAS-Mapper, the goal was to transform the 1-D habitat estimates into pseudo two-dimensional (2-D) results. RAS-Mapper overlays the water onto a prescribed terrain and interpolates the water surface elevation to create an estimate of the location of water inundation, which can then be used to predict locations of hydraulically suitable habitat for the Silvery Minnow.

The HEC-RAS geometry data that was necessary for the RAS-Mapper analysis (geo-referenced cross-sections and a LiDAR surface to generate a terrain) was available only for the year 2012. Therefore, only 2012 results were processed in RAS-Mapper. The original 2012 LiDAR data was used to develop a raster on ArcMap software (intellectual property of ESRI), which could be imported as a terrain in RAS-Mapper. The RAS-Mapper application distributes the water throughout the terrain, interpolating between the cross-sections, which results in a more accurate understanding of where water is present in a channel. RAS-Mapper will also predict the flow depth and velocity at a given discharge. ArcMap was used to combine the RAS-Mapper generated rasters for velocity and depth, so the RGSM depth and velocity criteria could be applied to identify the areas of suitable habitat. The results were used to create maps that show the areas of hydraulically suitable habitat for each life stage of the RGSM.

4.5 RAS-Mapper Habitat Results in 2012

While the width slice method quantitatively determined areas with increased potential for habitat, RAS-Mapper was used to spatially depict these areas of potential RGSM habitat throughout the MRG and overlay the results on a map of the Rio Grande River. The hydraulically suitable habitat for each life stage was mapped at discharges of 1,500 cfs, 3,000 cfs, and 5,000 cfs, which have daily exceedance probabilities of around 9.5%, 4.5%, and 0.72%, respectively (Figure 17). The 1,500 cfs and 3,000 cfs discharges were run with levees in place and the 5,000 cfs discharge was run with levees removed based on 25% overtopping in 2012 (Figure 65).

According to the RAS-Mapper results, there is more hydraulically suitable habitat in EB1 and EB5 than the middle portions of the Elephant Butte Reach with flow rates ranging from 1,000 cfs to 3,000 cfs (Figure 70). The results show that a 500 cfs to 1,500 cfs are the most conducive flow rates for suitable adult habitat at low flows, between 500 cfs and 3,000 cfs. This is due to the flow being confined to the main channel, but the flow rate is low enough that the Silvery Minnow's habitat requirements are met. When the flow is increased past 1,500 cfs the suitable habitat decreases. When increasing the flow rate and the flow is still confined to the main increases the velocities and depths (Table 5) outside the required range for the Silvery Minnow. At a discharge of 5,000 cfs, the amount of hydraulically suitable habitat increases greatly (Figure 71). An example of the habitat maps for subreach EB1 at discharges of 1,500 cfs and 5,000 cfs is shown in Figure 73. The habitat maps for the remainder of the subreaches at each discharge (1,500 cfs, 3,000 cfs, and 5,000 cfs) can be found in Appendix E.

Although a discharge of 5,000 cfs may not be commonly seen throughout the Elephant Butte Reach, maps at this discharge still provide the opportunity to examine possible areas that are more likely to meet the velocity and depth criteria for the RGSM. This can help in identifying which areas may have hydraulically suitable habitat that are connected to the main channel due to backwater or natural formation of pools and which subreaches contain habitat that may be found suitable but are disconnected to the main channel. This disconnection from the main channel is due to perching of the banks creating

natural levees above the floodplain. Both instances may be beneficial for the future of the RGSM, but different approaches may be needed in planning restoration efforts.

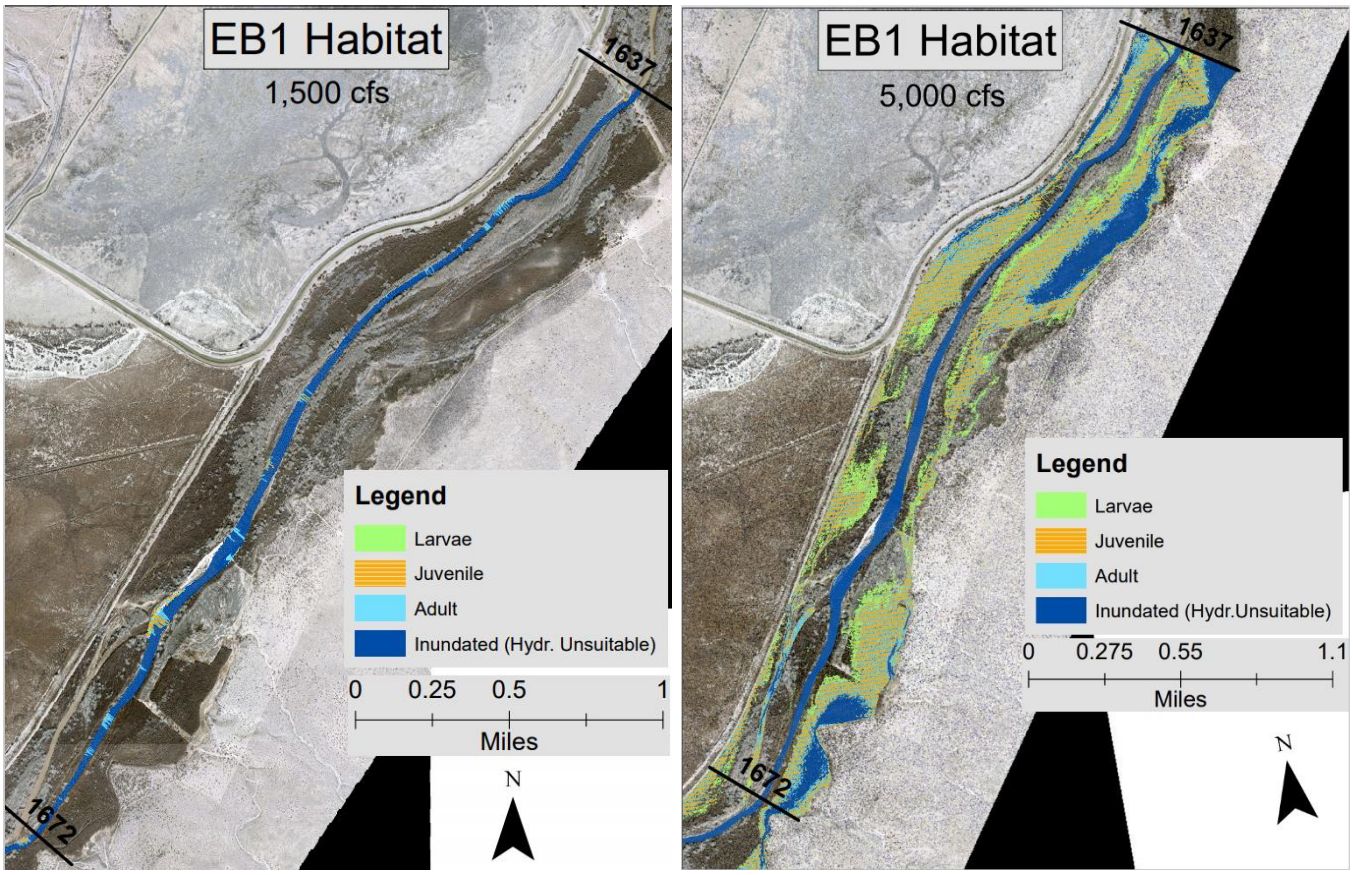

Figure 73 Suitable habitat in 2012 *for each life stage in subreach EB1 at 1,500 cfs (left) and 5,000 cfs (right)*

4.6 Disconnected Areas

RAS-Mapper provides the opportunity to identify areas that likely meet the velocity and depth requirements of the RGSM at specified discharges. RAS-Mapper may also be beneficial for identifying areas throughout the reach that may contain water but fail to remain connected to the main channel. These may be possible areas of focus for restoration efforts.

By connecting several of these disconnected areas, the Silvery Minnow may gain a great amount of possible habitat. Available hydraulically suitable habitat estimation will become more accurate if the disconnected areas can be connected back to the river and can be utilized by the RGSM. Figure 74 shows one instance of a disconnected area in the Elephant Butte Reach. The disconnected areas are emphasized in the zoomed in square on the right. It is possible to see that the main channel is deeper (darker blue) and at higher flows these floodplains and low-lying areas may become inundated. These disconnected areas could be used to identify potential spots on the Rio Grande where the RGSM may become stranded. Some areas may turn into pools once the high flow events subsides and the floodplain is no longer inundated. Conversely, these areas could become possible restoration sites leading to an increase in hydraulically suitable RGSM habitat. Locations of disconnected areas based off the RAS-Mapper habitat maps have been listed in a table in Appendix E.

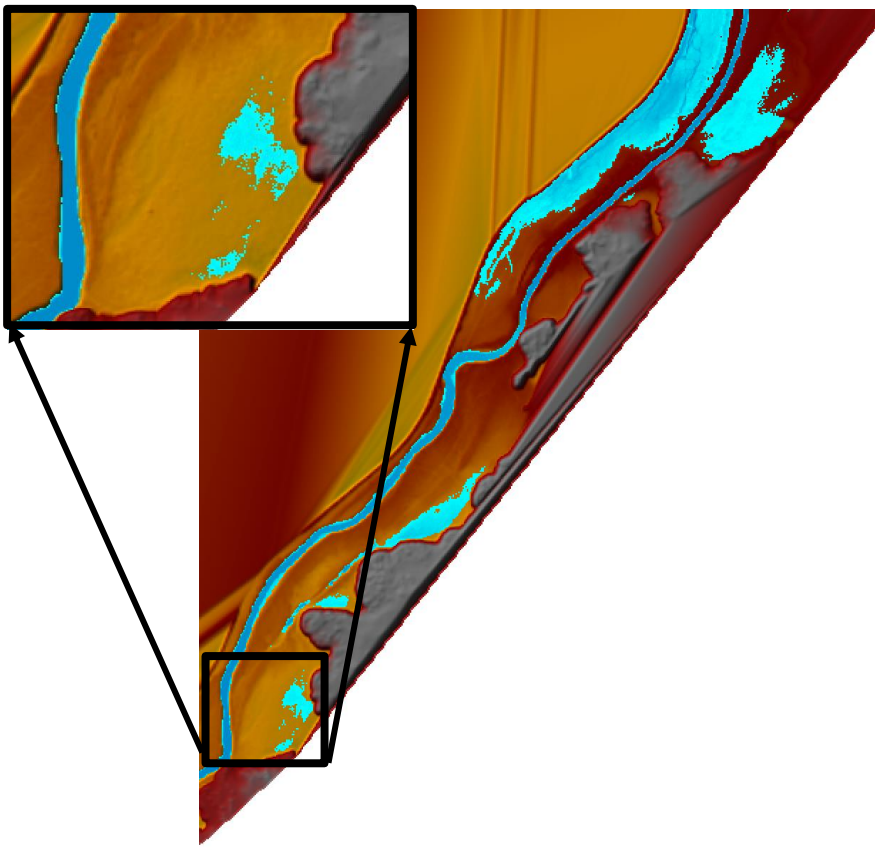

Figure 74 Example of a disconnected area that contains water, but no access to or from the main channel

After calculating the velocity and flow distribution, these disconnected areas often meet the depth and velocity criteria of the RGSM. However, the lack of connectivity eliminates the possibility of RGSM habitat. Figure 75, for example, predicts that the disconnected area shown is hydraulically suitable for the RGSM's adult, juvenile, larval life stages. RAS Mapper indicates that this area will not be accessible to the RGSM.

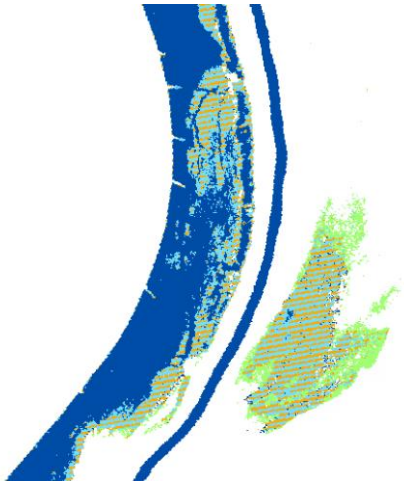

Figure 75 Disconnected area showing hydraulically suitable habitat for RGSM adult (green), juvenile (orange cross hatch), and larvae (green)

5. Elephant Butte Reservoir Synthesis

The complex system of the Rio Grande River's Elephant Butte Reach can be divided into different hydrologic and morpho dynamic effects that have shaped the river through time. This ultimately influences the inundation criteria of the river's floodplain and the Rio Grande Silvery Minnow (RGSM) habitat that may be present.

To understand the underlying processes driving the changes to the Elephant Butte Reach, first the trends in the hydrology of the river must be examined. As shown in Section 2, there have been changes in mean daily peak flow and annual flow volume. Figure 14 shows the cumulative annual discharge in the Elephant Butte Reach from 1949 to present, and the discharge trends during this time can be divided into three distinct periods. Most notably, the first period (late 1940s to late 1970s) was a time of low annual flow volume. During the period from 1949 to 1978 the annual flow volume was significantly less than from 1979 to 1999. Then from 2000 to the present (2021) annual flow volume was again lower. The periods when flow exceeded 5,000 cfs for the greatest number of days are consistent with the cumulative annual flow volume (Figure 20). During the period from 1949 to 1978 there were very few days when flows were greater than 5,000 cfs. Conversely, from 1979 to about 1999 there were a larger number of days with higher flows. From 2000 to the present there were only a few days above 5,000 cfs in 2005 (Figure 11), although 2008, 2017, and 2019 also had relatively large, long duration, spring runoff events. Although the Narrows at Elephant Butte and San Antonio gages are informative, their respective period of records are too short to use for this synthesis. It is evident from the San Marcial Gage raster hydrographs of daily discharge (Figures 10 and 11) that there were several large peaks over 10,000 cfs in the early 1900s up until about 1942. Peak flow decreased during the period from 1943 to the present due to a combination of upstream dams and drought. After the high flow year in 1942, peak flows have commonly been near or below 5,000 cfs. Although annual flow volumes are large between 1979 and 1999, the peak flow magnitude is much smaller than events in the early 1900s. Annual flow volumes and peak flow magnitudes have both been low during the current drought from 2000 to the present, with the 2005 spring runoff event being the most notable exception.

While there is sediment supply from upstream tributaries and channel erosion, a major source of sediment input to the Elephant Butte Reservoir is from the arroyos or ephemeral tributaries during the monsoon thunderstorm season in July, August, and September (Figures 22, 25, and 26). The main driver for flow rate and reservoir replenishment in the Reach is due to spring runoff. Figure 14 shows that the large increase in cumulative discharge occurs more often in the spring due to snowmelt runoff. There are large monsoonal rainfall events that cause the cumulative discharge to have a sharp increase, such as the 2013 monsoonal event (Figure 25). Figure 30 combines both the discharge and sediment load where the above results are corroborated. Sediment supply and transport capacity, combined with reservoir water surface stage, has a large effect on temporal and spatial changes to the river morphology. The sediment dynamics influences the amount of aggradation or degradation that occurs in the main channel and the channel banks, which causes perching above the adjacent floodplain to form natural levees.

Elephant Butte Reservoir was found to cause backwater effects that can propagate delta deposition upstream of the pool during full reservoir conditions for the entirety of the Elephant Butte Reach, where these effects diminish moving upstream. Due to the reservoir stage relying on snowmelt, the climate has a great effect on the water surface elevation (WSE) of the reservoir pool. The reservoir WSE dictates where

the delta forms and the location at which the backwater effect starts. A higher WSE in the reservoir means the delta will form farther upstream causing sediment in the river to settle resulting in channel aggradation. The backwater effect increases water depth while decreasing the velocity and sediment transport capacity of the river that propagates upstream. The reservoir water level through time can be observed in Figure 48 through 50. Figure 49 shows how the longitudinal profile of the river greatly changes in tandem with the reservoir water level. When the reservoir water level decreased between 1962 and 1972 the delta that had previously formed and the backwater effect was then moved farther into the reservoir. This led to head cutting and degradation of the main channel due to the decrease in backwater effects and increased transport capacity of the river. As the reservoir filled back up between 1972 and 2002 there was a large amount of aggradation increasing the channel elevation by around 20 feet in subreach EB5 (Figure 37). Then from 2002 to 2012 the reservoir water level decreased once again, causing head cutting to occur and degrading the river Reach by around 12 feet in subreach EB5. This amount of aggradation and degradation is quantified in Figure 38.

When aggradation of the main channel occurs, as seen from 1972 to 2002, this has ultimately led to perching of the channel, creating natural levees, and disconnecting surface flows of the main river channel from the floodplain. Disconnection occurs when the floodplain is inundated, the flood event starts to recede, and the natural levees prevent water from returning to the main channel. The mechanism for perching is due to channel aggradation causing sediment ladened water to rise allowing for sediment to be deposited to the riverbanks and into the riparian zone along the riverbank. Resistance to flow is higher in the overbank resulting in lower velocity and sediment deposition. An example of floodplain disconnection and the potential hydraulically suitable habitat for the Silvery Minnow is shown in Figure 73 and Figure 74. Figure 59 is a good example of perching of the main channel. As discussed above, this cross section shows that between 1972 and 2002 there was a large amount of deposition causing the main channel to fill with sediment. When incision occurs the top width of a channel is most likely to narrow and when aggradation occurs the channel is more likely to widen. Figure 41 shows the wetted top width at 1,000 and 3,000 cfs. The 1,000 cfs flow is a good indicator of the main channel characteristics due to 3,000 cfs potentially inundating the flood plain from 1992 to 2002. When the channel degraded a small amount from 1962 to 1972 the top width decreased. When the channel aggraded from 1972 to 2002 the channel widened. When the channel switches back to degradation the channel narrows and the top width decreases. These trends are more pronounced closer to the reservoir. This narrowing and widening effect can be seen in the cross-sectional views of the channel in Figures 55, 57, 59, 61, and 63. The widening effect of the channel when aggradation of the main channel occurs may also have been accelerated due to the mowing operations that occurred from the 1950s to the 1980s which is shown in Figure 2.

The reservoir effects have a very large impact on the channel aggradation, channel perching, bank height and amount of discharge needed to overtop the banks. The cycles of degradation and aggradation, as discussed, can cause large increases in natural levee formations and an increase in the main channel depth. When coupling these two factors the required flow rate to inundate the floodplain increased greatly from 2002 to 2012 (Figure 65). From 1972 to 2002 the required flow rate to overtop at least 25% of cross-sections greatly decreased from around 3,000 cfs to around 1,500 cfs. This was due to the backwater effect and deposition of sediment in the main channel in the delta that extends through this Reach. During this time, natural levees were being built up increasing the riverbank height. After this period the reservoir level dropped from 2002 to 2012 causing large amounts of incision, which coupled with the increase in bank height and hydraulic depth, increased the discharge required to overtop the banks to almost 5,000

cfs. Table 3 shows the probabilities of exceedance of different mean daily flow rates from a flow duration analysis. The probability of exceedance of 1,870 cfs and 4,962 cfs was 10% and 1% respectively for the Floodway at San Marcial. Due to the incision of the river, the mean daily exceedance flow required to overtop at least 25% of the cross sections went from 10% to 1% between 2002 to 2012.

The reservoir affects both the channel morphology and the hydraulically suitable habitat for the RGSM. The RGSM habitat availability spikes when the floodplain is inundated where the flow depth and velocity criteria is met. Figure 73 is a good example of how much available habitat there is once the floodplain is inundated compared to when the flow is contained in the main channel. Figure 67 to 69 shows each life stage's habitat availability. All three Silvery Minnow life stages' available habitat follows the same trend as the 25% overtopping analysis due to the reservoir effects. Between 1962 to 1972 there was a small amount of degradation. The habitat curves for both these years are similar but 1972 spikes a little later than 1962 due to floodplain inundation. After the rapid aggradation from 1972 to 2002, the floodplain inundation (sharp rise in habitat curve) shifted to a lower discharge. When the water in the reservoir dropped after 2002 and the river incised the required flow rate to inundate the floodplain increased to around 5,000 cf reducing the availability of suitable habitat. Figure 70 shows a breakdown of the available adult habitat in 2012 divided into subreaches for flows up to 3,000 cfs. Subreach EB5 has the most available habitat of this reach at lower flow rates. Figure 71 and Figure 72 show the available habitat for each RGSM life stage by subreaches from 500 cfs to 10,000 cfs in 2012. Subreach EB1 has most available habitat for all three life stages when flows are at or above 5,000 cfs. This may be because EB1 is located farther away from the reservoir. From 2012 to 2018 the river morphology was relatively stable and habitat availability is not expected to change, which is indicated by small fluctuations in the cross-section elevations and the Elephant Butte WSE (Figure 48 through Figure 50). Table 6 is a breakdown of the different morhological changes that the river has experienced to aid with trends that can be observed from 1962 to 2012. Appendix D shows the complete analysis of hydraulically suitable habitat for the Silvery Minnow. Appendix E shows aerial imagery of the subreaches and the mapping of the RGSM habitat.

Figure 76 is a sketch of the reservoir delta and the sedimentation effects that occur with the change in reservoir water surface elevation. When the reservoir water level is held constant the sediment that enters the water body continues to lengthen the pivot point (point between the topset and foreset delta slope (shown in Figure 76) and continues to deposit sediment upstream of the pivot point, which moves progressively more upstream over time. Except in the backwater region of active delta deposition, the channel will remain about the same planform as prior to reservoir construction. When the reservoir water level rises (Figure 76 middle panel), the pivot point moves upstream as does delta deposition. This results in development of distributary channels forming a braided condition. Braids are indicative of reduced sediment transport capacity in the active delta region created by reduced hydraulic energy gradient from the rising reservoir. Far upstream the channel may remain in its current plan form but could experience channel aggradation such as stage A5 (Massong et al. 2010) with the formation of sediment plugs. If the reservoir continues to rise the upstream length of the braided channel may also increase. Continued reservoir water surface elevation rise will inundate the delta formed at lower reservoir stages. These events occurred when water level in the reservoir rose from 1972 to 2002, the formed delta was submerged, and the backwater effects propagated reducing sediment transport and causing channel aggradation. Also, during times when the reservoir is raising and channel aggradation occurs, there will likely be the formation of natural levees along the channel banks in the riparian zone (Figure 76 middle

panel & cross section view). When the reservoir WSE falls some of the delta deposits are eroded and transported downstream causing the pivot point to move downstream. The foreset slope, which was formerly underwater, becomes an over-steepened section of the channel profile that has a high local sediment transport capacity. The once braided channel will begin to incise creating a single thread channel that over time may begin to migrate laterally. The greatest incision will occur at the previously formed delta where there is the thickest zone of previously deposited sediment. The incision will start to head cut up stream, which will cause channel degradation and potentially some narrowing of the main channel.

Table 6 Observed Trends of The Elephant Butte Reach

	Period	Reservoir WSE Change	Change in Bed Elevation	Change in Top Width	Change in Bed Slope (avg reach)	Change in Sinuosity
Subreach EB1	1962-1972	Fluctuation	Slight Decrease	Decrease	Increase	Increase
	1972-1992	Increase	Increase	Decrease	Decrease	Decrease
	1992-2002	Constant, Slight Decrease	Increase	Increase	Decrease	Decrease
	2002-2012	Decrease	Decrease	Decrease	Increase	Slight Increase
Subreach EB2	1962-1972	Fluctuation	Decrease	Decrease	Decrease	Decrease
	1972-1992	Increase	Increase	Increase	Decrease	Decrease
	1992-2002	Constant, Slight Decrease	Increase	Increase	Increase	Slight Decrease
	2002-2012	Decrease	Decrease	Decrease	Increase	Slight Increase
Subreach EB3	1962-1972	Fluctuation	Decrease	Decrease	Slight Decrease	Increase
	1972-1992	Increase	Increase	Increase	Slight Increase	Decrease
	1992-2002	Constant, Slight Decrease	Increase	Increase	Decrease	Increase
	2002-2012	Decrease	Decrease	Decrease	Increase	No Change
Subreach EB4	1962-1972	Fluctuation	Decrease	Decrease	Decrease	Slight Increase
	1972-1992	Increase	Increase	Increase	Decrease	Increase
	1992-2002	Constant, Slight Decrease	Increase	Increase	Decrease	No Change
	2002-2012	Decrease	Decrease	Decrease	Increase	Slight Increase
Subreach EB5	1962-1972	Fluctuation	Decrease	Increase	Increase	Increase
	1972-1992	Increase	Increase	Increase	Slight Decrease	Increase
	1992-2002	Constant, Slight Decrease	Increase	Increase	Decrease	No Change
	2002-2012	Decrease	Decrease	Decrease	Increase	Decrease

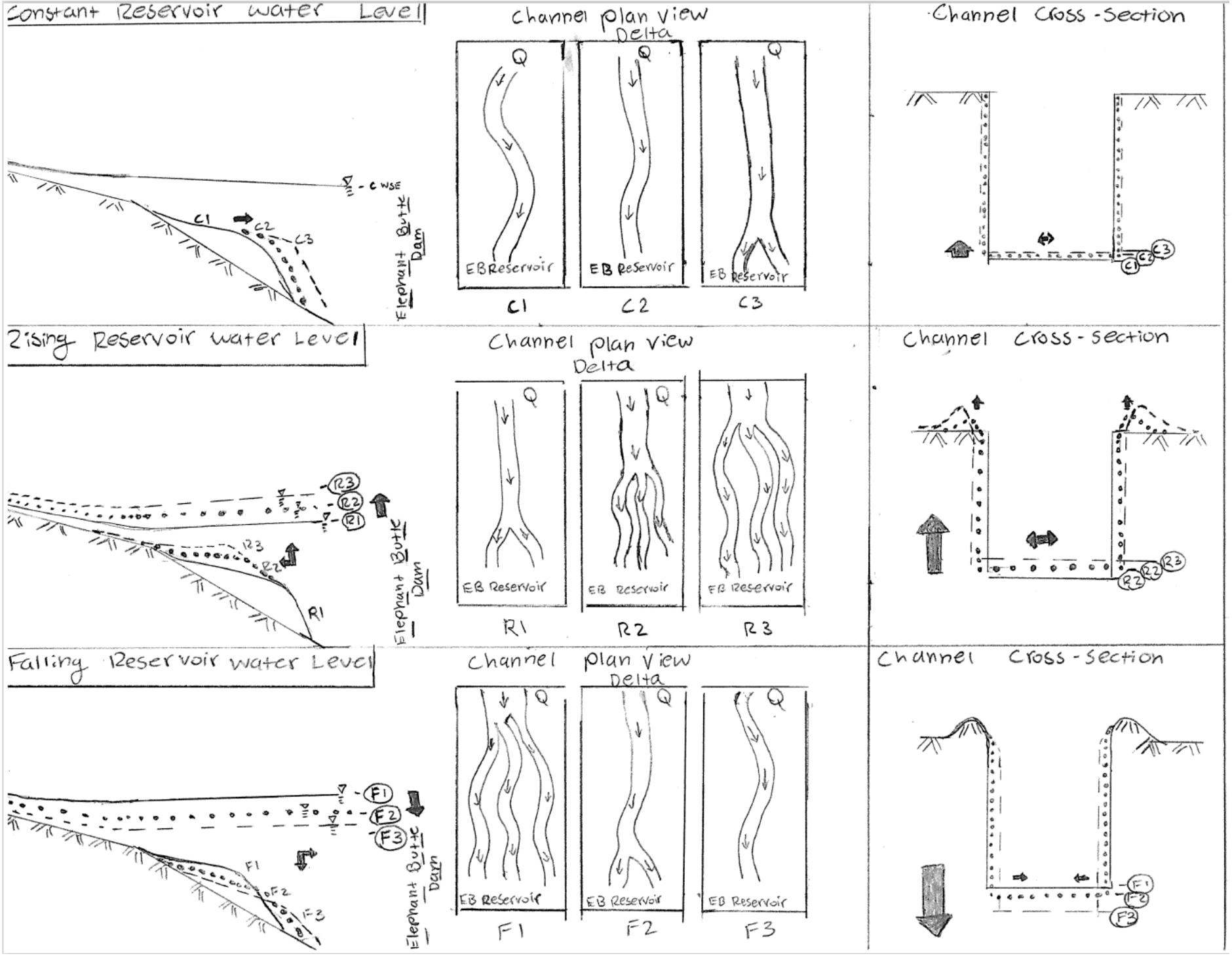

Figure 76 Reservoir Evolution Model

5. Conclusions

The Elephant Butte Reach extends from the southern boundary of the Bosque Del Apache National Wildlife Refuge to the Elephant Butte Reservoir near Truth or Consequences, New Mexico. The purpose of the report is to analyze the hydrologic, hydraulic and geomorphic trends between 1918 and 2021. HEC-RAS and GIS were used to find geomorphic and river characteristics such as sinuosity, width, bed elevation and other hydraulic parameters. Hydraulically suitable RGSM habitat was determined quantitatively and spatially throughout the reach.

Major findings include:

- While spring snowmelt typically brings the largest increases in the discharge volumes in the Elephant Butte Reach, summer thunderstorms have a greater impact on the amount of suspended sediment transported. Spring runoff is regulated and captured in upper reservoirs above Elephant Butte Reach. Which will have a direct effect on the sediment input from spring runoff and erosion of the main channel. Below the San Acacia dam there are no major tributaries that enter the MRG but there are several small arroyos that enter the river and two flood controlled channels (Towne 2007). Where there is suspended sediment from channel erosion and spring runoff the main source of sediment is from the arroyos that enter the river from convective thunderstorms. Strong monsoonal storms have led to flooding of the MRG in September of 2013, resulting in large increases in both cumulative discharge and sediment.
- Peak discharges topped 6,000 cfs on September 17th, 2013 at the HWY 380 gage San Antonio (08355490), with the maximum suspended sediment load measuring 403,000 tons per day on September 14th, 2013, and the maximum sediment concentration of 54,900 mg/l on September 13th, 2013. Downstream at the San Marcial gage (08358400) the discharge reached 4,500 cfs on September 19th, 2013, and the maximum suspended sediment load of 328,000 tons per day on September 15th, 2013, and maximum sediment concertation of 61,600 mg/l on September 14th, 2013. The delay in peak discharge from peak sediment load indicates that the rising limb of storm events is what brings greatest sediment load and highest sediment concentration. Looking at another severe thunderstorm in May of 2017 resulted in larger flows in the MRG. At the HWY 380 gage San Antonio (08355490) the peak discharge of 4,250 cfs on May 24th, 2017, the maximum suspended sediment load measuring 28,000 tons per day on May 22th, 2017, and the maximum sediment concentration of 2,520 mg/l on May 22th, 2017. Downstream at the San Marcial gage (08358400) the discharge reached 3,970 cfs on May 25th, 2017, and the maximum suspended sediment load of 13,900 tons per day on May 25th, 2017, and maximum sediment concertation of 1,530 mg/l on May 16th, 2017. This also indicates that there is a localized effect of the sediment loading which is dependent on rainfall location and there is still strong evidence that the rising limb brings the highest concertation of sediment into the river.
- While the HWY 380 San Antonio gage (08355490) had a peak discharge of about 1,800 cfs on August 4th with suspended sediment transport of 285,000 tons per day on Aug 5th. For both storms the sediment concentration peaked around the same value: 54,000 mg/l. Downstream at the San Marcial gage (08358400) recorded a peak discharge of about 1,900 cfs on August 5th with suspended sediment transport of 295,000 tons per day on Aug 5th. For both storms the sediment concentration peaked around the same value: 53,700 mg/l.

- Significant narrowing of the channel occurred between 1935 and 1972. This can be seen in the active channel widths. Since 2004 the active channel widths for EB1, EB2, and EB4 have remained relatively stable around 100ft where EB3, EB5 and EB6 are still fluctuating between about 100ft and 300ft. The width of all reaches is less than the predicted 250 ft equilibrium width predicted by JW equations.
- There has been a cycle of degradation (1962-1972), aggradation (1972-2002), degradation (2002-2012) within the reach. This trend is even more amplified the farther down Elephant Butte Reach toward the narrows of the Elephant Butte reservoir. Subreach EB1 shows small changes in aggradation and degradation cycle, where EB5 is much greater. Subreach EB1 has had about 5 feet aggradation and 3 feet degradation whereas EB5 has had 15 feet aggradation, and 13 feet degradation.
- Reservoir water levels are the base level control for the Elephant Butte Reach and aggradation is associated with higher reservoir water surface elevations (WSE) and degradation with subsequent lower WSEs.
- Throughout the reach the grain size is classified as mainly fine sand. Where the Elephant Butte Reach has a grain size range from medium sand to some coarse silt (1mm to 0.002mm). Where the bulk of the grain sizes measured has a diameter range of 0.1mm to 0.0625mm.
- The sinuosity has remained relatively close to 1 and has had an overall small decrease in subreaches EB1, EB3, EB4, and EB5. Subreaches EB4 and EB5 showed a decrease then a small increase. Subreach EB2 showed a small increase in sinuosity 1 to 1.07. Subreach EB3 has shown the greatest fluctuation where from 1918 to 1935 the sinuosity dropped from around 1.7 to around 1.2, then has increased and plateaued to around 1.3.
- Cross-sectional tends show the same aggradation and degradation cycles as determined by changes in base level control of Elephant Reservoir WSE. The cross-sectional view provides insight as to what stages in the Massong's planform model the river has gone through and delta formation at the mouth of the Elephant Butte Reservoir. Where Section 5 gives an introductory reservoir evolution model for delta formation and backwater effects. The trend is more prevalent the father downstream in the Elephant Butte Reach, where EB5 shows greatest trends. The river consistently degrades from 1962 to 1972, indicative of stages 3 and M4 where the channel vertically erodes. From 1972 to 1992 there is extreme aggradation where A4 is occurring. The river's sediment transport capacity is lower than the sediment input which causes perching of the channel to then occur. From 1992 to 2002 the river is at an A4 stage where perching is occurring, but the main channel is filing with sediment. This decreases the hydraulic depth. In 2012 the channel stays at an A4 stage where the banks are aggrading but the hydraulic depth increases.
- The river has been experiencing dramatic changes, effecting the discharge at which bankfull occurs (or 25% of levee overtopping is achieved). Currently in 2012, it was found that the required flow rate to reach 25% overtopping was 4,773 cfs compared to 1962 which required 2,866 cfs. Where there was a drop of required flow rate in 1992 and 2002 to reach the 25% overtopping which has been linked to the reservoir WSE being more full causing sedimentation and deposition. Thus, the hydraulic depth decreases making overtopping occur at a lower flow rate (1972 to 2002). Once the water level in the reservoir decreased after 2002 then there was degradation and head cutting from the reservoir narrows upriver. The incision increased the hydraulic depth and subsequently increased the required flow rate to reach overtopping. For 50%

overtopping for 2012, 2002, 1992, 1972, and 1962 the required flow rate to achieve this was 5,728, 1,928, 2,375, 4,150 cfs respectively.

- While the width slices method estimates the greatest amount of hydraulically suitable habitat, the RAS-mapper habitat maps show that much of the habitat is disconnected from the main channel in many locations. Based on the RAS-mapper habitat maps for 2012, subreach EB1 provides hydraulically suitable habitat that may be more accessible for the RGSM due to connectivity to the main channel. Where at flows below 3,000 cfs, habitat maps indicate that inundation of the floodplain is unlikely. The habitat maps also indicate that subreach EB5 still does not reach bankfull discharge at 3,000 cfs and may need up around 4,800 cfs to achieve inundation of the floodplain. This is corroborated in the analysis at which 25% bankfull is reached.
- The results for the 2012 RGSM habitat maps show that EB1 through EB4's flood plains become inundated between 3,000 and 5,000 cfs allowing for the suitable habitat for the RGSM to greatly increase. EB5 indicates that a greater flow needs to occur for the floodplain to be inundated due to the greater aggradation / degradation cycles that this subreach has experienced so close to the reservoir.

6. Bibliography

Beckwith, T and Julien, P.Y (2020) "Middle Rio Grande Escondida Reach Report:Morpho-dynamic Processes and Silvery Minnow Habitat from Escondida Bridge to US-380 Bridge (1918-2018.)" Colorado State University, Fort Collins, CO.

Bovee, K.D., Waddle, T.J., and Spears, J.M. (2008). "Streamflow and endangered species habitat in the lower Isleta reach of the middle Rio Grande." *U.S. Geological Survey Open-File Report 2008-1323*.

Doidge, S and Julien, P.Y. (2019). Draft Report. *Middle Rio Grande San Acacia Reach: Morphodynamic Processes and Silvery Minnow Habitat from San Acacia Diversion Dam to Escondida Bridge*, Colorado State University, Fort Collins, CO.

Fitzner, A. (2018). Draft Report "Reclamation Managing Water in the West." *Bureau of Reclamation Draft Lower Reach Plan*, Albuquerque Area Office, Albuquerque, NM, 36 p.

Greimann B. and N. Holste (2018). *Analysis and Design Recommendation of Rio Grande Width,* Technical Report. SRH-2018-24, Sedimentation and River Hydraulics Group Technical Service Center, US Bureau of Reclamation, Denver, Colorado, 20p.

Holste, N. (2020) "One-Dimensional Numerical Modeling of Perched Channels." U.S. Bureau of Reclamation, Denver, CO.

Julien, P.Y. (2002). *River Mechanics*, Cambridge University Press, New York

Julien, P. Y., and Wargadalam, J. (1995). "Alluvial channel geometry: theory and applications." *Journal of Hydraulic Engineering*, American Society of Civil Engineers, 121(4), 312–325.

Klein, M., Herrington, C., AuBuchon, J., and Lampert, T. (2018a). *Isleta to San Acacia Geomorphic Analysis*, U.S. Bureau of Reclamation, Reclamation River Analysis Group, Albuquerque, New Mexico.

Klein, M., Herrington, C., AuBuchon, J., and Lampert, T. (2018b). *Isleta to San Acacia Hydraulic Modeling Report*, U.S. Bureau of Reclamation, Reclamation River Analysis Group, Albuquerque, New Mexico.

LaForge, K., Yang, C.Y., Julien, P.Y., and Doidge, S. (2019). Draft Report. *Rio Puerco Reach: Hydraulic Modeling and Silvery Minnow Habitat Analysis*, Colorado State University, Fort Collins, CO.

Larsen, A. (2007). *Hydraulic modeling Analysis of the Middle Rio Grande-Escondida Reach, New Mexico*. M.S thesis, Civil Engineering Department, Colorado State University, Fort Collins, CO.

Makar, P. (2006). "Channel Widths Changes Along the Middle Rio Grande, NM." *Proceedings of the Eith Federal Interagency Sedimentation Conference*, Bureau Of Reclamation, Denver, CO. 943 p.

Makar, P., Massong, T., and Bauer, T. (2006). "Channel Widths Change Along the Middle Rio Grande, NM." *Joint 8th Federal Interagency Sedimentation Conference, Reno, NV, April 2 -April6, 2006.*

Massong, T., Paula, M., and Bauer, T. (2010). "Planform Evolution Model for the Middle Rio Grande, NM." *2nd Joint Federal Interagency Conference, Las Vegas, NV, June 27 - July 1, 2010*.

MEI. (2002). *Geomorphic and Sedimentologic Investigations of the Middle Rio Grande between Cochiti Dam and Elephant Butte Reservoir*, Mussetter Engineering, Inc., Fort Collins, CO, 220 p.

Mortensen, J.G., Dudley, R.K., Platania, S.P., and Turner, T.F. (2019). Draft report. *Rio Grande Silvery Minnow Habitat Synthesis*, University of New Mexico with American Southwest Ichthyological Researchers, Albuquerque, NM.

Mortensen, J.G., Dudley, R.K., Platania, S.P., White, G.C., and Turner, T.F., Julien, P.Y., Doidge, S, Beckwith, T., Fogarty, C. (2020). Draft Report. *Linking Morpho-Dynamics and Bio-Habitat*

Conditions on the Middle Rio Grande: Linkage Report 1- Isleta Reach Analyses. Submitted to the U.S. Bureau of Reclamation, Albuquerque, New Mexico.

Owen, T. E., Anderson, K., and Julien, P. (2011). *Elephant Butte Reach: South boundary of Bosque del Apache NWR to Elephant Butte Reservoir hydraulic modeling analysis, 1962- 2010.* Colorado State University, Fort Collins, CO.

Owen, T. E., (2012). *Geomorphic Analysis Of the Middle Rio Grande - Elephant Butte Reach, New Mexico.* Colorado State University, Fort Collins, CO.

Pinson, A.O., Scissons, S.K., Brown, S.W., Walther, D.E. (2014). Post Flood Report: Record Rainfall and Flooding Events during September 2013 in New Mexico, Southeastern Colorado and Far West Texas, U.S. Army Corps of Engineers, Albuquerque, New Mexico.

Pinson, A.O., Scissons, S.K., Brown, S.W., Walther, D.E. (2014). *Post Flood Report: Record Rainfall and Flooding Events during September 2013 in New Mexico, Southeastern Colorado and Far West Texas,* U.S. Army Corps of Engineers, Albuquerque, New Mexico

Posner, A. J. (2017). Draft report. *Channel conditions and dynamics of the Middle Rio Grande River,* U.S. Bureau of Reclamation, Albuquerque, New Mexico.

Scurlock, D. (1998). "From the Rio to the Sierra: an environmental history of the Middle Rio Grande Basin." *General Technical Report RMRS-GTR-5. Fort Collins, CO: US Department of Agriculture, Forest Service, Rocky Mountain Research Station, 440 p.*

Shah-Fairbank, S. C., Julien, P. Y., and Baird, D. C. (2011). "Total sediment load from SEMEP using depth-integrated concentration measurements." Journal of Hydraulic Engineering, 137(12), 1606–1614.

Schied, A., Sperry, D. J., and Julien, P.Y (2022) "Middle Rio Grande Bosque del Apache Reach Report: Morpho-dynamic Processes and Silvery Minnow Habitat from US-380 Bridge to Southern Boundary of Bosque Del Apache National Wildlife Refuge (BDANWR)" Colorado State University, Fort Collins, CO.

Shrimpton, C. P, (2012). *Analysis of Sediment Plug Hypotheses Middle Rio Grande, NM.* Colorado State University, Fort Collins, CO.

Towne, L. (2007). "Infrastructure and Management of the Middle Rio Grande." *The Middle Rio Grande Today, Burequ of Reclamation,* 17 p.

U.S. Bureau of Reclamation. (2012). "Middle Rio Grande River Maintenance Program - Comprehensive Plan and Guide." Albuquerque Area Office, Albuquerque, New Mexico, 202p.

U.S. Bureau of Reclamation. (2021). "Water Operations: Historic Data." Online Resource. https://www.usbr.gov/rsvrWater/HistoricalApp.html

U.S. Fish and Wildlife Service. (2007). "Rio Grande Silvery Minnow (Hybognathus amarus)." Draft Revised Recovery Plan, Albuquerque, New Mexico, 174 p.

Varyu, D. (2013). *Aggradation / Degradation Volume Calculations: 2002-2012*. U.S. Department of the Interior, Bureau of Reclamation, Technical Services Center, Sedimentation and River Hydraulics Group. Denver, CO.

Varyu, D. (2016). *SRH-1D Numerical Model for the Middle Rio Grande: Isleta Diversion Dam to San Acacia Diversion Dam*. U.S. Department of the Interior, Bureau of Reclamation, Technical Services Center, Sedimentation and River Hydraulics Group. Denver, CO.

Yang, C.Y. (2019). *The Sediment Yield of South Korean Rivers*, Colorado State University, Fort Collins, CO.

Yang, C.Y. and Julien, P.Y. (2019). "The ratio of measured to total sediment discharge." *International Journal of Sediment Research,* 34(3), pp.262-269.

Yang, C.Y., LaForge, K., Julien, P.Y., and Doidge, S. (2019). Draft Report. *Isleta Reach: Hydraulic Modeling and Silvery Minnow Habitat Analysis*, Colorado State University, Fort Collins, CO.

Appendix A

Cumulative Plots used in the Subreach Delineation, Aerial Imagery with Agg/deg Line Labels

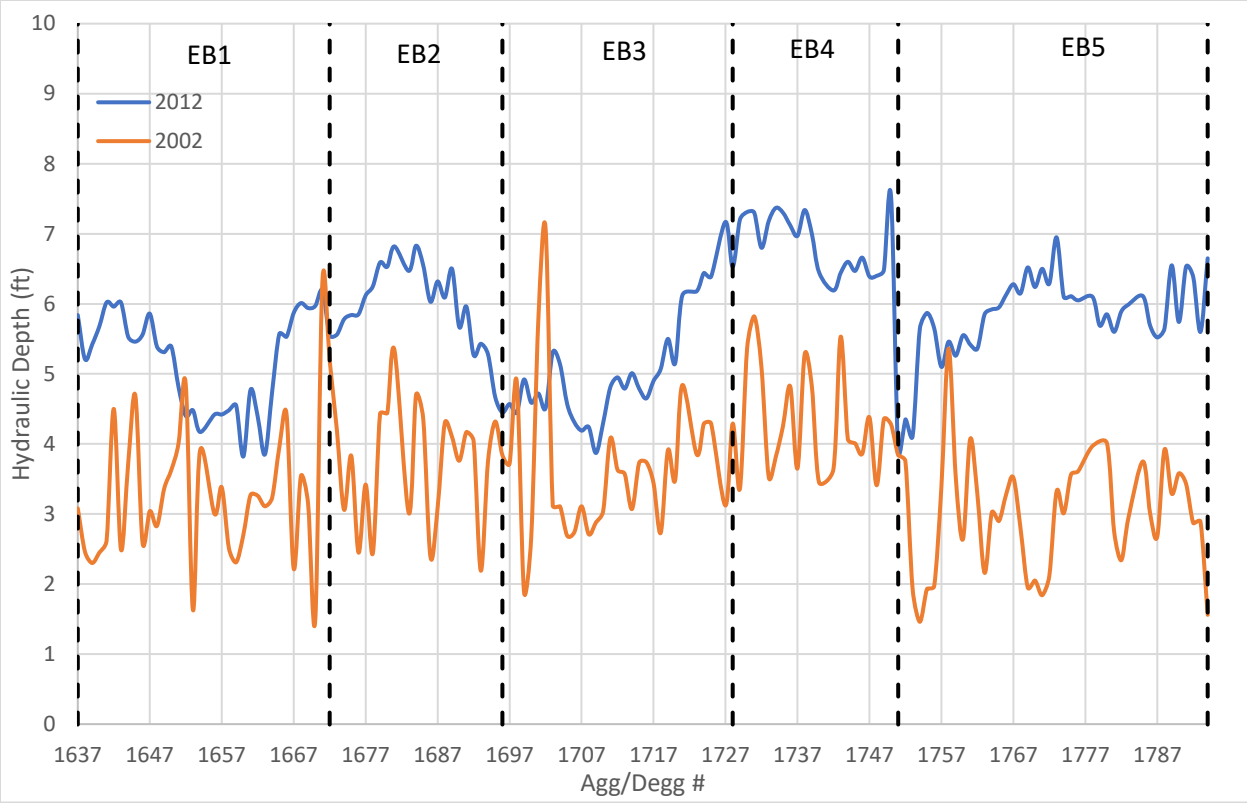

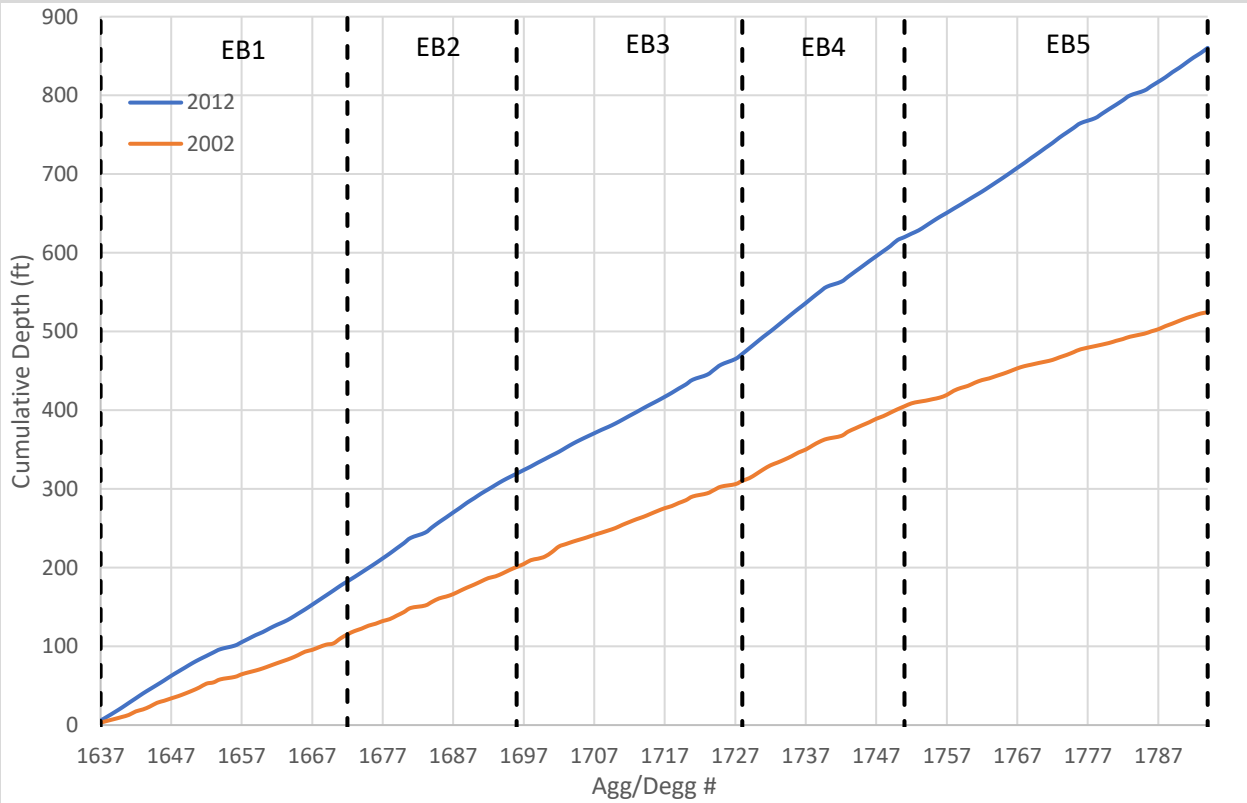

Figure A- 2 Depth (top) and cumulative depth (bottom) throughout the Elephant Butte Reach for the years 2002 (orange) and 2012 (blue).

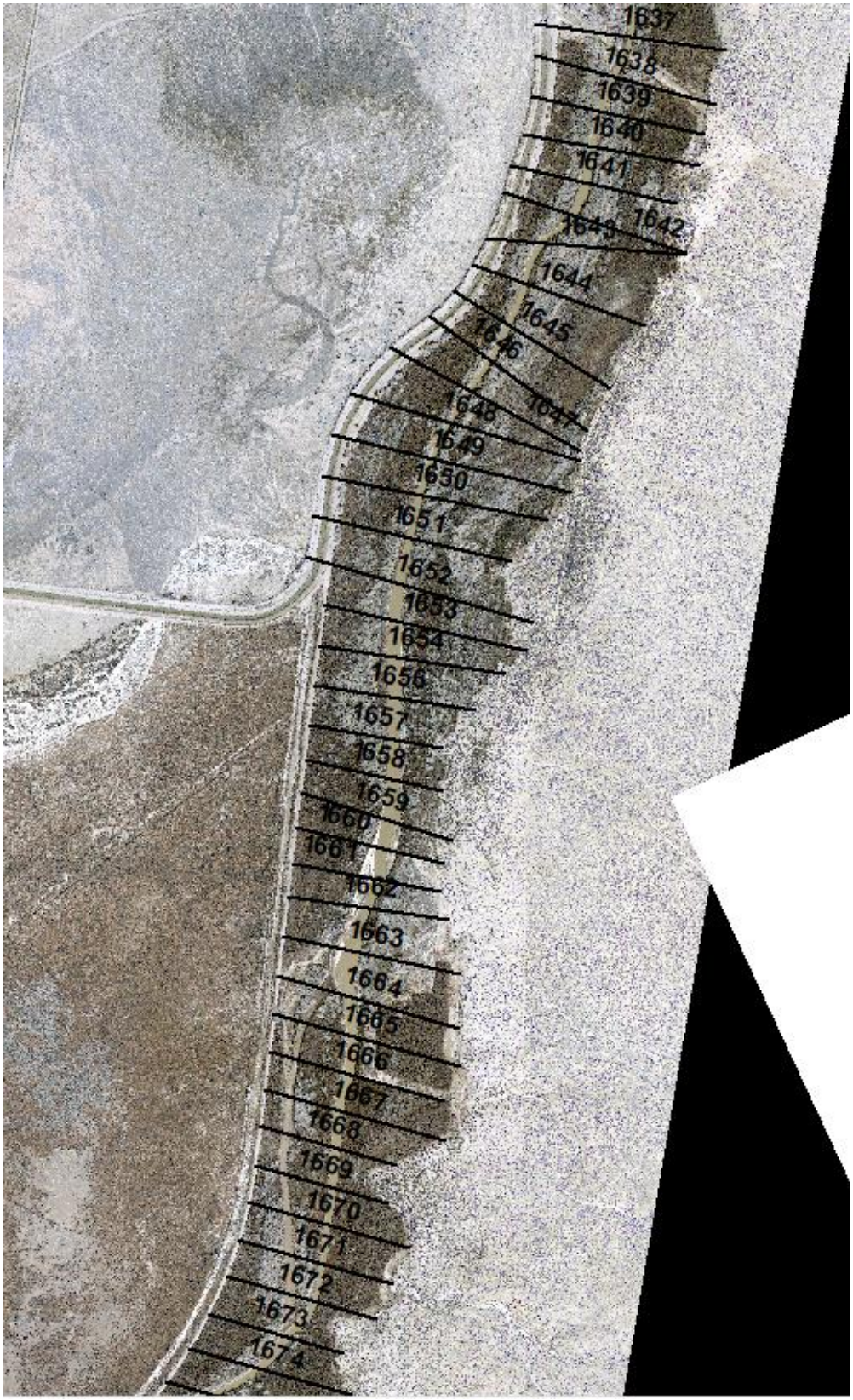

Figure A- 3 2012 Aerial imagery with agg/deg line labels

Figure A- 4 2012 Aerial imagery with agg/deg line labels

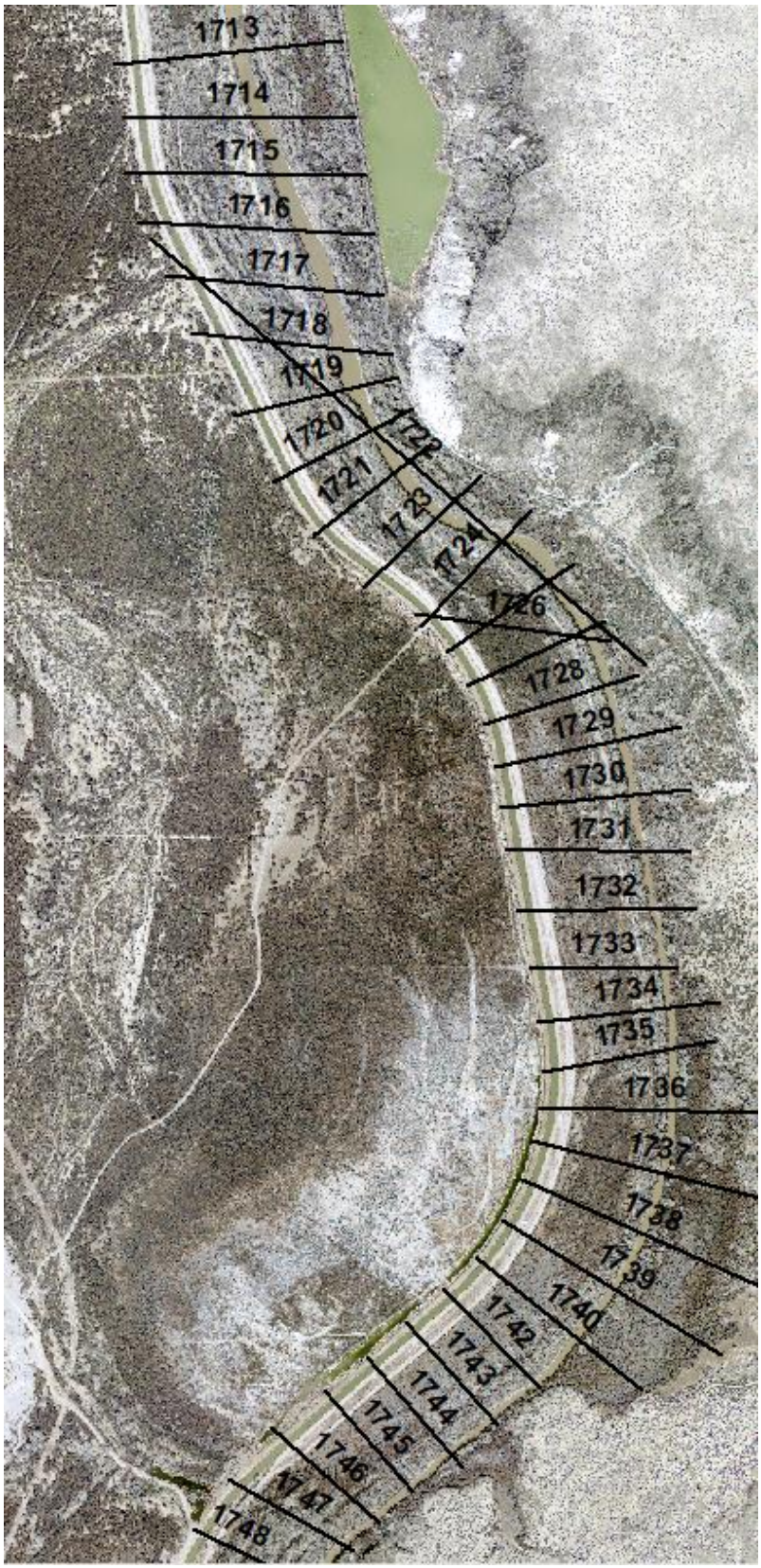

Figure A- 5 2012 Aerial imagery with agg/deg line labels

Figure A- 6 2012 Aerial imagery with agg/deg line labels

Figure A- 7 2012 Aerial imagery with agg/deg line labels

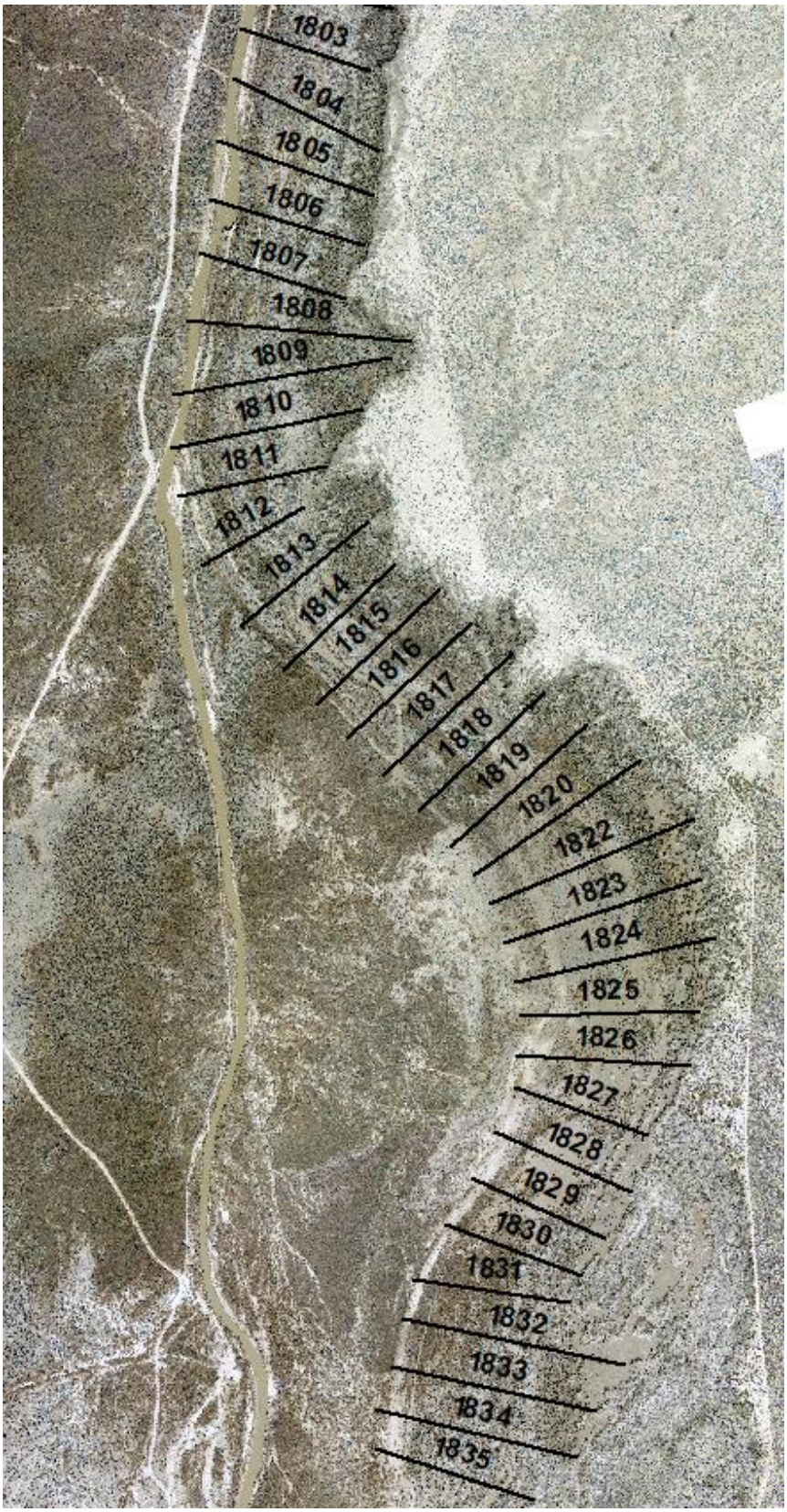

Figure A- 8 2012 Aerial imagery with agg/deg line labels

Figure A- 9 2012 Aerial imagery with agg/deg line labels

Figure A- 10 2012 Aerial imagery with agg/deg line labels

Figure A- 11 2012 Aerial imagery with agg/deg line labels

Figure A- 12 2012 Aerial imagery with agg/deg line labels

Figure A- 13 2012 Aerial imagery with agg/deg line labels

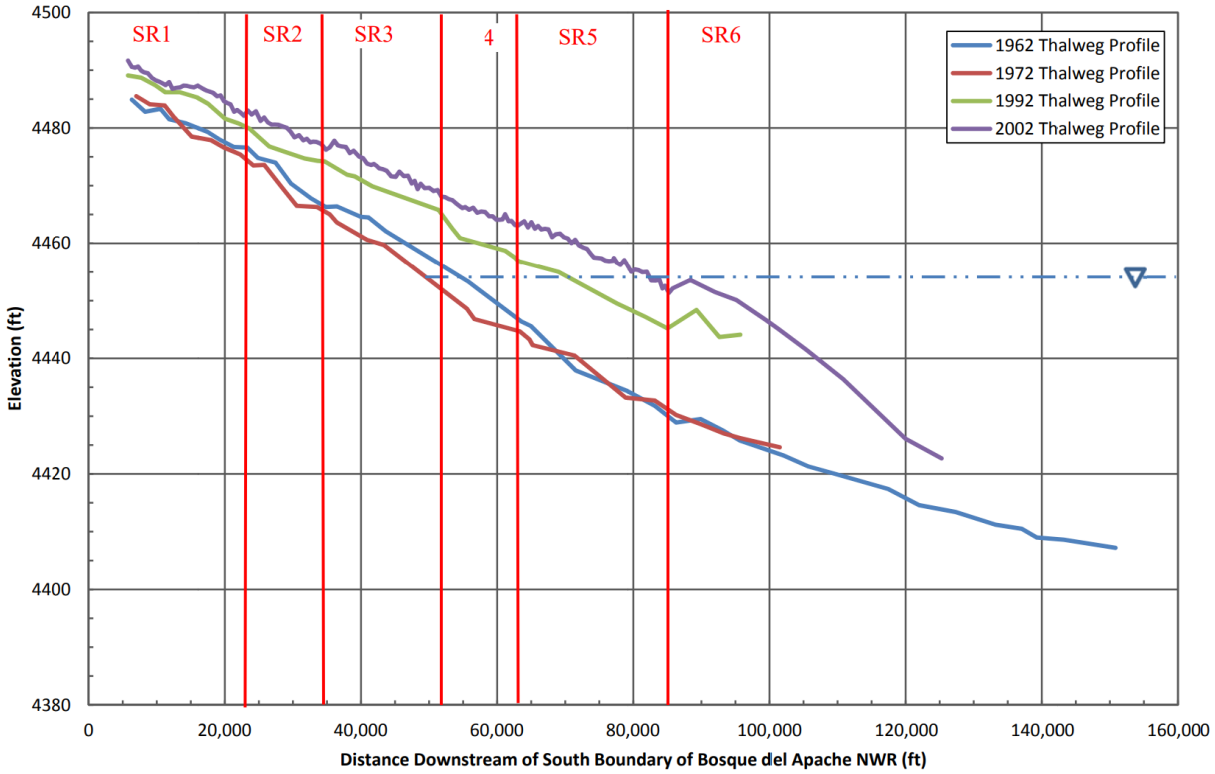

Figure A- 14 Thalweg Elevation Profile from Agg/Deg Surveys (Owens, 2012)

Appendix B

Total Sediment Load using SEMEP Analysis (Shah-Fairbank et al., 2011)

&

Years Used For Julien and Wargadalam (JW) Equation Calculations

The Series Expansion of Einstein Procedure (SEMEP) was used in this study to estimate the total sediment load in the Middle Rio Grande (Yang, C.Y. 2019). The method was developed at CSU with the procedure detailed in Shah-Fairbank et al. (2011) as a function of shear velocity u_* and fall velocity ω. In this report, SEMEP is applied at three stations on the Rio Grande, at San Acacia gage 08354900, as well as Albuquerque and Bernardo at gages 08330000 and 08332010. The number of field samples calculated by the SEMEP are 306, 211, and 173, respectively, at gages 08330000, 08332010, and 08354900. For these stations, the values of u_*/ω range from 1.5 to 37,600. According to Shah-Fairbank et al. (2011), SEMEP performs accurately when $u_*/\omega > 5$, so good results are expected from this application.

It can be seen in Figure B-1 that the SEMEP predictions and total sediment load measurements fall close to the 45-degree line of perfect agreement. Figure B-1 also shows the prediction errors between SEMEP calculations and measurements as a function of u_*/ω. The mean absolute percent difference is 27%. Figure B-2 shows the sediment rating curves for total sediment discharges at gage 08354900.

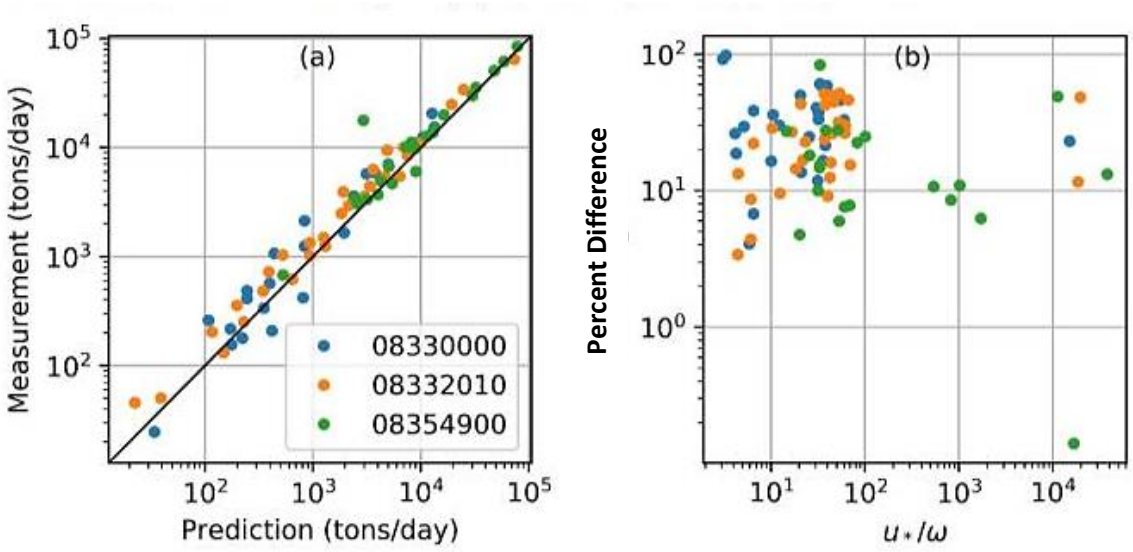

Figure B- 1 Comparison between predicted and measured total sediment load (left) and percent difference vs u/w (right)*

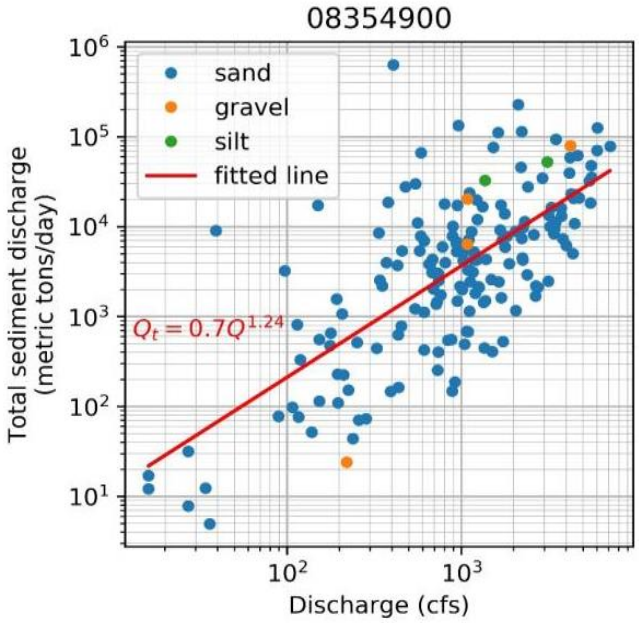

Figure B- 2 Total sediment rating curve at the San Acacia gage

The ratio of measured to total sediment discharge is a function of flow depth h, grain size d_s, and Rouse number Ro (Ro = $\omega/2.5u_*$) according to SEMEP (Shah-Fairbank et al. 2011; Yang and Julien 2019). In addition, the ratio of suspended to total sediment discharge is a function of the ratio h/d_s and Ro. The calculated ratio Q_m/Q_t and the ratio Q_s/Q_t are plotted with the analytical solutions in Figure B-3 for the San Acacia gaging stations, where Q_m is the measured sediment discharge, Q_t is the total sediment discharge, and Q_s is the suspended sediment discharge. As expected, when the value of Ro is low (Ro < 0.3), the ratio Q_s/Q_t is close to 100% during floods when h/d_s > 100. These ratios are also in good agreement with the theory for both sands and gravels.

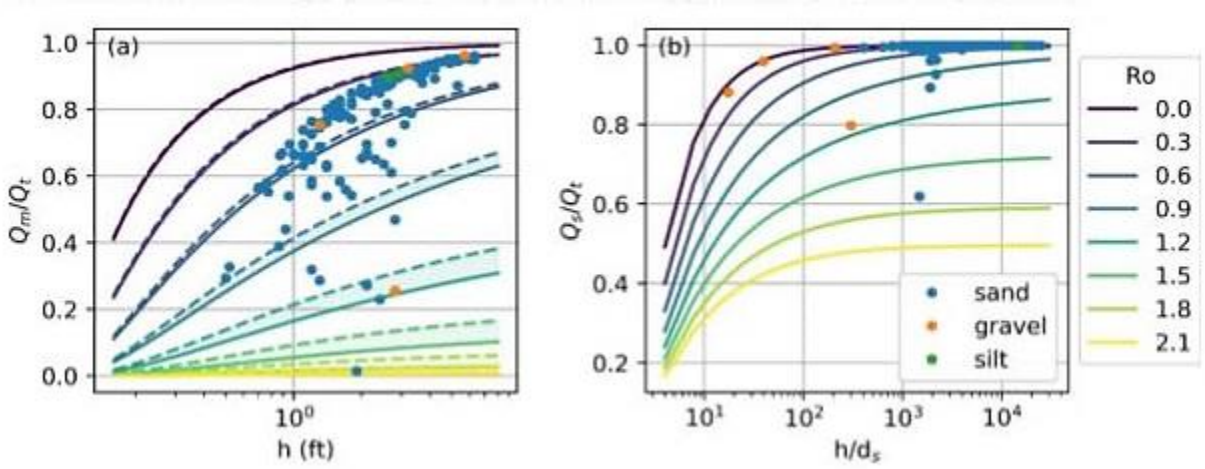

Figure B- 3 the ratio of measured to total sediment discharge vs depth; and (b) the ratio of suspended to total sediment discharge vs h/ds at the San Acacia gage

Table 7 Years used in JW Calculations for D50

Year Analyzed	Subreach	Year Used
1992	EB1	1991
	EB2	1999
	EB3	1992
	EB4	1993
	EB5	1994
2002	EB1	2002
	EB2	1999
	EB3	2002
	EB4	2002
	EB5	2002
2012	EB1	2016
	EB2	1992
	EB3	2017
	EB4	2017
	EB5	2017

Appendix C

Additional Figures from Geomorphology Analyses

(Wetted Top Width Plots, Sediment Rating Curve/Alpha Method Example)

Wetted Top Width Plots

In section 3.1, the cross-section moving averaged top width was plotted for all agg/deg lines in the Elephant Butte Reach. Figures C-1 and C-2 show each cross-section top width plotted against the agg/deg lines rather than the moving average at discharges of 1,000 cfs and 3,000 cfs with levees in place.

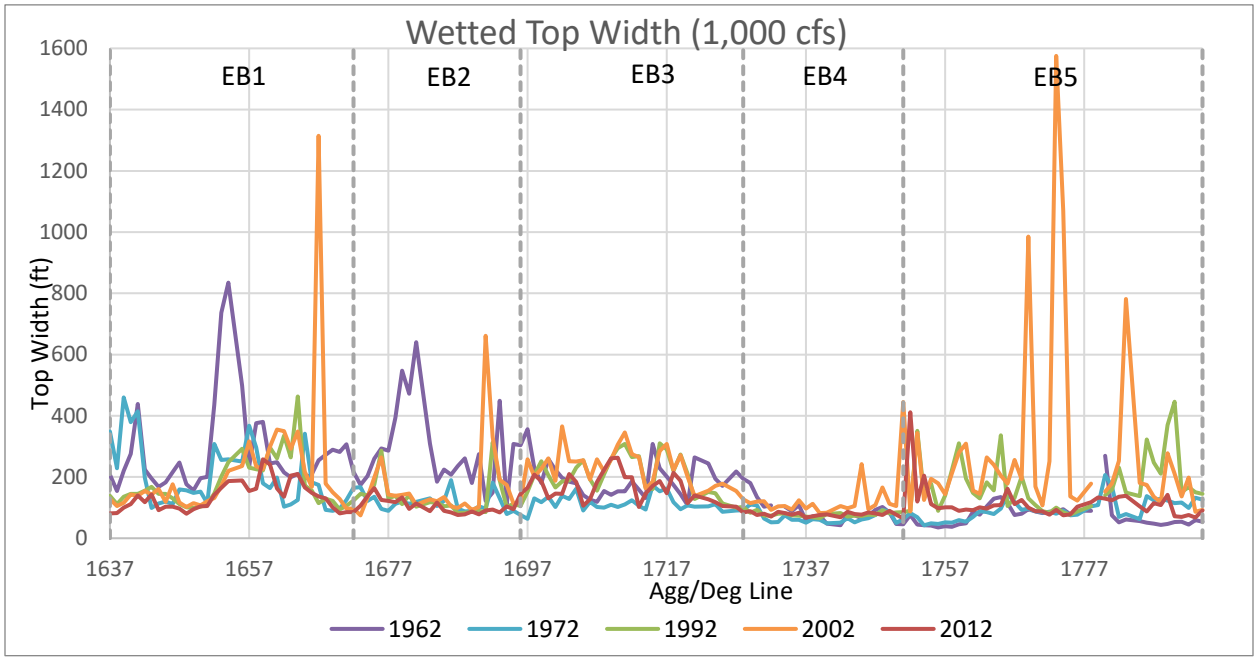

Figure C-1 Wetted top width at each agg/deg line throughout the Elephant Butte Reach at a discharge of 1,000 cfs

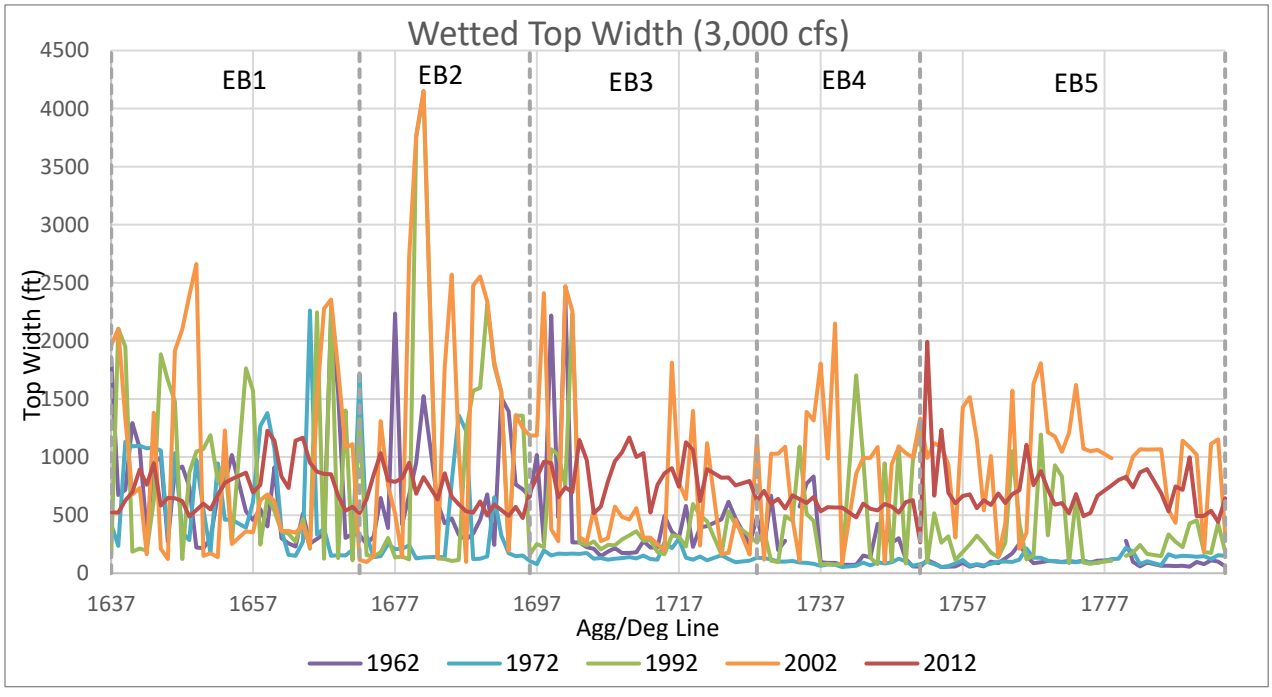

Figure C-2 Wetted top width at each agg/deg line throughout the Elephant Butte Reach at a discharge of 3,000 cfs

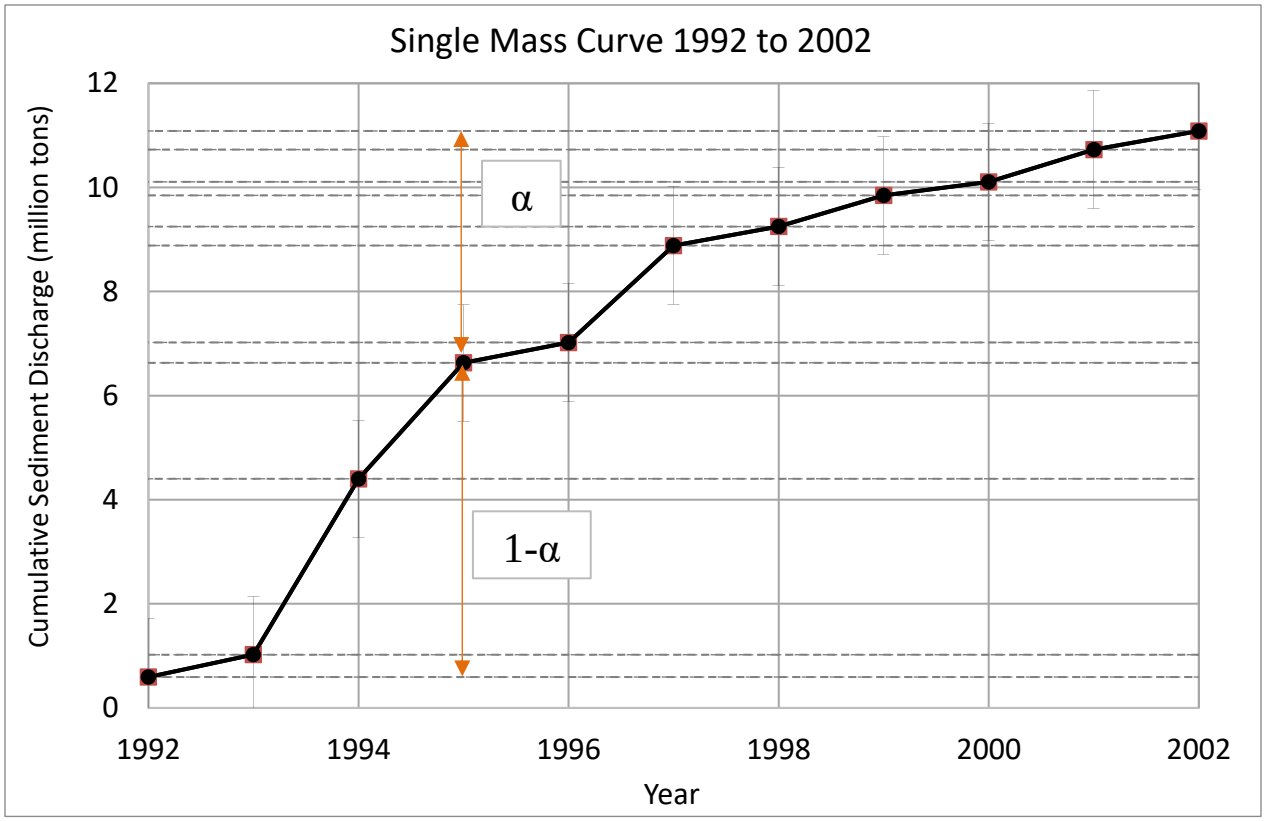

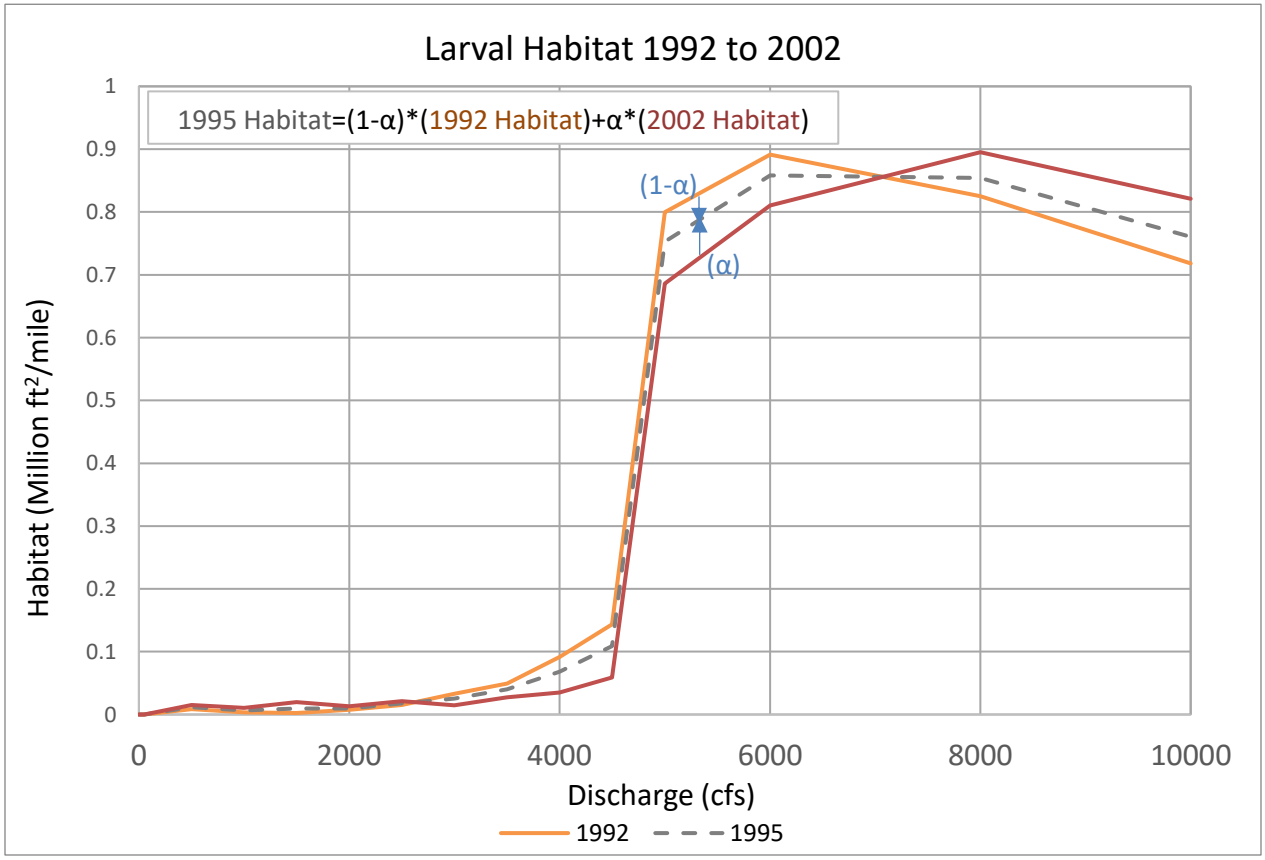

Figure C-3 Example of annual habitat interpolating using the sediment rating curve and alpha technique

Appendix D

Additional Figures from Habitat Analyses

(Habitat Charts by Subreach, Spatially Varying Habitat Charts, Habitat Curves)

Width Slices: Habitat Bar Charts

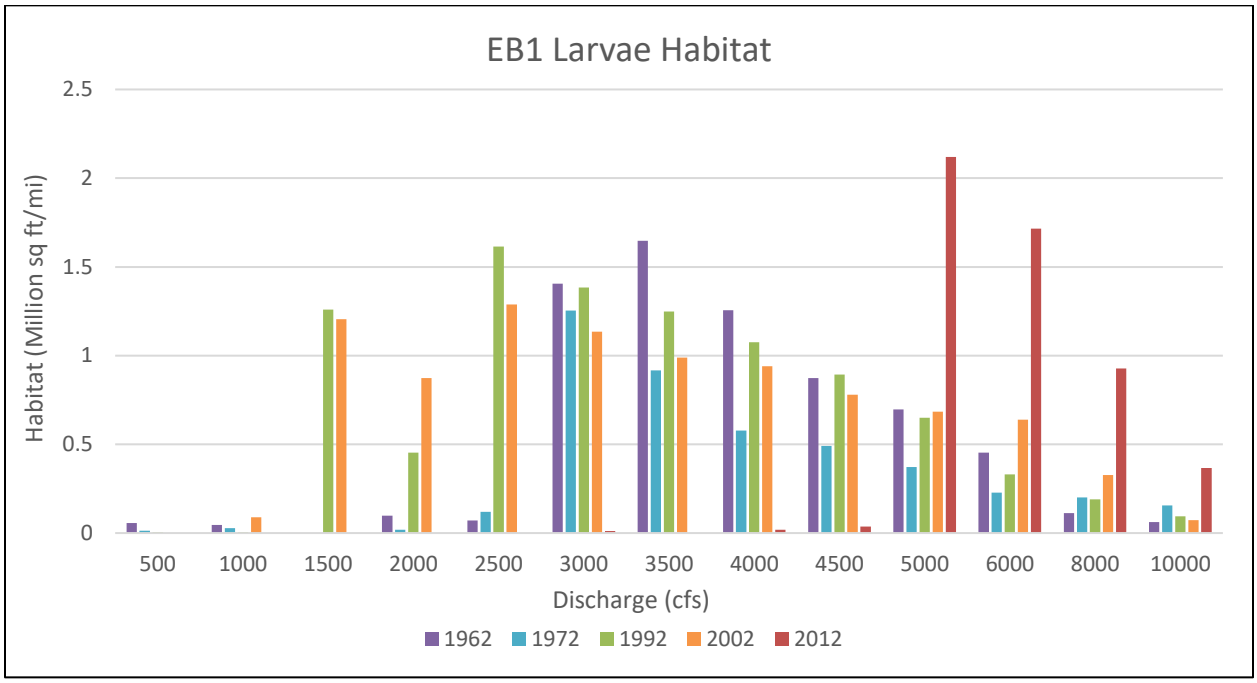

Figure D-1 Subreach EB1 larva habitat

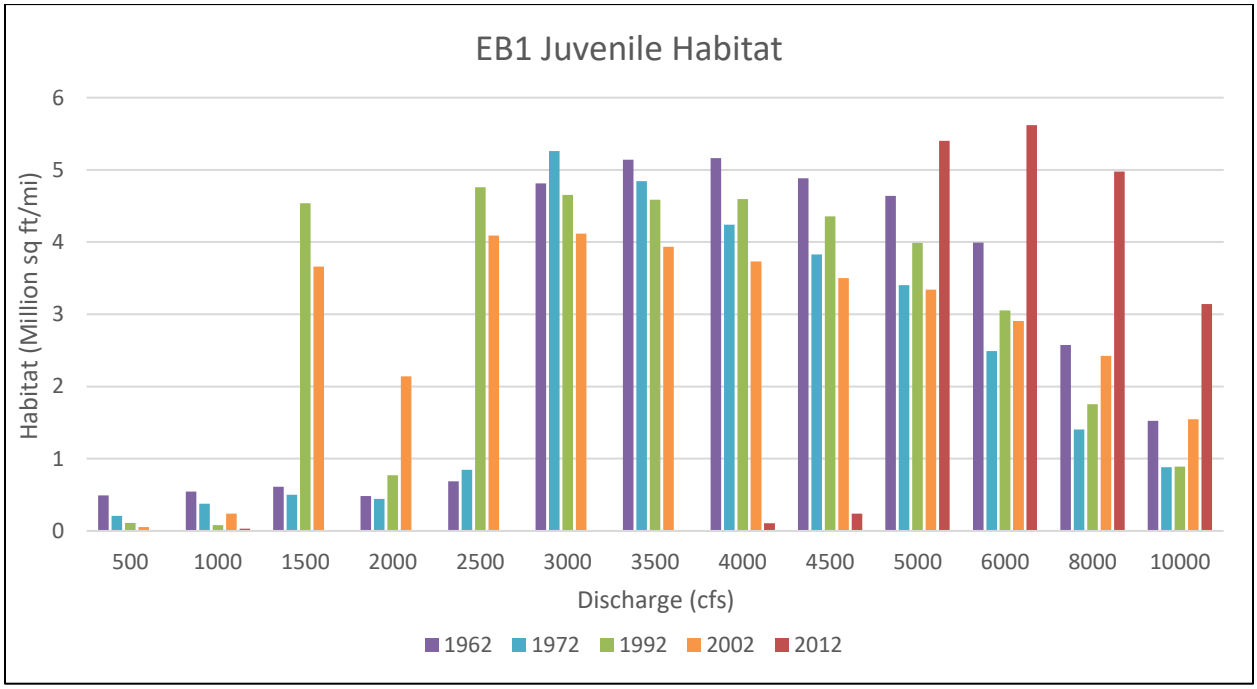

Figure D-2 Subreach EB1 juvenile habitat

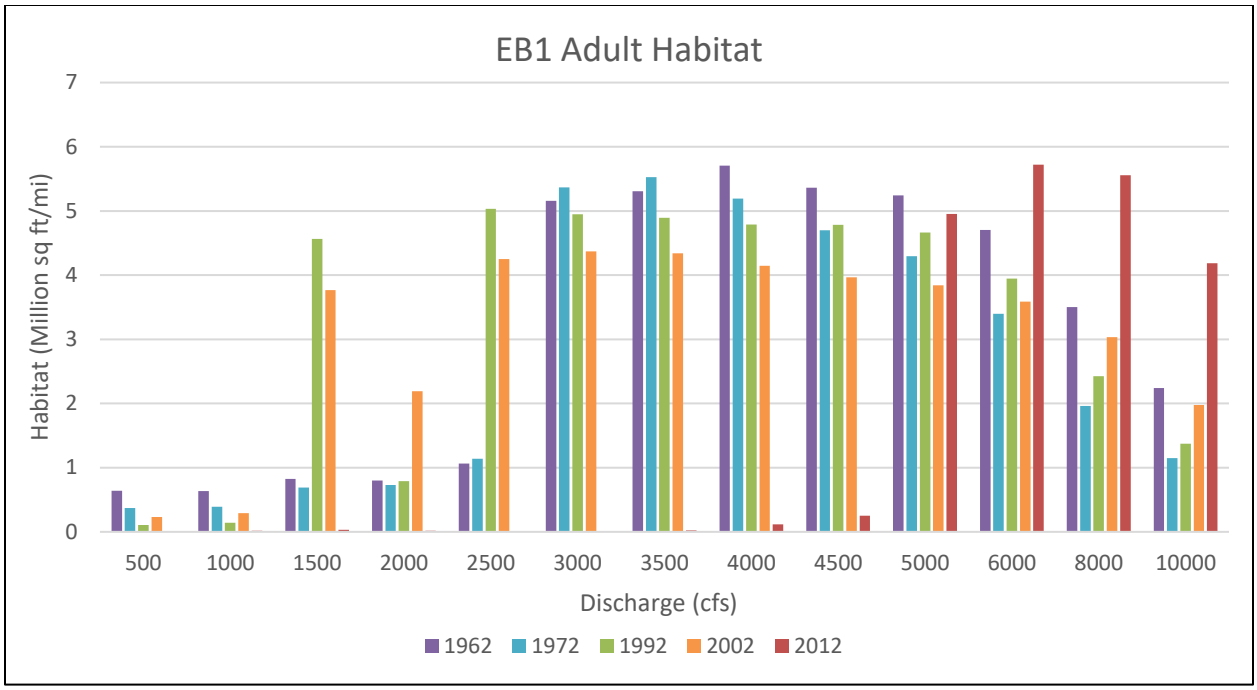

Figure D-3 Subreach E1 adult habitat

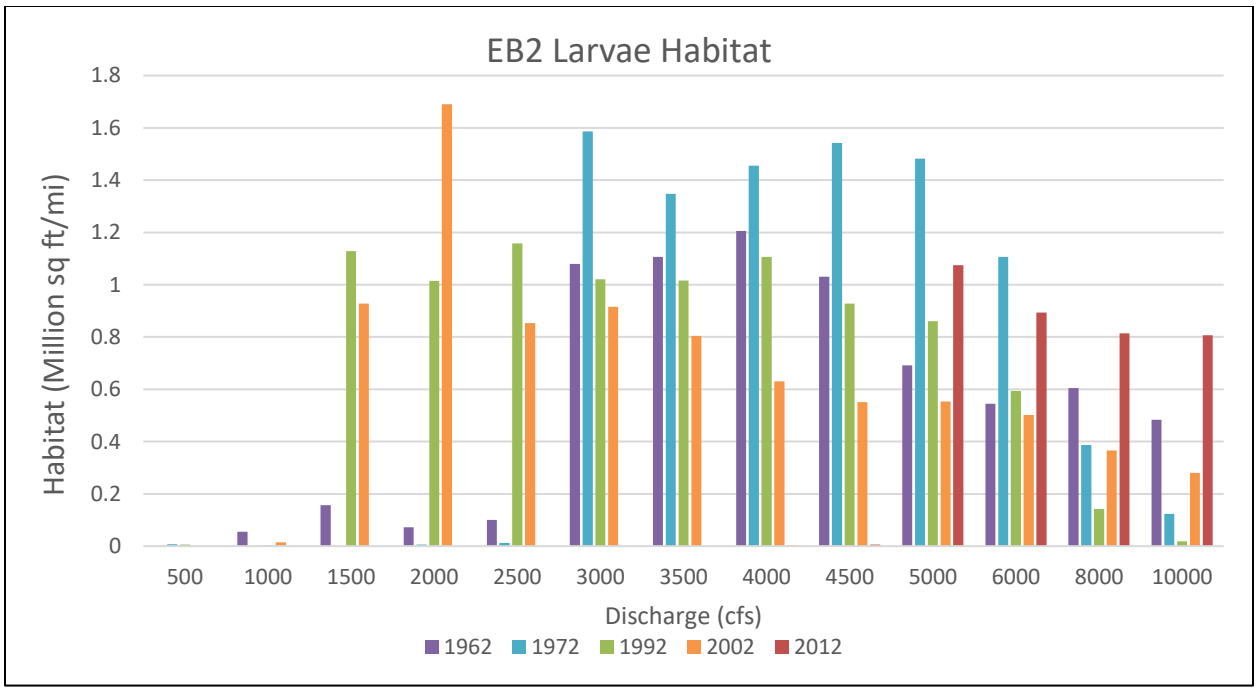

Figure D-4 Subreach EB2 larva habitat

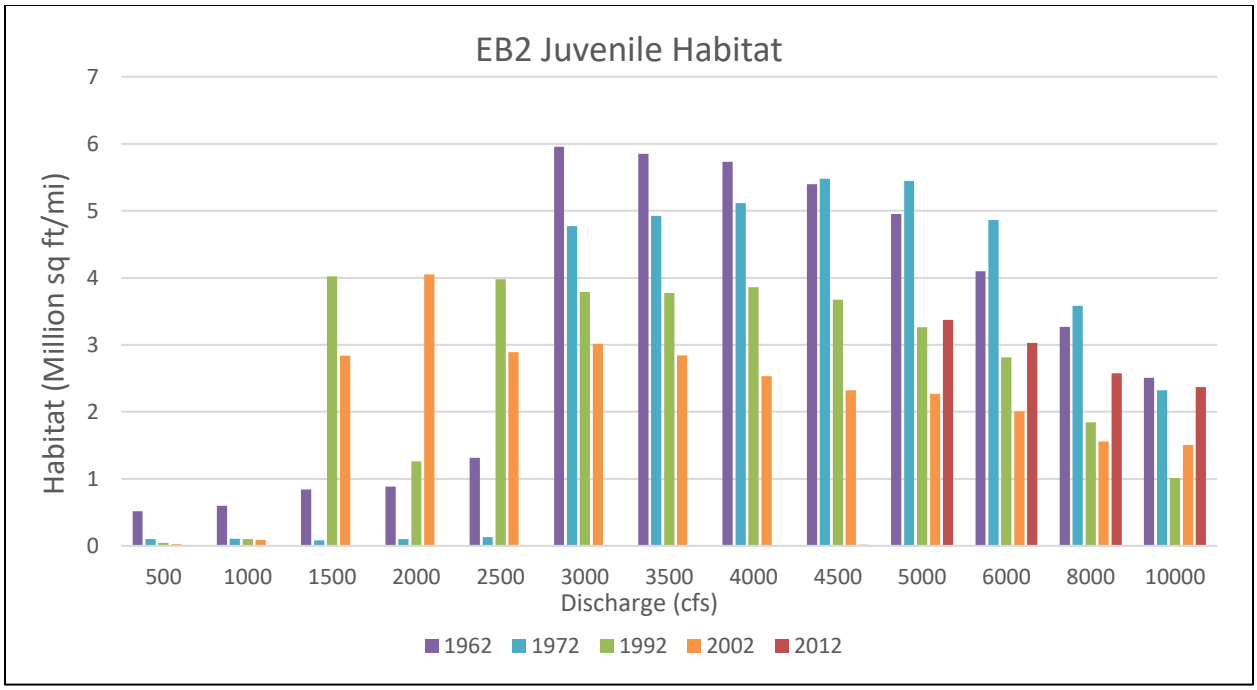

Figure D-5 Subreach EB2 juvenile habitat

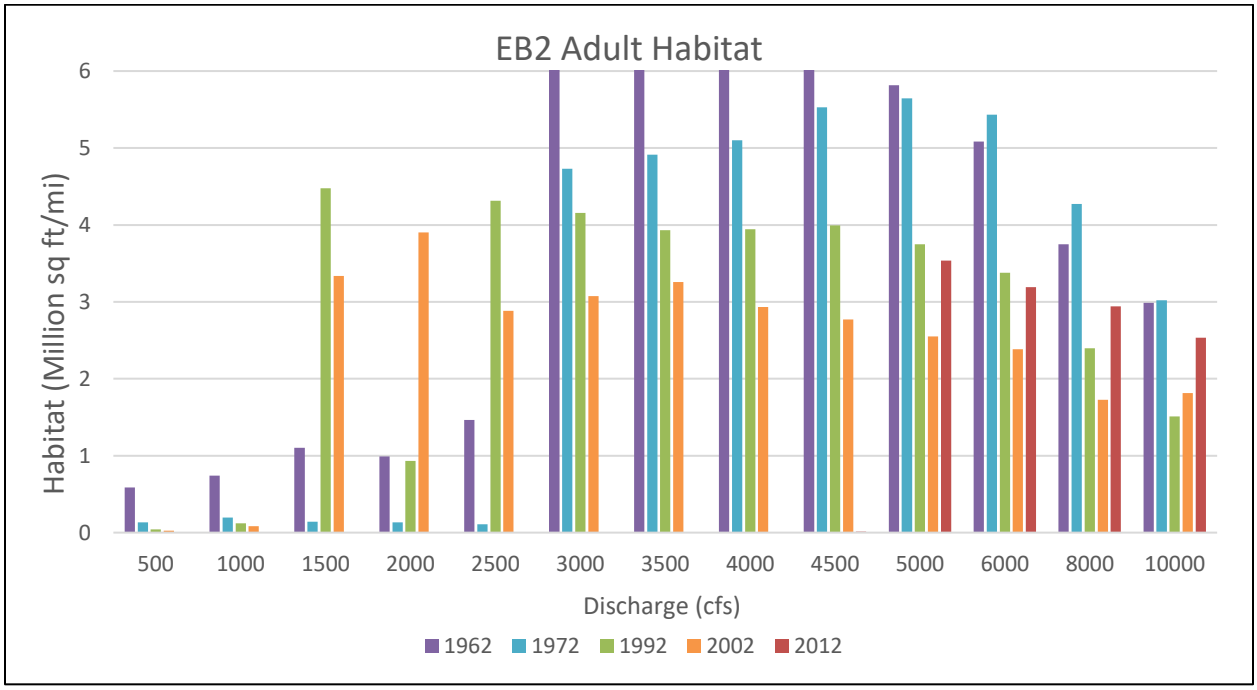

Figure D-6 Subreach EB2 adult habitat

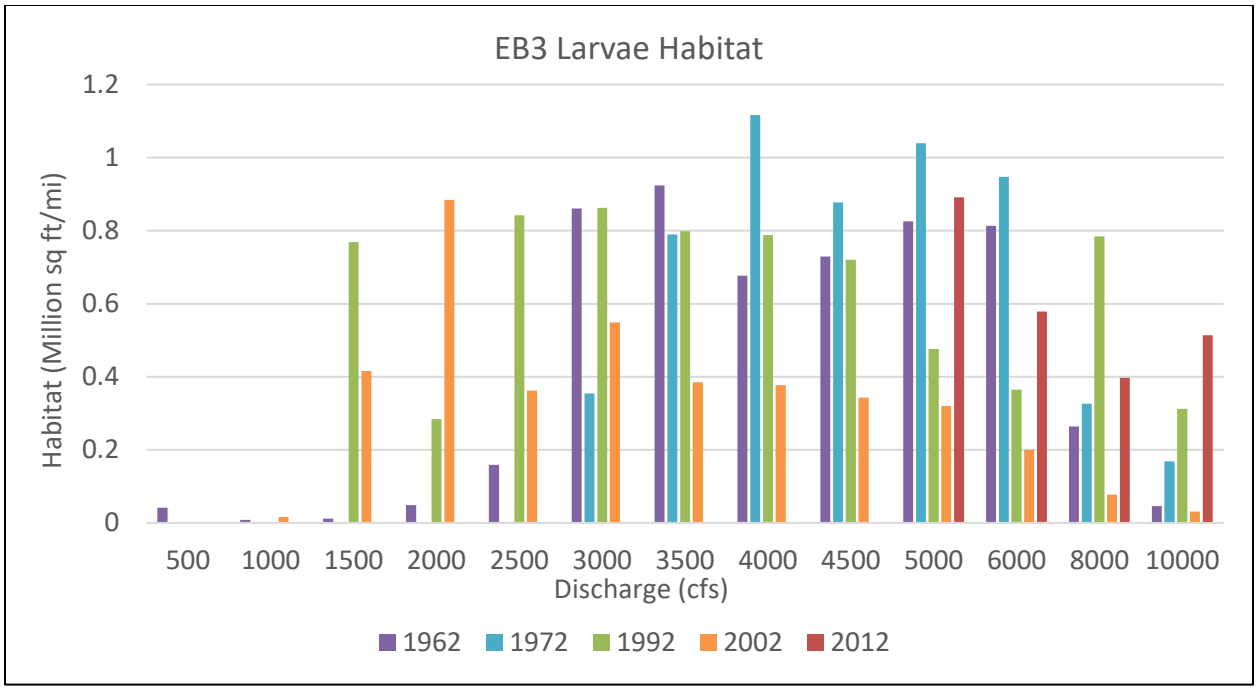

Figure D-7 Subreach EB3 Larva Habitat

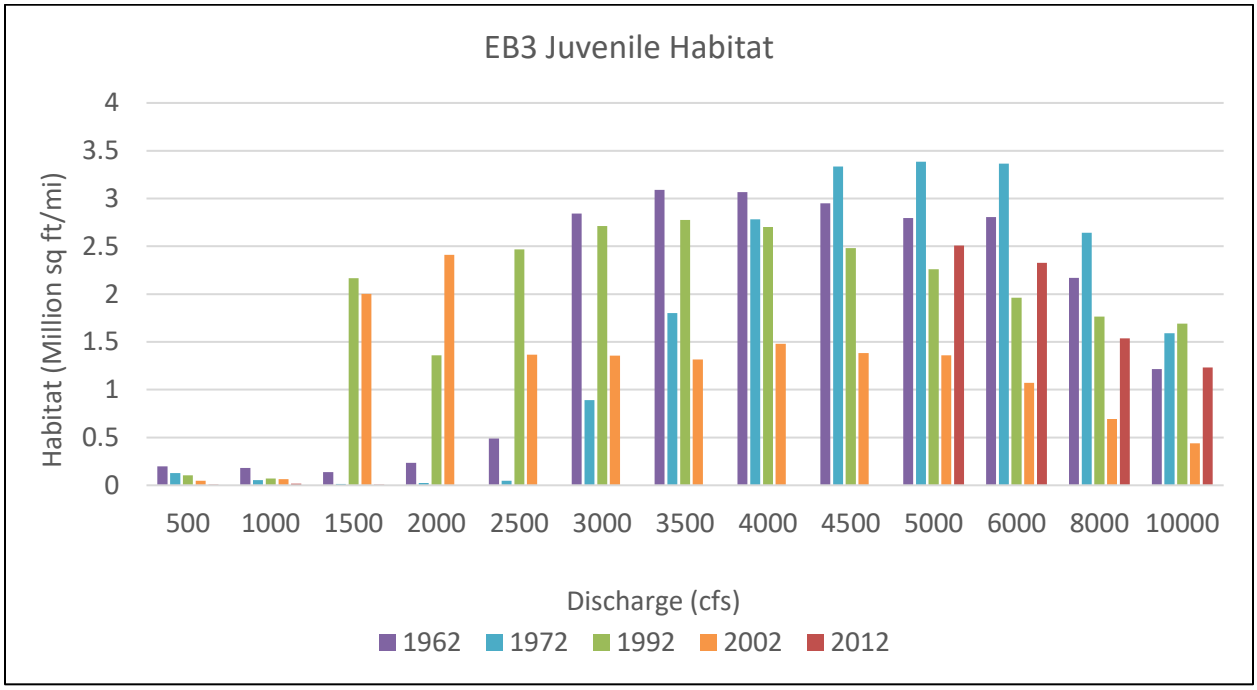

Figure D-8 Subreach EB3 Juvenile Habitat

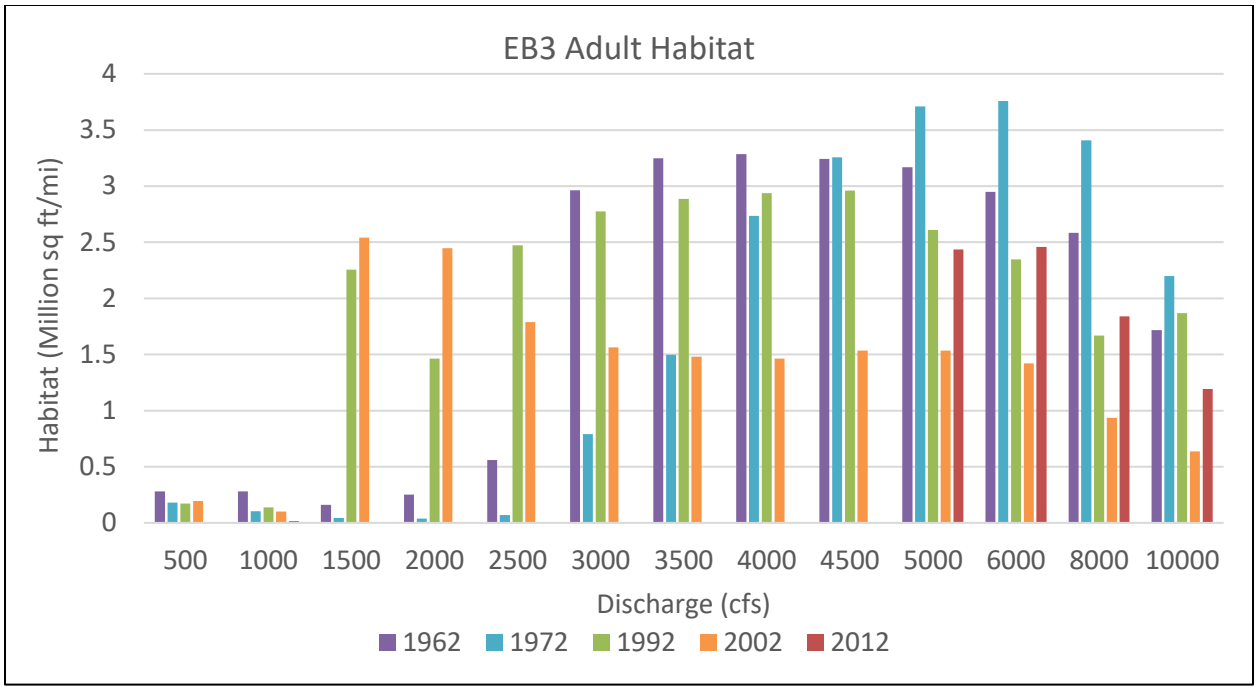

Figure D-9 Subreach EB3 Adult Habitat

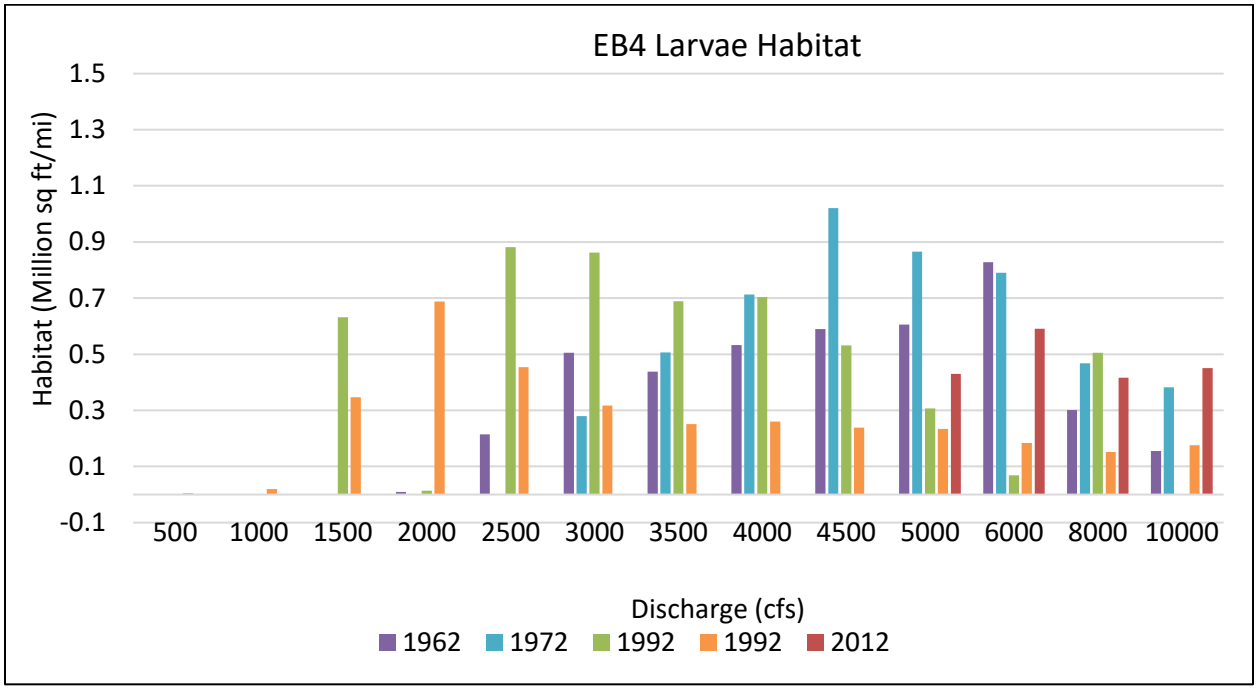

Figure D-10 Subreach EB4 Larva Habitat

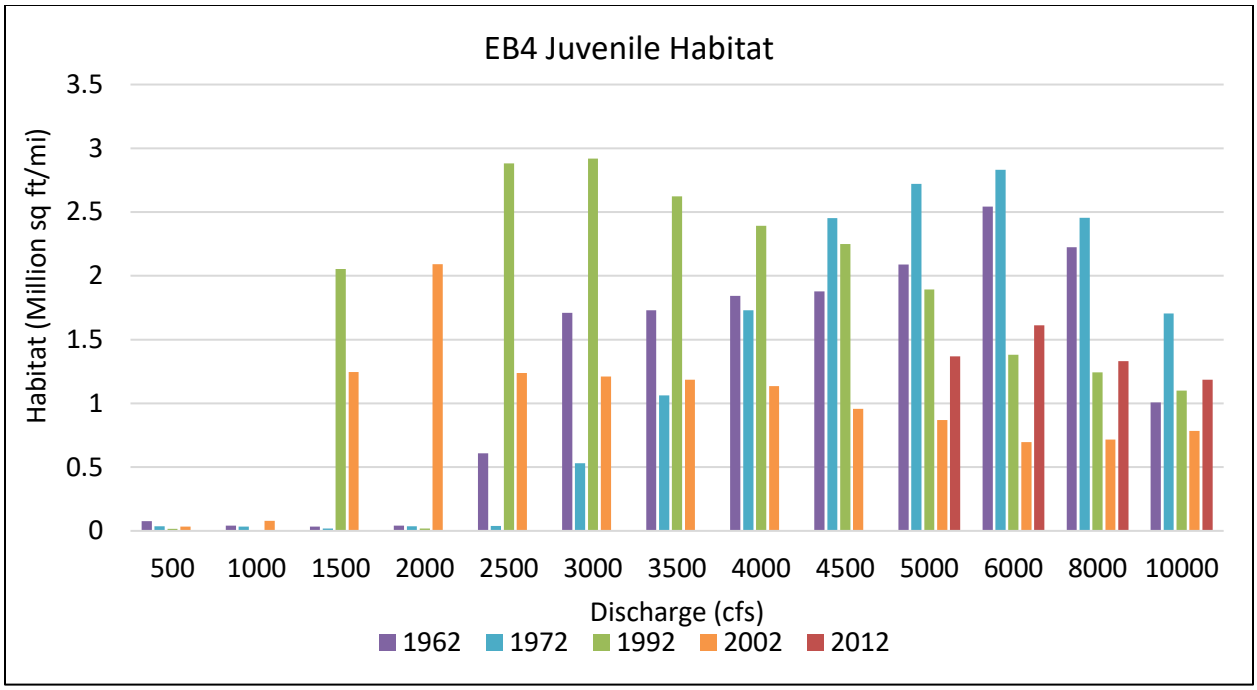

Figure D-11 Subreach EB4 Juvenile Habitat

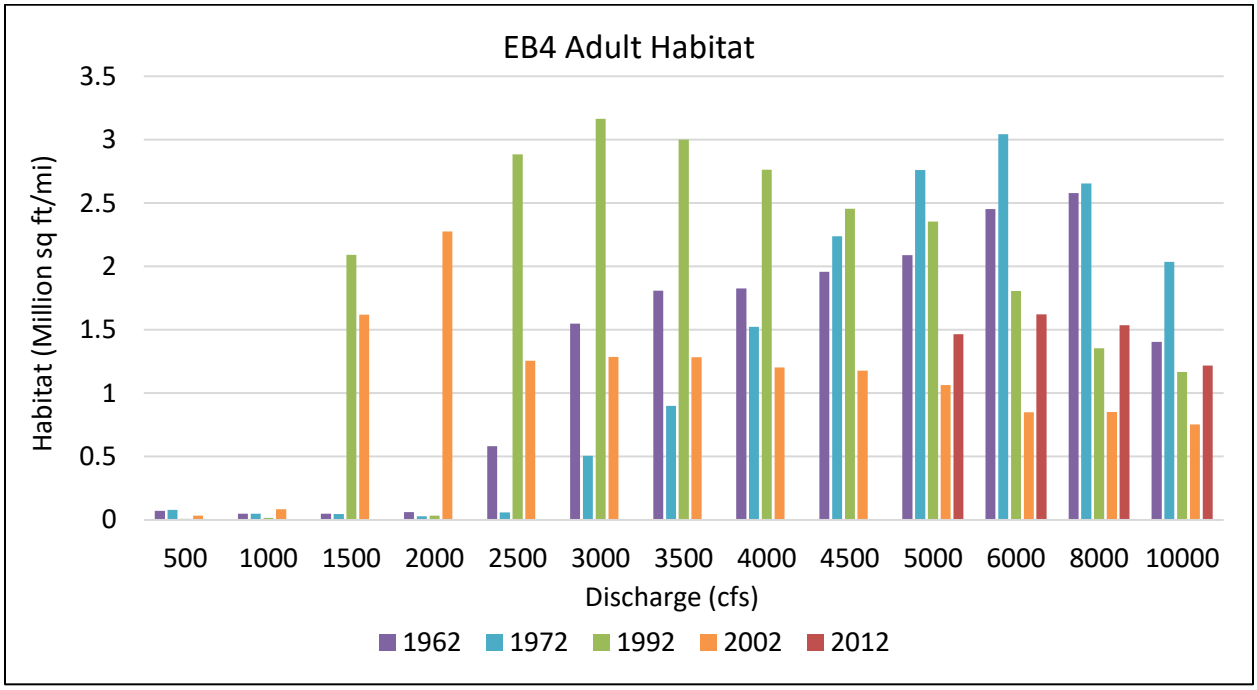

Figure D-12 Subreach EB4 Adult Habitat

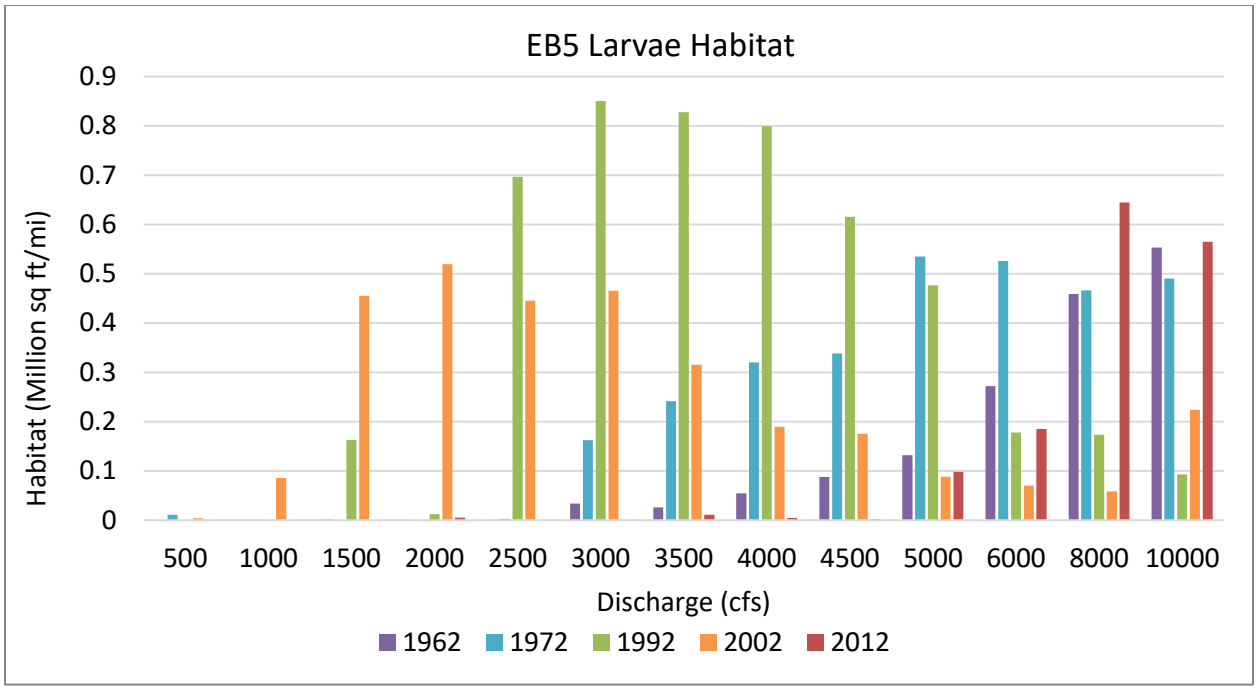

Figure D-13 Subreach EB5 Larva Habitat

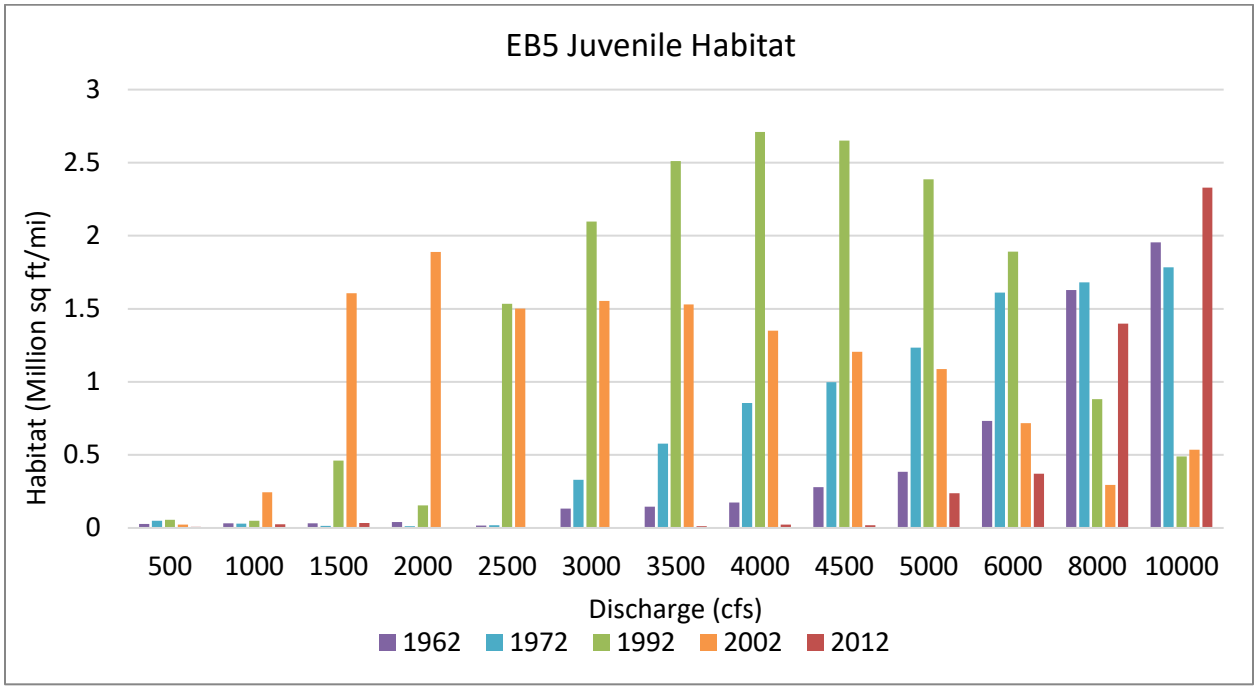

Figure D-14 Subreach EB5 Juvenile Habitat

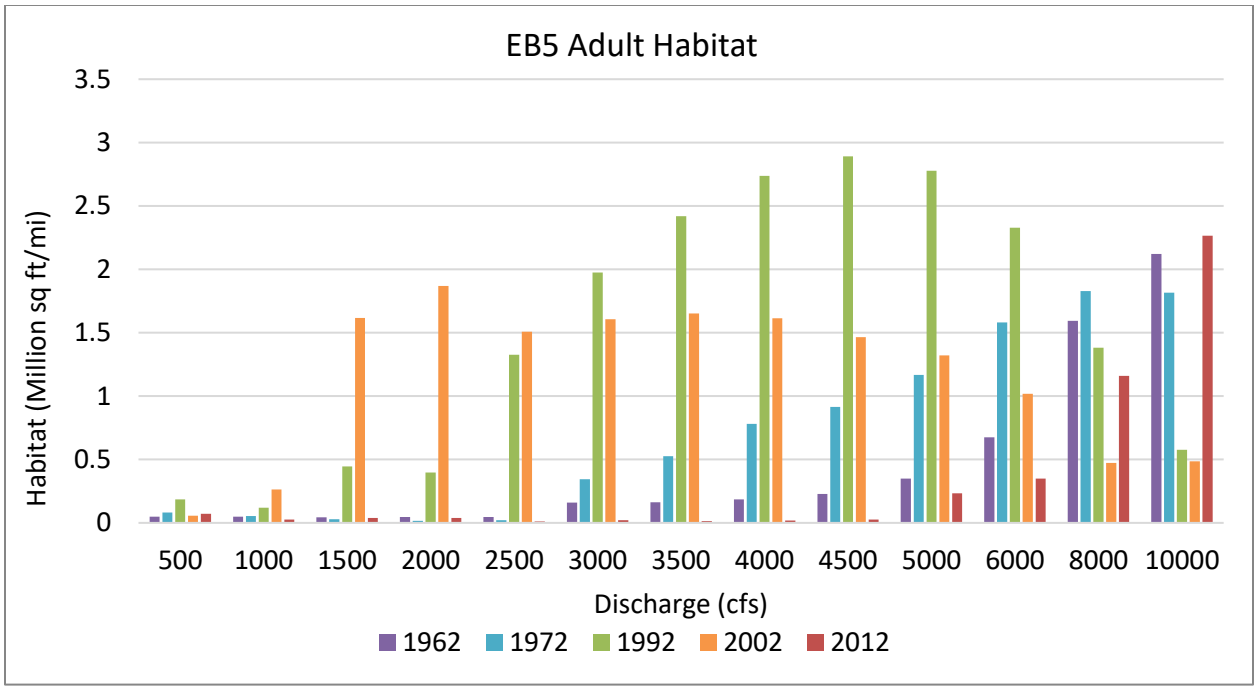

Figure D-15 Subreach EB5 Adult Habitat

Stacked Habitat Charts

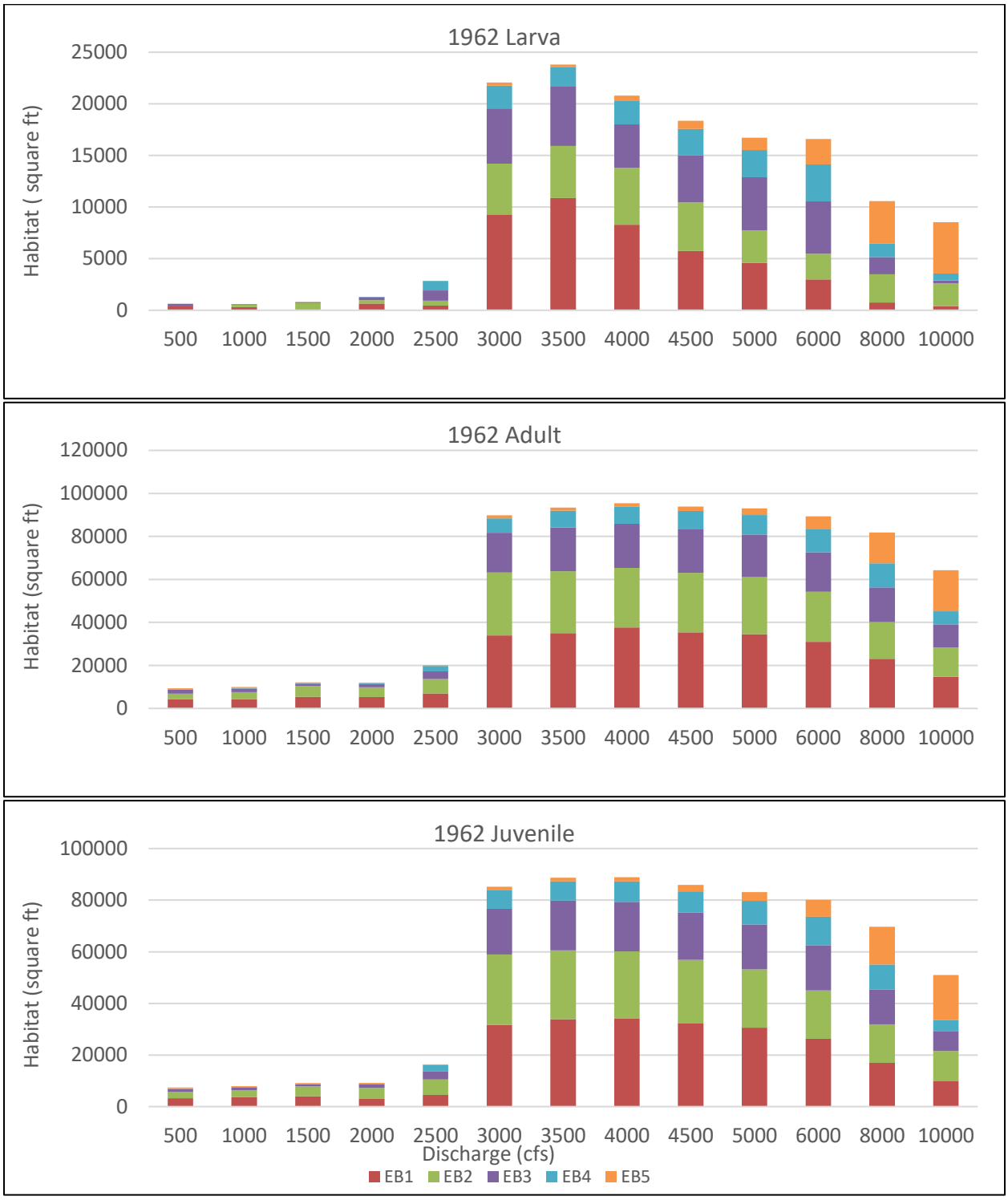

Figure D-16 Stacked habitat charts to display spatial variations of habitat throughout the Elephant Butte Reach in 1962

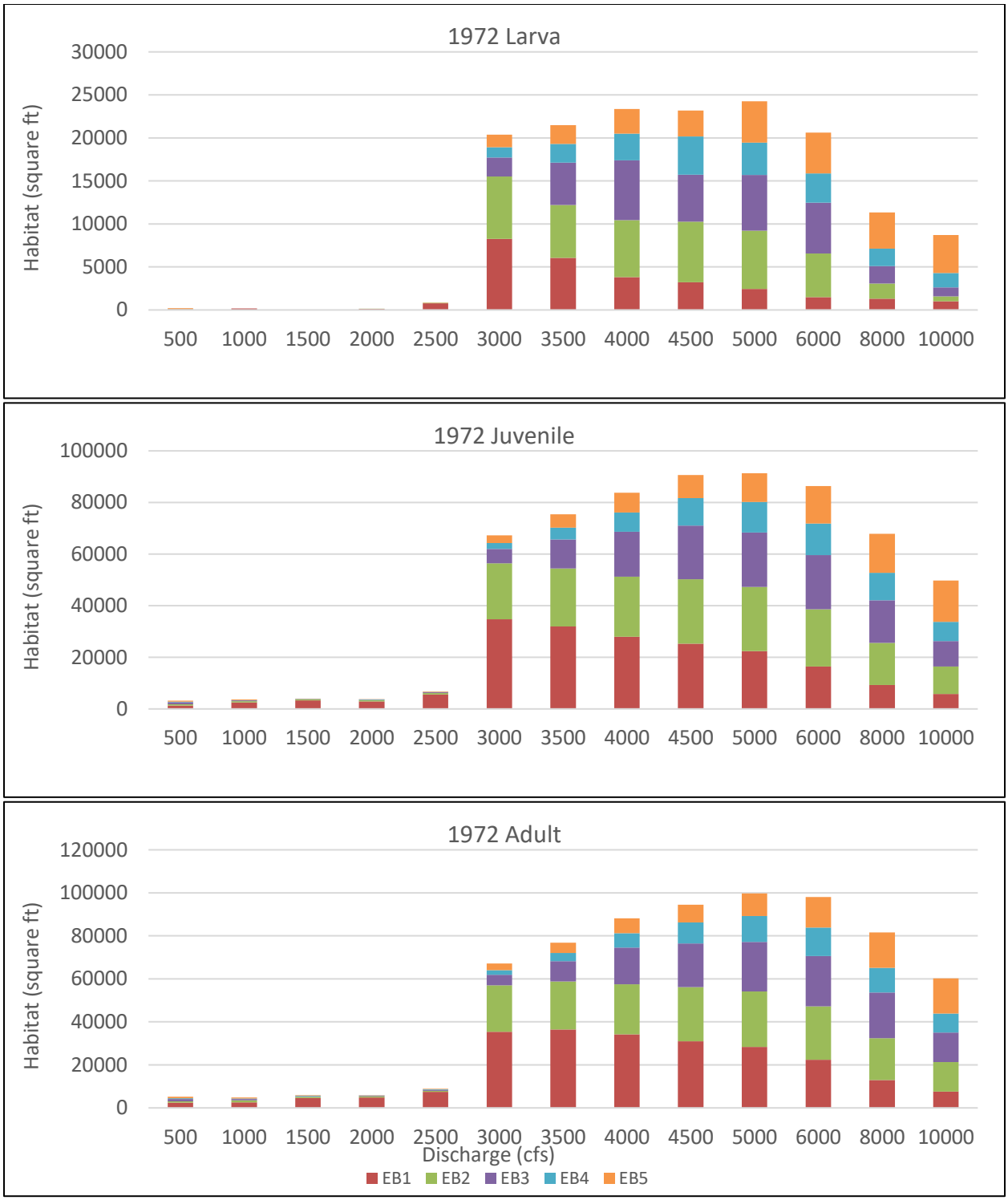

Figure D-17 Stacked habitat charts to display spatial variations of habitat throughout the Elephant Butte Reach in 1972

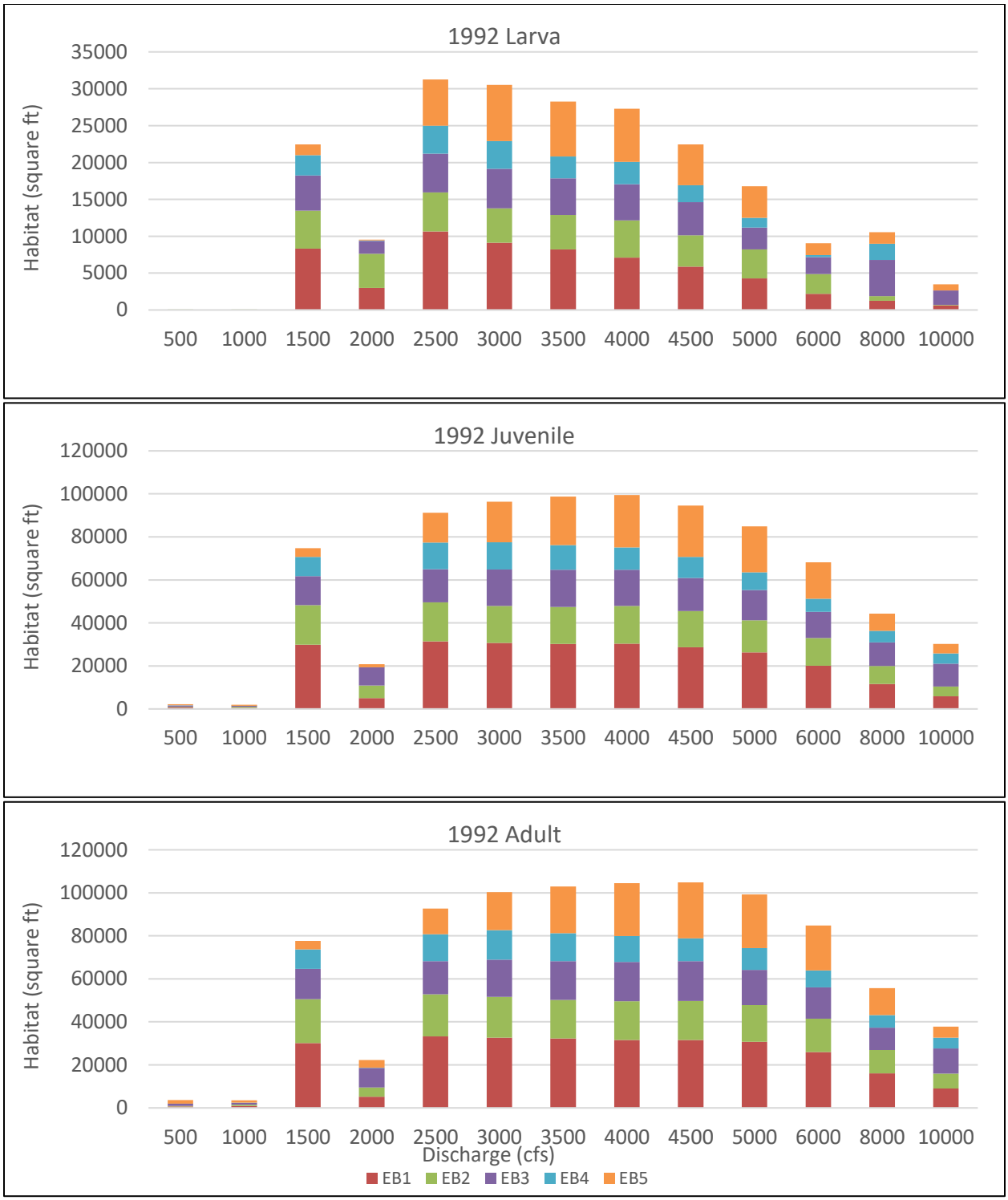

Figure D-18 Stacked habitat charts to display spatial variations of habitat throughout the Elephant Butte Reach in 1992

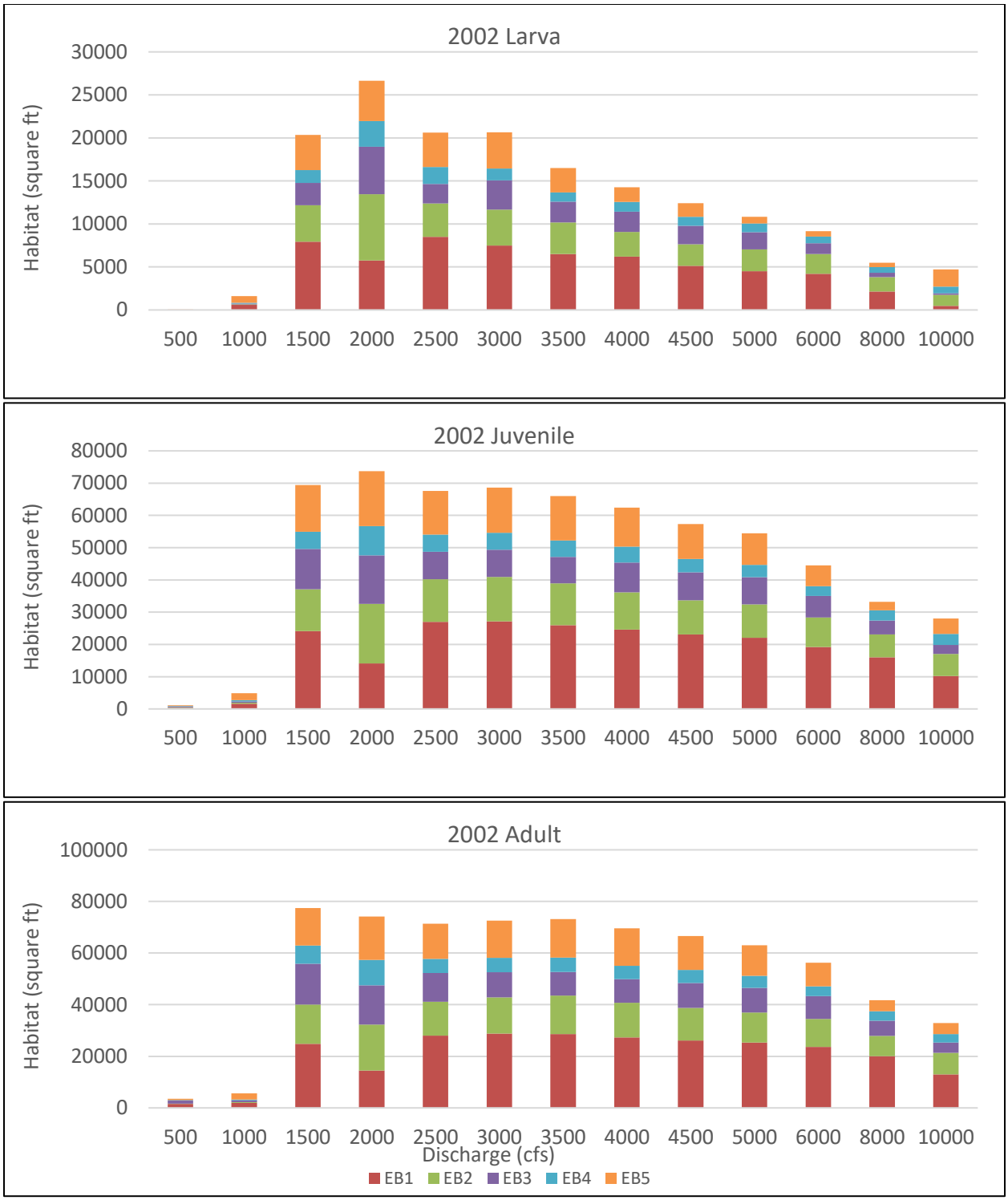

Figure D-19 Stacked habitat charts to display spatial variations of habitat throughout the Elephant Butte Reach in 2002

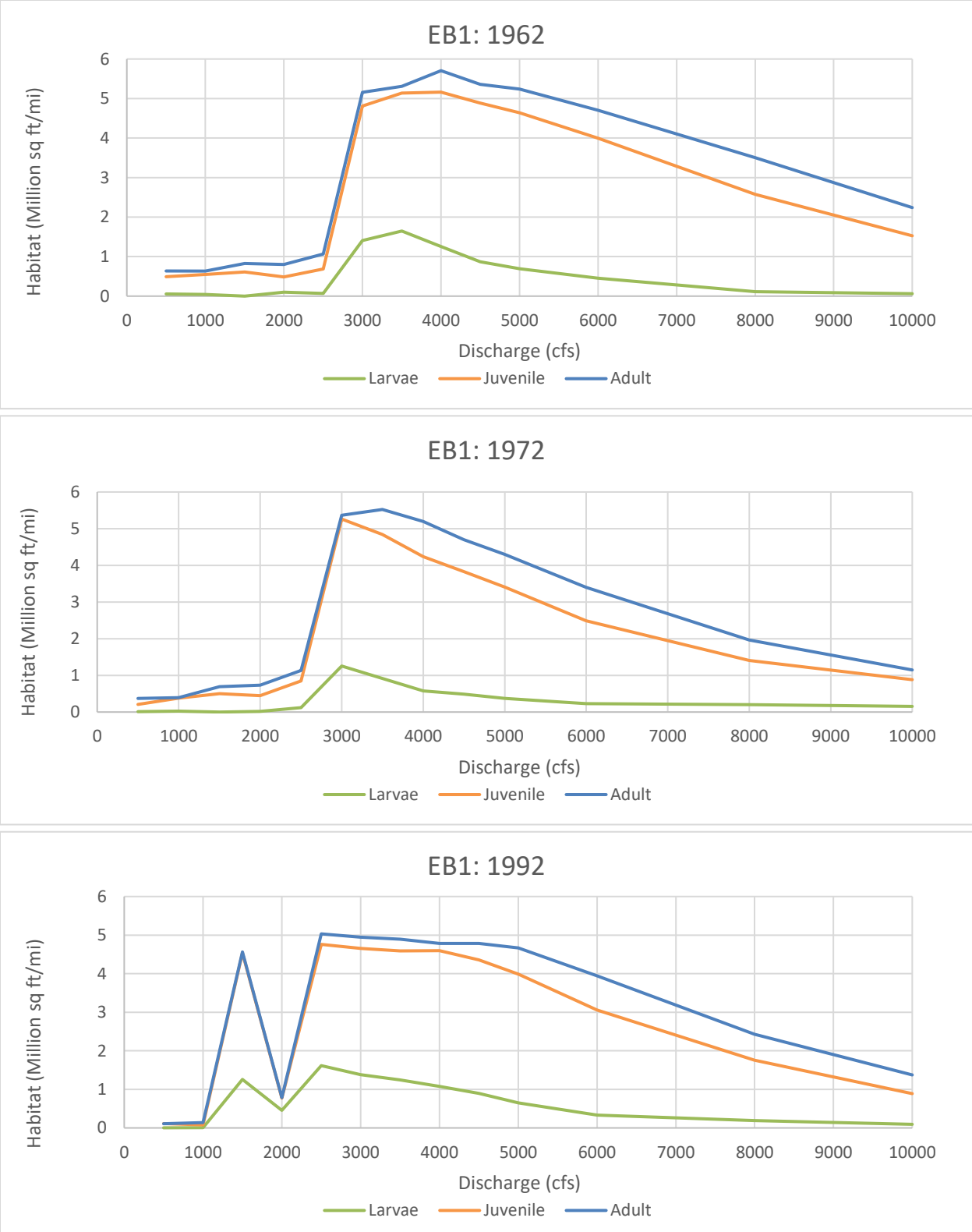

Figure D-20 Life stage habitat curves for subreach EB1 at the years 1962 (top), 1972 (middle), and 1992 (bottom).

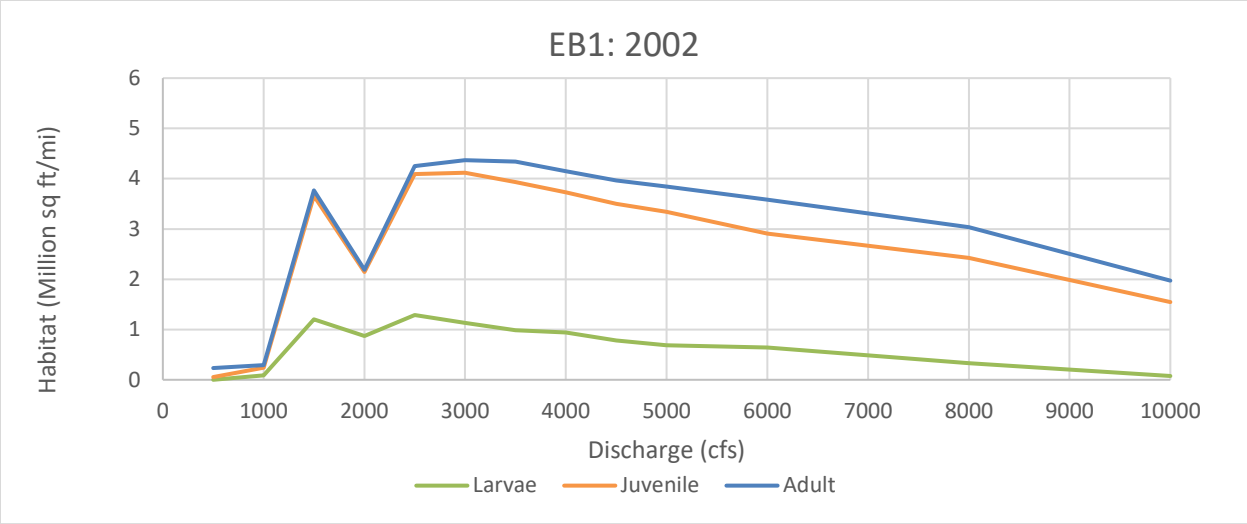

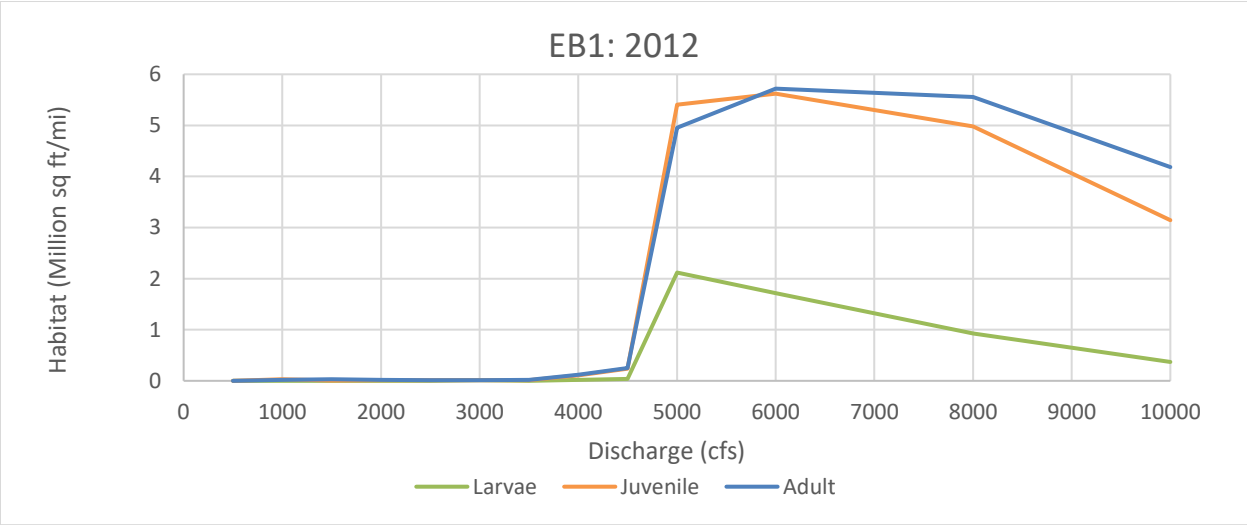

Figure D-21 Life stage habitat curves for subreach EB1 for the years 2002 (top) and 2012 (bottom).

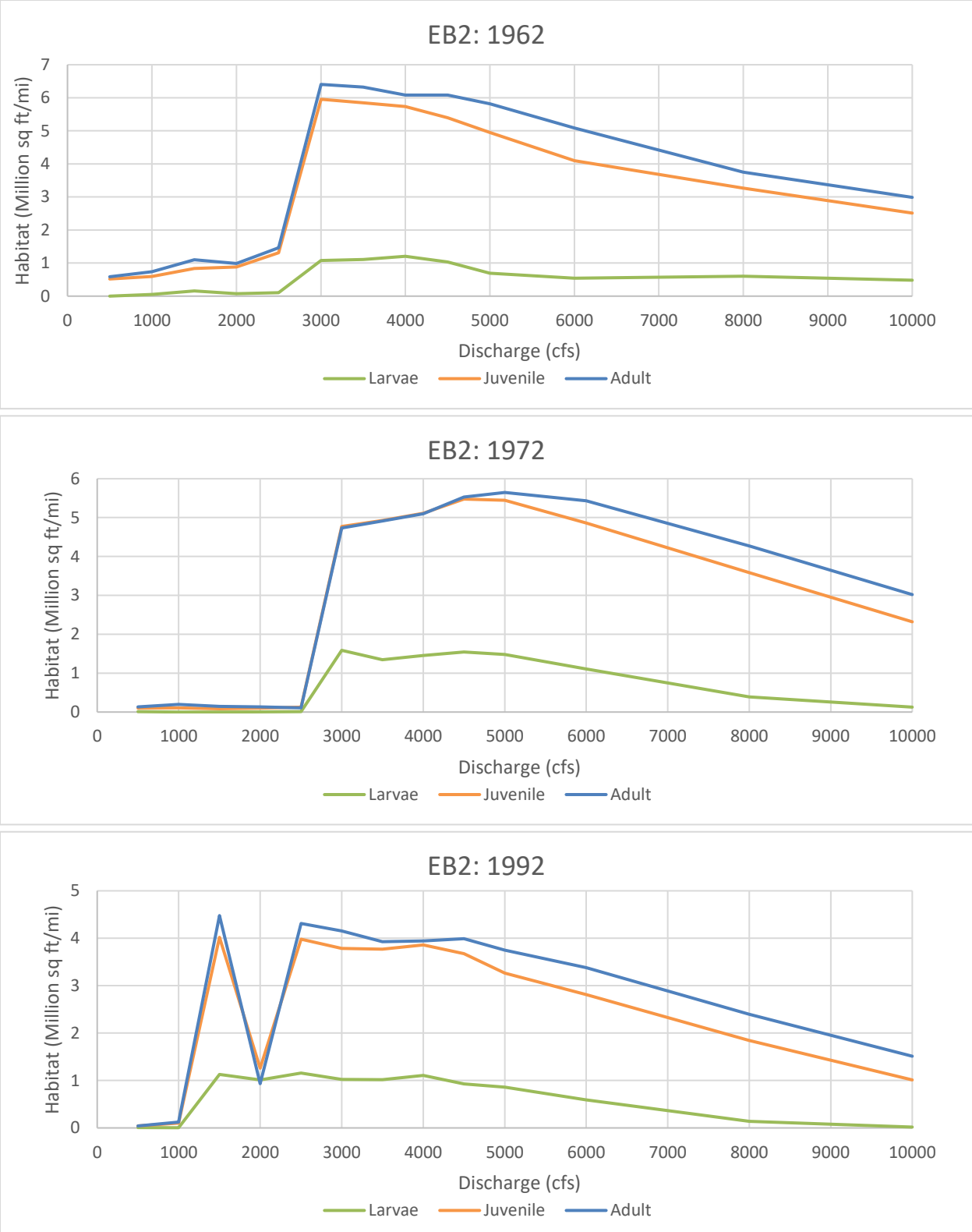

Figure D-22 Life stage habitat curves for subreach EB2 at the years 1962 (top), 1972 (middle), and 1992 (bottom).

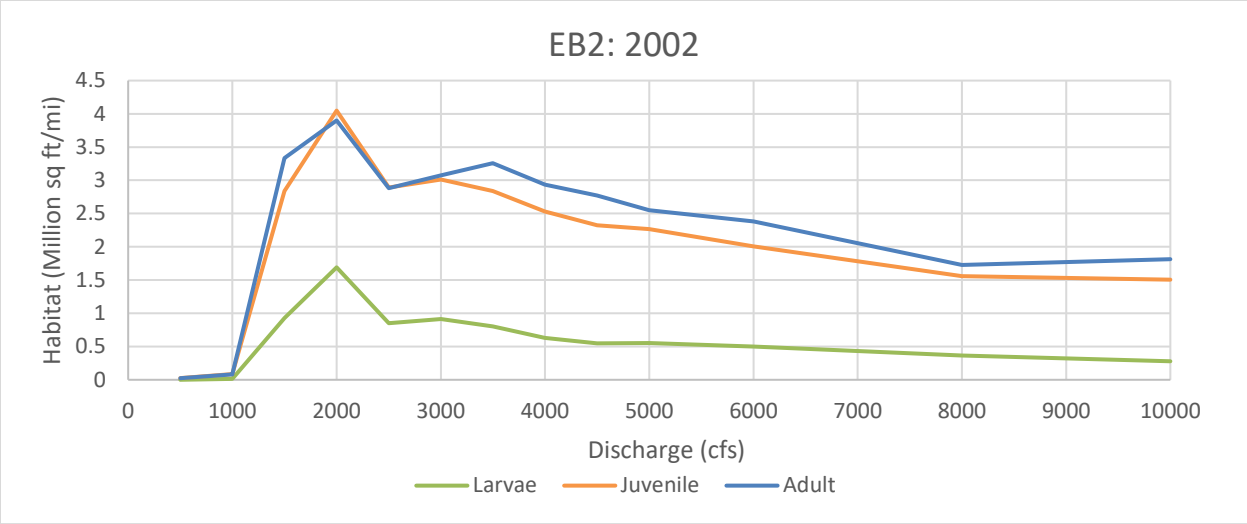

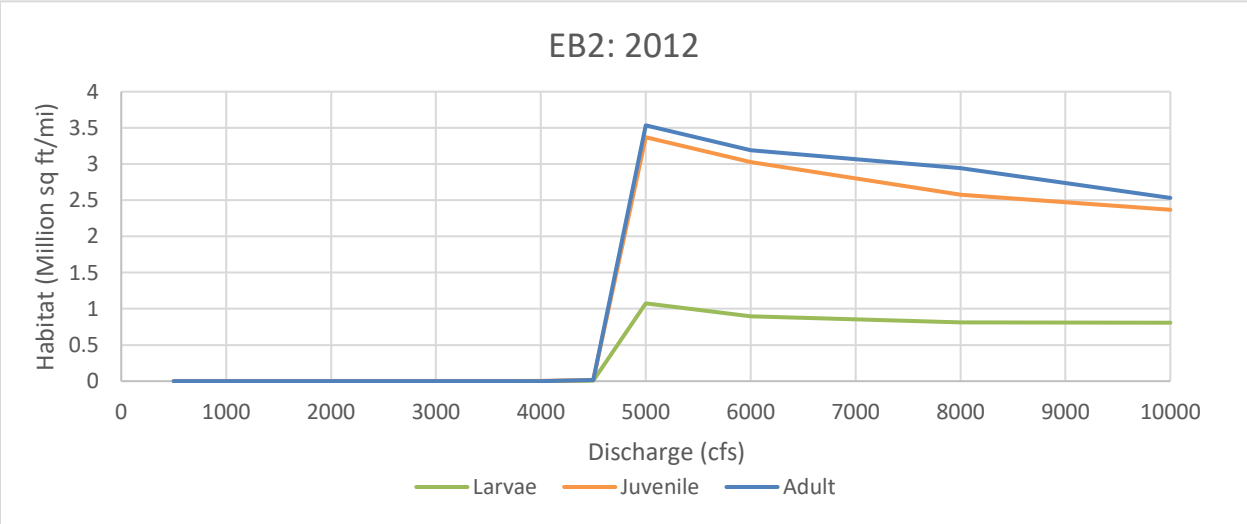

Figure D-23 Life stage habitat curves for subreach EB2 for the years 2002 (top) and 2012 (bottom).

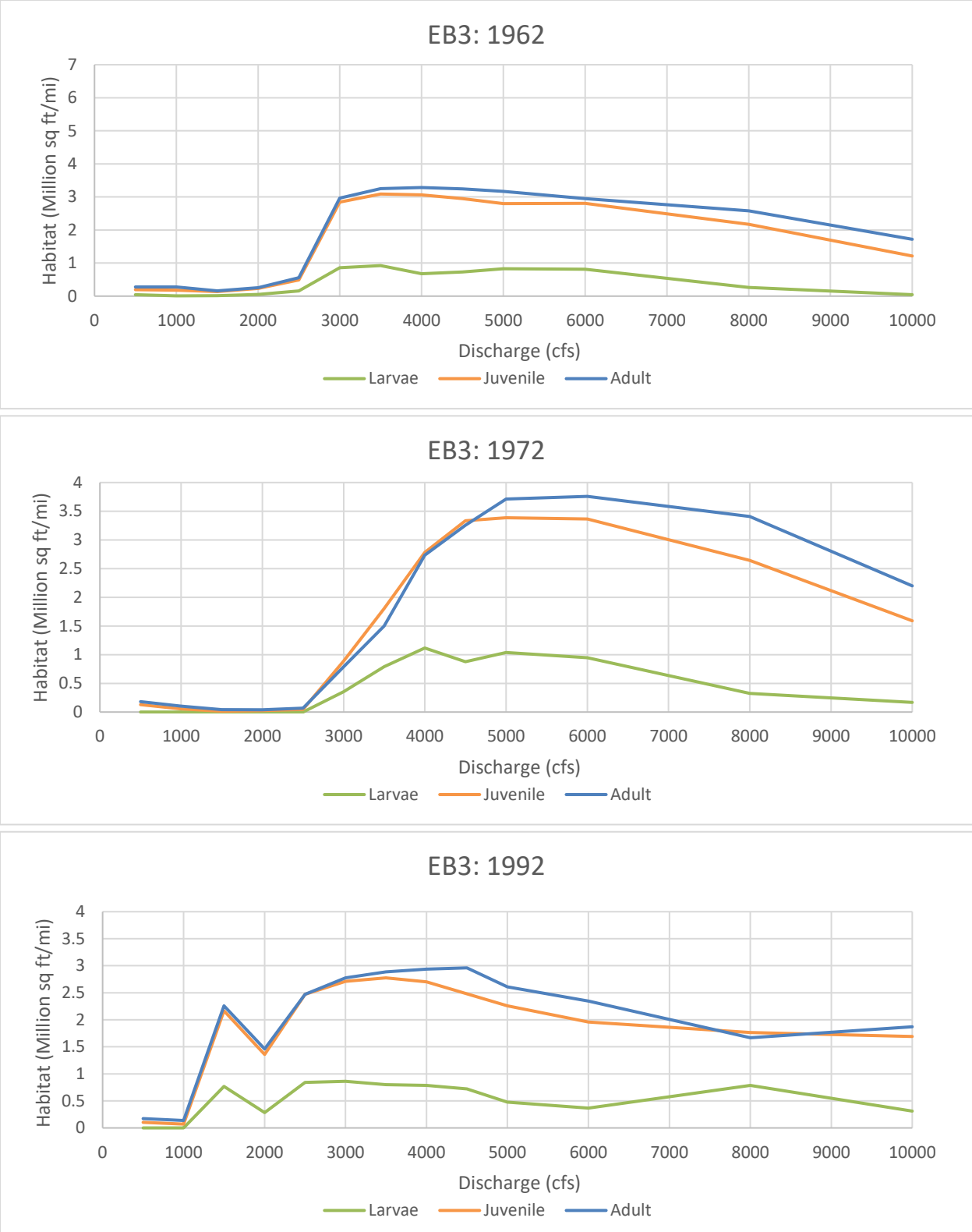

Figure D-24 Life stage habitat curves for subreach EB3 at the years 1962 (top), 1972 (middle), and 1992 (bottom)

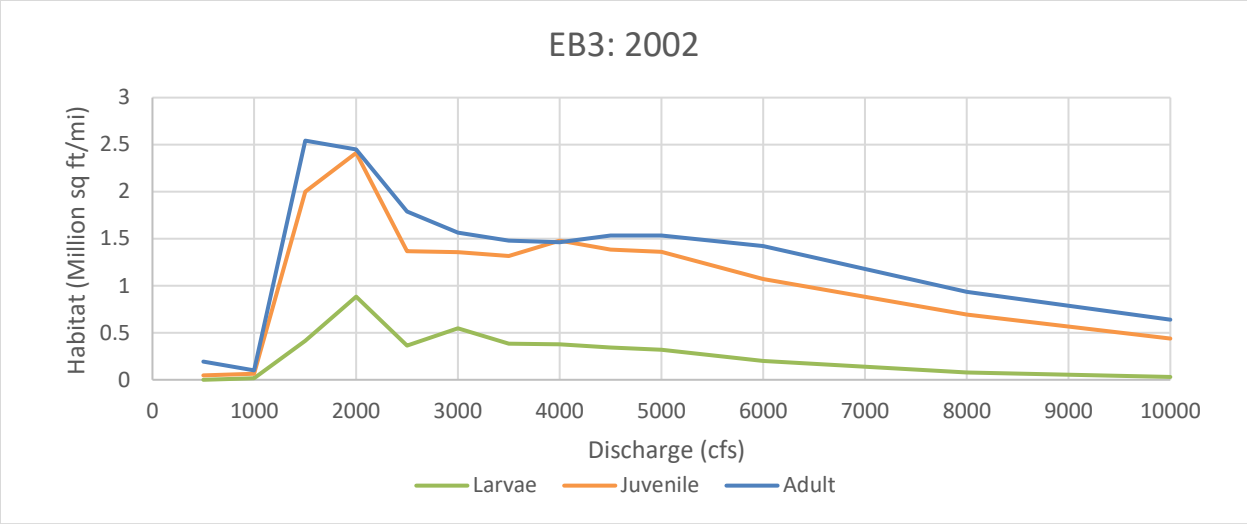

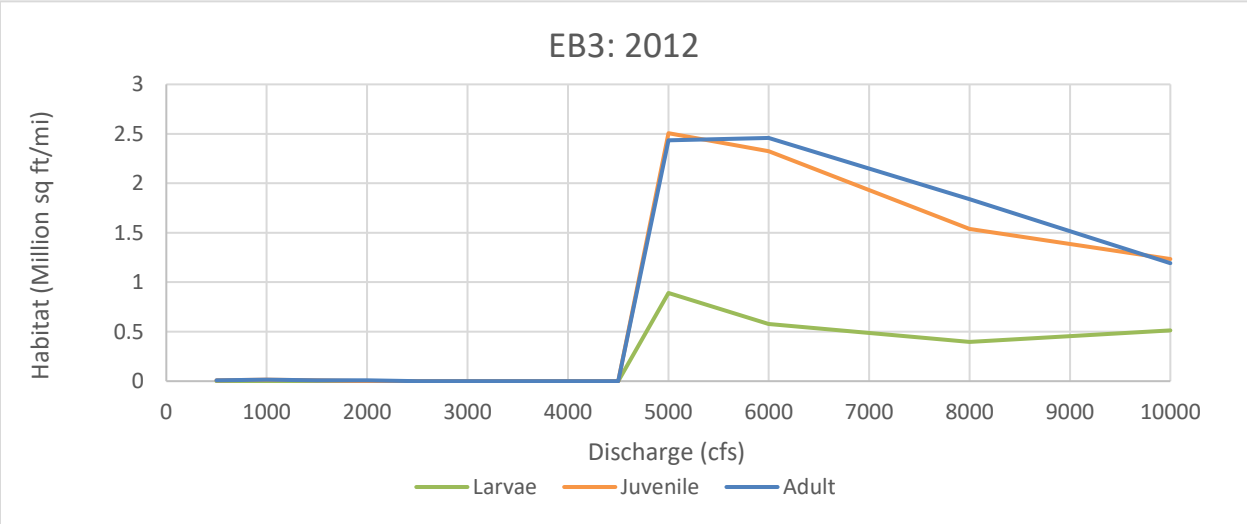

Figure D-25 Life stage habitat curves for subreach EB3 for the years 2002 (top) and 2012 (bottom)

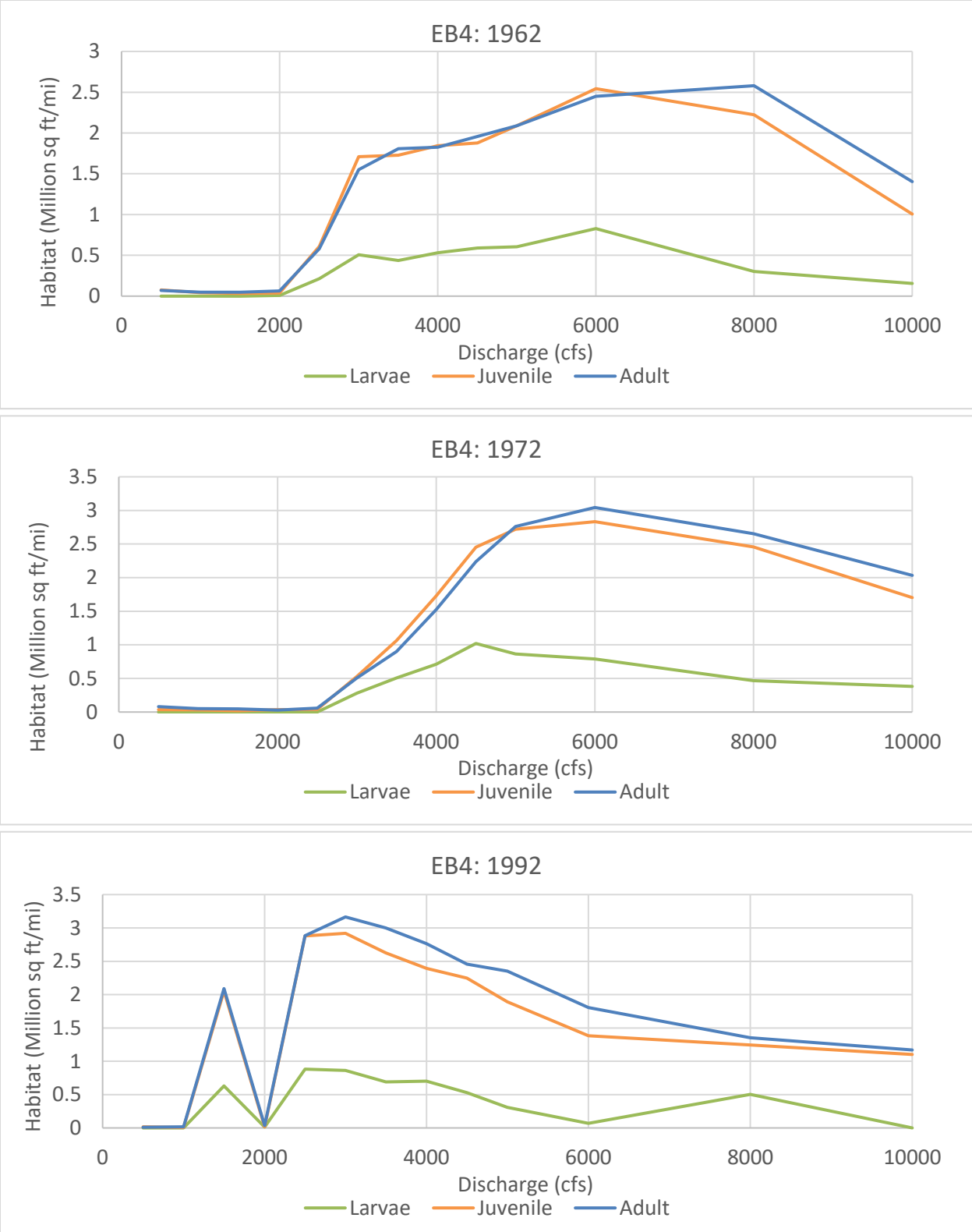

Figure D-26 Life stage habitat curves for subreach EB4 at the years 1962 (top), 1972 (middle), and 1992 (bottom).

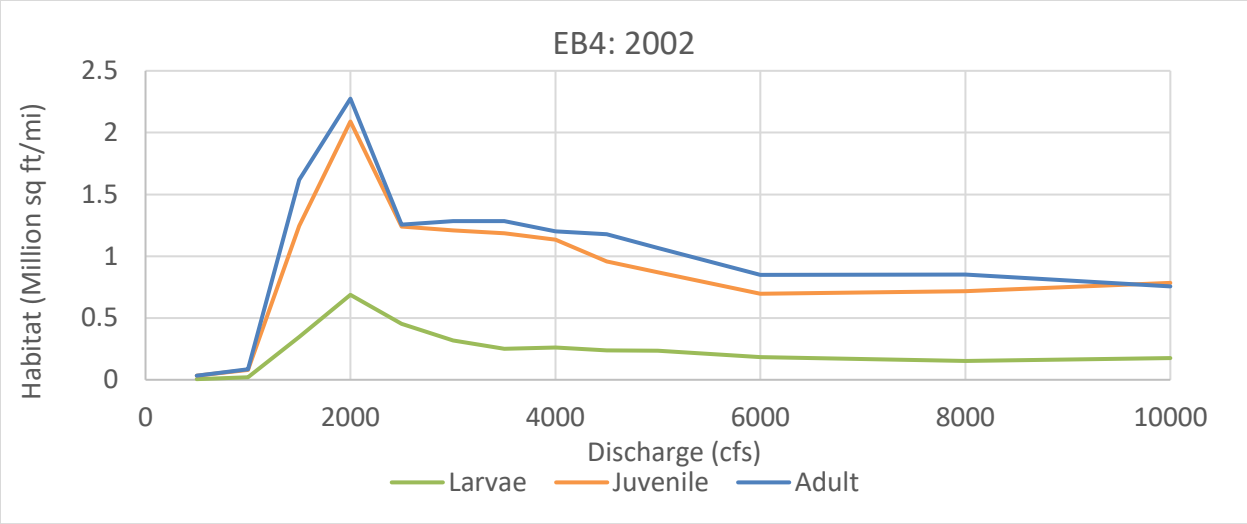

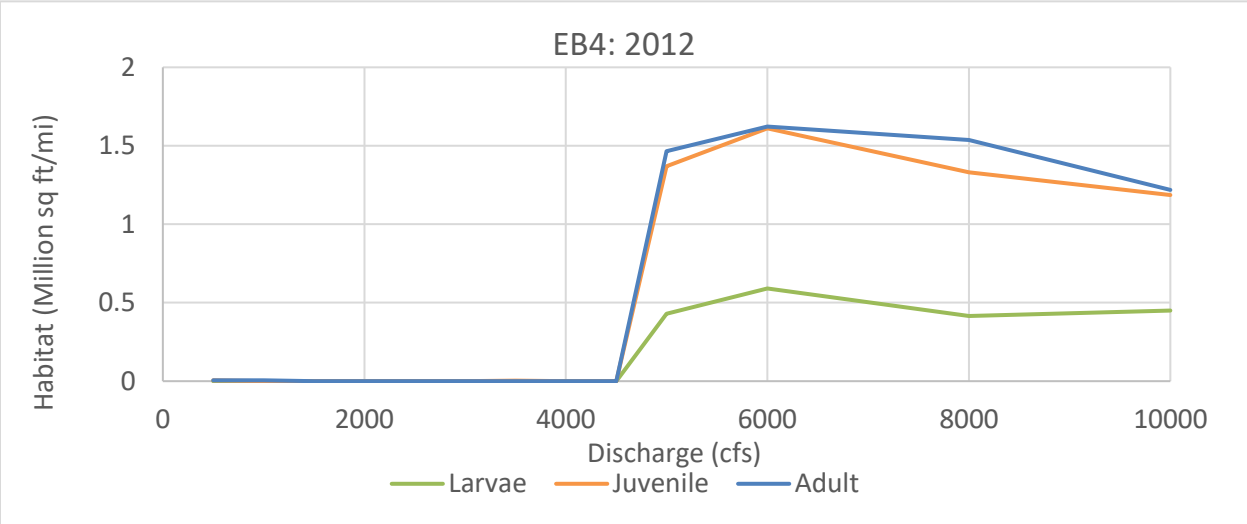

Figure D-27 Life stage habitat curves for subreach EB4 for the years 2002 (top) and 2012 (bottom).

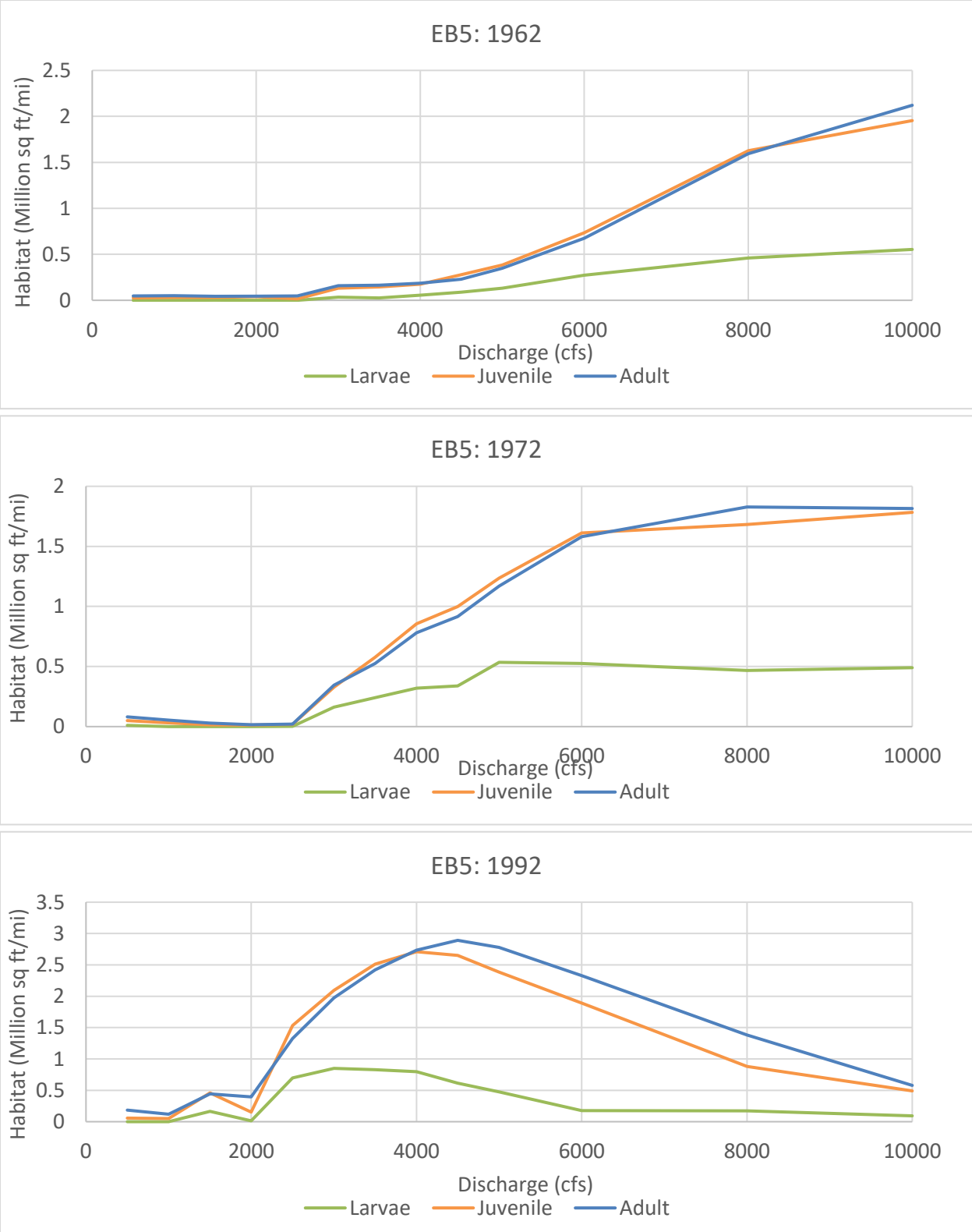

Figure D-28 Life stage habitat curves for subreach EB5 at the years 1962 (top), 1972 (middle), and 1992 (bottom).

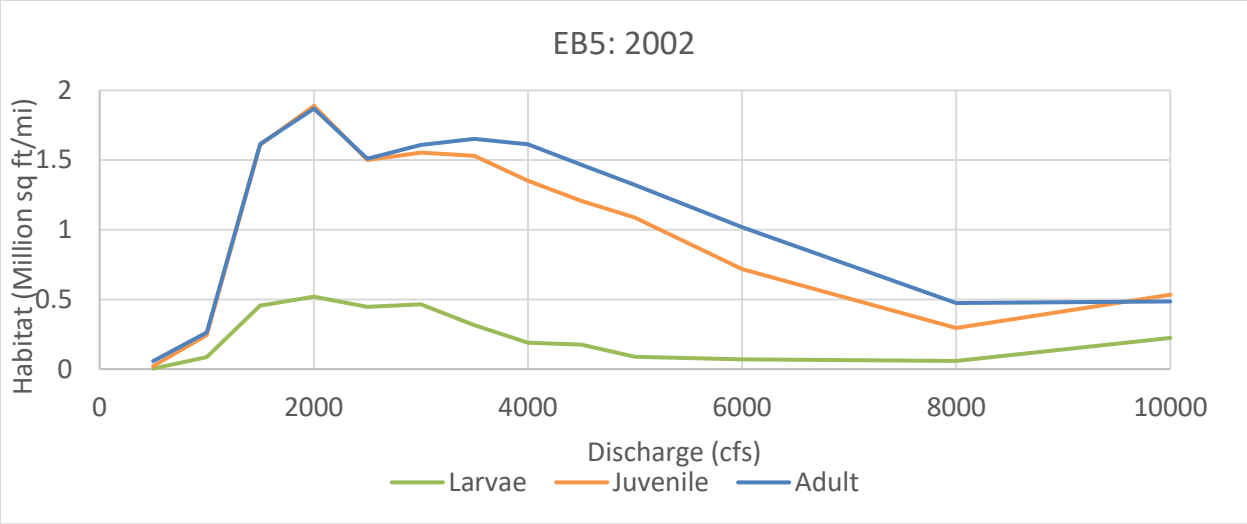

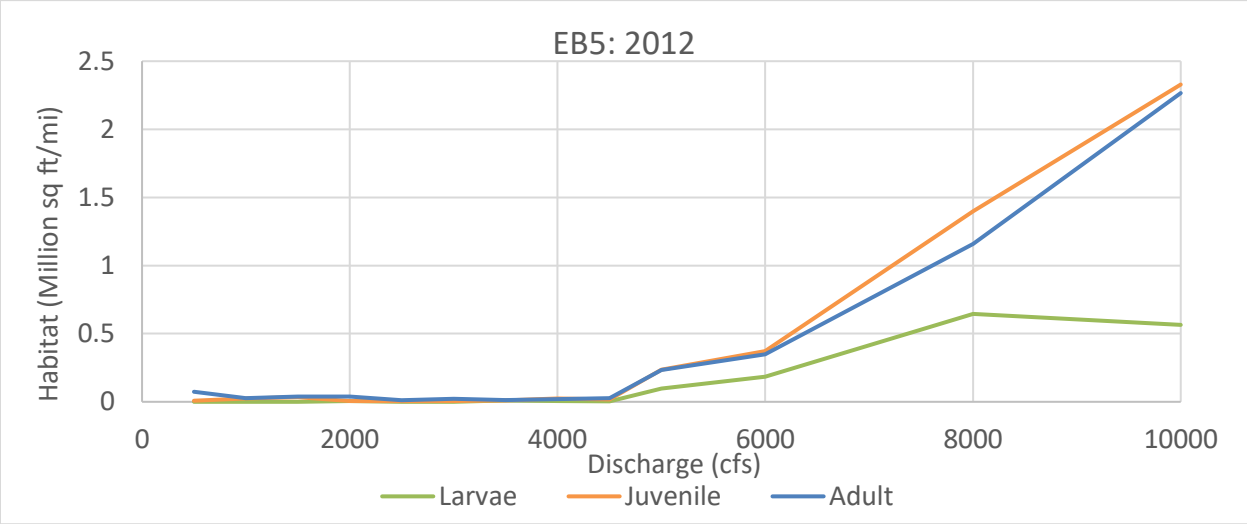

Figure D-29 Life stage habitat curves for subreach EB5 for the years 2002 (top) and 2012 (bottom).

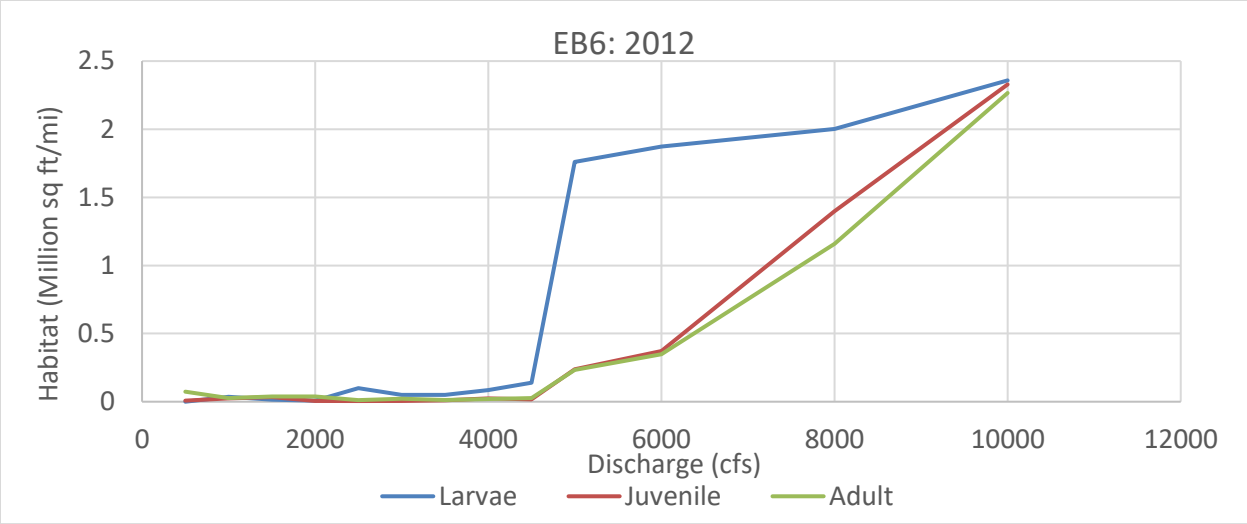

Figure D-30 Life stage habitat curves for subreach EB6 2012.

Appendix E

Habitat Maps, Table of Disconnected Areas of Hydraulically Suitable Habitat

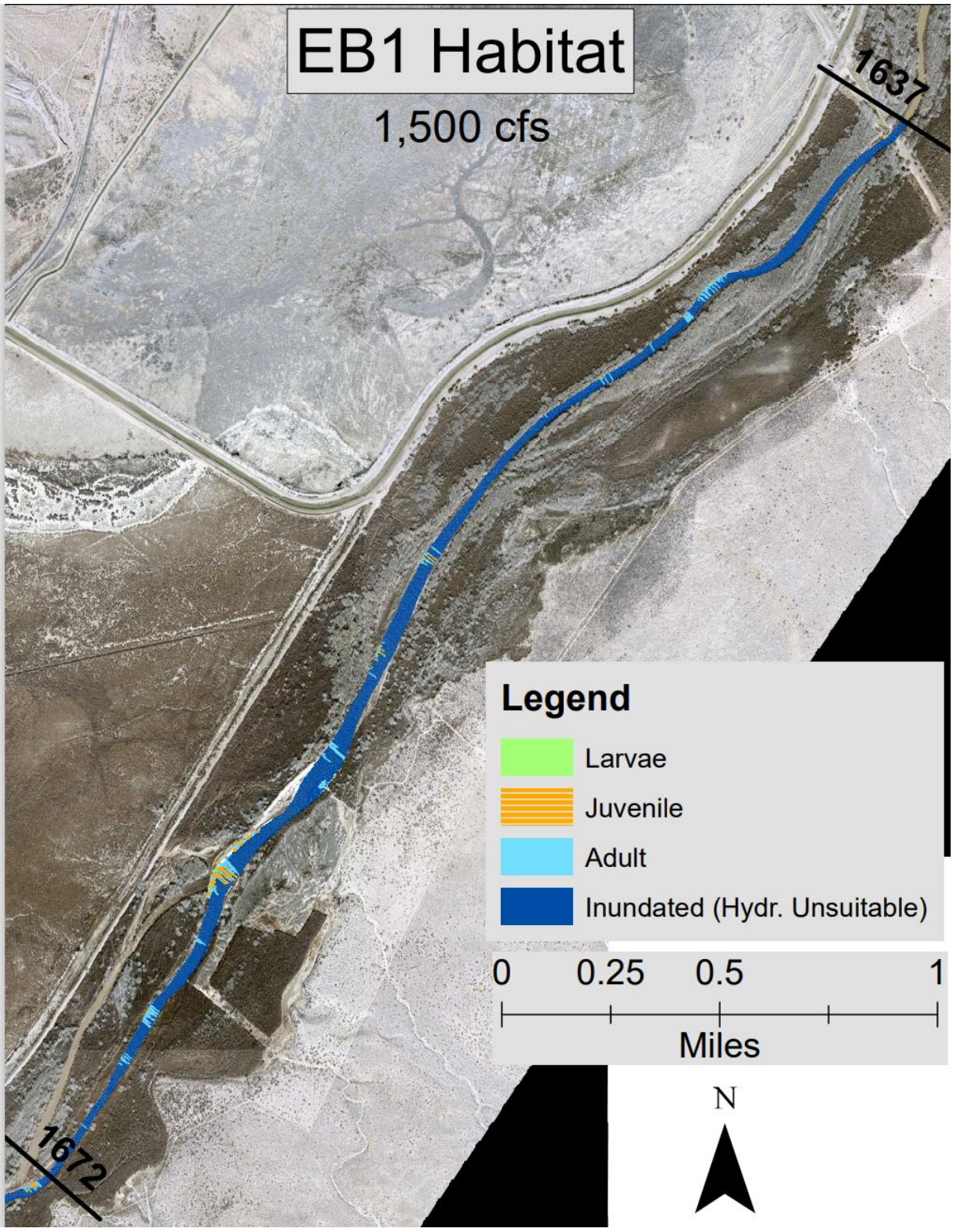

Figure E- 1 RGSM Habitat in subreach EB1 at 1500 cfs with hydraulically suitable areas labeled for larvae (green), juvenile (orange), and adult (light blue) and unsuitable inundated areas in dark blue.

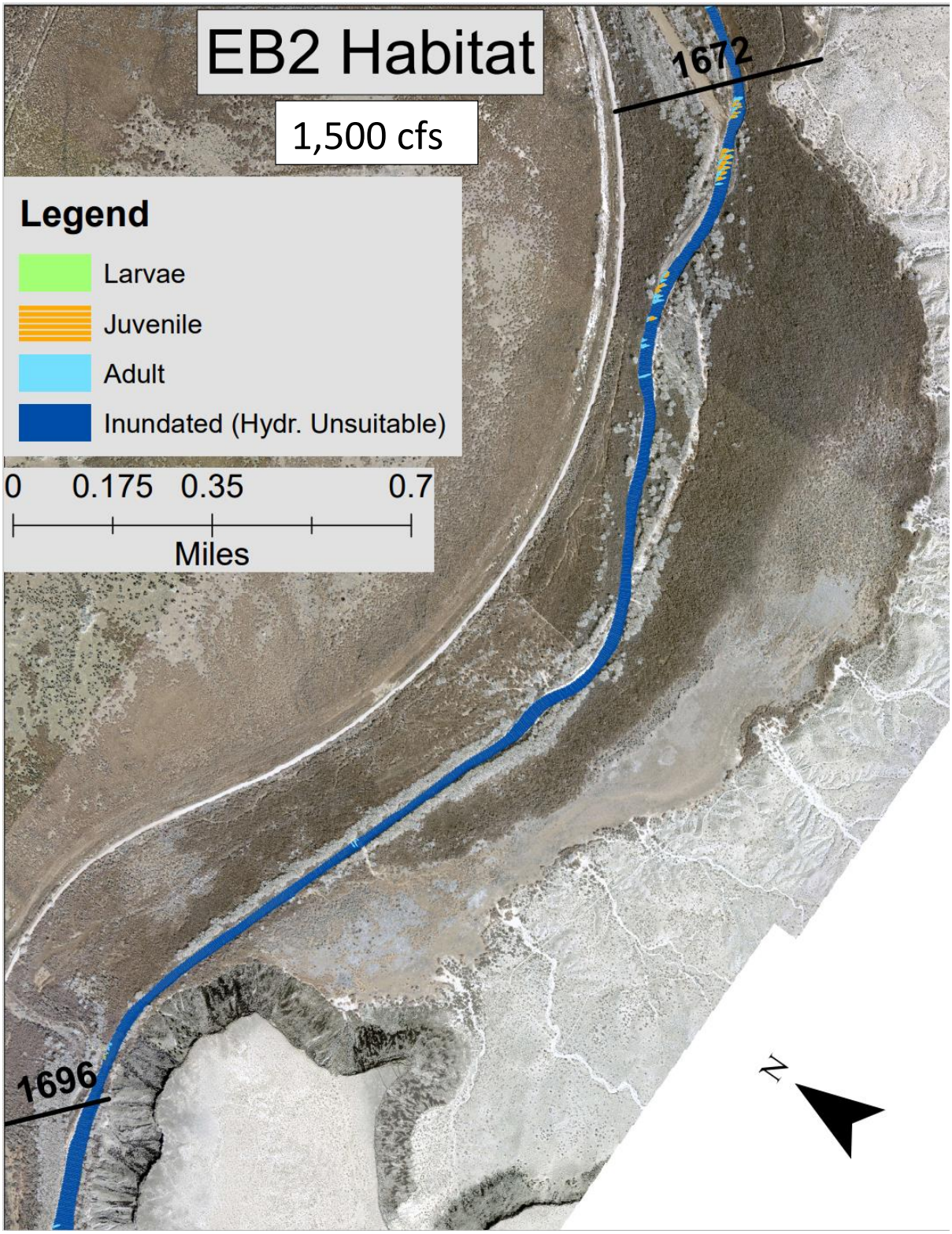

Figure E- 2 RGSM Habitat in subreach EB2 1500 cfs with hydraulically suitable areas labeled for larvae (green), juvenile (orange), and adult (light blue) and unsuitable inundated areas in dark blue.

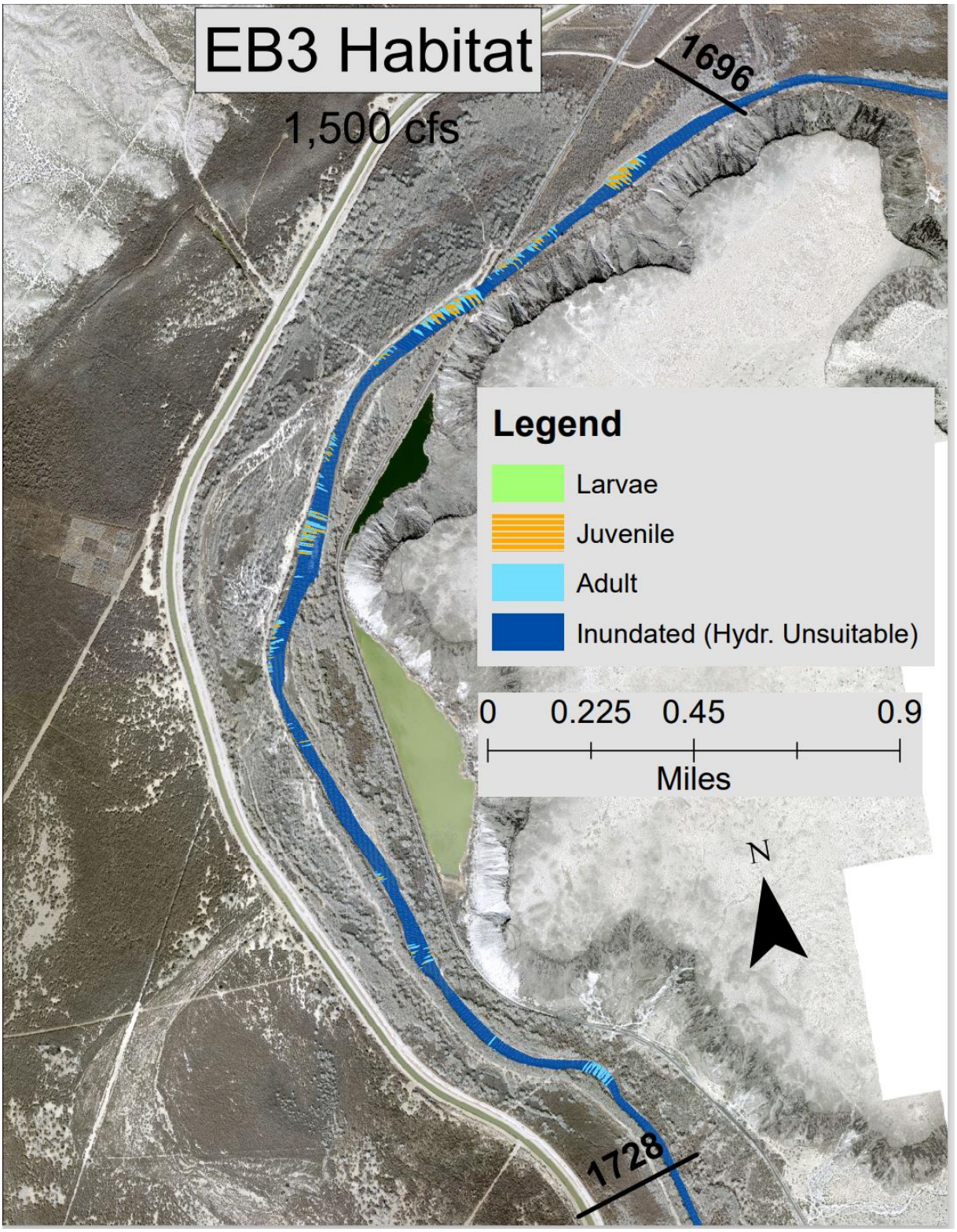

Figure E- 3 RGSM Habitat in subreach EB3 at 1500 cfs with hydraulically suitable areas labeled for larvae (green), juvenile (orange), and adult (light blue) and unsuitable inundated areas in dark blue.

Figure E- 4 RGSM Habitat in subreach EB4 at 1500 cfs with hydraulically suitable areas labeled for larvae (green), juvenile (orange), and adult (light blue) and unsuitable inundated areas in dark blue.

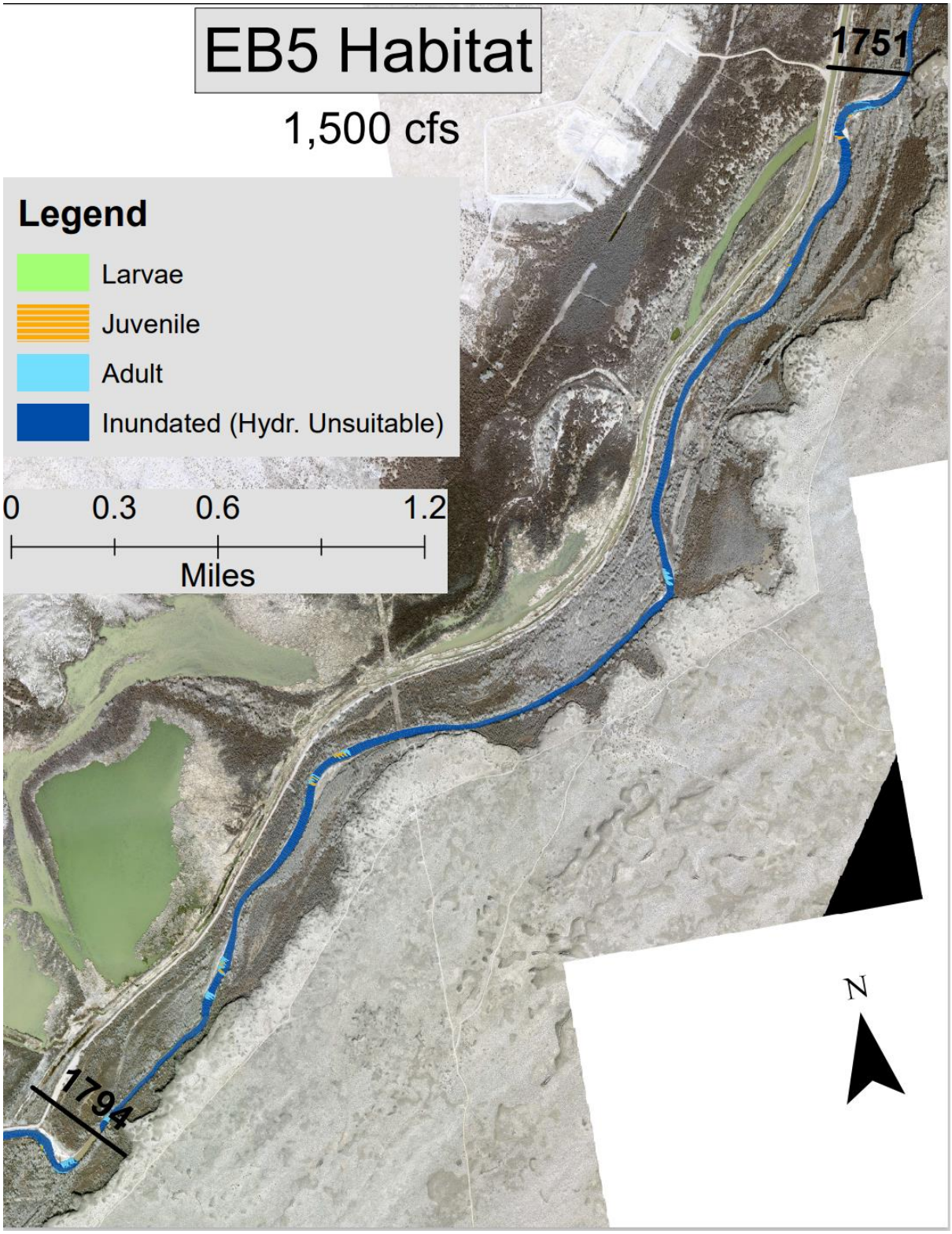

Figure E- 5 RGSM Habitat in subreach EB5 at 1500 cfs with hydraulically suitable areas labeled for larvae (green), juvenile (orange), and adult (light blue) and unsuitable inundated areas in dark blue.

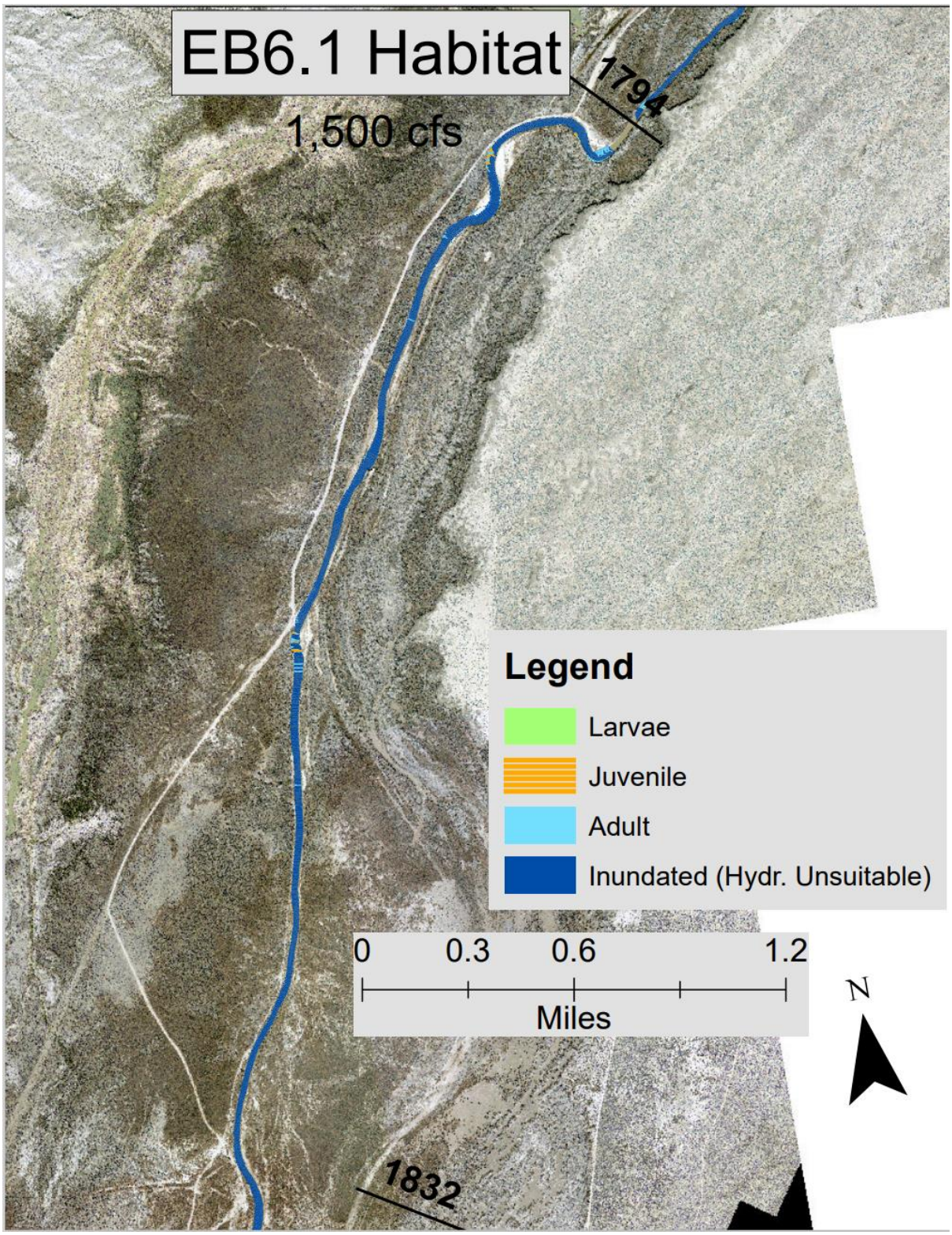

Figure E- 6 RGSM Habitat in subreach EB6.1 at 1500 cfs with hydraulically suitable areas labeled for larvae (green), juvenile (orange), and adult (light blue) and unsuitable inundated areas in dark blue.

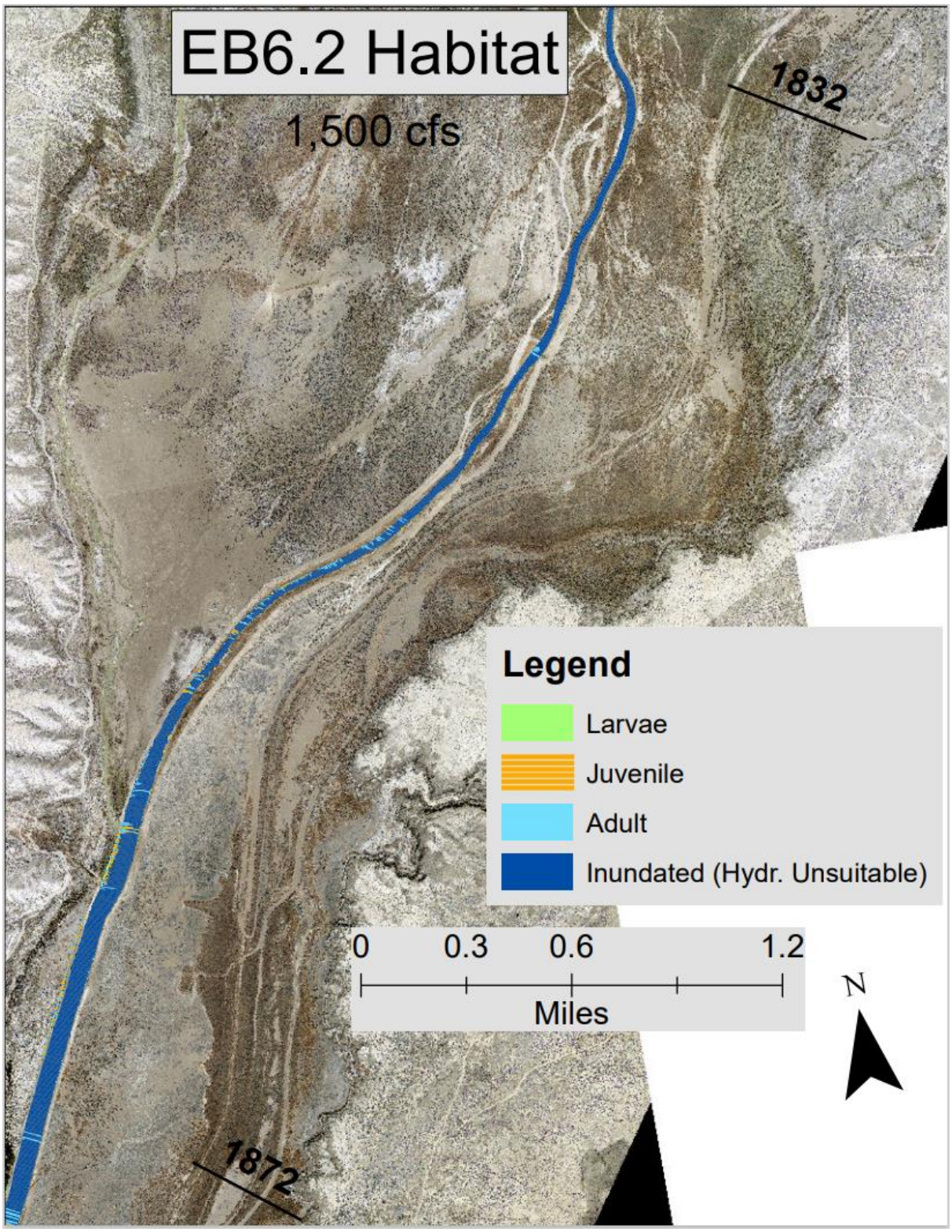

Figure E- 7 RGSM Habitat in subreach EB6.2 at 1500 cfs with hydraulically suitable areas labeled for larvae (green), juvenile (orange), and adult (light blue) and unsuitable inundated areas in dark blue.

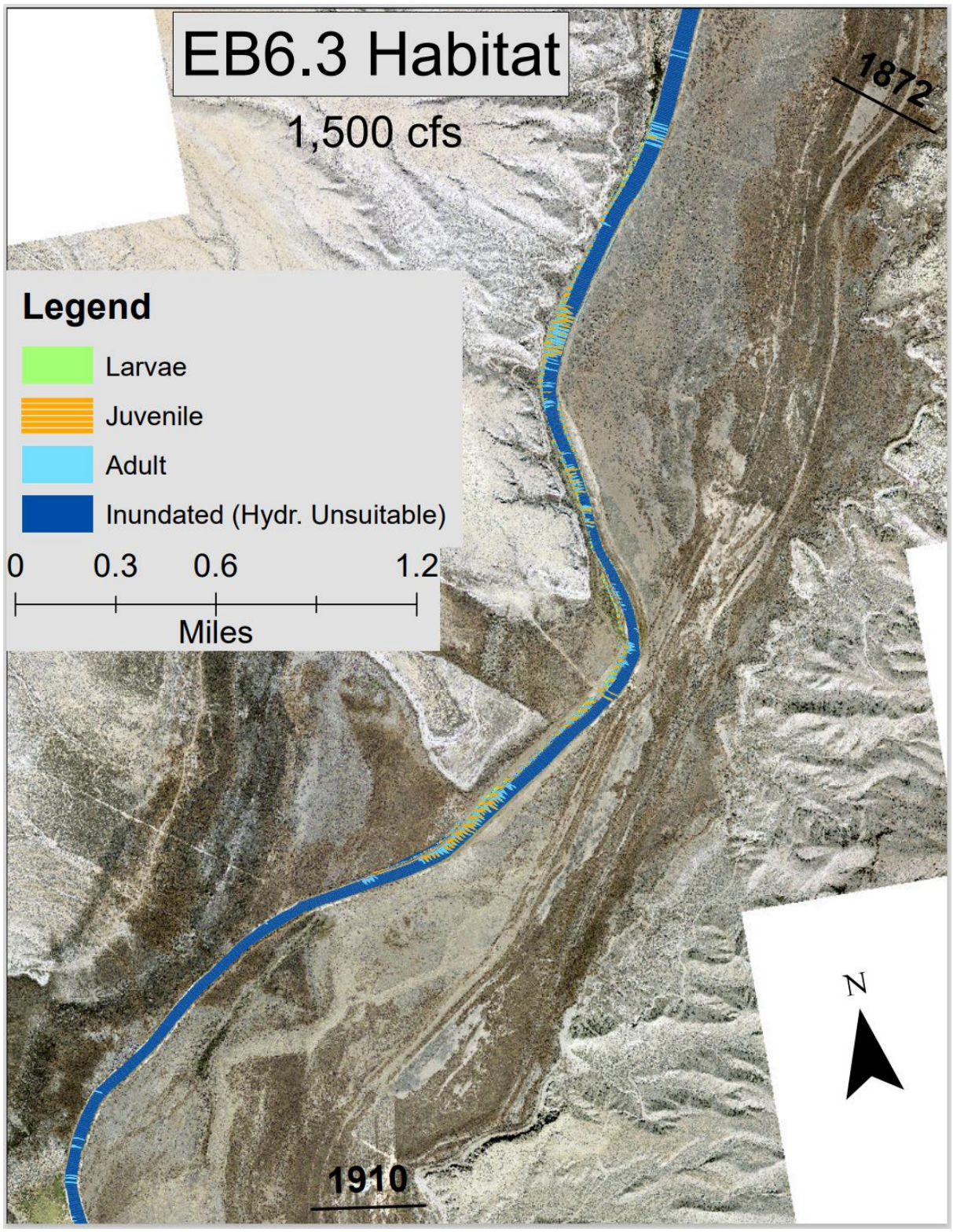

Figure E- 8 RGSM Habitat in subreach EB6.3) at 1500 cfs with hydraulically suitable areas labeled for larvae (green), juvenile (orange), and adult (light blue) and unsuitable inundated areas in dark blue.

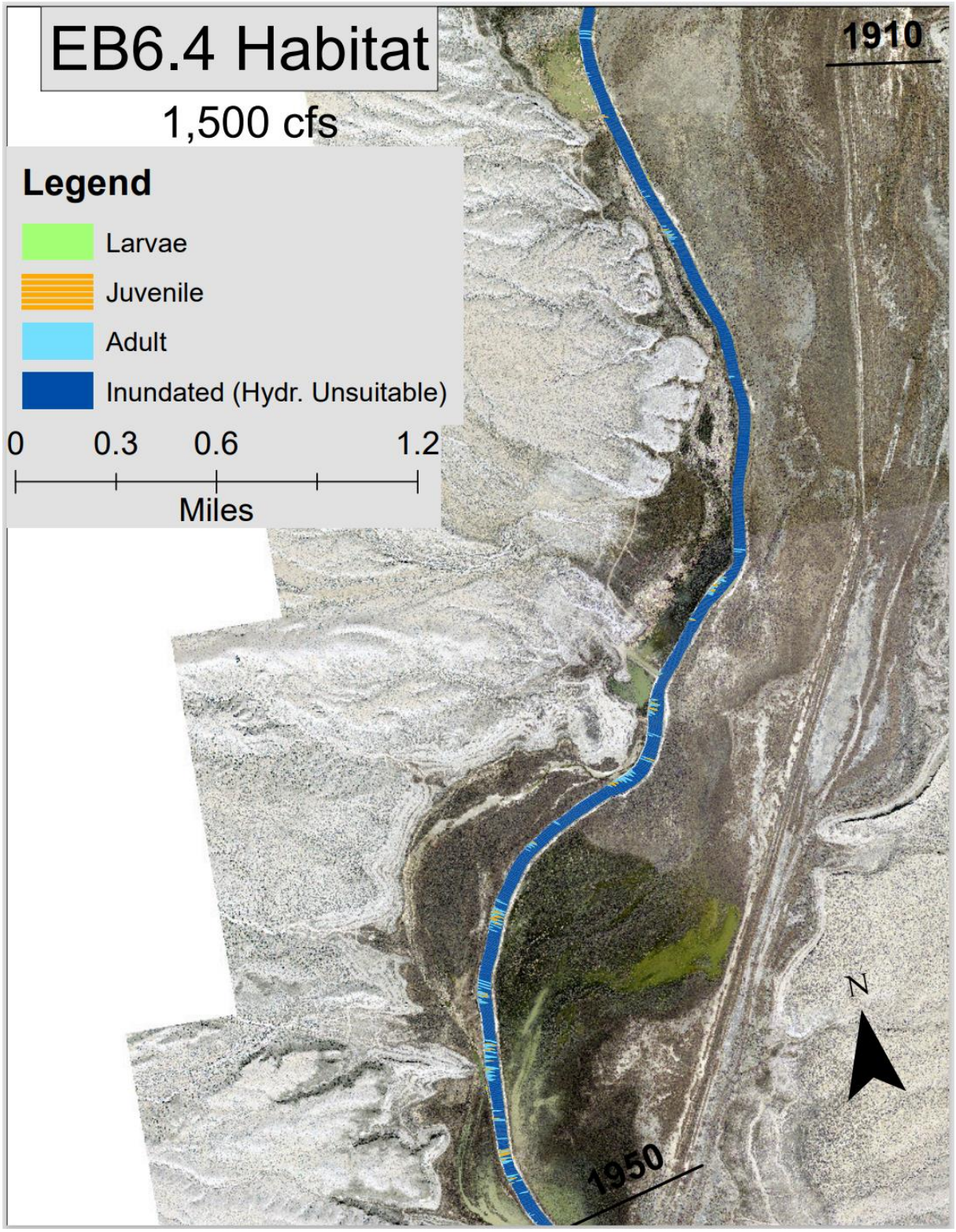

Figure E- 9 RGSM Habitat in subreach EB6.4 at 1500 cfs with hydraulically suitable areas labeled for larvae (green), juvenile (orange), and adult (light blue) and unsuitable inundated areas in dark blue.

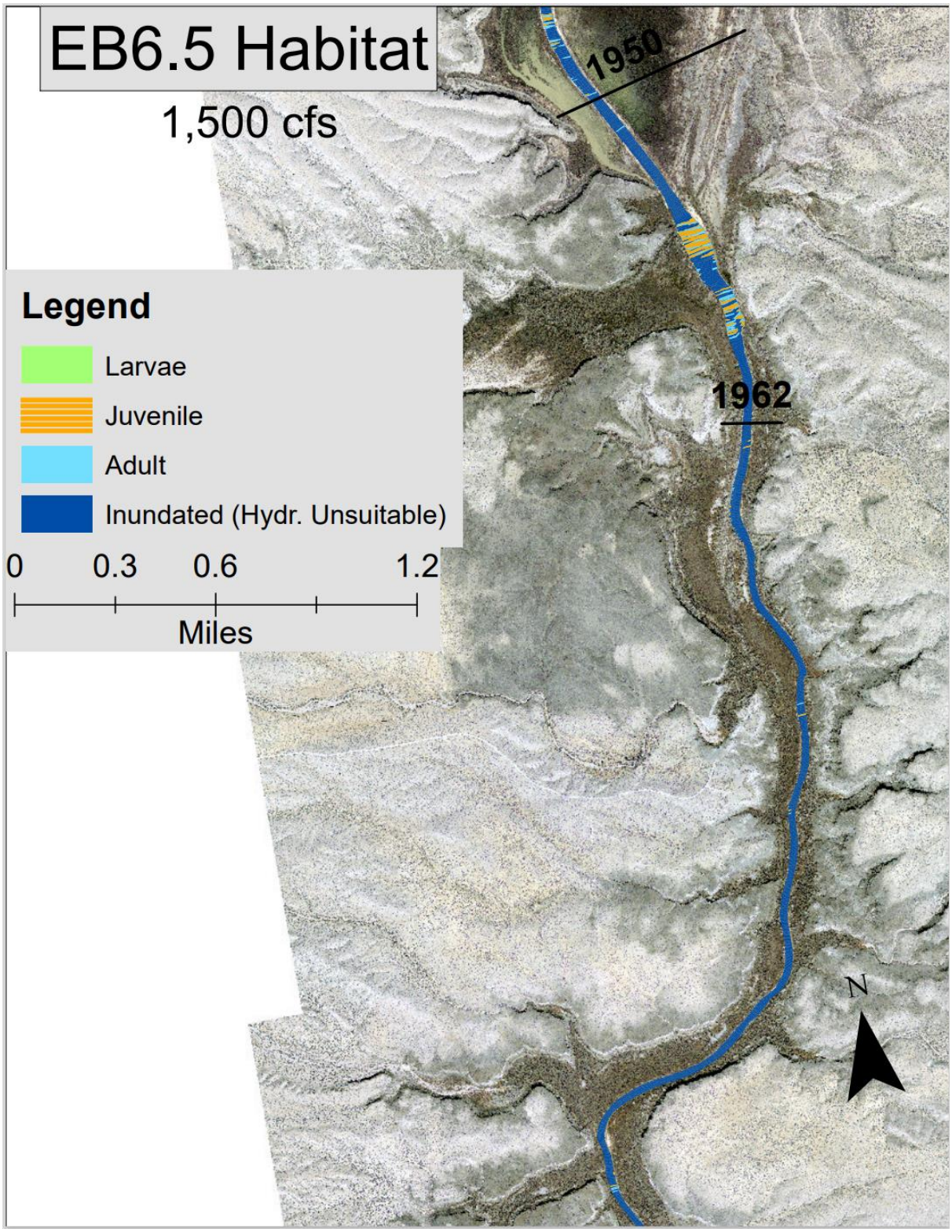

Figure E- 10 RGSM Habitat in subreach EB6.5 at 1500 cfs with hydraulically suitable areas labeled for larvae (green), juvenile (orange), and adult (light blue) and unsuitable inundated areas in dark blue.

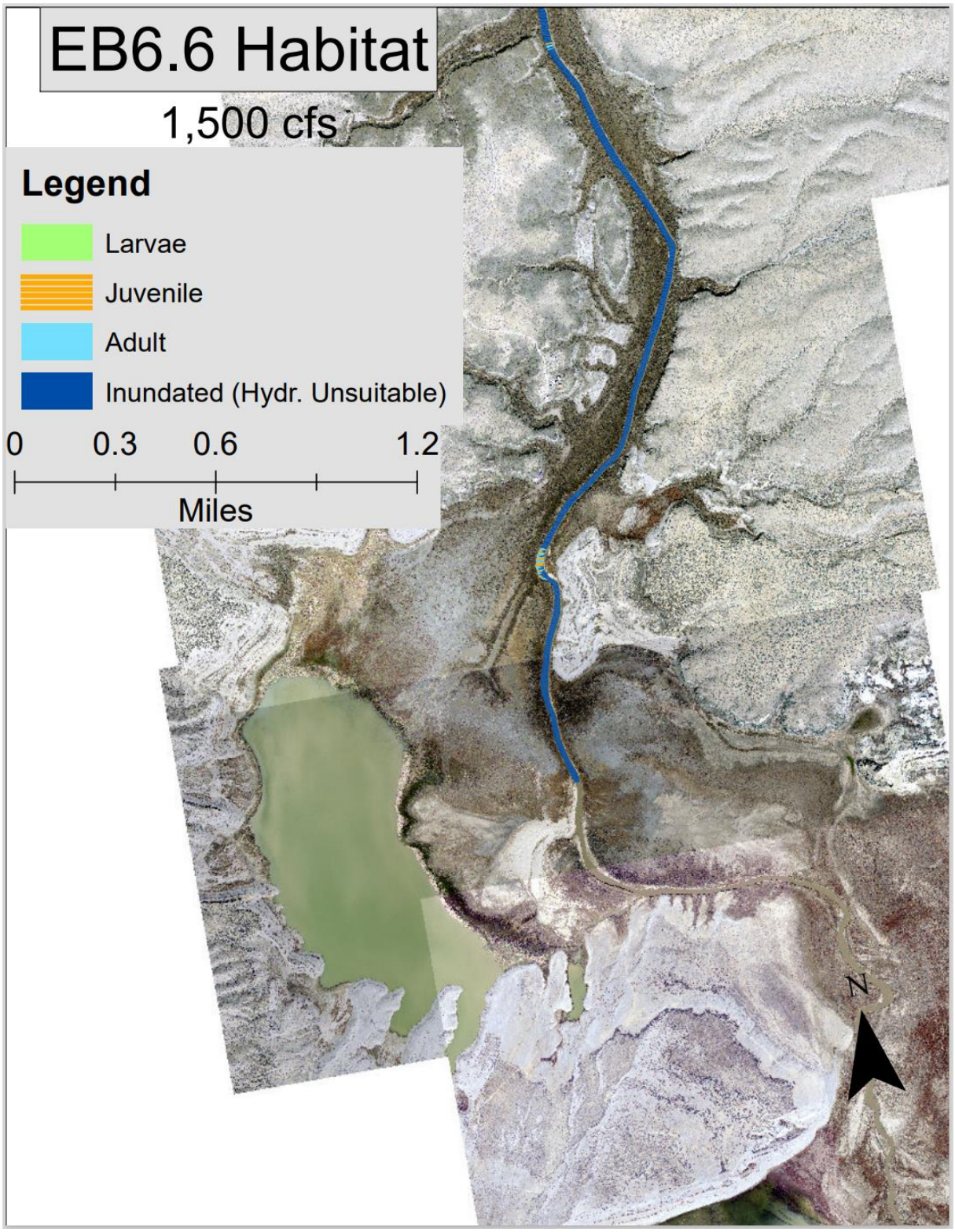

Figure E- 11 RGSM Habitat in subreach EB6.6 at 1500 cfs with hydraulically suitable areas labeled for larvae (green), juvenile (orange), and adult (light blue) and unsuitable inundated areas in dark blue.

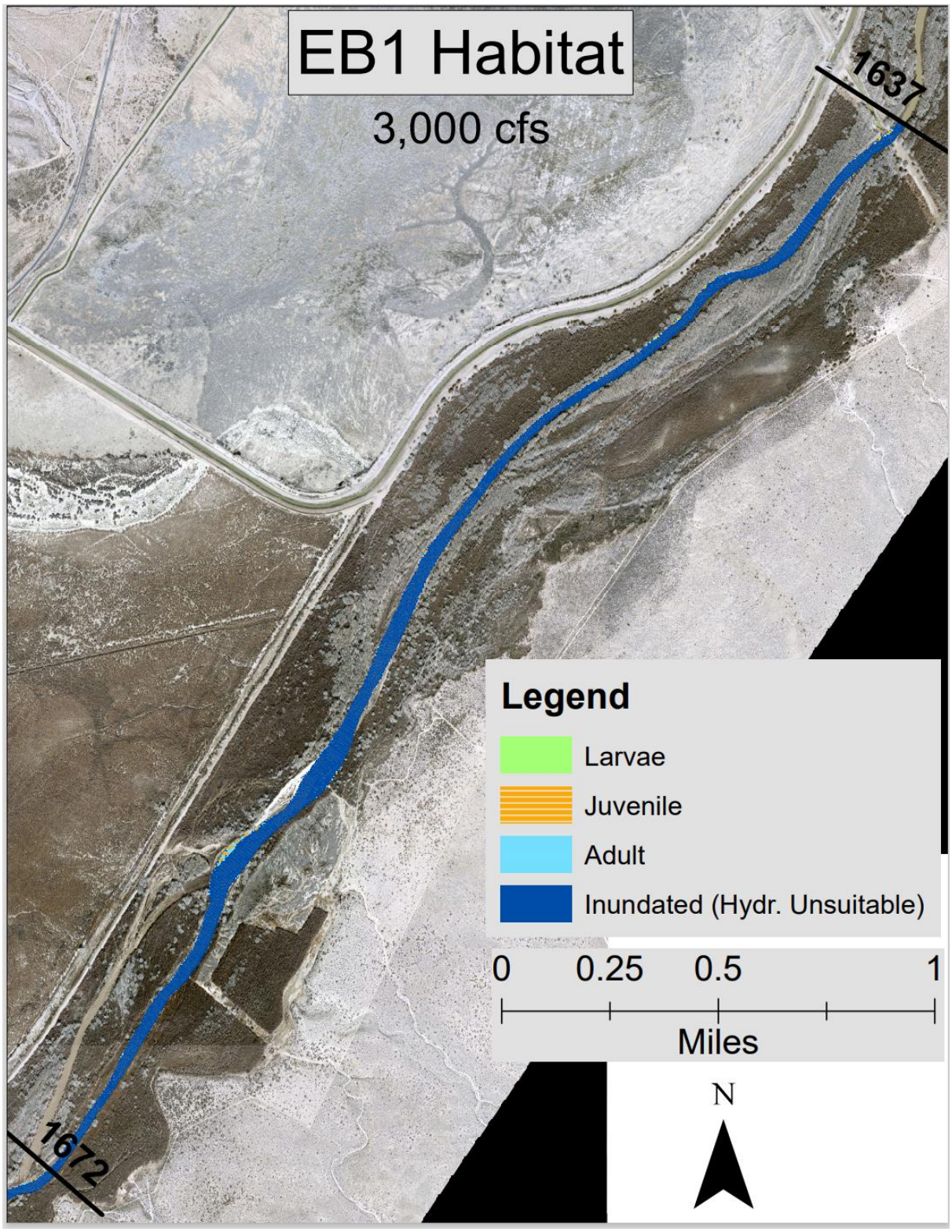

Figure E- 12 RGSM Habitat in subreach EB1 at 3000 cfs with hydraulically suitable areas labeled for larvae (green), juvenile (orange), and adult (light blue) and unsuitable inundated areas in dark blue.

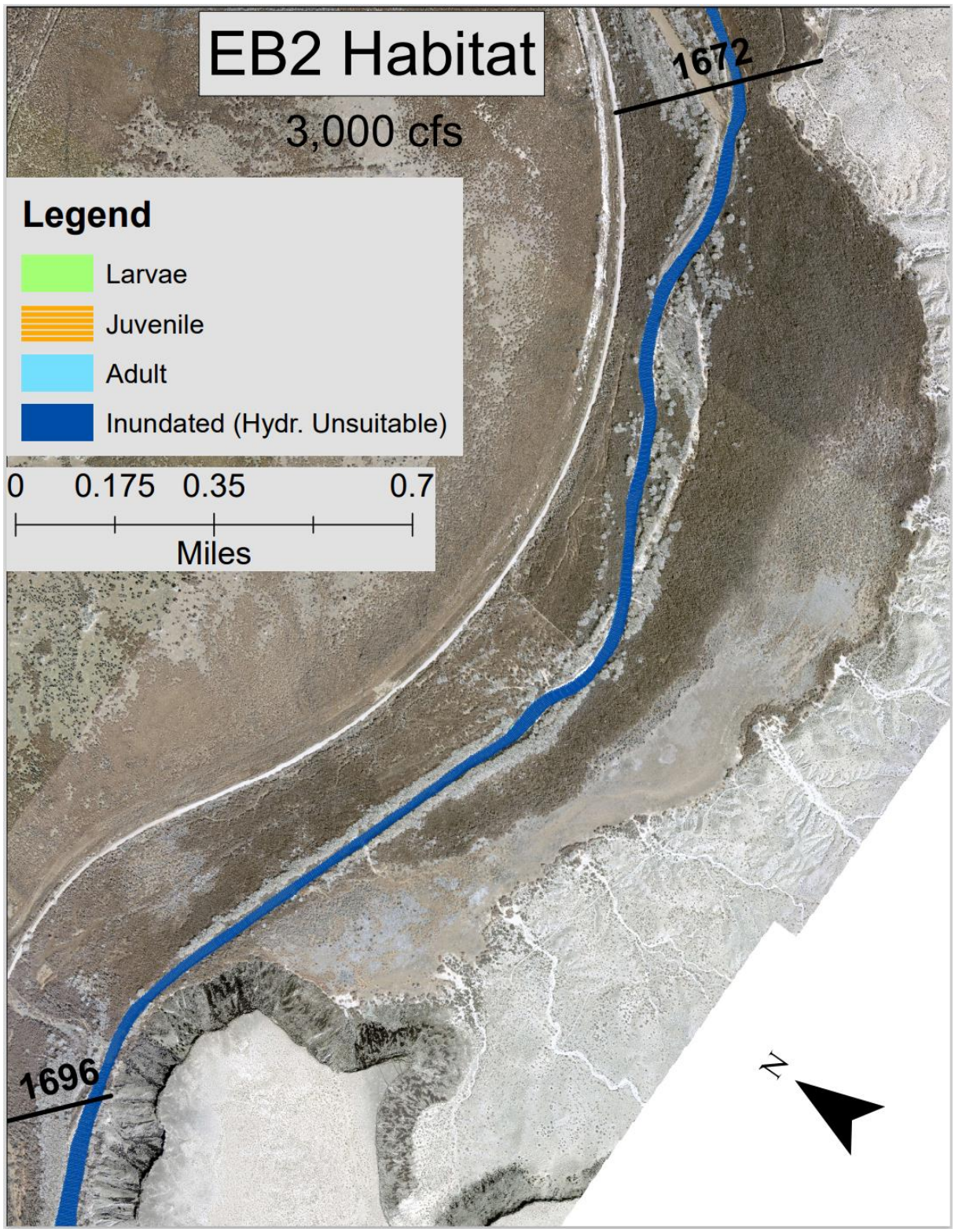

Figure E- 13 RGSM Habitat in subreach EB2 at 3000 cfs with hydraulically suitable areas labeled for larvae (green), juvenile (orange), and adult (light blue) and unsuitable inundated areas in dark blue.

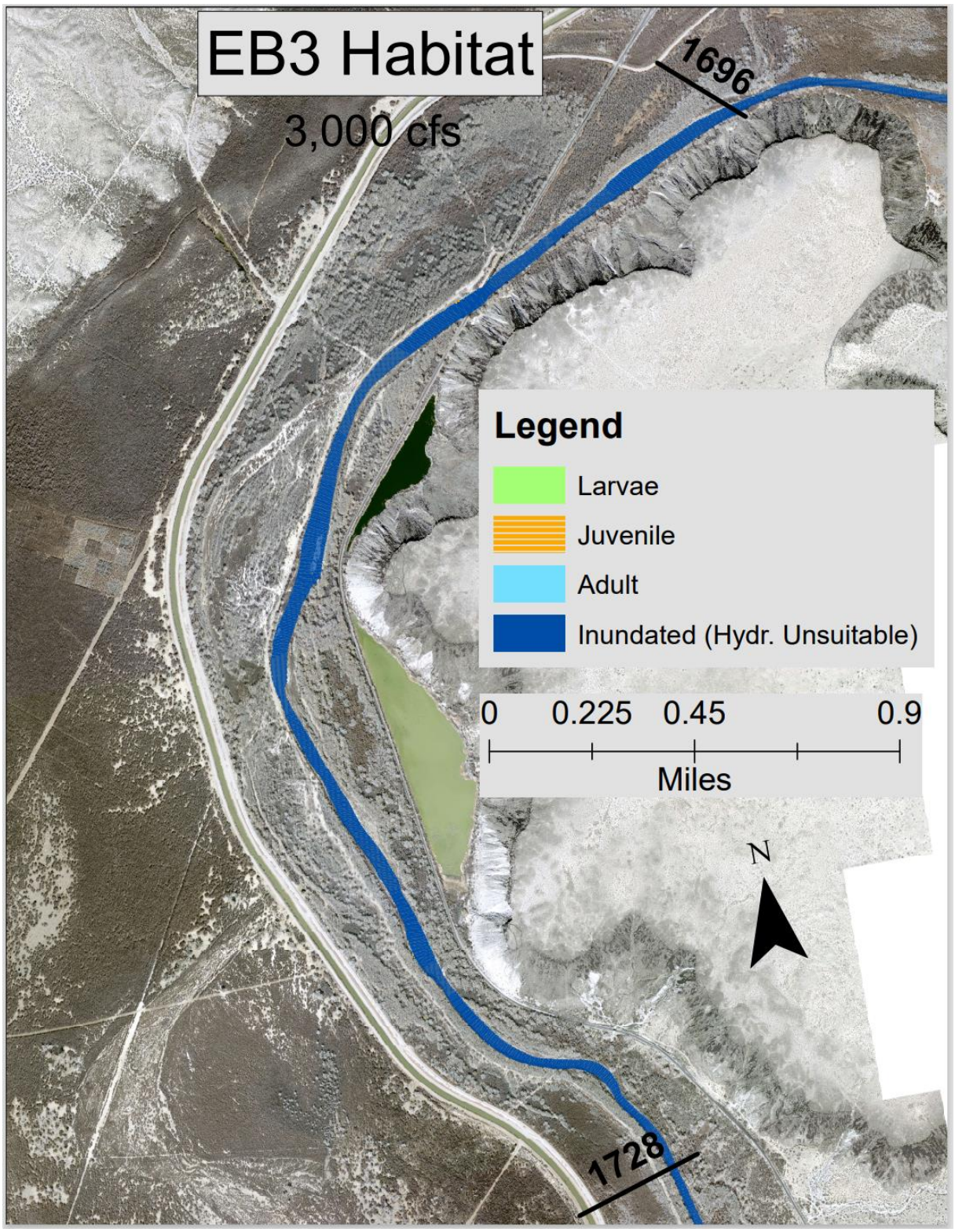

Figure E- 14 RGSM Habitat in subreach EB3 at 3000 cfs with hydraulically suitable areas labeled for larvae (green), juvenile (orange), and adult (light blue) and unsuitable inundated areas in dark blue.

. *Figure E- 15 RGSM Habitat in subreach EB4 at 3000 cfs with hydraulically suitable areas labeled for larvae (green), juvenile (orange), and adult (light blue) and unsuitable inundated areas in dark blue.*

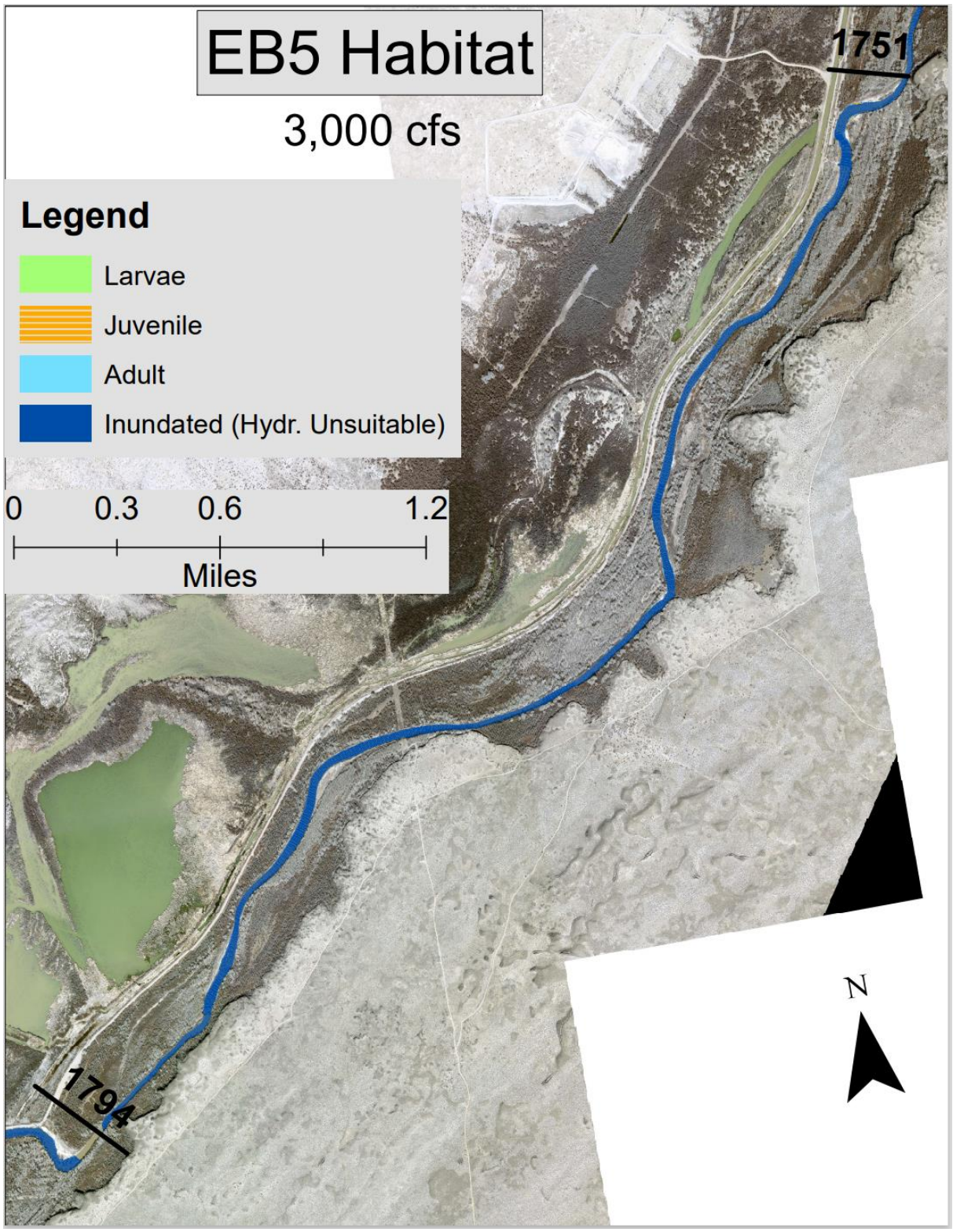

Figure E- 16 RGSM Habitat in subreach EB5 at 3000 cfs with hydraulically suitable areas labeled for larvae (green), juvenile (orange), and adult (light blue) and unsuitable inundated areas in dark blue.

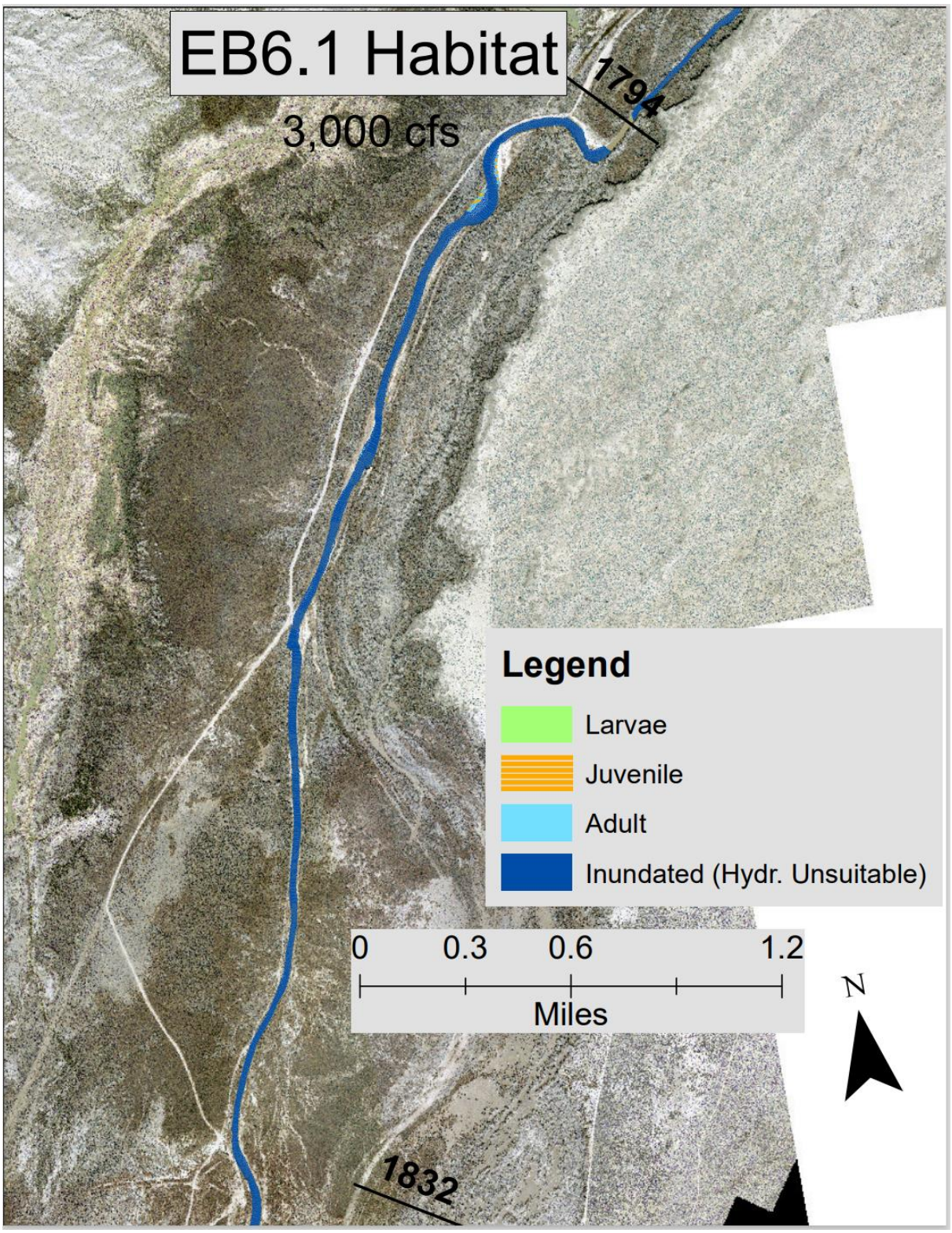

Figure E- 17 RGSM Habitat in subreach EB6.1 at 3000 cfs with hydraulically suitable areas labeled for larvae (green), juvenile (orange), and adult (light blue) and unsuitable inundated areas in dark blue.

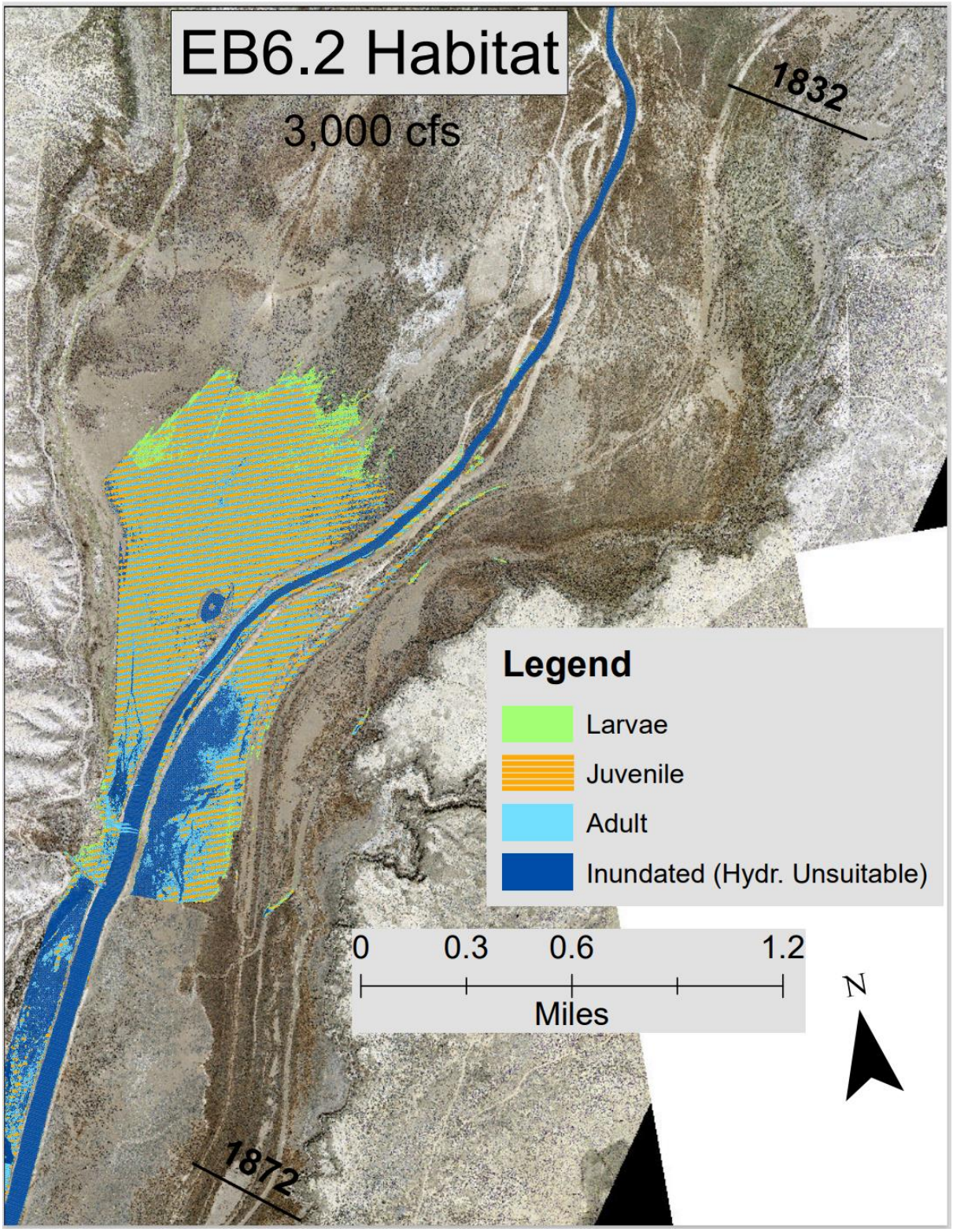

Figure E- 18 RGSM Habitat in subreach EB6.2 at 3000 cfs with hydraulically suitable areas labeled for larvae (green), juvenile (orange), and adult (light blue) and unsuitable inundated areas in dark blue.

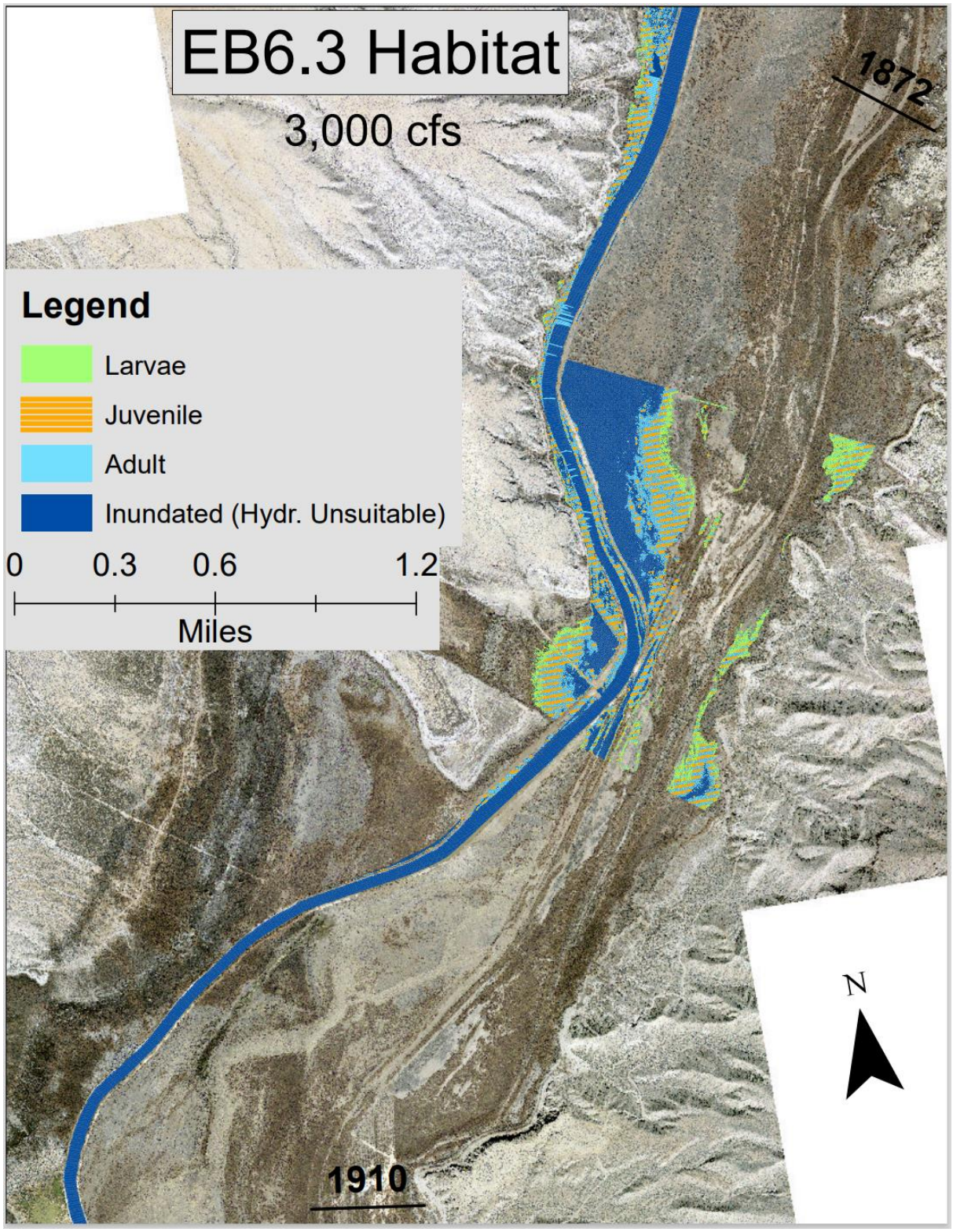

Figure E- 19 RGSM Habitat in subreach EB6.3 at 3000 cfs with hydraulically suitable areas labeled for larvae (green), juvenile (orange), and adult (light blue) and unsuitable inundated areas in dark blue.

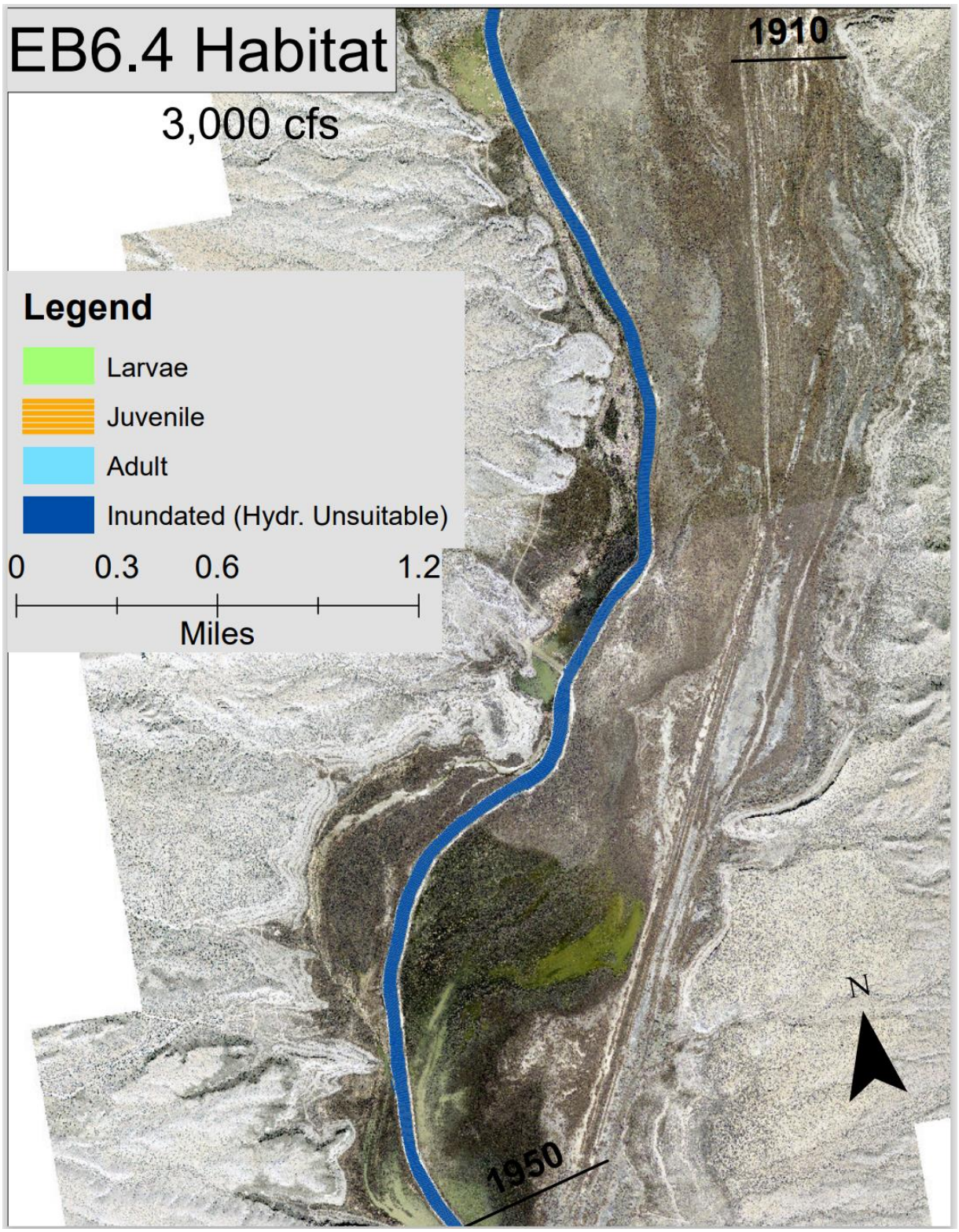

Figure E- 20 RGSM Habitat in subreach EB6.4 at 3000 cfs with hydraulically suitable areas labeled for larvae (green), juvenile (orange), and adult (light blue) and unsuitable inundated areas in dark blue.

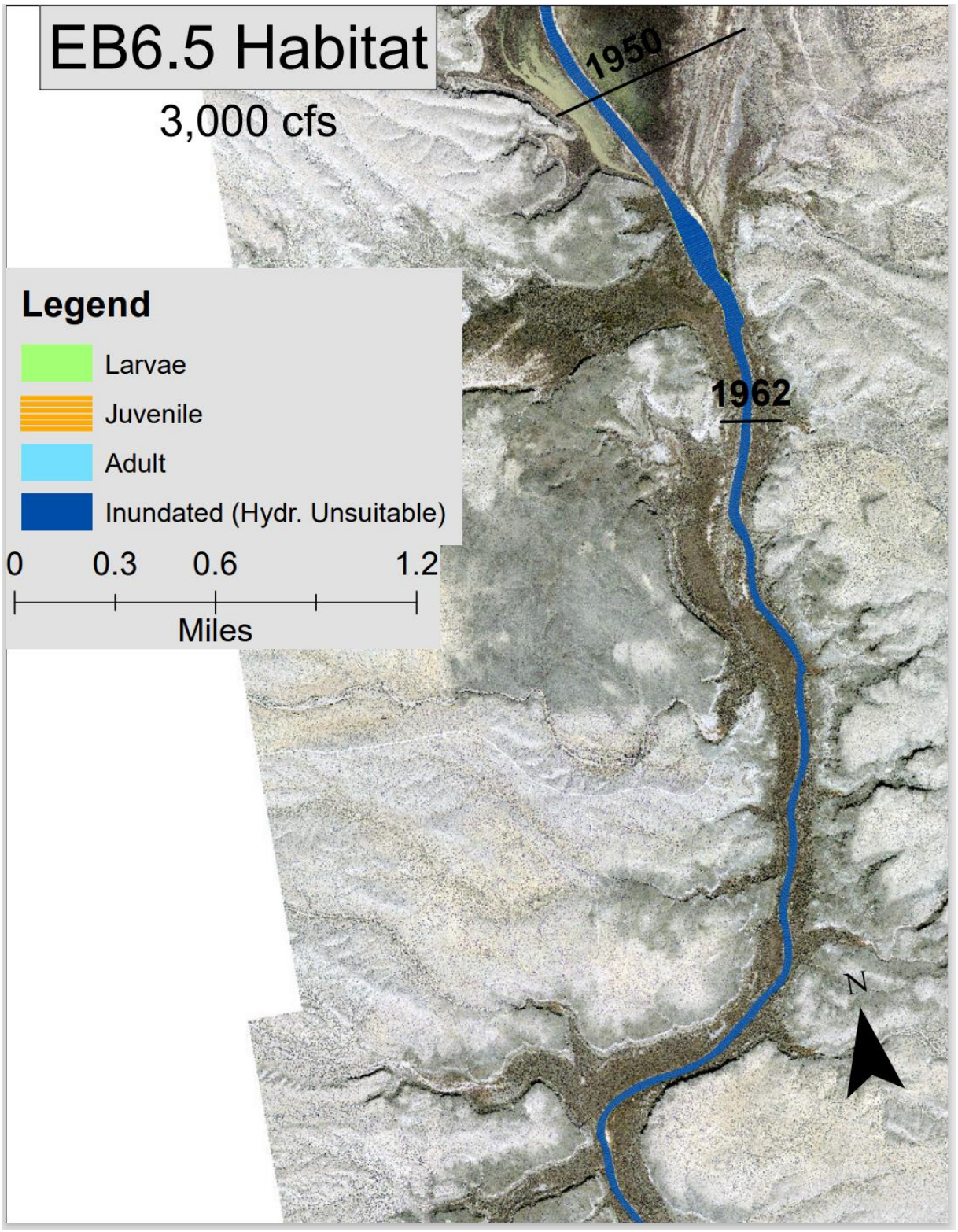

Figure E- 21 RGSM Habitat in subreach EB6.5 at 3000 cfs with hydraulically suitable areas labeled for larvae (green), juvenile (orange), and adult (light blue) and unsuitable inundated areas in dark blue.

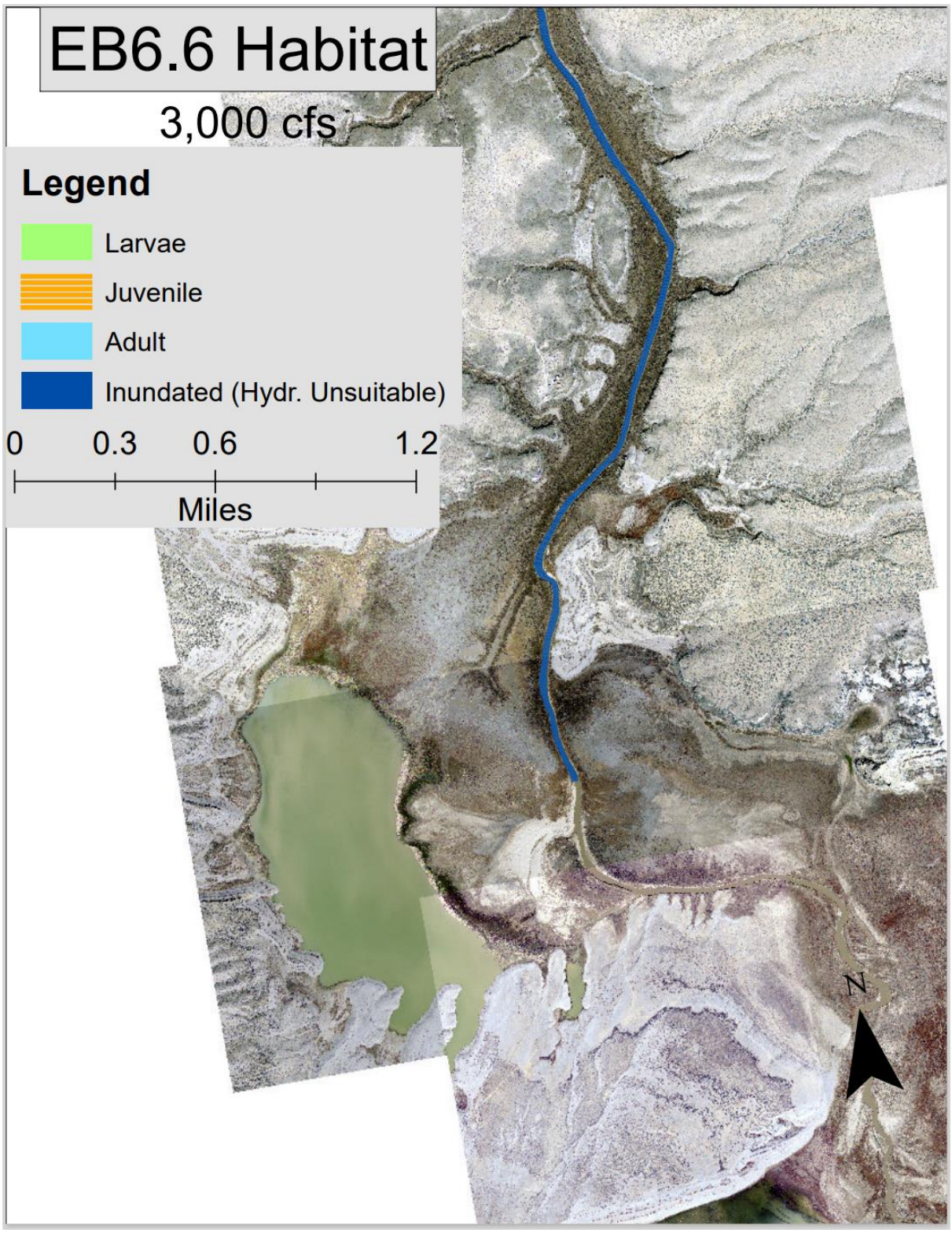

Figure E- 22 RGSM Habitat in subreach EB6.6 at 3000 cfs with hydraulically suitable areas labeled for larvae (green), juvenile (orange), and adult (light blue) and unsuitable inundated areas in dark blue.

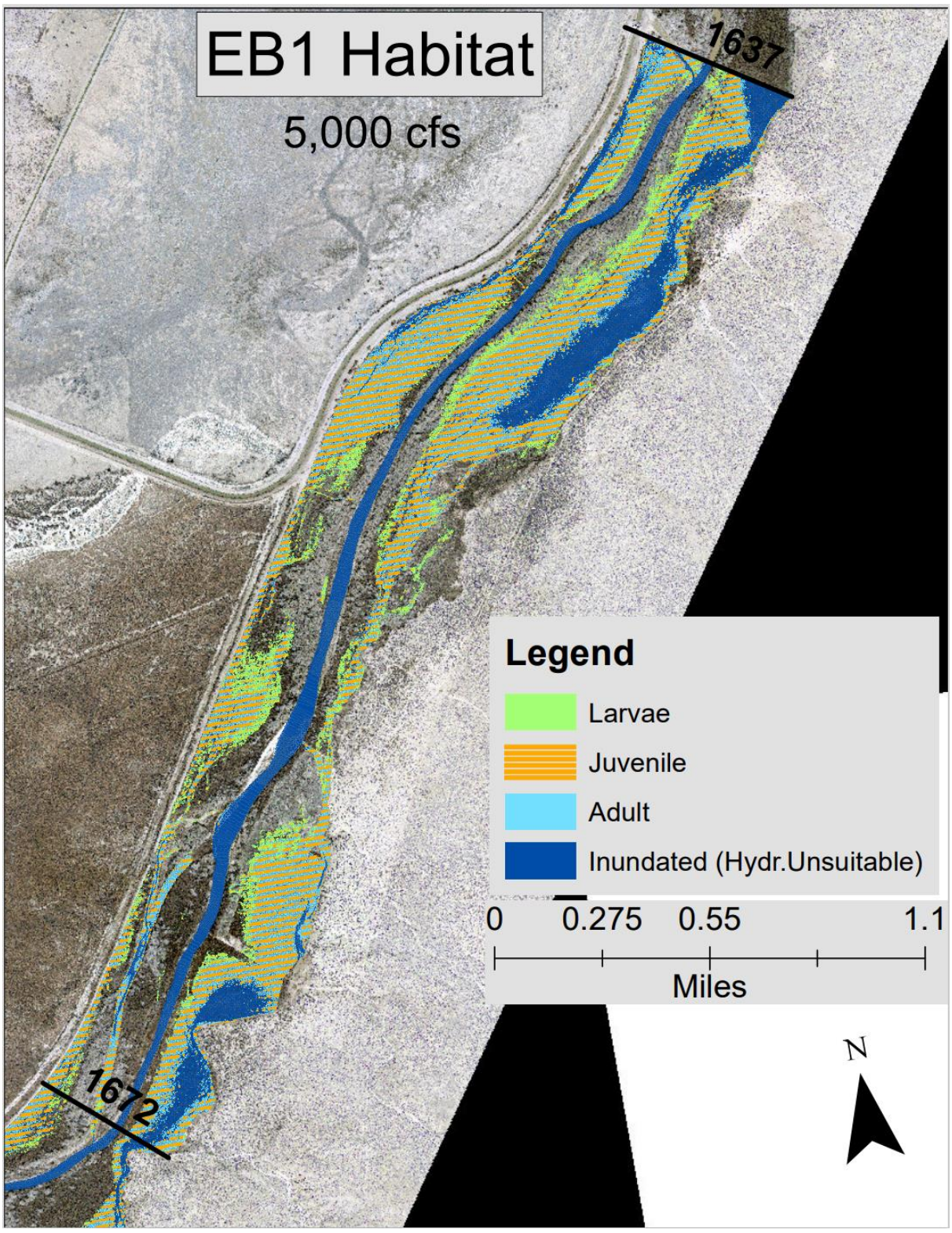

Figure E-23 RGSM Habitat in subreach EB1 at 5000 cfs with hydraulically suitable areas labeled for larvae (green), juvenile (orange), and adult (light blue) and unsuitable inundated areas in dark blue.

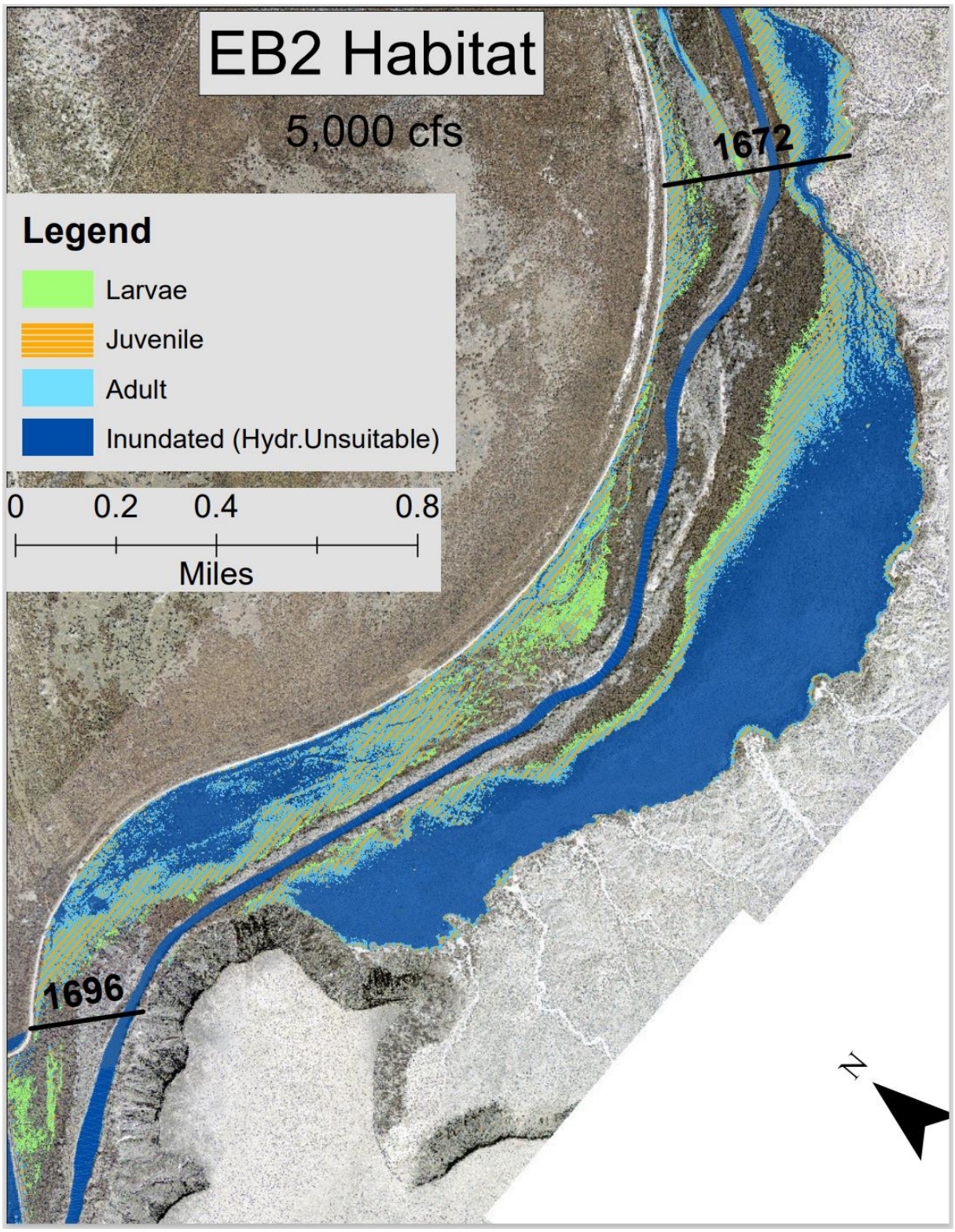

Figure E- 24 RGSM Habitat in subreach EB2 at 5000 cfs with hydraulically suitable areas labeled for larvae (green), juvenile (orange), and adult (light blue) and unsuitable inundated areas in dark blue.

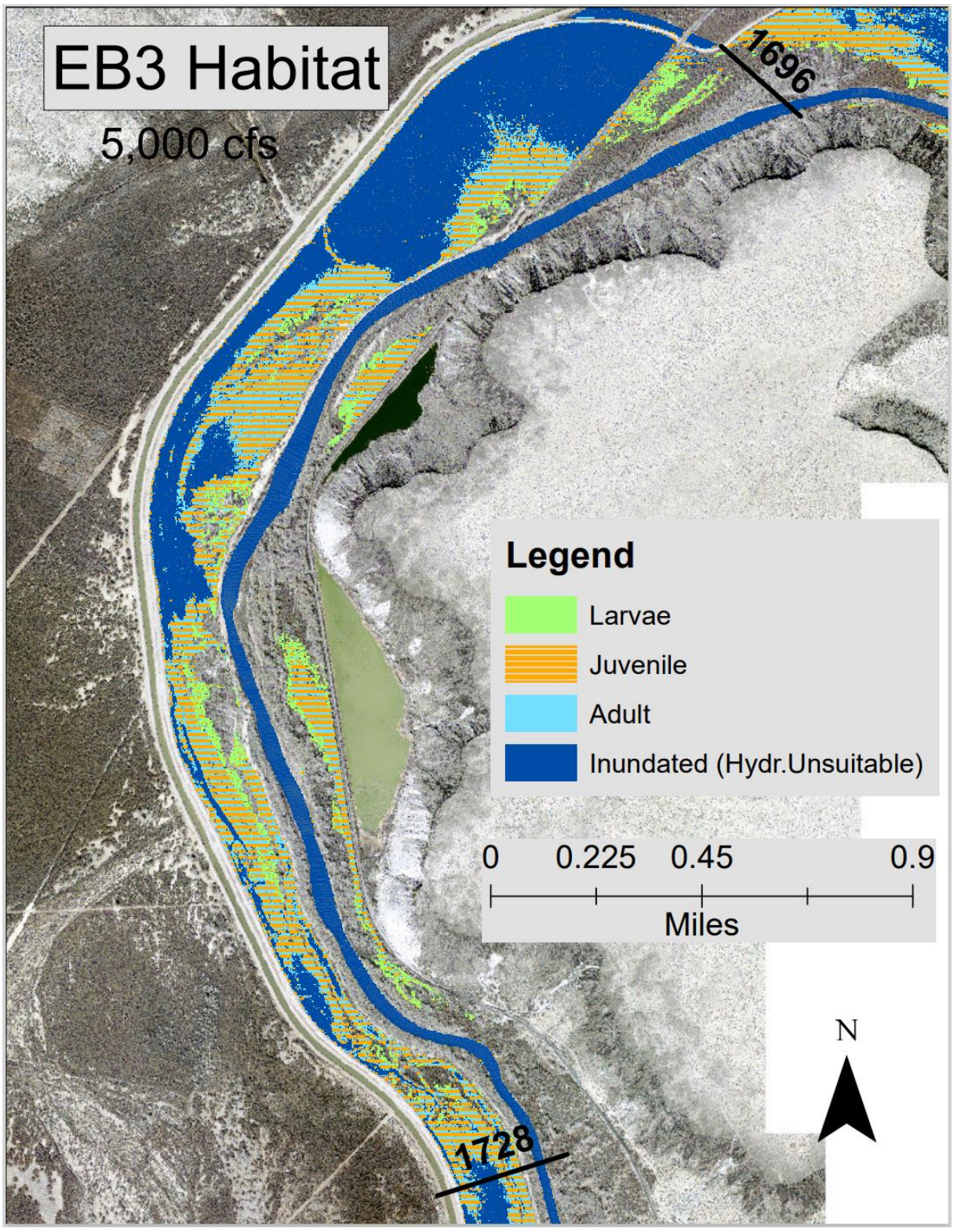

Figure E- 25 RGSM Habitat in subreach EB3 at 5000 cfs with hydraulically suitable areas labeled for larvae (green), juvenile (orange), and adult (light blue) and unsuitable inundated areas in dark blue

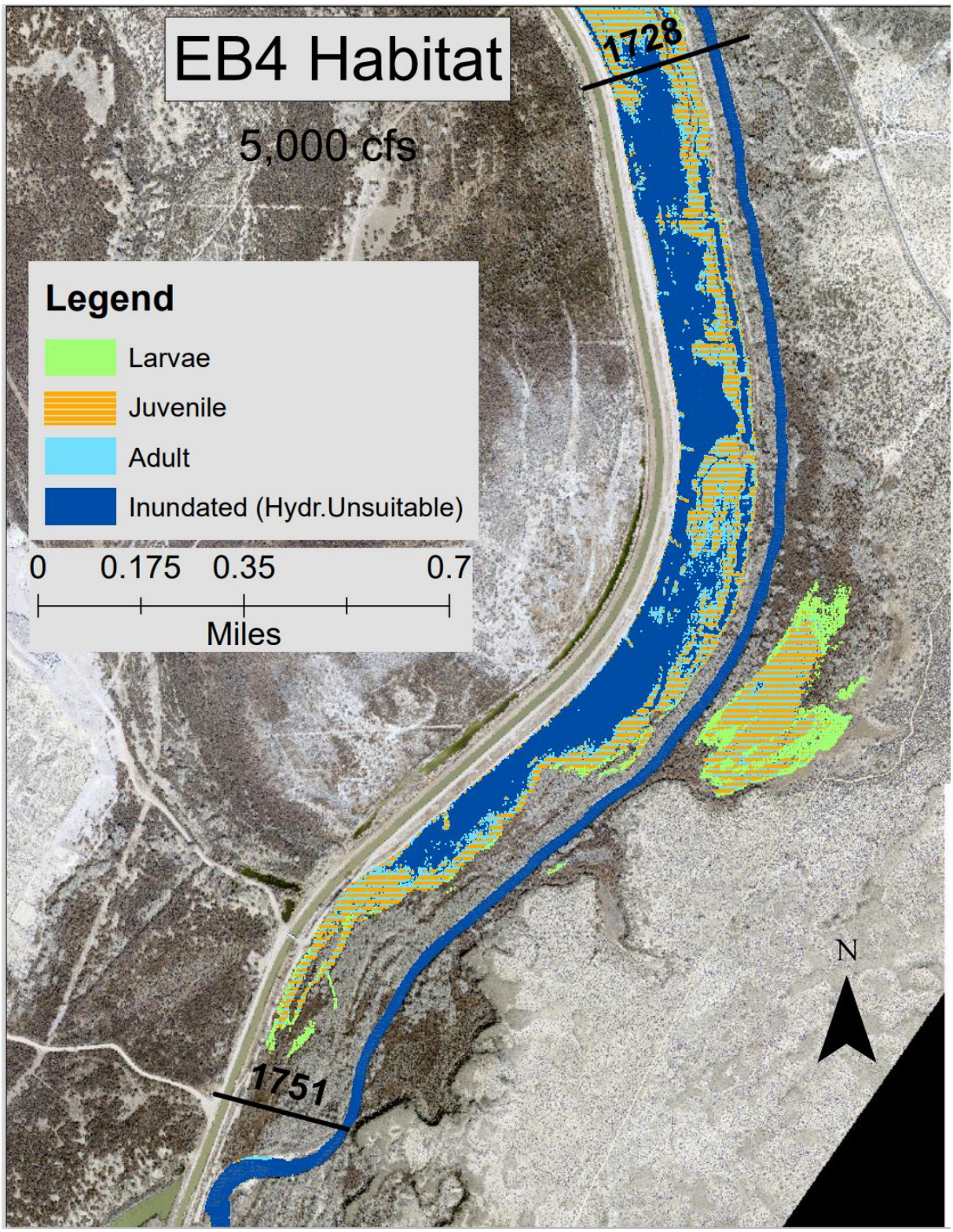

Figure E- 26 RGSM Habitat in subreach EB4 at 5000 cfs with hydraulically suitable areas labeled for larvae (green), juvenile (orange), and adult (light blue) and unsuitable inundated areas in dark blue.

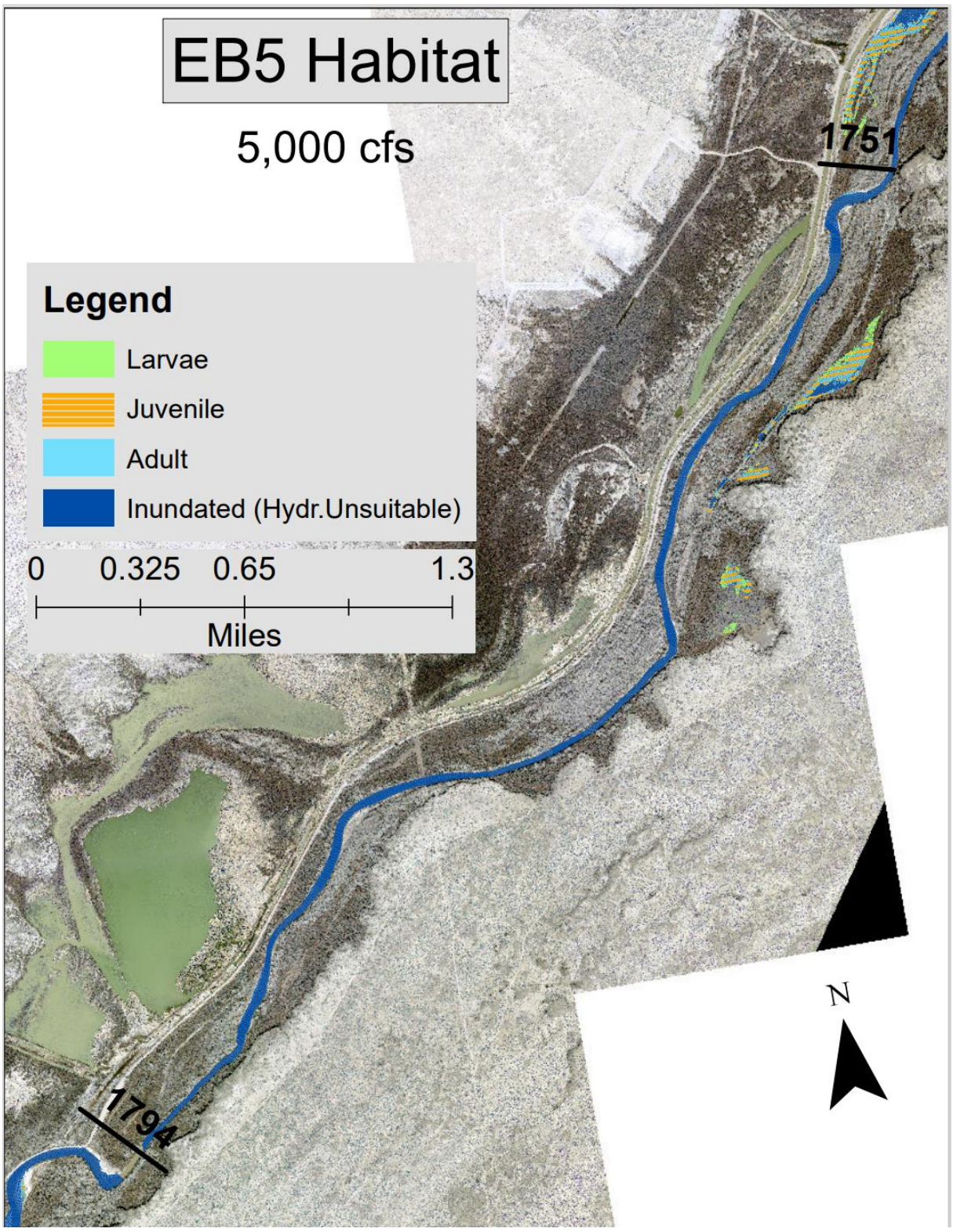

Figure E- 27 RGSM Habitat in subreach EB5 at 5000 cfs with hydraulically suitable areas labeled for larvae (green), juvenile (orange), and adult (light blue) and unsuitable inundated areas in dark blue

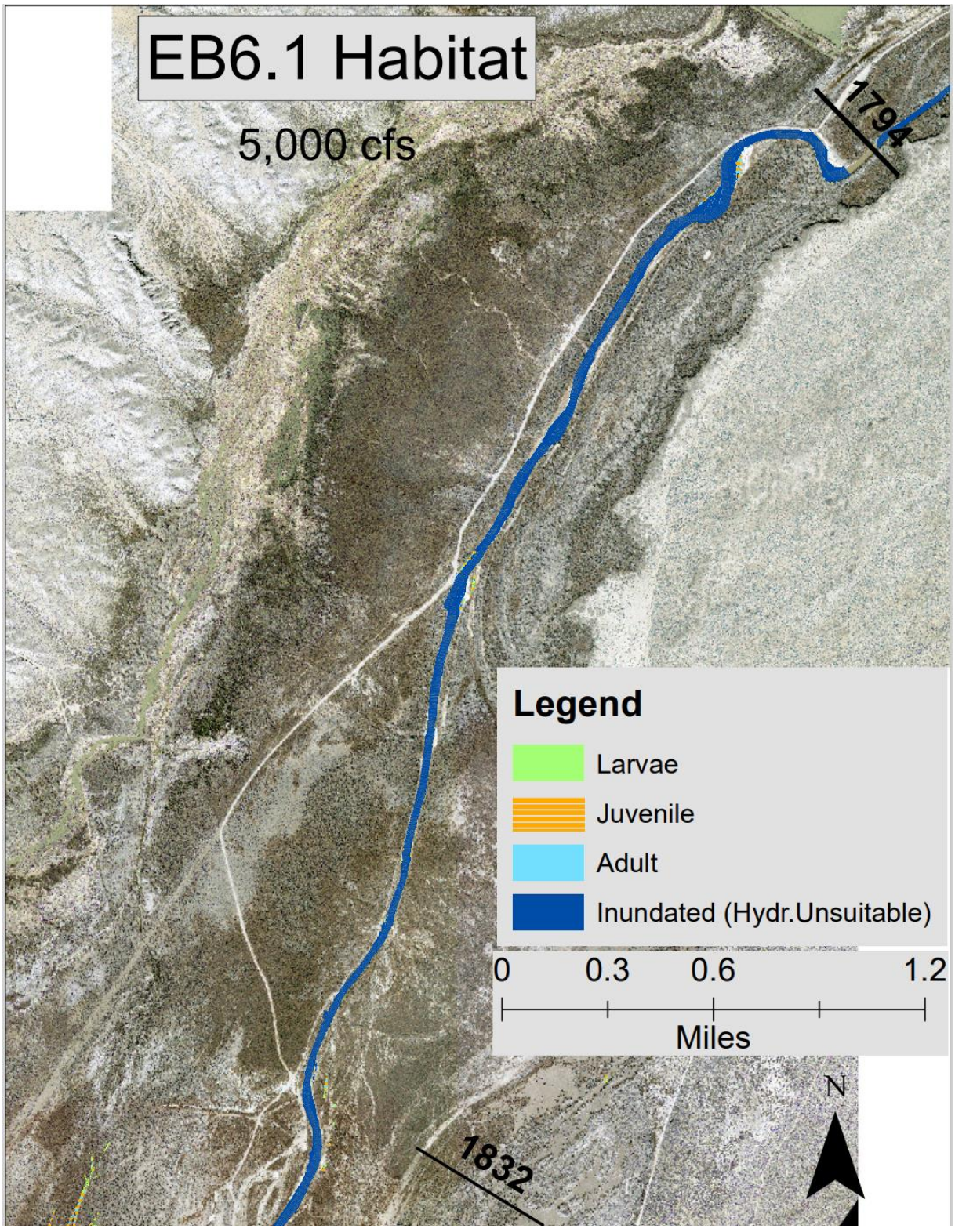

Figure E-28 RGSM Habitat in subreach EB6.1 at 5000 cfs with hydraulically suitable areas labeled for larvae (green), juvenile (orange), and adult (light blue) and unsuitable inundated areas in dark blue.

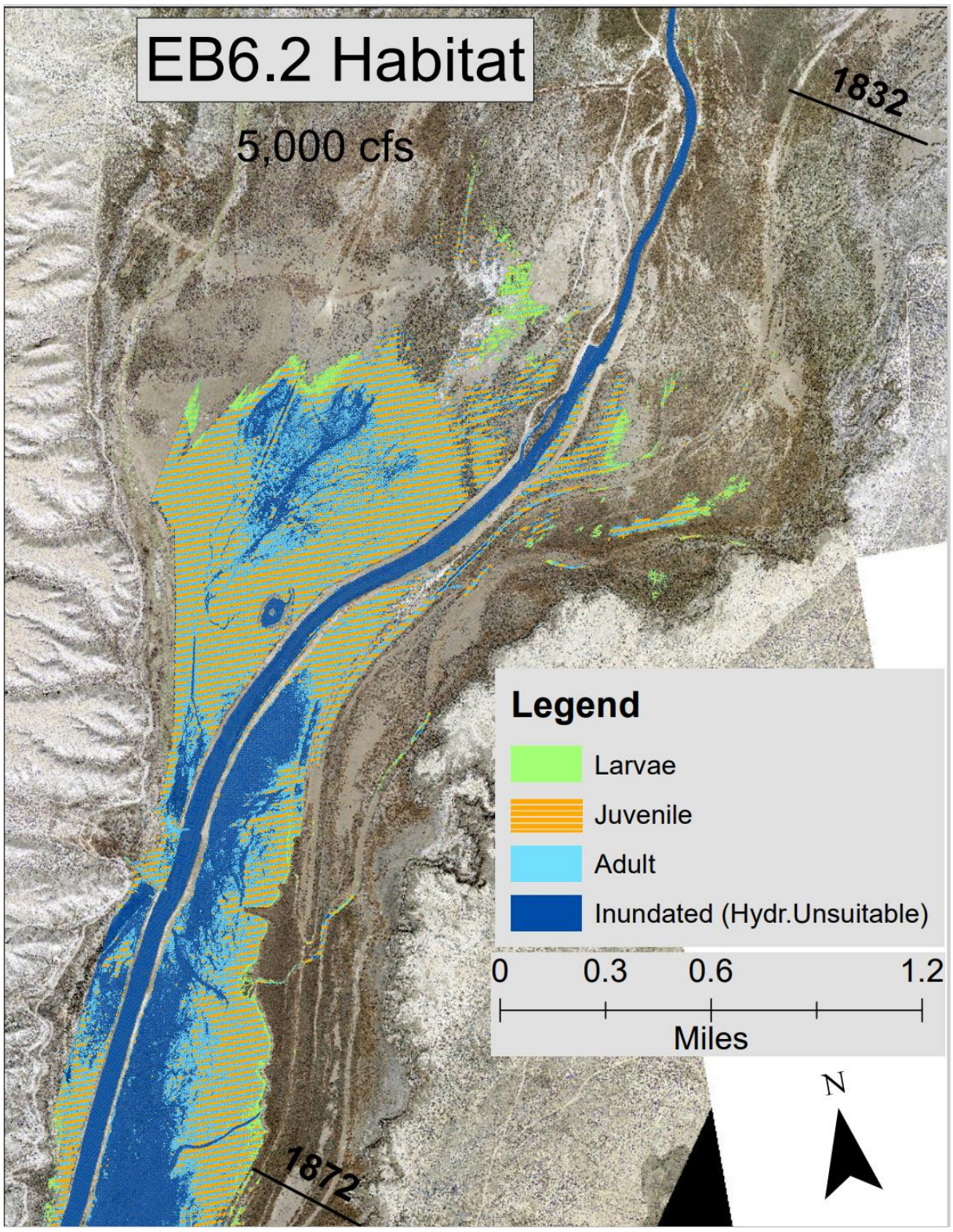

Figure E-29 RGSM Habitat in subreach EB6.2 at 5000 cfs with hydraulically suitable areas labeled for larvae (green), juvenile (orange), and adult (light blue) and unsuitable inundated areas in dark blue.

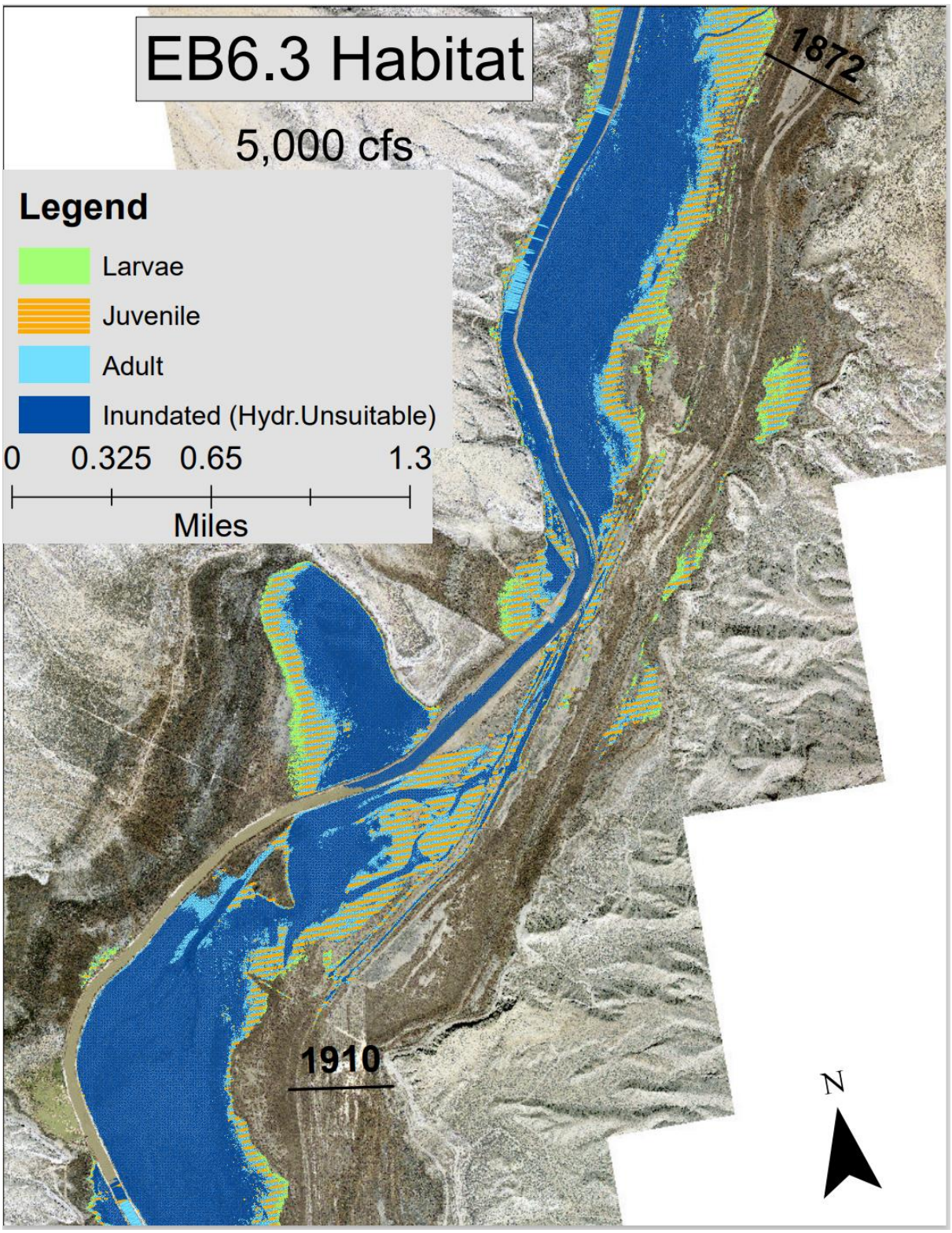

Figure E-30 RGSM Habitat in subreach EB6.3 at 5000 cfs with hydraulically suitable areas labeled for larvae (green), juvenile (orange), and adult (light blue) and unsuitable inundated areas in dark blue.

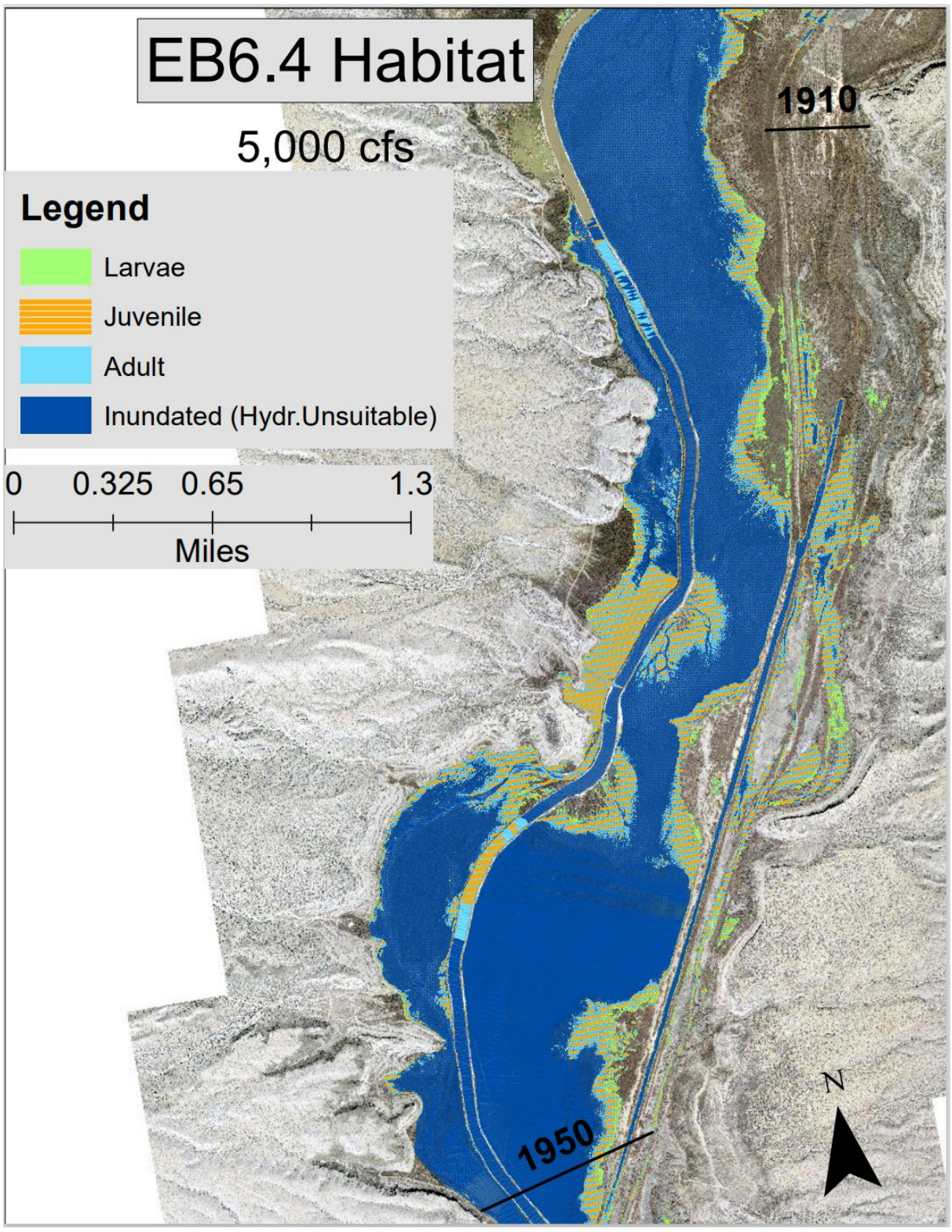

Figure E-31 RGSM Habitat in subreach EB6.4 at 5000 cfs with hydraulically suitable areas labeled for larvae (green), juvenile (orange), and adult (light blue) and unsuitable inundated areas in dark blue.

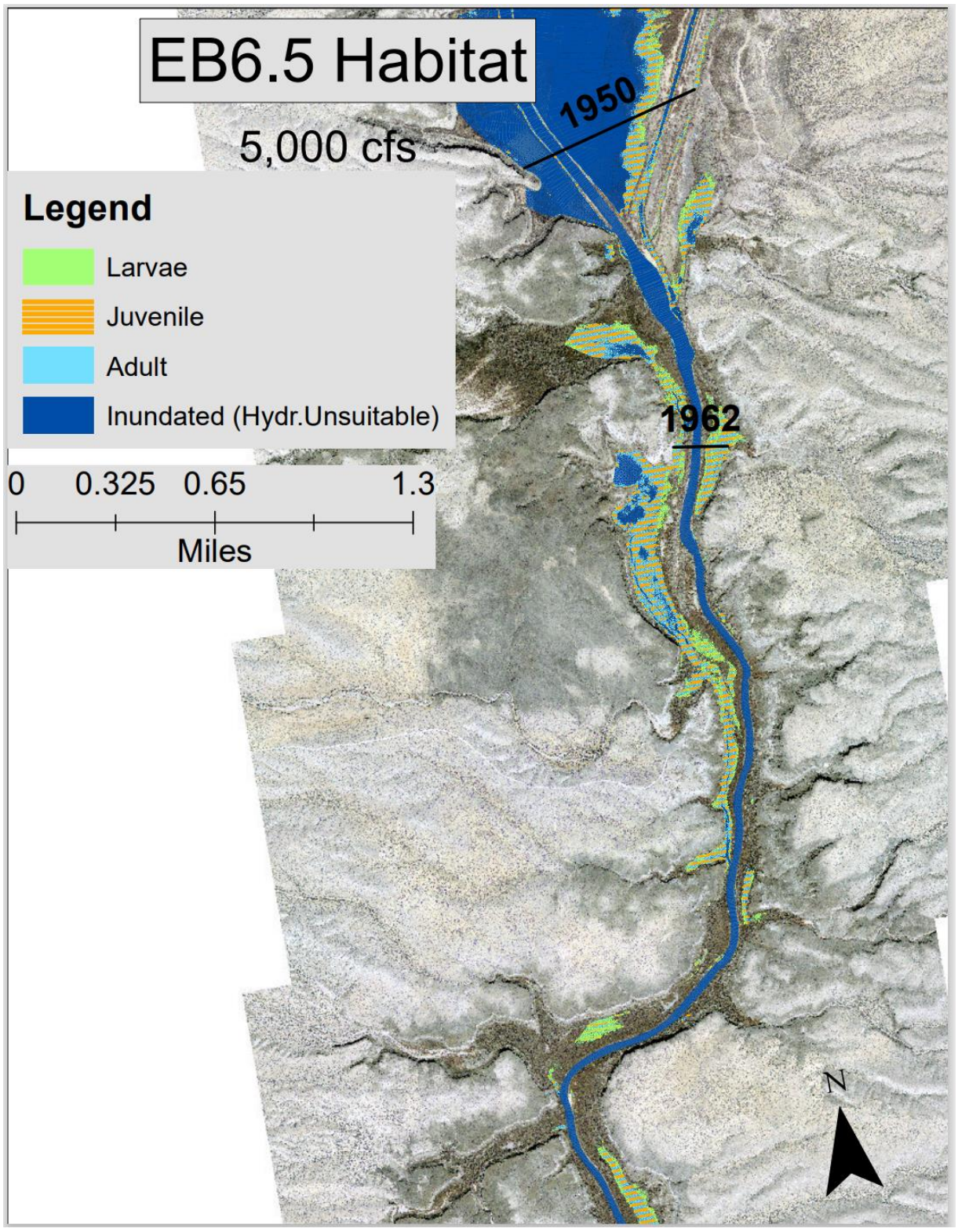

Figure E-32 RGSM Habitat in subreach EB6.5 at 5000 cfs with hydraulically suitable areas labeled for larvae (green), juvenile (orange), and adult (light blue) and unsuitable inundated areas in dark blue.

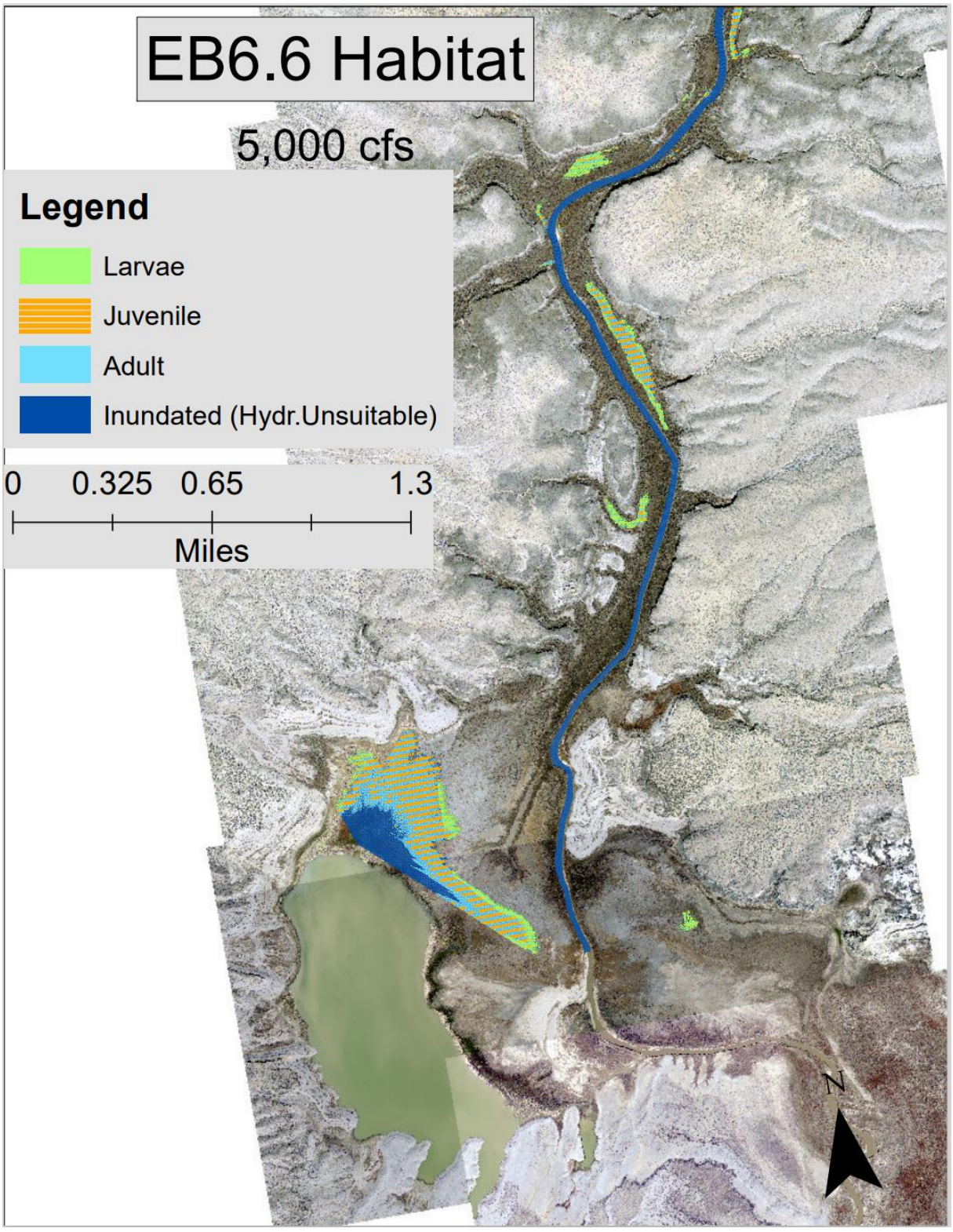

Figure E-33 RGSM Habitat in subreach EB6.6 at 5000 cfs with hydraulically suitable areas labeled for larvae (green), juvenile (orange), and adult (light blue) and unsuitable inundated areas in dark blue.

Appendix F

Geomorphology/Habitat Connection Figures for Process Linkage Report

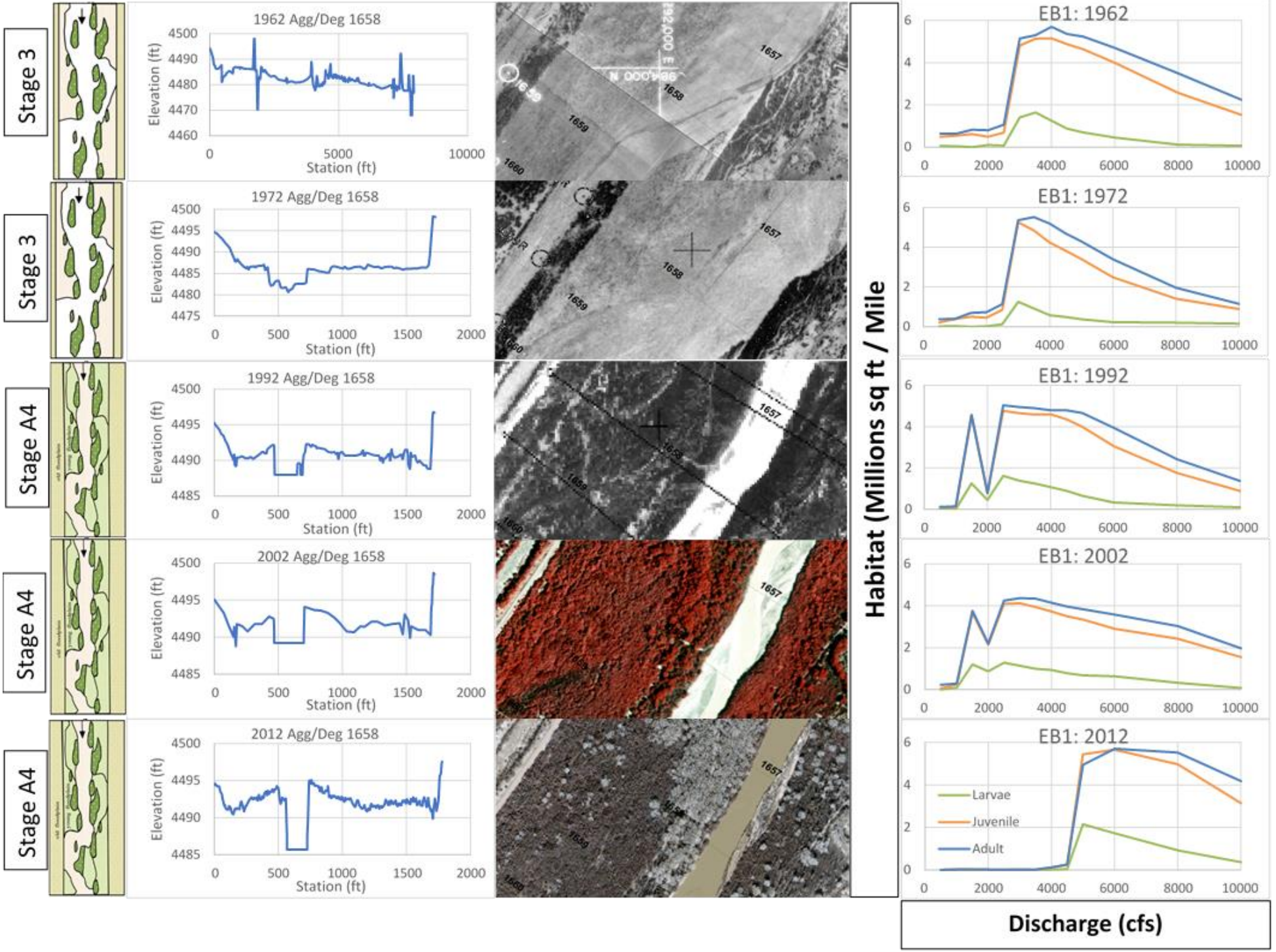

Figure F- 8 Geomorphology and habitat connections collage for subreach EB1

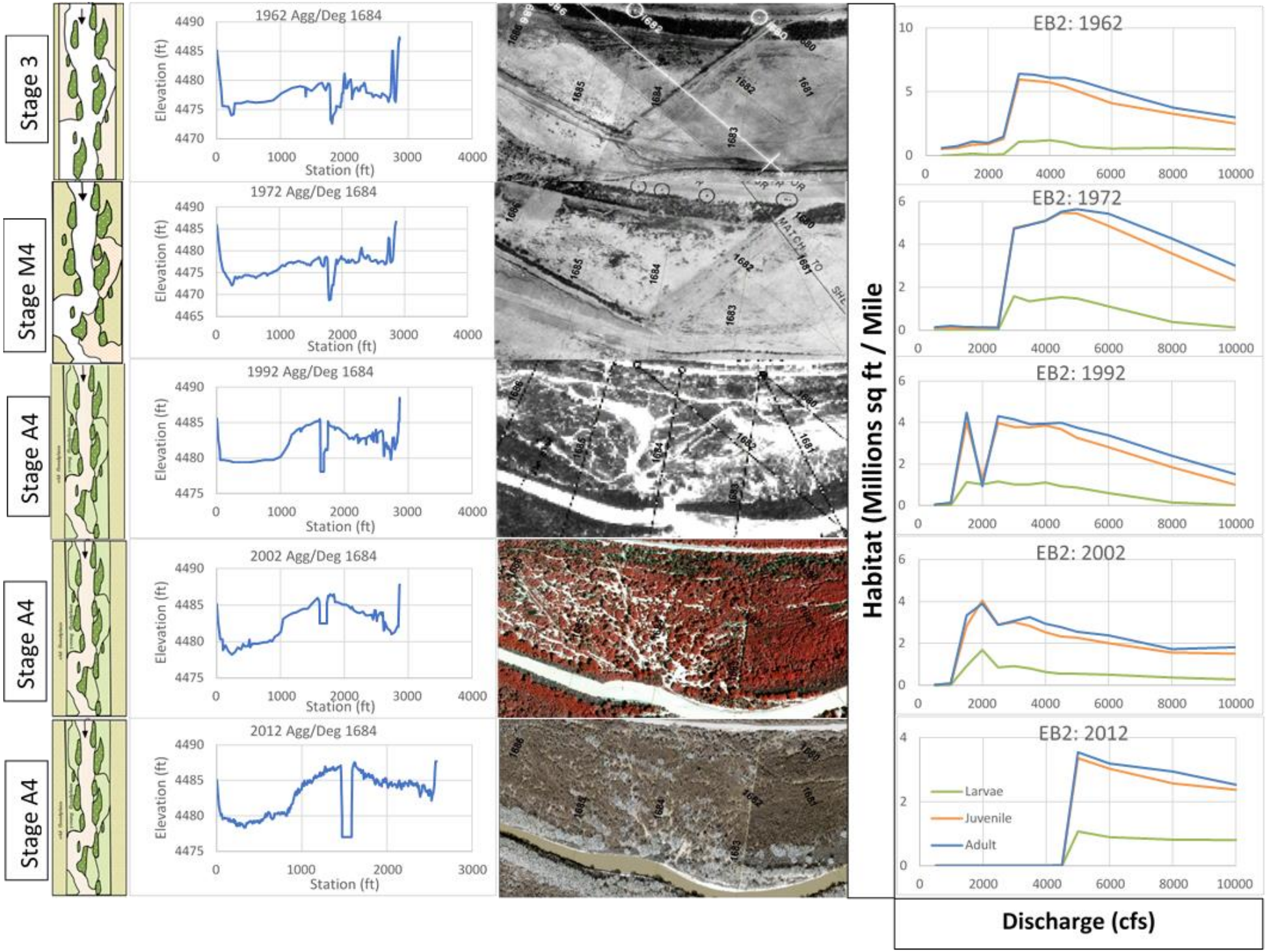

Figure F- 9 Geomorphology and habitat connections collage for subreach EB2

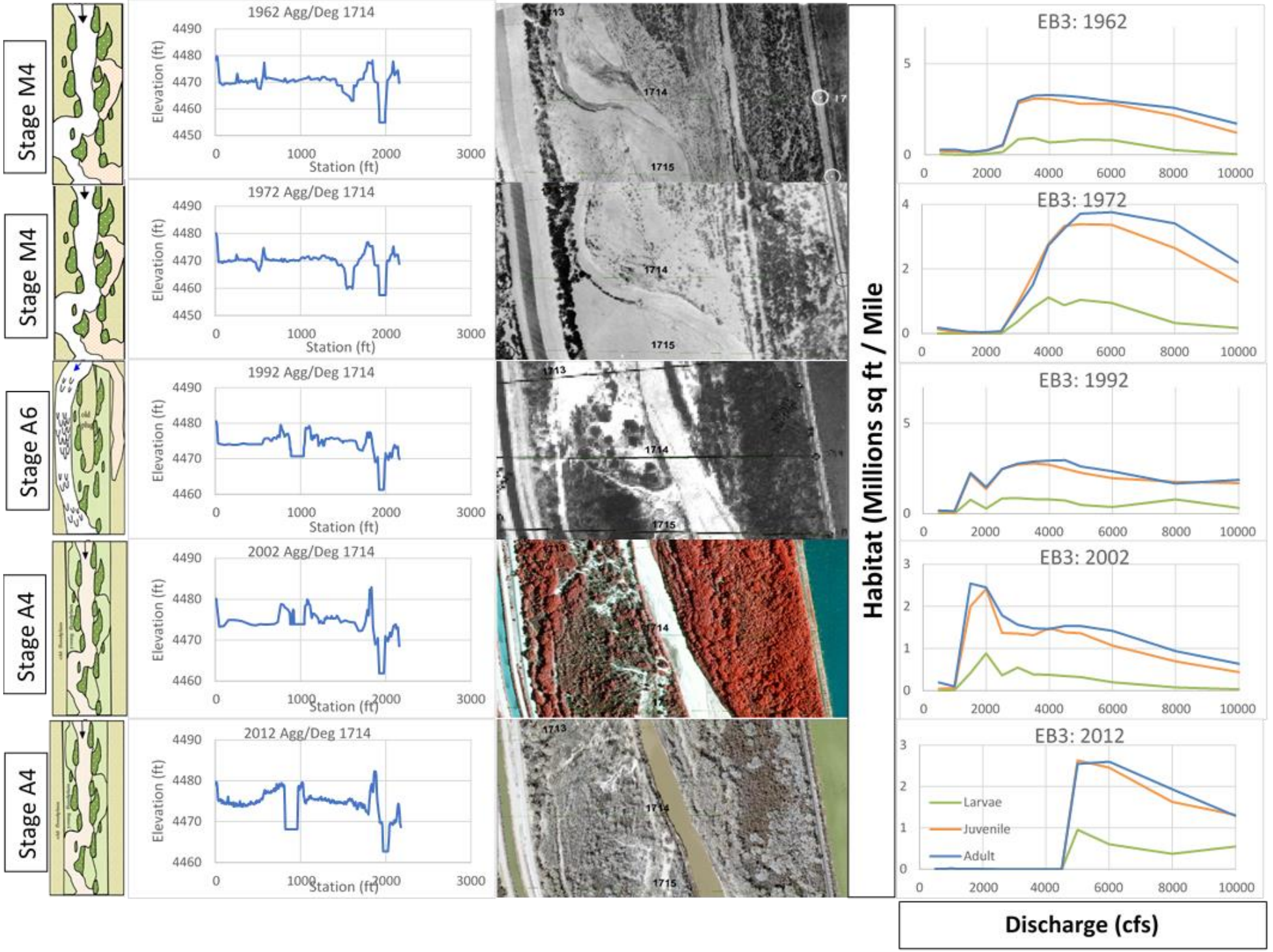

Figure F- 10 Geomorphology and habitat connections collage for subreach EB3

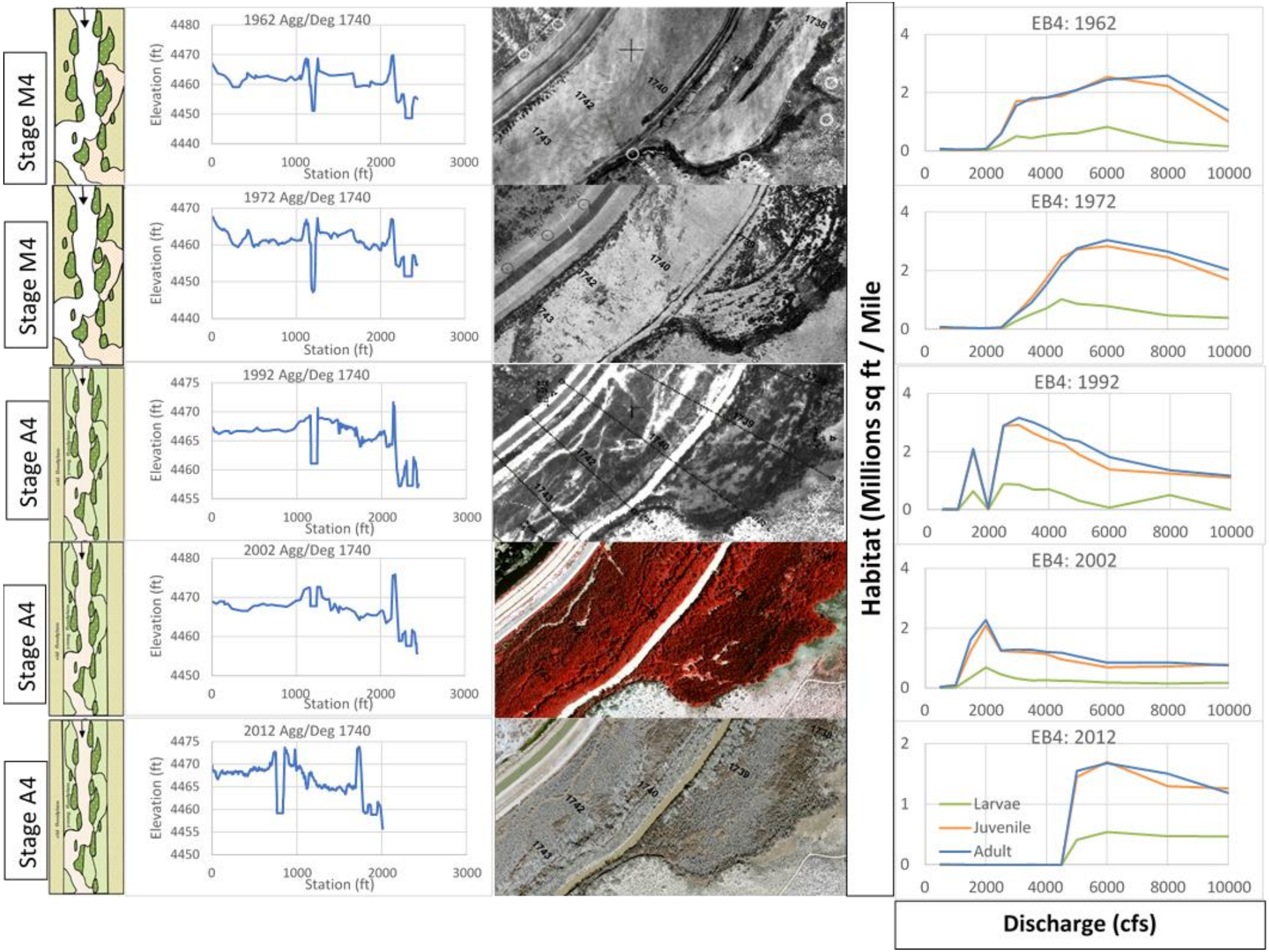

Figure F- 11 Geomorphology and habitat connections collage for subreach EB4

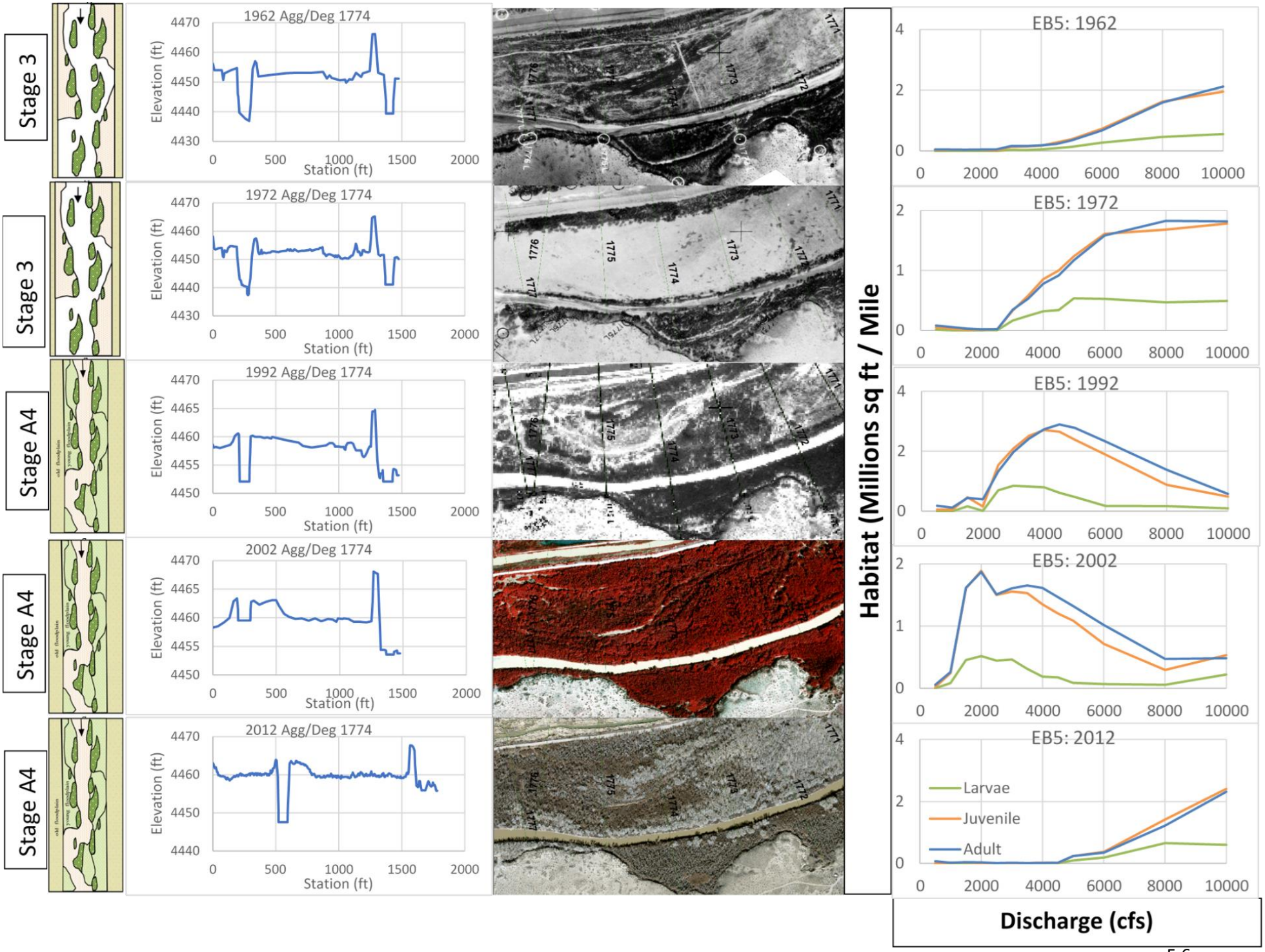

Figure F- 12 Geomorphology and habitat connections collage for subreach EB5